AD_____

AWARD NUMBER: DAMD17-01-1-0773

TITLE: Non-Invasive Gene Therapy of Experimental Parkinson's Disease

PRINCIPAL INVESTIGATOR: William M. Pardridge, M.D.

CONTRACTING ORGANIZATION: University of California
Los Angeles, California 90024-1406

REPORT DATE: September 2006

TYPE OF REPORT: Final

PREPARED FOR: U.S. Army Medical Research and Materiel Command
Fort Detrick, Maryland 21702-5012

REPORT DOCUMENTATION PAGE

Form Approved
OMB No. 0704-0188

1. REPORT DATE *(DD-MM-YYYY)*	**2. REPORT TYPE**	**3. DATES COVERED** *(From - To)*
01-09-2006	Final	27 Aug 2001 – 26 August 2006

4. TITLE AND SUBTITLE

Non-Invasive Gene Therapy of Experimental Parkinson's Disease

5a. CONTRACT NUMBER

5b. GRANT NUMBER
DAMD17-01-1-0773

5c. PROGRAM ELEMENT NUMBER

6. AUTHOR(S)

William M. Pardridge, M.D.

E-Mail: wpardridge@mednet.ucla.edu

5d. PROJECT NUMBER

5e. TASK NUMBER

5f. WORK UNIT NUMBER

7. PERFORMING ORGANIZATION NAME(S) AND ADDRESS(ES)

University of California
Los Angeles, California 90024-1406

8. PERFORMING ORGANIZATION REPORT NUMBER

9. SPONSORING / MONITORING AGENCY NAME(S) AND ADDRESS(ES)
U.S. Army Medical Research and Materiel Command
Fort Detrick, Maryland 21702-5012

10. SPONSOR/MONITOR'S ACRONYM(S)

11. SPONSOR/MONITOR'S REPORT NUMBER(S)

12. DISTRIBUTION / AVAILABILITY STATEMENT
Approved for Public Release; Distribution Unlimited

13. SUPPLEMENTARY NOTES

14. ABSTRACT

The present research has developed a non-viral gene targeting technology, whereby the effects of a neurotoxin on the brain can be reversed shortly after the intravenous injection of a therapeutic gene medicine without the use of viral vectors. The brain gene targeting technology developed in this work creates an "artificial virus" which is comprised of non-immunogenic lipids and proteins, wherein the therapeutic gene is packaged in the interior of the gene delivery vehicle, which is called a pegylated immunoliposome (PIL). The PIL carrying the gene is a 85 nm "stealth" nanocontainer, which is relatively invisible to the body's reticuloendothelial system, which normally removes nanocontainers from the blood. The surface of the nanocontainer is studded with a receptor-specific monoclonal antibody (MAb). This MAb acts as a moleculr Trojan horse, and triggers the transport of the stealth nanocontainer across the 2 biologicial membrane barriers that separate the blood from the interior of brain cells. These barriers are the brain microvascular endothelial wall, which forms the blood-brain barrier in vivo, and the brain cell plasma membrane. Both barriers express the transferrin receptor, and the anti-receptor MAb enables the PIL to cross the membrane barriers via normal physiological transport processes usually used for endogeneous ligands such as transferrin. With this approach non-viral, non-invasive gene therapy of the brain is now possible.

15. SUBJECT TERMS
neurotoxin, brain gene therapy, non-viral gene transfer

16. SECURITY CLASSIFICATION OF:			**17. LIMITATION OF ABSTRACT**	**18. NUMBER OF PAGES**	**19a. NAME OF RESPONSIBLE PERSON**
a. REPORT	**b. ABSTRACT**	**c. THIS PAGE**			USAMRMC
U	U	U	UU	130	**19b. TELEPHONE NUMBER** *(include area code)*

Standard Form 298 (Rev. 8-98)
Prescribed by ANSI Std. Z39.18

Table of Contents

INTRODUCTION

Neurotoxins can cause serious derangements in brain biochemistry that can compromise the cognitive and motor function of the individual. In the present studies an animal model of neurotoxin exposure is used, wherein the neurotoxin, 6-hyrdoxydopamine, is injected into a specific region of the rat brain called the medial forebrain bundle, followed approximately 4 weeks later by a biochemical picture resembling Parkinson's disease (PD). On the side of the brain where the neurotoxin is injected, there is a 90% reduction in the level of a key enzyme, tyrosine hydroxylase (TH), which is a rate-limiting enzyme involved in dopamine production. Dopamine is the neurotransmitter that is deficient in PD. One way that brain TH levels can be restored in conditions such as PD is through gene therapy, wherein the TH gene is given to the individual afflicted with PD. However, with the conventional approach to gene therapy of the brain, there are two serious problems. First, virtually all present-day approaches use viral vectors to carry the gene to brain cells. However, these viral vectors are either highly inflammatory (such as adenovirus or herpes simplex virus) or stably alter the host genome in a random way (retrovirus, adeno-associated virus), which can lead to insertional mutagenesis and cancer. These viruses do not enter the brain from blood, because they do not cross the blood-brain barrier (BBB). This creates the second problem with present-day approaches to gene therapy, which is the viral vector is administered to the brain by craniotomy and drilling a hole in the head. However, this only distributes the virus to a tiny region of the brain at the tip of the injection needle. What is needed is a non-invasive, non-viral form of brain gene therapy wherein the therapeutic gene can be administered intravenously without viral vectors followed by widespread expression of the exogenous gene throughout the brain. This is the goal of the present research.

The present research uses a completely new form of brain gene targeting technology which uses a novel gene delivery vehicle called pegylated immunoliposomes (PIL). PILs are comprised of non-immunogenic lipids and proteins, wherein the therapeutic gene is packaged within the interior of the gene delivery vehicle, which is called a pegylated immunoliposome (PIL). The PIL carrying the gene is an 85 nm "stealth" nano-container, which is relatively invisible to the body's reticuloendothelial system, that normally removes nano-containers from the blood. This stealth effect is created by conjugating approximately 2000 strands of 2000 Dalton polyethylene glycol (PEG) to the surface of the liposome carrying the gene inside. Approximately 1-2% of the tips of the PEG strands are studded with receptor-specific monoclonal antibodies (MAb). This MAb is a targeting ligand and acts as a molecular Trojan horse, which triggers the transport of the stealth nano-container across the two biological membrane barriers which separate the blood from the interior of brain cells: the brain microvascular endothelial wall, which forms the blood-brain barrier (BBB) in vivo, and the brain cell plasma membrane (BCM). Both the BBB and the BCM express a targeted receptor, in this case, the transferrin receptor (TfR), and the anti-TfR MAb enables the PIL to cross the membrane barriers via normal physiological transport processes which are usually used for endogenous ligands such as transferrin. With this approach, non-viral gene therapy, non-invasive gene therapy of the brain is now possible.

The TH expression plasmid is encapsulated in the interior of the 85 nm PIL which is targeted to rat brain with the OX26 murine MAb to the rat TfR. The TfRMAb-PIL carrying the plasmid DNA is injected intravenously in rats at a dose of 1-10 μg plasmid DNA per adult rat. These rats all have drug-confirmed experimental PD, owing to the intracerebral injection of the

6-hydroxydopamine neurotoxin into the brain four weeks earlier. The goal is to normalize the striatal TH activity based on both brain biochemistry assays, immunocytochemistry assays, and pharmacologic behavioral testing.

BODY

Original Statement of Work (SOW). The original statement of work outlined experiments in 5 areas:

(1) formulation of PILs (01 year)
(2) single dose efficacy study with SV40 promoter (01-02 years)
(3) toxicity study with focus on brain inflammatory response (02-03 years)
(4) single dose efficacy study with glial fibrillary acidic protein (GFAP) gene promoter (02-03 years)
(5) multi-dose efficacy study (03 year)

Progress toward these goals has been achieved on time, although the work period has been extended by 2 consecutive 1-year no cost extensions. The purpose of the no-cost extension period was to extend the last of the specific aims, and to find new ways for prolonging the therapeutic effect of the gene therapy. The work performed in the extended years culminated in the publication of Appendix 15 in the 2006 Pharmaceutical Research.

KEY RESEARCH ACCOMPLISHMENTS

- First demonstration of global expression of a trans-gene in the brain following an intravenous injection of small volumes of a non-viral formulation. This was accomplished in mice, rats, and Rhesus monkeys. This was made possible by the development of a completely new non-viral gene transfer technology that utilizes pegylated immunoliposomes or PILs, which carry encapsulated plasmid DNA.
- First demonstration that the expression of the transgene in organs outside the brain could be eliminated by the combined use of PILs and brain-specific gene promoters. This was demonstrated in mice, rats, and Rhesus monkeys.
- First demonstration that the biochemical abnormalities, and the behavior abnormalities in neurotoxin-induced Parkinson's disease could be completely normalize, albeit temporarily, with intravenous injections of PILs carrying an expression plasmid encoding cDNA forms of the rat tyrosine hydroxylase (TH) trans-gene.
- The mechanism of the transient nature of TH gene expression in brain was shown by real time PCR studies in the primate brain to be due to degradation of cDNA forms of the trans-gene. This provides the basis for future work using chromosomal-derived forms of the therapeutic gene, which are less susceptible to DNAases in the cell, which degrade the exogenous DNA delivered to brain cells with the PIL gene transfer technology.

REPORTABLE OUTCOMES

(1) Manuscripts: listed below in Publications.

(2) Plasmids developed: tyrosine hydroxylase expression plasmids driven by either the SV40 or the GFAP promoter were produced as described in prior reprots.

CONCLUSIONS

The US Army support of this work has led to the development of a transformational technology that revolutionizes our approach to gene therapy of the brain and to gene therapy of brain neurotoxin exposure. Unlike the conventional approach to brain gene therapy, we achieve the desired pharmacological effect without viruses and without craniotomy. The use of viral vectors will probably never be widely used in gene therapy in humans, owing to their toxic effects. The use of craniotomy for delivering genes to the brain is problematic because the gene is only delivered to a tiny area of the brain. Moreover, craniotomy-based gene therapy of the brain in soldiers in the field is virtually impossible. We have created a form of brain gene therapy that could be administered to soldiers in the field.

This approach to gene therapy enables adult transgenics in 24 hours.

This new technology for non-invasive delivery of non-viral genes to the brain should be developed further in the following directions:

- Chromosomal (genomic) forms of the trans-gene should be used instead of cDNA forms of the gene. This past work has shown that large genomic constructs of 15-20 kb can be incorporated in eukaryotic expression plasmids. The genomic forms of the gene have longer periods of action in vivo than do the cDNA forms.
- This work should be replicated not with the TH gene but with a gene encoding a nigral-striatal trophic factor, such as glial derived neurotrophic factor (GDNF). The toxic effects of neurotoxins can be ameliorated with a single dose of GDNF gene therapy.
- GDNF gene therapy of neurotoxin exposed brain should be coupled with gene promoters that enable transgene expression only in the nigral-striatal tract. This will eliminate “off target” expression of the transgene in areas outside the therapeutic target.
- The Army needs to continue this work, as it will eventually lead to the development of powerful neuroprotective agents that can be easily administered to at risk soldiers in the field.

PUBLICATIONS FUNDED BY THIS WORK:

1. Shi, N., Zhang, Y., Boado, R.J., Zhu, C., and Pardridge, W.M. (2001): Brain-specific expression of an exogenous gene following intravenous adminstration. Proc. Natl. Acad. Sci. U.S.A., 98: 12754-12759. **APPENDIX 1.**

2. Pardridge, W.M. (2002): Drug and gene targeting to the brain with molecular Trojan horses. Nature Reviews-Drug Discovery, 1: 131-139. **APPENDIX 2.**

3. Pardridge, W.M. (2002): Drug and gene delivery to the brain: the vascular route. Neuron, 36: 555-558. **APPENDIX 3.**

4. Zhang, Y., Boado, R.J., and Pardridge, W.M. (2003): Marked enhancement in gene expression by targeting the human insulin receptor. J. Gene Med., 5: 157-163. **APPENDIX 4.**

5. Zhang, Y., Calon, F., Zhu, C., Boado, R.J., and Pardridge, W.M. (2003): Intravenous non-viral gene therapy causes complete normalization of striatal tyrosine hydroxylase and reversal of motor impairment in experimental Parkinsonism. Hum. Gene Ther. 14: 1-12. **APPENDIX 5.**

6. Zhang, Y., Schlachetzki, F., and Pardridge, W.M. (2003): Global non-viral gene transfer to the primate brain following intravenous administration. Mol. Ther., 7: 11-18. **APPENDIX 6.**

7. Zhang, Y., Boado, R.J., and Pardridge, W.M. (2003): Absence of toxicity of chronic weekly intravenous gene therapy with pegylated immunoliposomes. Pharm. Res., 20: 1770-1785. **APPENDIX 7.**

8. Zhang, Y., Schlachetzki, F., Li, J.Y., Boado, R.J., and Pardridge, W.M. (2003): Organ-specific gene expression in the Rhesus monkey eye following intravenous non-viral gene transfer. Mol. Vis., 9: 465-472. **APPENDIX 8.**

9. Pardridge, W.M. (2003): Gene targeting in vivo with pegylated immunoliposomes. Methods in Enzymology (Liposomes, Part C), 373: 507-528. **APPENDIX 9.**

10. Zhang, Y., Schlachetzki, F., Zhang, Y., Boado, R.J., and Pardridge, W.M. (2004): Normalization of striatal tyrosine hydroxylase and reversal of motor impairment in experimental Parkinsonism with intravenous non-viral gene therapy and a brain –specific promoter. Human Gene Therapy, 15: 339-350. **APPENDIX 10.**

11. Schlachetzki, F., Zhang, Y., Boado, R. J., and Pardridge, W.M. (2004): Gene therapy of the brain: the transvascular approach. Neurology, 62: 1275-1281. **APPENDIX 11.**

12. Zhu, C., Zhang, Y., Zhang, Y.F., Li, J.Y., Boado, R.J., and Pardridge, W.M. (2004): Organ specific expression of LacZ gene controlled by the opsin promoter after intravenous gene administration in adult mice. J. Gene Med., 6: 906-912. **APPENDIX 12.**

13. Pardridge, W.M. (2005): Tyrosine hydroxylase replacement in experimental Parkinson's disease with trans-vascular gene therapy. NeuroRx, 2: 129-138. **APPENDIX 13.**

14. Chu, C., Zhang, Y., Boado, R.J., and Pardridge, W.M. (2006): Loss of exogenous gene expression in primate brain following intravenous administration is due to plasmid degradation. Pharm. Res., 23: 1586-1590. **APPENDIX 14.**

Brain-specific expression of an exogenous gene after i.v. administration

Ningya Shi, Yun Zhang, Chunni Zhu, Ruben J. Boado, and William M. Pardridge*

Department of Medicine, University of California School of Medicine, Los Angeles, CA 90024

Communicated by M. Frederick Hawthorne, University of California, Los Angeles, CA, August 24, 2001 (received for review June 8, 2001)

The treatment of brain diseases with gene therapy requires the gene to be expressed throughout the central nervous system, and this is possible by using gene targeting technology that delivers the gene across the blood–brain barrier after i.v. administration of a nonviral formulation of the gene. The plasmid DNA is targeted to brain with pegylated immunoliposomes (PILs) using a targeting ligand such as a peptidomimetic mAb, which binds to a transporting receptor on the blood–brain barrier. The present studies adapt the PIL gene targeting technology to the mouse by using the rat 8D3 mAb to the mouse transferrin receptor. Tissue-specific expression in brain and peripheral organs of different exogenous genes (β-galactosidase, luciferase) is examined at 1–3 days after i.v. injection in adult mice of the exogenous gene packaged in the interior of 8D3-PIL. The expression plasmid is driven either by a broadly expressed promoter, simian virus 40, or by a brain-specific promoter taken from the 5′ flanking sequence of the human glial fibrillary acidic protein (GFAP) gene. The transgene is expressed in both brain and peripheral tissues when the simian virus 40 promoter is used, but the expression of the exogenous gene is confined to the brain when the transgene is under the influence of the brain-specific GFAP promoter. Confocal microscopy colocalizes immunoreactive bacterial β-galactosidase with immunoreactive GFAP in brain astrocytes. These studies indicate that tissue-specific gene expression in brain is possible after the i.v. administration of a nonviral vector with the combined use of gene targeting technology and tissue-specific gene promoters.

blood–brain barrier | gene therapy | transferrin receptor | β-galactosidase | liposomes

Brain-specific expression of a therapeutic gene requires the use of (*i*) organ-specific promoter elements and (*ii*) a transcellular targeting system that enables delivery of the transgene across both the blood–brain barrier (BBB) and the brain cell plasma membrane. Prior work has demonstrated the widespread expression of exogenous genes in the brain of rats after the i.v. injection of pegylated immunoliposomes (PILs) that carry the plasmid DNA in the interior of the nanocontainer (1). The PIL/DNA was targeted to brain cells with a peptidomimetic mAb to the rat transferrin receptor (TfR). Owing to the abundance of the TfR on the brain capillary endothelium, which forms the BBB *in vivo*, the mAb targeted the exogenous gene to brain cells *in vivo* in the rat (1). However, the TfR is also abundant in some peripheral tissues, such as liver and spleen, and the exogenous gene, driven by the simian virus 40 (SV40) promoter, also was expressed in liver and spleen after the i.v. injection of the PIL (2).

The present studies test the hypothesis that the expression of an exogenous gene can be restricted to the brain with the use of both the PIL gene targeting technology and a brain-specific promoter. The expression in brain and peripheral organs is measured for either a luciferase or a β-galactosidase exogenous gene. The plasmid DNA encapsulated in the 8D3-PIL is administered i.v., and the exogenous gene is under the influence of either the SV40 promoter or the human glial fibrillary acidic protein (GFAP) promoter (3, 4). A second goal of this work was to develop a gene targeting system specific for the mouse, given the availability of transgenic mouse models of human disease. Prior work in rats used the mouse OX26 mAb to the rat TfR (1, 2), but the OX26 mAb is not active in mice (5). The rat 8D3 mAb to the mouse TfR is an active BBB transport vector in mice (5), and the present studies describe the production of PILs targeted with the 8D3 mAb.

The structure of the PIL gene targeting system is shown in Fig. 1*A*, and this formulation is to be contrasted with conventional cationic lipid/DNA complexes. The PIL has a net negative charge (2) and internalizes the DNA in the interior of the liposome to render the plasmid DNA resistant to the endogenous endonucleases, which are ubiquitous *in vivo* (6). Any exteriorized DNA is removed from the PIL formulation by nuclease treatment and gel filtration chromatography (1, 2). The liposome surface is decorated with 2,000–3,000 strands of 2,000-Da polyethylene glycol, designated PEG^{2000}. The "pegylation" of the liposome prevents absorption of serum proteins to the surface of the structure and minimizes uptake of the liposome by cells lining the reticuloendothelial system (7). The pegylated liposome is directed to tissues *in vivo* by tethering to the tips of 1–2% of the PEG strands a targeting peptidomimetic mAb (Fig. 1*A*). The anti-TfR mAb binds to the BBB TfR to trigger receptor-mediated transcytosis across the BBB *in vivo*, and this process is followed by Tfr-mediated endocytosis of the PIL into brain cells (1, 2).

Experimental Procedures

Materials. Adult male BALB/c mice (25–30 g) were purchased from Harlan Breeders, Indianapolis. dCTP (specific activity: 800 Ci/mmol) was from Perkin–Elmer. *N*-succinimidyl[2,3-^{3}H] propionate (specific activity: 97.0 Ci/mmol) was supplied by Amersham Pharmacia. DNase I, exonuclease III, and the Nick Translation Kit were from GIBCO/BRL. Traut's reagent was purchased from Pierce. Lipids for liposome synthesis were supplied by Avanti Polar Lipids. The LiposoFAST-Basic extruder and polycarbonate filters were from Avestin, Ottawa. 5-Bromo-4-chloro-3-indoyl-β-D-galactoside, rat IgG, and all other chemicals were purchased from Sigma. The pSV-β-galactosidase expression plasmid driven by the SV40 promoter, the pGL3-control luciferase expression plasmid driven by the SV40 promoter, the luciferase reagent, and recombinant luciferase were obtained from Promega. The pGfa-lacZ β-galactosidase expression plasmid was provided by Jose Segovia, Centro de Investigaciòn y de Estudios Avanzados, San Pedro Zacatenco, Mexico (3, 4). In this plasmid, the *lacZ* gene is driven by the human GFAP promoter (nucleotides −2163 to +47). The GFAP ATG at position +15 was mutated to TTG, so translation

Abbreviations: BBB, blood–brain barrier; GFAP, glial fibrillary acidic protein; PIL, pegylated immunoliposome; PEG, polyethylene glycol; TfR, transferrin receptor; HIR, human insulin receptor; SV40, simian virus 40.

*To whom reprint requests should be addressed at: Warren Hall, Room 13-164, University of California, 900 Veteran Avenue, Los Angeles, CA 90024. E-mail: wpardridge@mednet.ucla.edu.

The publication costs of this article were defrayed in part by page charge payment. This article must therefore be hereby marked "*advertisement*" in accordance with 18 U.S.C. §1734 solely to indicate this fact.

 www.pnas.org/cgi/doi/10.1073/pnas.221450098

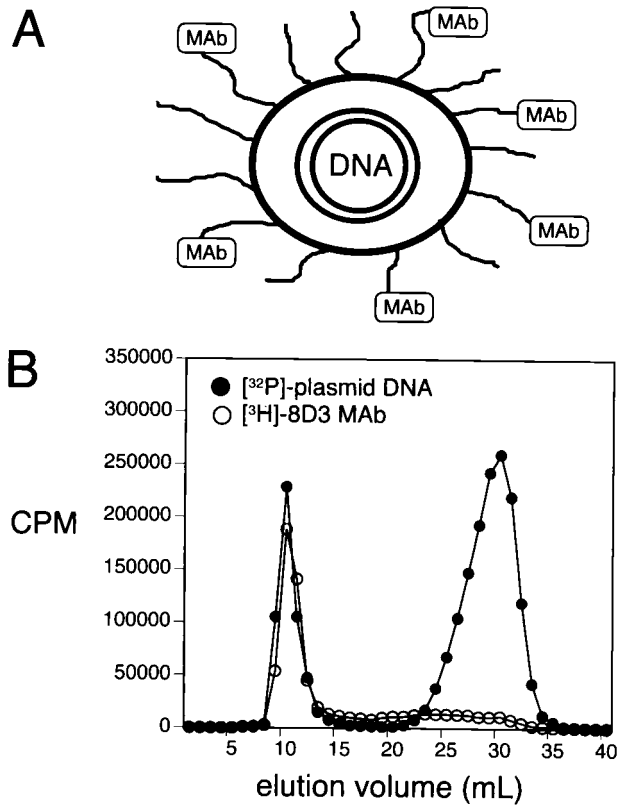

Fig. 1. (*A*) A double-stranded supercoiled plasmid DNA is encapsulated in the interior of 75- to 85-nm liposomes, which are pegylated with PEG^{2000}, and 1–2% of the PEG strands are conjugated with a targeting ligand, such as a mAb (1, 2). (*B*) Elution of 8D3 PILs through a Sepharose CL-4B gel filtration column allowed for separation of the PILs from unconjugated mAb and from exteriorized nuclease-digested DNA. The comigration of the interiorized [^{32}P]-DNA and the [^{3}H]8D3 mAb demonstrated the plasmid DNA and the targeting mAb were incorporated in the same structure.

begins at the *lacZ* ATG initiation codon. The 3′ untranslated region (UTR) following the *lacZ* gene is derived from the mouse protamine gene-1 3′ UTR, and contains an intron and poly(A) sequence (3, 4). The orientation of the GFAP promoter within the plasmid was confirmed by DNA sequencing. The 8D3 hybridoma line, secreting a rat IgG to the mouse Tfr (8), was obtained from Britta Engelhardt, Max Planck Institute, Bad Naoheim, Germany.

Plasmid DNA Preparation and Radiolabeling. β-Galactosidase or luciferase plasmid DNA was purified from *Escherichia coli* with the maxiprep procedure and desalted by using the Qiagen (Chatsworth, CA) Plasmid Maxi Kit and QIAquick PCR purification kit, respectively. The size of the DNA was confirmed by 0.8% agarose gel electrophoresis. DNA was labeled with ^{32}P-dCTP using nick translation. The specific activity of ^{32}P-DNA was 15–20 μCi/μg. The purity measured by trichloroacetic acid precipitability was 99%.

mAb Purification and Radiolabeling. The rat 8D3 anti-mouse TfR mAb was purified with protein G Sepharose affinity chromatography from ascites generated in nude mice. All animal procedures were performed with protocols approved by the University of California Los Angeles Animal Research Committee. The 8D3 hybridoma was grown on a feeder layer of newborn mouse thymocytes and peritoneal cells, as described by Kissel *et al.* (8). The antibody was tritiated with *N*-succinimidyl[2,3-^{3}H] propionate as described (9). The specific activity and trichloroacetic acid precipitability of the ^{3}H-8D3 mAb were 100–150 μCi/mg and 95%, respectively.

PIL Synthesis. PILs were synthesized by using a total of 20 μmmol of lipids, including 18.8 μmmol of 1-palmitoyl-2-oleoyl-sn-glycerol-3-phosphocholine (POPC), 0.4 μmmol of didodecyldimethylammonium bromide (DDAB), 0.6 μmmol of distearoylphosphatidylethanolamine (DSPE-PEG), and 200 nmol of DSPE-PEG-maleimide, as described (1, 2). The supercoiled plasmid DNA (150 μg) and 2 μCi of ^{32}P-plasmid DNA were encapsulated in the pegylated liposomes, and exteriorized DNA was degraded by nuclease digestion, as described (1, 2). The thiolated 8D3 mAb was conjugated to the pegylated liposome overnight at room temperature. The 8D3 PIL/DNA was separated from degraded DNA absorbed to the exterior of the liposome, and from unconjugated mAb, using a 1.6 × 18 cm column of Sepharose CL-4B (Fig. 1*B*). The average number of 8D3 mAbs conjugated on one liposome was 50 and was computed from the measurement of radioactive mAb, as described (10). The DNA encapsulation efficiency was 20%. The control rat IgG PIL/β-galactosidase plasmid DNA was prepared by following the same procedure.

***In Vivo* Administration and Gene Expression Assays.** Male BALB/c mice weighing 25–30 g were anesthetized with ketamine (50 mg/kg) and xylazine (4 mg/kg) i.p. PIL conjugated with either the 8D3 mAb or nonspecific rat IgG, and carrying either the pSV-β-galactosidase plasmid DNA, the pGfa-lacZ plasmid DNA, or the pGL3-control plasmid DNA was injected i.v. in mice via the jugular or femoral vein with a 30-g needle at a dose of 3–5 μg of PIL-encapsulated plasmid DNA per mouse. Mice were killed at 24, 48, and 72 h postinjection. Brain, liver, spleen, kidney, heart, and lung were removed and frozen in OCT embedding medium for β-galactosidase histochemistry, or homogenized in 4 vol of lysis buffer for measurements of organ luciferase activity, as described (1). For histochemistry, frozen sections of 18-μm thickness were fixed in 0.1% glutaraldehyde in 0.1 M NaH_2PO_4 for 5 min and incubated with 0.1% 5-bromo-4-chloro-3-indoyl-β-D-galactoside at pH = 7.0 at 37°C overnight, as described (1, 2). Whole-mount images of the organs were obtained by scanning the section with a UMAX PowerLookIII scanner with transparency adapter, and the image was cropped in Adobe PHOTOSHOP 5.5 on a G4 Power Macintosh computer. The luciferase enzyme activity was measured in organ supernatants with a Luminometer (Biolumat LB 9507, Berthold, Nashua, NH), as described (1). A standard curve was assayed in parallel with recombinant luciferase, and the relative light units were converted to pg of luciferase. The protein concentration in the tissue extract was determined with the BCA protein assay reagent (Pierce), and the luciferase activity in the organ was expressed as pg luciferase/mg protein.

Confocal Microscopy. Mouse brain frozen sections (20 μm) were fixed with 100% acetone at −20°C for 20 min. The sections were incubated in primary antibody for 1 h at room temperature. The primary antibodies were mixed and included a goat anti-human/rodent GFAP 1:20 polyclonal antiserum (Research Diagnostics, Chicago), and a mouse mAb against *E. coli* β-galactosidase, 20 μg/ml (Promega). After a PBS wash, a rhodamine-conjugated donkey anti-goat IgG 1:200 (Research Diagnostics) secondary antibody was added for 30 min at room temperature. The slides were then washed and incubated with fluorescein-conjugated goat anti-mouse IgG (Sigma) for 30 min at room temperature. The sections were mounted on slides with Vector Shield (Vector Laboratories) mounting media, and viewed with a ×10 or ×100 objective and a Zeiss LSM 5 PASCAL confocal microscope with dual argon and heli-

Table 1. Organ luciferase activity

Organ	pg Luciferase/mg protein	
	48 h	72 h
Brain	0.76 ± 0.09	0.50 ± 0.10
Heart	0.015 ± 0.001	0.018 ± 0.004
Liver	3.1 ± 0.5	1.4 ± 0.1
Spleen	1.1 ± 0.1	0.52 ± 0.11
Lung	0.74 ± 0.06	0.34 ± 0.09
Kidney	0.0092 ± 0.0009	0.0082 ± 0.0003

Data are mean ± SE ($n = 5$ mice per time point). Mice were administered a single i.v. injection of 5 μg/mouse of SV40 promoter-pGL3 plasmid DNA encapsulated in 8D3-PIL.

um/neon lasers. The sample was scanned with multitrack mode to avoid leakage of the fluorescein signal into the rhodamine channel. Sections were scanned at intervals of 0.48 μm and reconstructed with Zeiss LSM software. Control experiments used either a mouse IgG (Cappel) or reagent grade goat IgG (Sigma) as primary antibody in lieu of the anti-β-galactosidase or the anti-GFAP antibody, respectively.

Results

The organ luciferase activity at 48 and 72 h after a single i.v. injection of the pGL3 plasmid DNA encapsulated in the 8D3-PIL is shown in Table 1 and indicates the 8D3 mAb targets the gene to TfR-rich organs such as brain, liver, spleen, and lung, with very little gene expression in kidney or heart. The results with the 8D3 TfR mAb in the mouse replicate previous work with the OX26 TfR mAb in the rat (1).

Administration of the pSV-β-galactosidase plasmid encapsulated in the 8D3-PIL resulted in gene expression in both brain and peripheral tissues, such as spleen (Fig. 2*A*). The pGfa-lacZ plasmid also was encapsulated in 8D3-PIL and injected i.v. in mice, and organs were removed 2 days later for β-galactosidase histochemistry (Fig. 2*B*). Whereas the GFAP/β-galactosidase gene was widely expressed throughout the mouse brain, there was no expression of the transgene in mouse spleen, liver, heart, or lung (Fig. 2*B*). Gene targeting of organs *in vivo* was determined by the specificity of the targeting mAb. When the 8D3 rat mAb to the murine TfR was replaced with nonspecific rat IgG (rIgG), and the GFAP/β-galactosidase plasmid was encapsulated in the interior of the rIgG-PIL, there was no gene expression in brain or peripheral tissues (lung, spleen, liver, or heart) (Fig. 2*C*). Owing to high expression of endogenous mammalian β-galactosidase in mouse kidney, this organ serves as a positive control for the histochemical assay (Fig. 2*C*). The β-galactosidase activity in mouse kidney represents endogenous mammalian enzyme, and this activity does not arise from expression of the bacterial β-galactosidase gene in kidney.

The extent to which the exogenous gene is expressed throughout the central nervous system is demonstrated with serial coronal sections through the septo-striatum, the rostral dien-

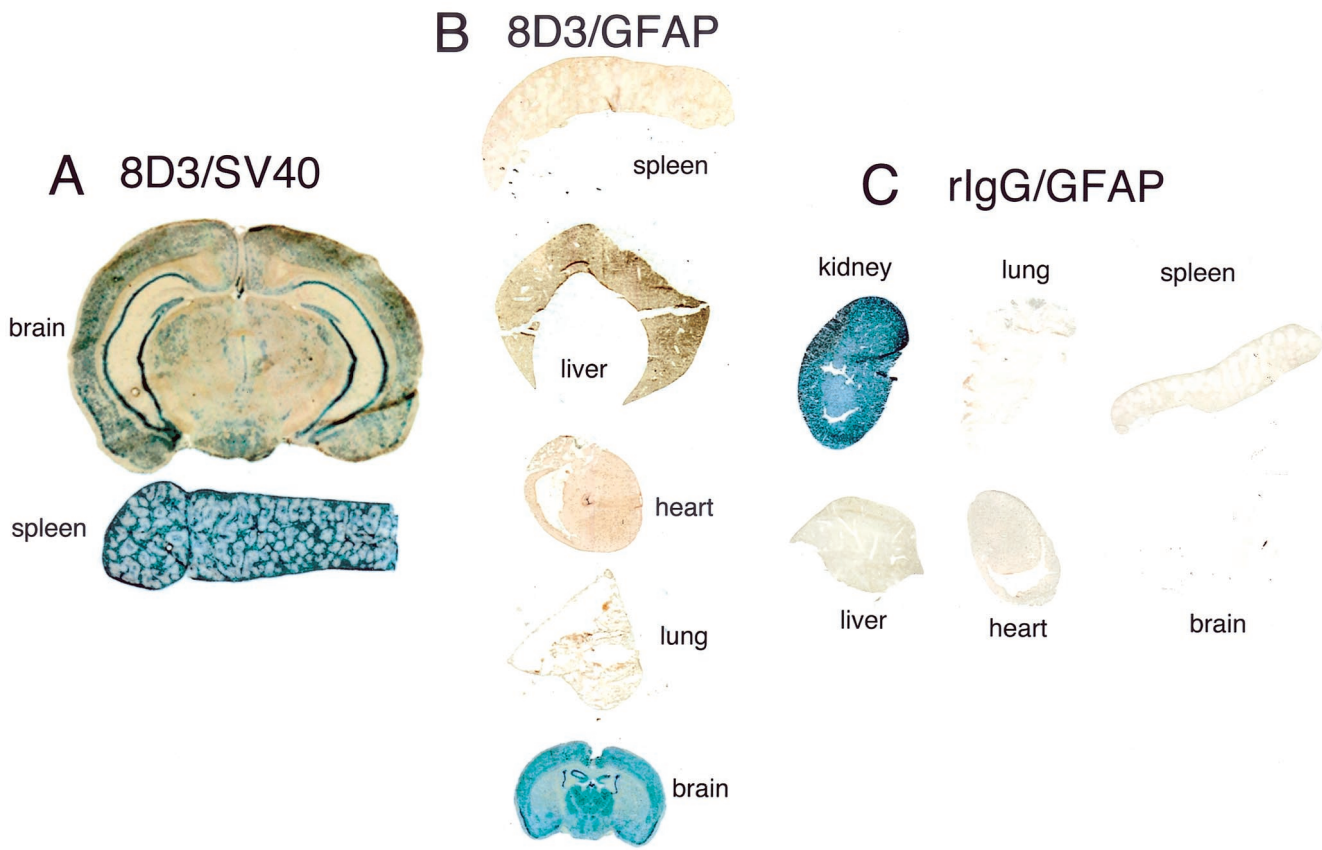

Fig. 2. (*A*) β-Galactosidase histochemistry was performed on organs removed 2 days after an i.v. injection of PILs carrying the pSV-β-galactosidase plasmid, driven by the SV40 promoter, and conjugated with the 8D3 rat mAb. (*B*) 5-Bromo-4-chloro-3-indoyl-β-D-galactoside histochemistry of organs removed from mice 2 days after a single i.v. injection of 8D3 PILs carrying the GFAP/β-galactosidase plasmid. (*C*) β-Galactosidase gene expression in mouse organs removed 48 h after a single i.v. injection of the GFAP/β-galactosidase plasmid incorporated in PILs that were targeted with nonspecific rat IgG (rIgG). All organs were negative except for kidney. The histochemical product in kidney is derived from endogenous mammalian β-galactosidase-like activity in that organ. Kidney removed from noninjected mice yielded similar β-galactosidase reaction product.

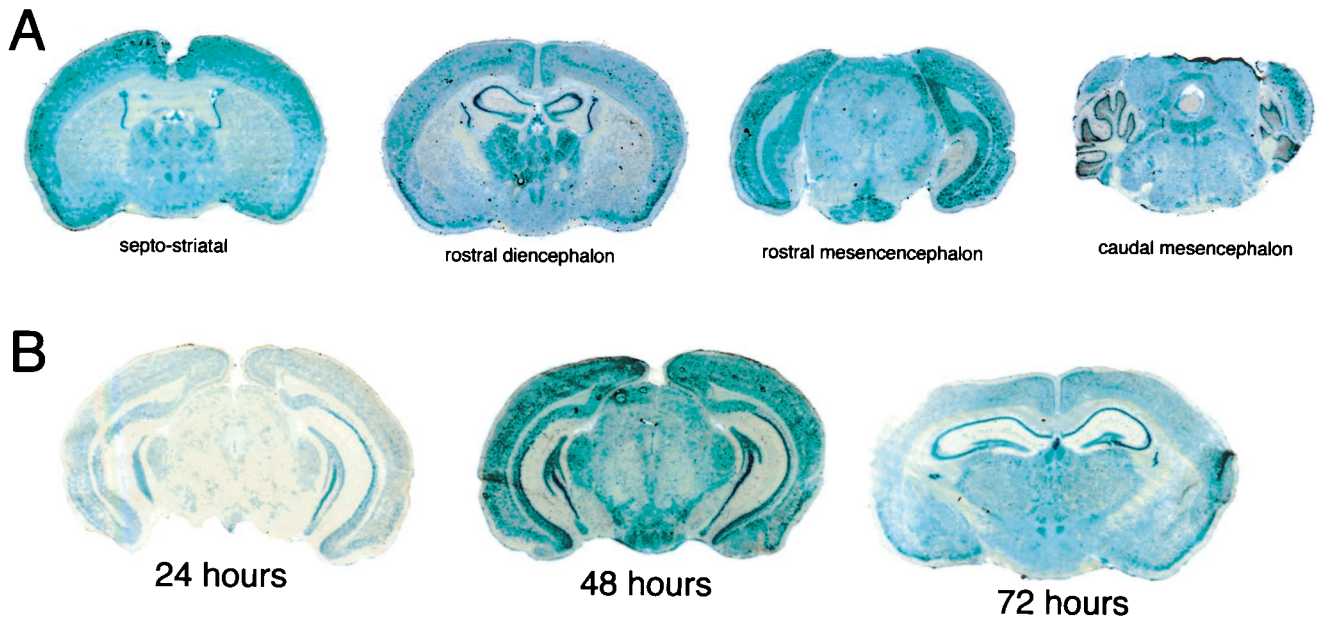

Fig. 3. (*A*) β-Galactosidase histochemistry in mouse brain removed 48 h after a single i.v. injection of the GFAP/β-galactosidase plasmid encapsulated in the interior of 8D3-targeted PILs. Coronal sections at different levels of the brain are shown. (*B*) β-Galactosidase histochemistry is shown for brain removed from mice at 24, 48, and 72 h after a single i.v. injection of the GFAP/β-galactosidase plasmid encapsulated in the interior of 8D3 PILs.

cephalon, the rostral mesencephalon, and the caudal mesencephalon (Fig. 3*A*). Gene expression is detected widely throughout the cortical and subcortical structures at all levels of brain. In the septo-striatum, the GFAP/β-galactosidase gene is expressed in the caudate putamen nucleus and the epithelium of the choroid plexus lining the lateral ventricles and the third ventricle. At the level of the rostral diencephalon, there is gene expression in the parietal cortex, the hippocampus, and the thalamic nuclei (Fig. 3*A*). In the caudal mesencephalon, gene expression is observed throughout the cerebellum and the posterior colliculus anteriorly and various hindbrain nuclear structures posteriorly. The expression in mouse brain of the GFAP/β-galactosidase gene peaks at 48 h after a single i.v. injection as shown in Fig. 3*B*. Temporal studies were performed with a SV40/β-galactosidase plasmid, which showed a reduced gene expression at 24 h compared with the GFAP/β-galactosidase and a level of β-galactosidase gene expression in the brain at 72 h that was comparable to the activity at 48 h in Fig. 2*A*.

Confocal microscopy confirmed the expression of the β-galactosidase transgene in astrocytes (Fig. 4). The expression of immunoreactive β-galactosidase and immunoreactive GFAP in the same brain cell is shown in Fig. 4 *A* and *B*, respectively, and the yellow signal in the superimposed image demonstrates immune labeling of both the cell body and the processes of the astrocyte (Fig. 4*C*). Astrocyte foot processes invest the basement membrane surface of the cerebral microvasculature, and these structures express immunoreactive GFAP, as shown in Fig. 4 *E* and *H*. Immunoreactive bacterial β-galactosidase is also expressed in the astrocyte foot processes investing the microvasculature as shown in Fig. 4 *D* and *G*. The orange/yellow signal in the superimposed image demonstrates colocalization of the GFAP and the bacterial β-galactosidase in the astrocyte processes (Fig. 4 *F* and *I*).

Discussion

These studies are consistent with the following conclusions. First, exogenous genes encoding for either luciferase or β-galactosidase and under the influence of the SV40 promoter are targeted to brain in the mouse using PILs and the rat 8D3 mAb to the mouse TfR. However, the transgene is also targeted to TfR-rich peripheral tissues such as spleen, liver, and lung (Table 1, Fig. 2*A*). Second, the expression of the exogenous gene in peripheral organs can be eliminated when the exogenous gene is under the influence of a brain-specific promoter, such as the 2 kb of the 5′ flanking sequence of the human GFAP gene (Fig. 2*B*). Third, the PIL gene targeting technology enables the widespread expression throughout the central nervous system of an exogenous gene after the noninvasive i.v. administration of a nonviral formulation of the gene (Fig. 3*A*). Fourth, the expression of the exogenous gene in brain persists for at least 3 days after the single i.v. administration (Table 1, Fig. 3*B*). Fifth, the β-galactosidase transgene, under the influence of the GFAP promoter, is widely expressed in both cell bodies and processes of astrocytes, as demonstrated by confocal microscopy (Fig. 4).

The 8D3-PIL delivers the exogenous gene both to brain and TfR-rich peripheral tissues (Table 1). However, when the transgene is under the influence of a brain-specific promoter, there is no gene expression in peripheral tissues (Fig. 2*B*). The absence of measurable expression of the transgene in lung (Fig. 2*B*) contrasts the PIL gene targeting system with conventional cationic lipid/DNA complexes. After the i.v. injection of cationic liposome/DNA complexes, the level of gene expression in the lung is log orders greater than in peripheral tissues such as liver or spleen, and there is no gene expression in brain (11). The absence of significant gene expression in liver (Fig. 2*B*) contrasts the PIL system with the adenovirus gene delivery system, wherein >90% of the exogenous gene is expressed in mouse liver after the i.v. administration of adenoviral vector systems (12).

Transgene expression peaks at 2 days after a single i.v. injection and starts to decline by 3 days, when the gene is driven by a GFAP promoter (Fig. 3*B*). The SV40 promoter gives a greater persistence of the transgene in both mice (Table 1) and rats (2). The level of gene expression does not decline to the 50% level until 6 days after i.v. administration of the SV40/β-galactosidase in rats, as measured by either histochemistry or Southern blotting (2). The persistence of a therapeutic gene may

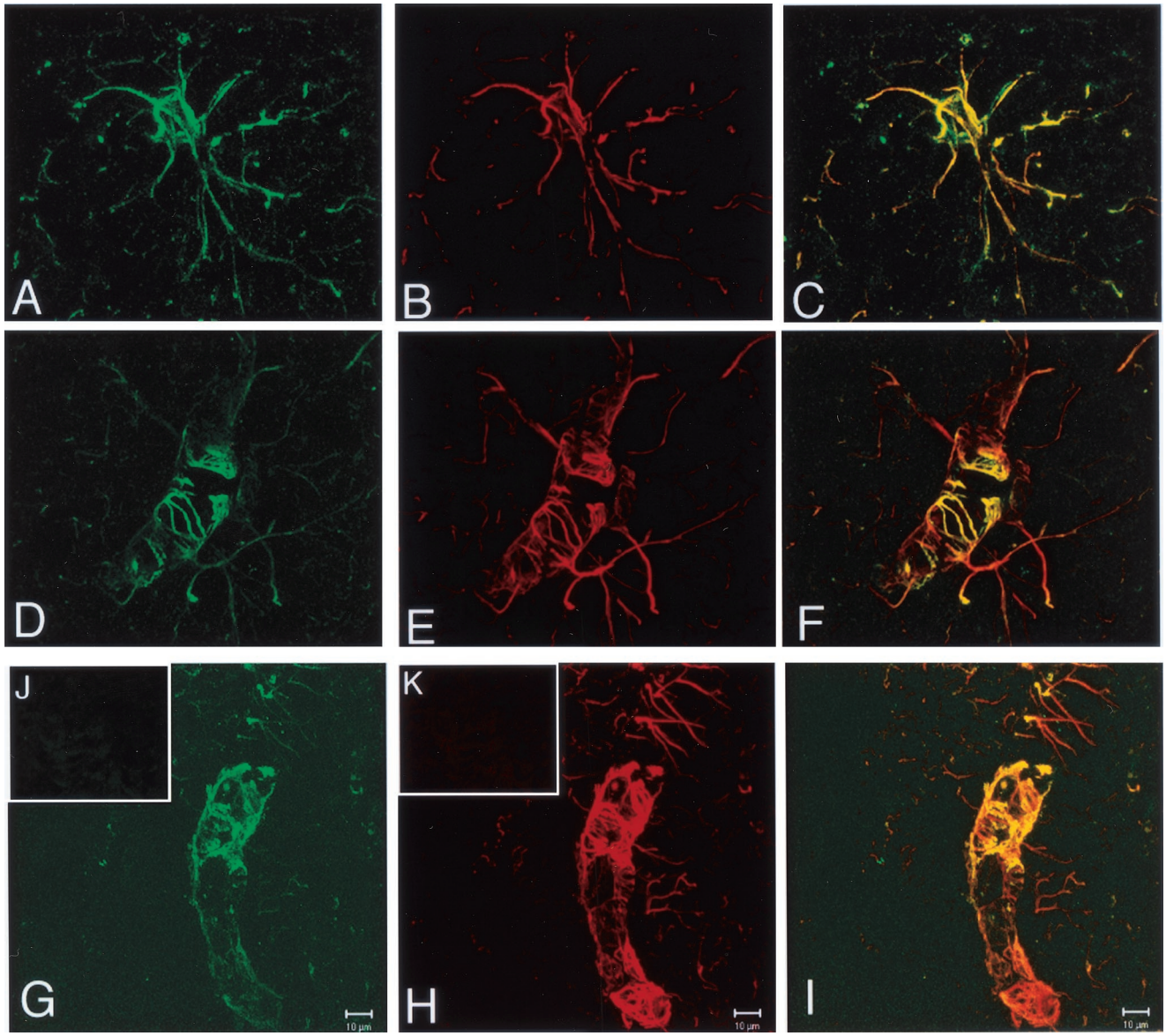

Fig. 4. Confocal microscopy of mouse brain removed 48 h after a single i.v. injection of the GFAP/β-galactosidase plasmid encapsulated in the interior of 8D3 PILs. (*A*, *D*, and *G*) The confocal microscopy of immunoreactive β-galactosidase, stained with a fluorescein-labeled secondary antibody. (*B*, *E*, and *H*) Immunoreactive GFAP, stained with a rhodamine-labeled secondary antibody. (*C*, *F*, and *I*) The respective superimposed images showing colocalization of the β-galactosidase and the GFAP in astrocyte cell bodies (*C*) and astrocyte processes (*F* and *I*). The yellow/orange images in are the result of the superimposition of the green (β-galactosidase) and red (GFAP) images. No staining of brain was obtained with either mouse IgG/fluorescein-conjugated goat anti-mouse IgG (*J*) or goat IgG/rhodamine-conjugated donkey anti-goat IgG (*K*). (Scale bar: 10 μm.)

be increased with the use of expression plasmids that contain gene elements that enable extra-chromosomal replication of the plasmid DNA (13). In addition to persistence of gene expression, a goal of gene targeting is the organ specificity, and even cellular specificity, of transgene expression. This degree of specificity is possible with the use of organ- or cell-specific promoter elements.

The expression in the mouse of the β-galactosidase gene was restricted to the brain, if the β-galactosidase gene was under the influence of the GFAP promoter (Fig. 2*B*). The pattern of β-galactosidase brain histochemistry shown in Fig. 3 for adult mice administered the transgene i.v. is similar to the β-galactosidase histochemistry of the brain of transgenic mice expressing the β-galactosidase gene under the influence of the human GFAP promoter (3). The expression of the β-galactosidase transgene in astrocytes was confirmed in the present studies with confocal microscopy (Fig. 4). Three-dimensional reconstruction of the confocal images of peri-vascular astrocytes reveals the rosette-like structures that invest the basement membrane surface of the brain capillary (Fig. 4 *E* and *H*), and these structures express the bacterial β-galactosidase (Fig. 4 *D* and *G*). These rosette-like structures of the astrocyte foot processes are identical to those in normal rat brain, as described by Kacem *et al.* (14). The β-galactosidase transgene also is expressed in the cell bodies of astrocytes as shown in Fig. 4 *A–C*.

In summary, brain-specific expression of an exogenous gene is possible with the combined use of a brain-specific promoter and a gene targeting system using PILs. This gene delivery system offers the same advantages of viral delivery systems, such as (*i*) interiorization of the exogenous gene in a nanocontainer, and protection from ubiquitous endonucleases *in vivo*, and (*ii*) surface proteins that trigger uptake of the gene by target cells.

However, humans have pre-existing immunity to either adenovirus or herpes simplex virus, and the single injection of either virus into either animal or human brain results in an inflammatory reaction in brain that can lead to demyelination (15, 16). In contrast, the immunogenicity of the PIL is restricted to the targeting mAb, and the antibody immunogenicity can be eliminated with the use of genetically engineered "humanized" mAbs. A mAb to the human insulin receptor (HIR) is an active BBB delivery system in Old World primates and humans and delivers 4% of the injected dose to the primate brain (17). This murine HIR mAb has been genetically engineered for use in humans (18). The reactivity of the genetically engineered form of the anti-HIR mAb is identical to that of the original murine HIR mAb, both with respect to binding to the HIR and *in vivo* targeting to the primate brain (18). The combined use of genetically engineered mAbs that are nonimmunogenic, and the PIL gene targeting system, may enable the widespread expression of a therapeutic gene throughout the brain in humans after i.v. administration. Brain specificity of gene expression can be controlled with the use of specific promoter and enhancer elements taken from brain-specific genes.

The pGfa-lacZ plasmid was provided by Dr. Jose Segovia, and the 8D3 rat hybridoma line was provided by Dr. Britta Engelhardt. Daniel Jeong skillfully prepared the manuscript. This work was supported by a grant from the University of California, Davis/Medical Investigation of Neurodevelopmental Disorders Institute Research Program, and the U.S. Department of Defense. The communicating member is a member of the Scientific Advisory Board of Lexrite Labs.

1. Shi, N. & Pardridge, W. M. (2000) *Proc. Natl. Acad. Sci. USA* **97,** 7567–7572. (First Published June 6, 2000; 10.1073/pnas.130187497)
2. Shi, N., Boado, R. J. & Pardridge, W. M. (2001) *Pharm. Res.* **18,** 1091–1095.
3. Brenner, M., Kisseberth, W. C., Su, Y., Besnard, F. & Messing, A. (1994) *J. Neurosci.* **14,** 1030–1037.
4. Segovia, J., Vergara P. & Brenner, M. (1998) *Neurosci. Lett.* **242,** 172–176.
5. Lee, H. J., Engelhardt, B., Lesley, J., Bickel, U. & Pardridge, W. M. (2000) *J. Pharmacol. Exp. Ther.* **292,** 1048–1052.
6. Barry, M. E., Pinto-Gonzalez, D., Orson, F. M., McKenzie, G. J., Petry, G. R. & Barry M. A. (1999) *Hum. Gene Ther.* **10,** 2461–2480.
7. Papahadjopoulos, D., Allen, T. M., Gabizon, A., Mayhew, E., Matthay, K., Huang, S. K., Lee, K. D., Woodle, M. C., Lasic, D. D., Redemann, C., *et al.* (1991) *Proc. Natl. Acad. Sci. USA* **88,** 11460–11464.
8. Kissel, K., Hamm, S., Schulz, M., Vecchi, A., Garlanda, C. & Engelhardt, B. (1998) *Histochem. Cell Biol.* **110,** 63–72.
9. Pardridge, W. M., Buckiak, J. L. & Yoshikawa, T. (1992) *J. Pharmacol. Exp. Ther.* **261,** 1175–1180.
10. Huwyler, J., Wu, D. & Pardridge, W. M. (1996) *Proc. Natl. Acad. Sci. USA* **93,** 14164–14169.
11. Osaka, G., Carey, K., Cuthbertson, A., Godowski, P., Patapoff, T., Ryan, A., Gadek T. & Mordenti, J. (1996) *J. Pharmacol. Sci.* **85,** 612–618.
12. Zinn, K. R., Douglas, J. T., Smyth, C. A., Liu, H. G., Wu, Q., Krasnykh, V. N., Mountz, J. D., Curiel, D. T. & Mountz, J. M. (1998) *Gene Ther.* **5,** 798–808.
13. Pardridge, W. M. (2001) *Brain Drug Targeting* (Cambridge Univ. Press, Cambridge, U.K).
14. Kacem, K., Lacombe, P., Seylaz, J. & Bonvento, G. (1998) *GLIA* **23,** 1–10.
15. Lawrence, M. S., Foellmer, H. G., Elsworth, J. D., Kim, J. H., Leranth, C., Kozlowski, D. A., Bothwell, A. L., Davidson, B. L., Bohn, M. C. & Redmond, D. E., Jr. (1999) *Gene Ther.* **6,** 1368–1379.
16. Dewey, R. A., Morrissey, G., Cowsill, C. M., Stone, D., Bolognani, F., Dodd, N. J., Southgate, T. D., Klatzmann, D., Lassmann, H., Castro, M. G. & Lowenstein, P. R. (1999) *Nat. Med.* **5,** 1256–1263.
17. Pardridge, W. M., Kang, Y.-S., Buciak, J. L. & Yang, J. (1995) *Pharm. Res.* **12,** 807–816.
18. Coloma, M. J., Lee, H. J., Kurihara, A., Landaw, E. M., Boado, R. J., Morrison, S. L. & Pardridge, W. M. (2000) *Pharm. Res.* **17,** 266–274.

DRUG AND GENE TARGETING TO THE BRAIN WITH MOLECULAR TROJAN HORSES

William M. Pardridge

Getting drugs and genes into the brain is a tall order. This is because the presence of the blood–brain barrier prevents many molecules from crossing into the brain. Overcoming this problem will have a profound effect on the treatment of many neurological disorders, allowing larger water-soluble molecules to pass into the brain. Transport vectors, such as endogenous peptides, modified proteins or peptidomimetic monoclonal antibodies, are one way of tricking the brain into allowing these molecules to pass. This article will review such molecular Trojan Horses, and the progress that has been made in the delivery of drugs and genes to the brain.

PEPTIDOMIMETIC
A molecule that binds to a blood–brain barrier (BBB) receptor and initiates receptor-mediated transcytosis (RMT) across the BBB. A peptidomimetic monoclonal antibody binds to an extracellular projecting epitope on the receptor to trigger RMT in a manner similar to the endogenous ligand for the receptor.

ENDOTHELIUM
Consists of cells of mesenchymal origin that comprise the innermost cellular lining of the capillary.

Department of Medicine, UCLA School of Medicine, Los Angeles, California 90024, USA.
e-mail: wpardridge@mednet.ucla.edu
DOI: 10.1038/nrd725

After ten years of fighting the Trojans, the Greeks played the most famous trick in military history — building a wooden horse. Once taken within the walls of Troy, Greek soldiers hidden inside the Trojan Horse slipped out in the middle of the night and opened the city gates. The Greek army thus entered and destroyed the city. As this strategy worked for the Greeks, so it can work for transporting molecules across the blood–brain barrier (BBB). Molecular Trojan Horses are brain transport vectors that include endogenous peptides, modified proteins and PEPTIDOMIMETIC monoclonal antibodies. These vectors target specific receptor/transport systems of the brain capillary ENDOTHELIUM and undergo receptor-mediated TRANSCYTOSIS through the BBB. This technology has allowed the brain targeting of recombinant proteins for neuroprotection, antisense radiopharmaceuticals for *in vivo* imaging of brain gene expression, and non-viral genes.

The blood–brain barrier

Getting most molecules into the brain is certainly a Herculean task (BOX 1). The BBB prevents the brain uptake of >98% of all potential neurotherapeutics[1]. It is found in the brain of all vertebrates[2], and is laid down in the first trimester of human fetal life[3]. The anatomical basis of the BBB arises from special cellular features of brain capillary endothelial cells, which include tight junctions and minimal PINOCYTOSIS[4].

The surface area of the human BBB is ~20 m^2, or the size of a small room, and the total length of capillaries in the human brain is ~400 miles[1]. The intracellular space of the brain capillary endothelium is ~0.8 $\mu l\ g^{-1}$, or about 1 ml for a 1,200-g human brain[1]. The distance between capillaries in the brain is ~40 μm (BOX 1): a small molecule diffuses a distance of 40 μm in one second, and the plasma transit time through the brain MICROVASCULATURE is also about one second[1]. The angioarchitecture of the brain has evolved to allow instantaneous drug or solute equilibration throughout the entire brain interstitial fluid, once the drug or solute traverses the limiting membrane between blood and brain — the BBB.

The brain microvasculature comprises four types of cell[5]: endothelial cells, PERICYTES, astrocyte foot processes and an occasional nerve ending (FIG. 1). The endothelial cells in the brain share the capillary basement membrane with pericytes — cells that have an important role in immune surveillance at the brain microvasculature[6]. Nearly 99% of the surface on the brain side of the capillary basement membrane is surrounded by astrocyte foot processes (FIG. 1). The distance between the astrocyte foot process and the capillary

Box 1 | **BBB, brain microvasculature and capillary endothelium**

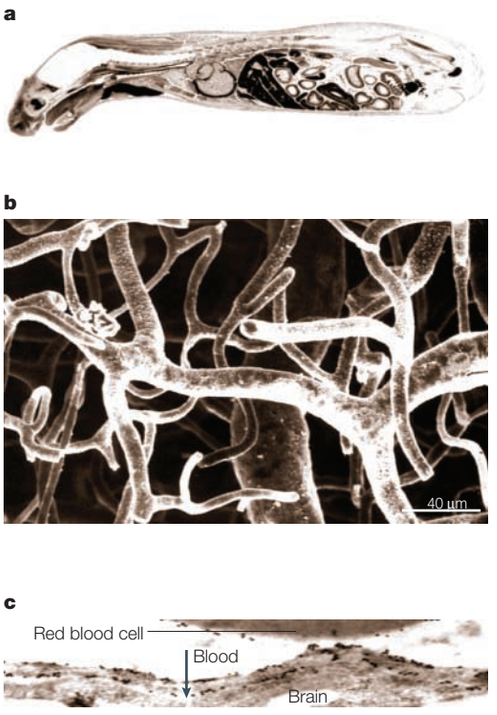

The blood–brain barrier (BBB) problem is illustrated in panel **a**, which is a whole-body film autoradiogram of a mouse that was sacrificed 30 minutes after the intravenous injection of radiolabelled histamine, a small molecule of ~100-Da molecular mass[55]. The study shows that a small molecule, such as histamine, readily traverses the porous capillary beds of all organs in the body except for the brain or spinal cord. Even though histamine is a relatively lipid-soluble small molecule, there is no transport into the brain owing to the presence of the BBB. In panel **b**, the brain microvasculature or capillary bed is visualized by a scanning electron micrograph of a vascular cast of the human cerebellar cortex[56]. The capillaries are separated by a distance of ~40 μm. The BBB consists of two membranes in series, the luminal and abluminal membranes, which are separated by ~300 nm of endothelial cytoplasm. Panel **c** illustrates the distribution of the GLUT1 glucose transporter on the luminal and abluminal membranes of the capillary endothelium in human brain, which can be determined using immunogold electron microscopy[57]. The GLUT1 glucose transporter is also expressed on the plasma membrane of human red blood cells. In addition to transporters, the cells of the brain microvasculature also express enzymes[58], and these form a second line of defence, or an 'enzymatic BBB'. (Part **a** reprinted with permission from REF. 55 © (1986) American College of Physicians–American Society of Internal Medicine; part **b**, reprinted from REF. 56 © (1983), with permission from Elsevier Science.)

basement membrane is only 20 nm (REF. 7). So, the topological relationships between the capillary endothelial cells, microvascular pericytes and astrocyte foot process are as intimate as any non-junctional cell–cell interactions in biology. There is also direct innervation of the capillary bed by nerve endings of either intracerebral or extracerebral origin (FIG. 1). Several cells interact at the brain microvasculature, but the site of permeability restriction is the endothelial cell.

Brain capillary endothelial cells are cemented together by epithelial-like high-resistance tight junctions. The formation of the tight junctions is associated with a 100-fold reduction of pinocytosis across the endothelium. The tight junctions segregate the endothelial plasma membrane into two domains: the luminal membrane on the blood side, and the abluminal membrane on the brain side of the BBB.

The usual pathways of solute-free diffusion across capillary endothelial barriers are the paracellular pathway, through open endothelial junctions, and the transcellular pathway, which involves either endothelial pinocytosis for large molecules or direct transfer across the endothelial cell plasma membrane for small molecules. However, there is minimal pinocytosis and no paracellular pathway at the brain microvasculature. Therefore, molecules circulating in the blood gain access to the brain interstitial fluid by transport through endothelial cells, and this transport may occur by one of two processes: lipid-mediated free diffusion or catalysed transport.

The lipid-mediated free diffusion of a drug through the BBB requires that it has both lipid solubility and a molecular mass under a threshold of 400–500 Da (REF. 8). All of the small-molecule neurotherapeutics that are used in clinical practice at present have both of these characteristics. Lipid-mediated free diffusion through the BBB is reduced if the drug is either water soluble or has a molecular mass above the 400–500-Da threshold. Most of the drugs that are selected as drug candidates by receptor-based high-throughput screening programmes lack these dual characteristics, and will not undergo transport across the BBB without the intervention of brain drug-targeting technology.

TRANSCYTOSIS
Transport across the endothelial barrier by movement through the endothelial cytoplasm (the transcellular pathway), in contrast to transport across the endothelial barrier by movement through the inter-endothelial junctional spaces (the paracellular pathway).

PINOCYTOSIS
Transcytosis across the endothelial cell through endosomal vesicles and/or a tubulovesicular network within the endothelial cell.

MICROVASCULATURE
The capillary network that perfuses the brain and delivers to the brain circulating nutrients and oxygen.

PERICYTE
A multifunctional cell that shares the basement membrane of the microvasculature with the endothelium, and sits on the brain side of the capillary.

Physiological transport across the BBB

Small or large water-soluble molecules can cross the BBB by means of catalysed transport by accessing specific transport systems that are located on the luminal and/or abluminal membranes of the brain capillary endothelium[1]. Accessing a transport system on the luminal membrane allows blood-borne molecules to enter the intra-endothelial compartment. The molecule must then traverse the abluminal membrane of the capillary endothelium to gain access to the brain interstitium. The three broad classes of BBB catalysed-transport systems are carrier-mediated transport (CMT), active-efflux transport (AET) and receptor-mediated transcytosis (RMT) (BOX 2).

Transporting drugs across the BBB

Knowledge of the cellular and molecular biology of the BBB transport systems provides the basis for brain drug-targeting technology. This knowledge leads to new strategies for the reformulation of a drug, so that BBB transport is increased to such a degree that the drug

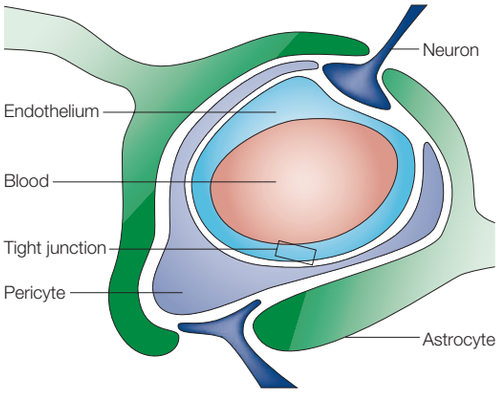

Figure 1 | **Four-cell model of the brain microvasculature.** The capillary endothelium shares a basement membrane with pericytes, and >99% of the brain surface of the capillary basement membrane is surrounded by astrocyte foot processes. There is occasional neuronal innervation of the capillary. The permeability properties of the blood–brain barrier are controlled by the endothelial cells, which express high-resistance tight junctions[4].

enters the brain in pharmacologically significant amounts. For example, a monoamine drug might be converted to the corresponding amino acid, which would then access the brain by CMT through the BBB LAT1 large neutral amino-acid transporter. By contrast, a drug that is a substrate for a BBB AET system might gain access to the brain by the administration of a 'co-drug' that inhibits the targeted AET system[1]. Neither the CMT system nor the AET system is a portal of entry to the brain for large-molecule drugs. However, large-molecule drugs, such as recombinant proteins, antisense drugs, monoclonal antibodies or gene medicines, can be targeted to the brain using RMT systems.

RMT systems can either be selectively localized to the luminal membrane or the abluminal membrane of the capillary endothelium, or be expressed on both membranes. An RMT system that is exclusively expressed on the luminal membrane allows uptake from the blood into only the intracellular compartment of the brain capillary endothelial cell. The model receptor for this pathway is the scavenger receptor, which mediates the uptake of acetylated low-density lipoprotein[1]. An RMT system that is selectively localized to the abluminal membrane mediates asymmetric transcytosis across the BBB in the brain-to-blood direction only. The model receptor for this pathway is the immunoglobulin Fc receptor (FcR). Because of the presence of the FcR on the brain side of the BBB, immunoglobulin G (IgG) molecules are actively transported from brain to blood[9], and there is no transport of IgG in the blood-to-brain direction[5]. RMT systems that are located on both the luminal and abluminal membranes of the BBB, such as the transferrin receptor (TFR)[1], mediate the transport of their substrates (in this case, transferrin; TF) in either the blood-to-brain[10] or brain-to-blood[11] directions.

Chimeric peptide technology

The observation that BBB RMT systems mediate the brain uptake of circulating endogenous peptides or proteins, such as insulin or TF, provided the basis for an approach to brain drug targeting called chimeric peptide technology[1]. A chimeric peptide is formed when a drug that is not normally transported across the BBB is conjugated to a transport vector that does undergo transport across the BBB, by means of either RMT for endogenous ligands, or absorptive-mediated transcytosis for cationic proteins or lectins. The transport vector that uses an RMT system at the BBB could be an endogenous peptide, such as insulin or TF, or a receptor-specific peptidomimetic monoclonal antibody (MAb). Peptidomimetic MAbs are endocytosing antibodies that bind to EXOFACIAL epitopes on the receptor that are distinct from the binding site of the endogenous ligand. The MAb therefore crosses the BBB through the RMT system without interfering with transport of the endogenous ligand[10]. Because transport is mediated by the vector half of the chimeric peptide, this approach allows drugs to be transported across the BBB without being recognized by endothelial receptors.

Drugs can be conjugated to transport vectors using several approaches, including avidin–biotin technology. With this method, a genetically engineered fusion protein of the transport vector and either avidin or streptavidin is prepared in parallel with mono-biotinylation of the neurotherapeutic. Because of the extremely high binding affinity of avidin or streptavidin for biotin, ($K_d = 10^{-15}$ M; dissociation half-life, $t_{1/2} = 89$ days)[12], there is instantaneous capture of the biotinylated therapeutic by the vector–avidin or vector–streptavidin fusion protein. This approach lends itself to a 'two-vial' format of drug administration[1]. The vector–avidin fusion protein is prepared in one vial, and the mono-biotinylated drug is prepared in a second vial. Just before intravenous or subcutaneous administration, the two vials are mixed, which is followed by the instantaneous formation of a drug–vector complex. Alternatively, protein-based neurotherapeutics can be delivered to the brain after the production of a vector–drug fusion gene and fusion protein[1]. In either case, the chimeric peptide can be manufactured in large scale using existing methods for the production of biological pharmaceuticals. In the design of a chimeric peptide, the overriding principle is to retain the bifunctionality of the molecule, so that the chimeric peptide binds both the BBB RMT system and the target receptor in the brain. With chimeric peptide technology, virtually any large-molecule drug can be targeted to the brain.

RMT strategies

The availability of drug and gene brain-targeting technology that uses BBB RMT systems allows a nearly unlimited expansion of drug development programmes. Drugs and genes that were previously undeveloped as brain pharmaceuticals because of the BBB problem can now enter central nervous system (CNS) drug development. Some examples are reviewed here. Reformulation enables the delivery of these proteins to the brain after intravenous administration, allowing NEUROTROPHINS to be developed as drugs for stroke or neurodegenerative

EXOFACIAL
Part of a plasma-membrane receptor that projects outwards into the extracellular space.

NEUROTROPHIN
A protein produced within the brain that modulates neuronal function and structure.

Box 2 | **Three classes of BBB transport systems**

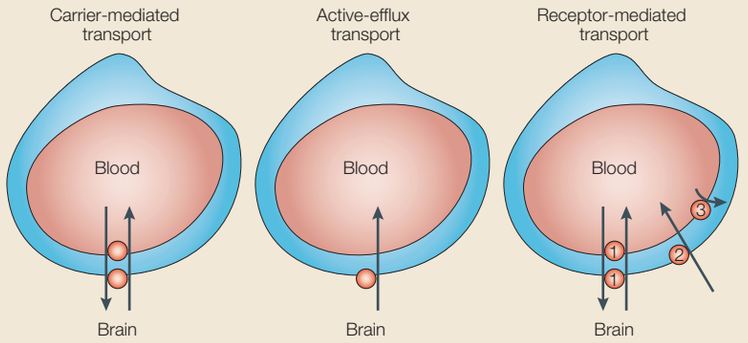

Carrier-mediated transport (CMT). CMT systems catalyse the bidirectional movement between blood and brain of small-molecule polar nutrients, such as glucose, amino acids, monocarboxylic acids, choline, purine nucleobases and nucleosides, thyroid hormone and water-soluble vitamins. All of these molecules access different CMT systems. CMT occurs through specialized transporter proteins that are stereospecific and mediate solute transport in the order of milliseconds. CMT systems are expressed on both the luminal and abluminal membranes of the capillary endothelium, so that transport in either the blood-to-brain or brain-to-blood direction can be mediated (panel **a**). Examples include the GLUT1 glucose transporters, MCT1 lactate transporters, LAT1 large neutral amino-acid transporters and CNT2 adenosine transporters.

Active-efflux transport (AET). AET systems mediate the unidirectional efflux from brain to blood of low-molecular-mass metabolic by-products and XENOBIOTICS. P-glycoprotein and organic anion-transporting polypeptide type 2 (OATP2) are examples of AET systems at the brain microvasculature[59,60]. The AET protein can be asymmetrically localized to the abluminal membrane of the endothelial cell, as shown in panel **b**, and can work in concert with equilibrative transport systems localized at the luminal endothelial membrane.

Receptor-mediated transcytosis (RMT). RMT systems comprise peptide-specific receptors, such as the insulin receptor, the transferrin receptor (TFR) or the leptin receptor, and these mediate the brain uptake of circulating endogenous peptides and proteins, such as insulin or transferrin[61]. The TFR, which is depicted as system 1 in panel **c**, is a bidirectional system that transports transferrin in either the blood-to-brain or brain-to-blood direction[11]. The blood–brain barrier Fc receptor, which is depicted as system 2 in panel **c**, selectively transports immunoglobulin G molecules in the brain-to-blood direction only[9]. The type I scavenger receptor, which is depicted as system 3 in panel **c**, can only mediate the uptake of circulating ligand, such as acetylated low-density lipoprotein, into the brain capillary endothelial compartment, without transcytosis or release into brain[1].

CNT2, sodium-coupled nucleoside transporter; MCT1, monocarboxylic-acid transporter.

disease. Peptide radiopharmaceuticals that cross the BBB have the potential to increase greatly the scope of neuroimaging modalities. These drugs can be delivered to the brain for the early diagnosis of brain disorders, including brain cancer and Alzheimer's disease (AD). Gene expression in the brain can be imaged non-invasively with sequence-specific antisense radiopharmaceuticals that have been reformulated to enable transport through the BBB. Finally, many intractable disorders of the brain might benefit from gene therapy. However, the only way that a gene can be widely dispersed to the human brain is by transport across the 400 miles of capillaries. This can be achieved with brain gene-targeting technology that uses BBB RMT systems to deliver non-viral gene medicines to all parts of the brain after intravenous administration.

CEREBRAL INFARCTION
Loss of brain tissue subsequent to the transient or permanent loss of circulation and/or oxygen delivery to that region of the brain; also known as a stroke.

XENOBIOTIC
A drug or naturally occuring alkaloid that has pharmacological properties.

Delivering neuroprotective drugs

Stroke is the third leading cause of death worldwide. There is no neuroprotective available for the acute treatment of stroke at present, and the cost for stroke rehabilitation in the United States alone is US$40 billion per year (see link to the American Heart Association). Small-molecule neuroprotectives have failed in clinical trials, because these drugs are either too toxic or do not cross the BBB. A new approach to neuroprotection in stroke is the development of recombinant neurotrophins that are engineered to cross the BBB.

Although the BBB is disrupted in experimental stroke[13,14], breakdown is delayed for 4–6 hours after the stroke, and by this time, the chances of permanent neuroprotection are minimal[15]. In the few hours after CEREBRAL INFARCTION, when neuroprotection is still possible, the BBB is intact, and circulating neurotrophins do not cross the BBB without the intervention of drug-targeting technology[16–18].

More than 30 naturally occurring neurotrophins are normally produced in the brain[19], and many are neuroprotective in stroke or brain injury when injected directly into the brain — not a practical or useful human therapeutic modality (BOX 3). However, neurotrophins are ineffective after intravenous administration because they do not cross the BBB *in vivo*. Present-day neurotrophin drug development programmes are focused only on the development of neurotrophin peptidomimetic small molecules. However, neurotrophin small-molecule mimetics are generally antagonists, not agonists[19]. These mimetics are either water-soluble or have molecular masses >500 Da, and either characteristic will preclude transport across the BBB in pharmacologically significant amounts[1]. Therefore, this type of drug probably needs to be reformulated to enable transport across the BBB.

The pharmacological activity of a neurotrophin chimeric peptide has been investigated using brain-derived neurotrophic factor (BDNF). The structure of the BDNF chimeric peptide is shown in FIG. 2. It is a bifunctional molecule that binds the neurotrophic tyrosine-kinase receptor (TRKB) on neurons to mediate neuroprotection, and the TFR at the BBB to mediate transport from blood to brain. BDNF is conjugated to an anti-TFR MAb using avidin–biotin technology (FIG. 2a). The BDNF chimeric peptide is neuroprotective in global ischaemia[16], and in both permanent[17] or reversible[18] regional brain ischaemia. The delayed intravenous administration of low doses (5–50 μg per rat) of the BDNF chimeric peptide results in a reduction of stroke volume by up to 70% in regional brain ischaemia[17,18], and a complete restoration of the pyramidal neuron density in the CA1 sector of a hippocampus subjected to transient global ischaemia[16].

This is a promising therapeutic avenue for stroke, providing that action can be taken within three hours after the event, when neuroprotection is still possible.

Delivering neurodiagnostic agents

Most present-day diagnostic-imaging modalities use small-molecule radiopharmaceuticals, which bind to

Box 3 | **Craniotomy-based drug delivery to the brain**

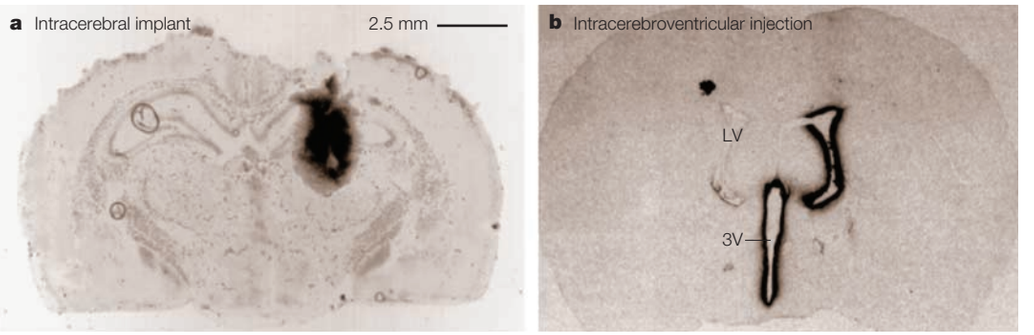

It is not practical to administer neurotrophins to humans by either intracerebroventricular (ICV) infusion or intracerebral injection. These invasive procedures allow the distribution of drugs to only the EPENDYMAL SURFACE **in the case of ICV infusion, or the local depot site where the treatment volume is <1 mm^3 in the case of intra-cerebral injection[1]. Panel a shows a film autoradiogram of a rat brain after the implantation of a polymeric disc embedded with 125-iodine ([^{125}I])-nerve growth factor (NGF)[62]. The diameter of the disc is 2 mm and the magnification bar is 2.5 mm, indicating that there has been minimal diffusion of the neurotrophin from the depot site. The picture in panel b is a film autoradiogram of a rat brain 24 hours after the ICV injection of [^{125}I]-brain-derived neurotrophic factor (BDNF)[63], which shows that there is minimal entry of the neurotrophin into the brain from the ependymal surface. 3V, third ventricle; LV, lateral ventricle. (Part a reprinted from** REF. 62 **© (1995), with permission from Elsevier Science; part b reprinted with permission from** REF. 63 **© (1994) Academic Press.)**

one of several monoaminergic or aminoacidergic neurotransmission systems. However, there are hundreds of peptidergic neuromodulation systems in the brain[5]. Peptide radiopharmaceuticals could prove to be neuroimaging agents, should these molecules be made transportable across the BBB *in vivo*.

Brain cancer. The epidermal growth factor receptor (EGFR) is overexpressed in brain cancer[22,23], so EGF peptide radiopharmaceuticals are potential imaging agents for the early diagnosis of brain cancer. However, EGF does not cross the BBB[24]. Therefore, this peptide radiopharmaceutical was reformulated to enable transport across the BBB for imaging experimental human brain cancer[25]. The structure of the EGF chimeric peptide is shown in FIG. 2b; it is a bifunctional molecule that binds to both the tumour cell EGFR, enabling imaging of the tumour, and to the BBB TFR, allowing transport from the blood into the tumour. The BBB in the brain tumour is called the brain–tumour barrier (BTB). Although the BTB is leaky in the core of the tumour in advanced stages, it is intact in the early stages of brain cancer, when diagnosis is desired. Even in advanced brain cancer, the BTB is intact to large-molecule drugs, such as EGF peptide radiopharmaceuticals[24]. Without brain drug-targeting technology, EGF is not transportable across either the BBB in normal brain or the BTB in a brain tumour. The EGF chimeric peptide that is shown in FIG. 2b has an extended 200-atom poly(ethyleneglycol) (PEG) linker between the EGF and the transport vector. If a shorter 14-atom linker is used, then the EGF is bound too tightly to the transport vector, and the EGF chimeric peptide no longer binds to the EGFR[26]. Replacing the short linker with a 200-atom extended PEG linker eliminates the steric hindrance of EGF binding to the EGFR. The PEG linker is attached to one of the internal lysine residues of the recombinant EGF. A diethylenetriaminepentacetic acid (DTPA) moiety is attached to the other lysine residue on human EGF to allow radiolabelling by chelation of 111-indium (FIG. 2b).

Experimental tumours that overexpress the human EGFR have been developed in the brains of nude rats[25]. When an EGF chimeric peptide radiopharmaceutical was administered, there was an uptake by small or large brain tumours. The ratio of radioactivity sequestered at the brain tumour relative to normal brain was 20:1 (REF. 25). The EGF chimeric peptide radiopharmaceutical was sequestered in the brain tumour due to binding to the tumour EGFR, but effluxed back to the blood from normal brain due to the absence of the EGFR in non-tumour brain regions. The radiopharmaceutical alone was not taken up. These studies show that it is possible to image the regional distribution of specific receptor systems in the brain with peptide radiopharmaceuticals that are enabled to cross the BBB using brain drug-targeting systems.

Alzheimer's disease. AD is caused by the long-term progressive deposition of AMYLOID within the brain; the principal component of this amyloid is a 43-amino-acid peptide designated amyloid-β^{1-43} ($A\beta^{1-43}$). Amyloid deposits start to develop years before the onset of dementia[27], so there is an urgent need for the development of a diagnostic test for people at risk for AD, so that early treatment can be initiated. It has been estimated that a delay in the onset of symptoms of AD by just five years will reduce US health-care costs by US$50 billion per year (see link to the Alliance for Aging Research). There is no blood test that is specific for the diagnosis of AD, so extensive efforts have been made to develop an AD diagnostic brain scan that could semi-quantitate the Aβ burden in the brains of people at risk of developing AD. Three types of amyloid imaging agent are now being developed: Congo red derivatives, anti-Aβ monoclonal

EPENDYMAL SURFACE
The surface of the brain that is lined by the ependymal epithelium, which is in contact with the cerebrospinal fluid.

AMYLOID
A silk-like protein aggregate that consists of a peptide that has a high degree of β-pleated-sheet secondary structure, which enables the aggregation of the peptide into plaques that deposit in the extracellular space of the brain.

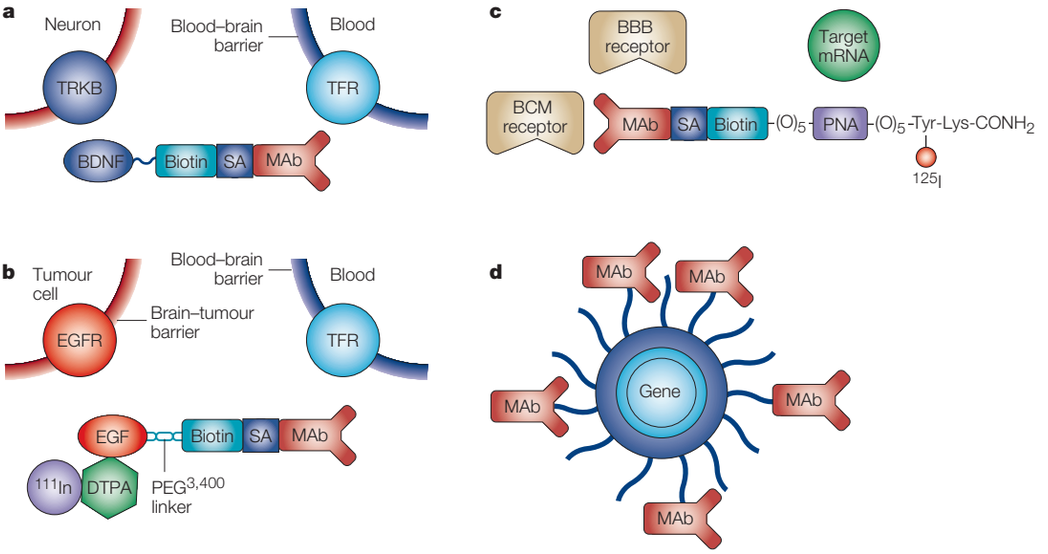

Figure 2 | **Structures of delivery vehicles for crossing the BBB. a** | Structure of a brain-derived neurotrophic factor (BDNF) chimeric peptide. The neurotrophin is conjugated to a monoclonal antibody (MAb) directed against the transferrin receptor (TFR). The BDNF chimeric peptide binds to both the TFR, to enable transport across the blood–brain barrier (BBB), and the neurotrophic tyrosine-kinase receptor (TRKB), to mediate neuroprotection. The BDNF is conjugated to the targeting MAb using avidin–biotin technology. A single biotin moiety is linked to the BDNF to enable high-affinity capture by a conjugate of streptavidin (SA) and the anti-TFR MAb. **b** | The structure of an epidermal growth factor (EGF) chimeric peptide is shown. Human recombinant EGF is conjugated to a MAb to the TFR. An extended 200-atom linker consisting of 3,400-Da poly(ethyleneglycol) ($PEG^{3,400}$) is placed between the EGF and the transport vector to release any steric hindrance of EGF binding to the EGF receptor (EGFR) that might be caused by attachment of the peptide to the transport vector. The EGF is also conjugated with diethylenetriaminepentaacetic acid (DTPA) to allow radiolabelling by chelation of 111-indium (^{111}In). **c** | Structure of an antisense radiopharmaceutical that is reformulated to enable transport across both the BBB and the brain cell membrane (BCM). The antisense imaging agent comprises four domains. First, a transport domain is formed by an anti-TFR MAb, which causes receptor-mediated transcytosis (RMT) across the BBB and receptor-mediated endocytosis across the brain cell membrane (BCM) *in vivo*. Second, a linker domain consists of SA, which is attached to the MAb transport vector, and a biotin moiety, which is attached to the amino terminus of a peptide nucleic acid (PNA). Third, an antisense domain consists of a sequence-specific PNA, which hybridizes to a target messenger RNA. Finally, a radiopharmaceutical domain contains either 125-iodine (^{125}I) attached to a carboxy-terminal tyrosine (Tyr) residue, or ^{111}In chelated to a DTPA moiety that is conjugated to a carboxy-terminal lysine (Lys) residue. **d** | A double-stranded supercoiled plasmid DNA containing an exogenous gene that is packaged into the interior of an 85-nm liposome. The surface of the liposome is conjugated with ~2,000 strands of PEG, and the tips of 1–2% of the PEG strands are conjugated with a targeting MAb. In these studies, the targeting MAb is directed at TFR, which is expressed at both the BBB and the BCM.

antibodies, and peptide radiopharmaceuticals consisting of shorter versions of $A\beta^{1-43}$, such as $A\beta^{1-40}$. However, none of the above amyloid-imaging agents crosses the BBB, so it is not possible to image the Aβ burden in the brain without BBB drug-targeting technology.

An $A\beta^{1-40}$ peptide radiopharmaceutical can be made to be transportable across the BBB by conjugation to BBB drug-targeting systems[28]. After dual modifications of $A\beta^{1-40}$ to enable both labelling with 111-indium and conjugation to BBB drug-delivery systems, the $A\beta^{1-40}$ still binds to amyloid plaques in autopsy sections of AD brains[29]. The neuroimaging of brain amyloid in transgenic mice *in vivo* has recently been reported using an Aβ peptide radiopharmaceutical conjugated to a BBB drug-targeting vector[30]. These chimeric peptides represent new amyloid-imaging agents for the early detection and semi-quantitation of the Aβ burden in patients with AD.

Delivering antisense radiopharmaceuticals

Several genes are selectively expressed in brain diseases, but only a small fraction of these are genes of known function[1]. This is illustrated by the Brain Tumor Cancer Genome Anatomy Project (see link to BT-CGAP). A review of the BT-CGAP database shows that >99% of the genes that are uniquely expressed in brain cancer are genes of unknown function. If the only information that is available about a new disease-specific gene is the sequence, then the only way it is possible to image gene expression *in vivo* is with sequence-specific antisense radiopharmaceuticals. An antisense radiopharmaceutical must be able to access the target messenger RNA molecule in the cytosol of brain cells. It must therefore be able to traverse two barriers in series: the BBB, followed by the brain cell membrane (BCM). The TFR is expressed at both the BBB and the BCM, and an anti-TFR MAb could be used as a transport vector to allow targeting of an antisense radiopharmaceutical across both the BBB and the BCM *in vivo*[1].

There are three general classes of antisense agents: phosphodiester oligodeoxynucleotides (PO-ODNs), phosphorothioate oligodeoxynucleotides (PS-ODNs) and peptide nucleic acids (PNAs). Unfortunately, the PO-ODNs are rapidly degraded by nucleases *in vivo*. The PS-ODNs are more metabolically stable *in vivo*, but

avidly bind to various cellular[31] and plasma proteins[32], including α_2-macroglobulin, a plasma protein of nearly 10^6-Da molecular mass. This binding to very large plasma proteins blocks the transport of PS-ODN–vector conjugates across the BBB *in vivo*[33]. PNAs are metabolically stable *in vivo*, do not bind non-specifically to a variety of proteins, and represent an ideal antisense agent to develop as a radiopharmaceutical. However, they do not cross the BBB[34], or cell membranes in general[35].

Nonetheless, PNAs can be made to be transportable across the BBB if they are reformulated and adapted using drug-targeting technology[36]. The structure of a PNA chimeric peptide, consisting of four domains, is shown in FIG. 2c. The nucleobase sequence of a model 18-mer PNA was designed to hybridize to luciferase mRNA around the methionine initiation codon[36]. RNase protection assays showed that the PNA still hybridized to the target mRNA sequence, despite conjugation to the BBB drug-targeting system. The imaging of luciferase gene expression in the brain *in vivo* was done with an experimental brain-tumour model[36] (FIG. 3). These studies indicate that to image gene expression *in vivo*, there must be sequence specificity of the antisense radiopharmaceutical, and the antisense radiopharmaceutical must be able to cross the BBB and BCM using drug-targeting technology.

Large sections of the human genome express novel genes of known sequence and unknown function. These genes are expressed in a disease-specific pattern. Therefore, the need to develop antisense-based gene-imaging technology will probably increase in the future. PNAs, or other classes of antisense agents, could be used to image gene expression *in vivo* if they are reformulated using brain drug-targeting technology.

Gene therapy for the brain

At present, brain gene therapy requires the intracerebral implantation of a therapeutic gene, which is inserted into a viral vector. However, the effective treatment volume after intracerebral injection is only the tip of a needle, or <1 mm^3, so it is not possible to have widespread expression of an exogenous gene throughout a significant volume of the brain using this method. Viral vectors that are commonly used are adenovirus and herpes simplex virus (HSV). However, virtually all humans, and many experimental animals, have a pre-existing immunity to both viruses[37,38]. Consequently, a single intracerebral administration of either adenovirus or HSV into animal or human brain results in a local inflammatory reaction that leads to demyelination[39–42]. Therefore, it is desirable to develop non-viral vectors for gene therapy. Cationic liposome–DNA complexes allow non-viral gene delivery into cells in tissue culture. However, these complexes immediately aggregate into micrometre-scale structures on mixing with physiological saline[43,44], and are not expressed in the brain after intravenous administration[45]. If the gene is reformulated to enable transport across the BBB, then there should be widespread expression of the exogenous gene throughout the brain after intravenous administration.

The reformulation of a double-stranded, supercoiled, non-viral plasmid DNA using brain gene-targeting technology is shown in FIG. 2d. The DNA is encapsulated in the interior of a PEGylated immunoliposome (PIL)[46]. This liposome has a net anionic charge[47], in contrast to cationic liposomes. Unlike cationic liposomes, which are unstable in both saline[43,44] and serum[48], the PIL formulation is stable in either medium[46,49]. The packaging of the plasmid DNA within the interior of the liposome eliminates the susceptibility of the DNA to the ubiquitous nucleases that are present in the body *in vivo*. In this respect, the packaging of the therapeutic gene into the interior of a nanocontainer such as a liposome is similar to packaging the gene in a viral vector. However, unlike viral vectors, the PIL is not coated with highly antigenic viral proteins. The simple encapsulation of the plasmid DNA into the interior of a 100-nm liposome would not yield significant gene expression *in vivo*, because the liposome would be immediately taken up by cells lining the RETICULO-ENDOTHELIAL system of the body. Uptake by the reticulo-endothelial system can be greatly reduced, and the blood residence time prolonged, by conjugating several thousand strands of 2,000-Da PEG[50], designated $PEG^{2,000}$, to the surface of

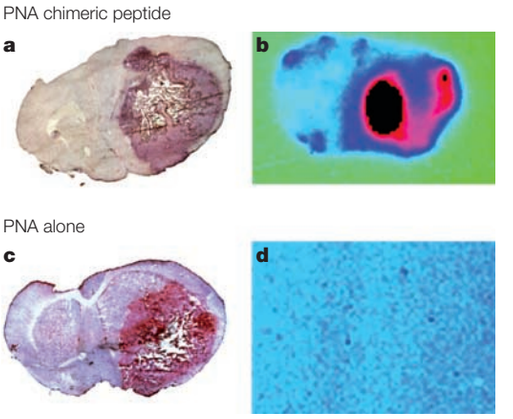

Figure 3 | **Imaging gene expression in the brain *in vivo*.** C6 rat glioma cells were permanently transfected with a gene that encodes luciferase, and these cells were implanted in the caudate-putamen nucleus of adult rats[36]. The experimental brain tumours selectively expressed the luciferase gene *in vivo*, based on measurements of tumour luciferase enzyme activity. **a**,**b** | Anti-luciferase peptide nucleic acid (PNA) conjugated to a brain drug-targeting system. **c**,**d** | Unconjugated anti-luciferase PNA. Figures **a** and **c** are autopsy stains, which show that large experimental tumours are formed. These tumour-bearing rats were given an anti-luciferase peptide nucleic acid (PNA) radiopharmaceutical intravenously two hours before sacrifice and film autoradiography of brain sections. When unconjugated anti-luciferase PNA was administered, there was no specific imaging of the brain tumour *in vivo* (**d**). However, when the PNA antisense radiopharmaceutical was conjugated to the brain drug-targeting system, the brain tumour that expressed the luciferase gene was imaged (**b**). By contrast, when a PNA that was specific to a viral messenger RNA was conjugated to the anti-Tfr MAb and injected intravenously into the tumour-bearing rats, there was no imaging of the experimental brain tumour *in vivo*[36], owing to the absence of the viral mRNA in the brain. MAb, monoclonal antibody; Tfr, rat transferrin receptor. (Reprinted with permission from REF. 36 © (2000) National Academy of Sciences, USA.)

RETICULO-ENDOTHELIAL
A system of phagocytic cells that line the microvasculature of the liver and spleen, and which remove foreign substances or particles from the blood.

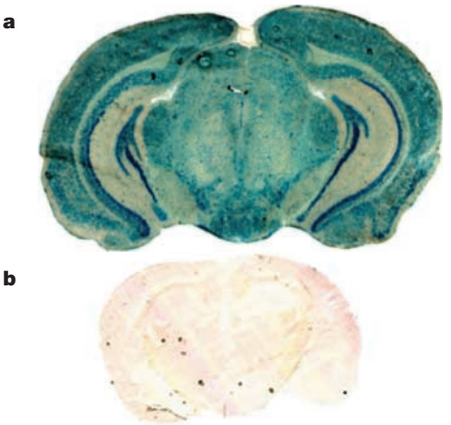

Figure 4 | **Non-viral, non-invasive gene targeting to the brain. a** | Targeting an exogenous gene encapsulated in a PEGylated immunoliposome (PIL) with a monoclonal antibody to the mouse transferrin receptor (Tfr) results in widespread gene expression in the brain following intravenous administration. The figure shows β-galactosidase histochemistry of a section of mouse brain that was removed 48 hours after a single intravenous injection of a β-galactosidase expression plasmid[51]. If the exogenous gene is under the influence of a widely expressed gene promoter, such as the SV40 promoter, the gene is also expressed in TFR-rich organs, such as the liver or spleen[47]. Conversely, if the expression of the exogenous gene is regulated by a brain-specific promoter, then gene expression is confined to the brain[51]. This was shown by replacing the SV40 promoter with the 5′-flanking sequence of the gene for the human glial fibrillary acidic protein (GFAP). A β-galactosidase expression plasmid, under the influence of the GFAP promoter, was packaged into the interior of a targeted PIL and injected intravenously into mice. Although the β-galactosidase gene was widely expressed in the brain, there was no gene expression in peripheral tissues[51]. These studies show that tissue-specific expression of exogenous genes can be achieved with tissue-specific gene promoters. **b** | There is no detectable expression of the β-galactosidase gene in mouse brain two days after an intravenous injection if the plasmid DNA is packaged into the interior of PILs that were targeted with a non-specific rat immunoglobulin-G control antibody[51]. (Reprinted with permission from REF. 51 © (2001) National Academy of Sciences, USA.)

the liposome. However, the PEGylated liposome will not cross biological barriers *in vivo*, and so will not cross either the BBB or the BCM.

PEGylated liposomes that are carrying plasmid DNA can be enabled to cross the BBB and BCM by conjugating a targeting ligand to the tips of 1–2% of the $PEG^{2,000}$ strands, as shown in FIG. 2d. Targeting ligands, such as peptidomimetic MAbs, trigger the RMT of the PIL across the BBB, and also cause the receptor-mediated endocytosis of the PIL across the BCM[49]. Then, the liposome lipids fuse with the endosomal membrane to release the plasmid into the cytosol, where it can then diffuse to the nucleus for transcription. The delivery of exogenous DNA to the nucleus with the PIL gene-targeting system has been shown with confocal microscopy[49].

The widespread expression of an exogenous gene throughout the brain after an intravenous injection of a non-viral formulation is shown in FIG. 4. In this study, a β-galactosidase expression plasmid was packaged into the interior of a PIL that was targeted with the 8D3 MAb, and injected intravenously into mice. The brain was removed 48 hours later for β-galactosidase histochemistry (FIG. 4a)[51]. Conversely, if the 8D3 targeting ligand on the PIL is replaced with a non-specific rat IgG, there is no expression of the exogenous β-galactosidase gene as shown by brain histochemistry (FIG. 4b). These control experiments using PILs prepared with non-specific IgGs show that organ uptake of the PIL is determined by the receptor specificity of the targeting ligand[46,47,51]. Gene targeting to mouse brain was accomplished with the rat 8D3 MAb to the mouse Tfr, as the OX26 murine MAb to the rat Tfr is inactive in mice[52].

Cell-specific gene expression in the brain will be beneficial for the treatment of certain neurological diseases. For example, in Parkinson's disease, the expression of a tyrosine hydroxylase exogenous gene could be restricted to the basal ganglia, with minimal expression in the cortex. Region-specific expression of an exogenous gene in the brain after intravenous administration might be possible with the combined use of gene-targeting technology, cloned therapeutic genes and region-specific gene promoters[51]. Gene-targeting technology can enable the widespread expression of an exogenous gene in the brain after intravenous administration (FIG. 4). The limiting factor is the discovery of cell-specific promoters in the brain that drive region-specific gene expression.

Conclusions

Despite the importance of solving the BBB problem to the overall neuroscience mission, there is surprisingly little worldwide effort in this area. The underdevelopment of BBB research and brain drug/gene-targeting technology is presumably derived from the dual assumptions that the BBB problem is not solvable, and that small-molecule drugs freely cross the BBB. Because most drugs do not cross the BBB, and because brain drug-targeting technology is generally not available, the fate of most CNS drug development programmes is termination. Furthermore, the BBB problem might not be recognized, and the drug development programme might not be terminated until the failure of a Phase II or even Phase III clinical trial. However, the BBB problem is solvable, and no CNS drug development programme need be terminated if brain drug/gene-targeting technology is developed. Because the processes of CNS drug discovery and CNS drug targeting are so different, it is important that independent brain drug-targeting programmes be developed in parallel with the brain drug discovery programmes. The interaction between the CNS drug discovery and the CNS drug-targeting programmes should take place as early as possible in the overall CNS drug development effort.

Technologies now exist to enable the delivery to the human brain of virtually any large-molecule neurotherapeutic, including recombinant proteins, antisense agents and gene medicines. Transport vectors specific for the human BBB are available[53], and have been genetically engineered to allow administration to humans[54]. Molecular Trojan Horses could be the vectors that launch a thousand drugs across the BBB.

1. Pardridge, W. M. *Brain Drug Targeting: the Future of Brain Drug Development* (Cambridge Univ. Press, Cambridge, 2001).
2. Cserr, H. F., Fenstermacher, J. D. & Rall, D. P. Comparative aspects of brain barrier systems for nonelectrolytes. *Am. J. Physiol.* **234**, R52–R60 (1978).
3. Mollgard, K. & Saunders, N. R. Complex tight junctions of epithelial and of endothelial cells in early fetal brain. *J. Neurocytol.* **4**, 453–468 (1975).
4. Brightman, M. W. Morphology of blood–brain interfaces. *Exp. Eye Res.* **25** (Suppl.), 1–25 (1977).
This paper reviews the classical electron-microscopic histochemistry that showed that the anatomical basis of the BBB is the capillary endothelial-cell tight junction.
5. Pardridge, W. M. *Peptide Drug Delivery to the Brain* (Raven, New York, 1991).
6. Pardridge, W. M., Yang, J., Buciak, J. & Tourtellotte, W. W. Human brain microvascular DR antigen. *J. Neurosci. Res.* **23**, 337–341 (1989).
7. Paulson, O. B. & Newman, E. A. Does the release of potassium from astrocyte endfeet regulate cerebral blood flow? *Science* **237**, 896–898 (1987).
8. Pardridge, W. M. CNS drug design based on principles of blood–brain barrier transport. *J. Neurochem.* **70**, 1781–1792 (1998).
9. Zhang, Y. & Pardridge, W. M. Mediated efflux of IgG molecules from brain to blood across the blood–brain barrier. *J. Neuroimmunol.* **114**, 168–172 (2001).
10. Skarlatos, S., Yoshikawa, T. & Pardridge, W. M. Transport of [^{125}I]-transferrin through the rat blood–brain barrier *in vivo*. *Brain Res.* **683**, 164–171 (1995).
11. Zhang, Y. & Pardridge, W. M. Rapid transferrin efflux from brain to blood across the blood–brain barrier. *J. Neurochem.* **76**, 1597–1600 (2001).
12. Green, N. M. Avidin. *Adv. Prot. Chem.* **29**, 85–133 (1975).
13. Belayev, L., Busto, R., Zhao, W. & Ginsberg, M. D. Quantitative evaluation of blood–brain barrier permeability following middle cerebral artery occlusion in rats. *Brain Res.* **739**, 88–96 (1996).
This investigation shows that the BBB is intact in the first 4–6 hours after experimental regional ischaemia, similar to other forms of acute brain injury. Neuroprotective agents will therefore not be effective unless they can cross the BBB.
14. Albayrak, S., Zhao, Q., Siesjo, B. K. & Smith, M. L. Effect of transient focal ischemia on blood–brain barrier permeability in the rat: correlation to cell injury. *Acta Neuropathol.* (Berl.) **94**, 158–163 (1997).
15. Kaplan, B. *et al.* Temporal thresholds for neocortical infarction in rats subjected to reversible focal cerebral ischemia. *Stroke* **22**, 1032–1039 (1991).
16. Wu, D. & Pardridge, W. M. Neuroprotection with non-invasive neurotrophin delivery to brain. *Proc. Natl Acad. Sci. USA* **96**, 254–259 (1999).
17. Zhang, Y. & Pardridge, W. M. Conjugation of brain-derived neurotrophic factor to a blood–brain barrier drug targeting system enables neuroprotection in regional brain ischemia following intravenous injection of the neurotrophin. *Brain Res.* **889**, 49–56 (2001).
18. Zhang, Y. & Pardridge, W. M. Neuroprotection in transient focal brain ischemia following delayed, intravenous administration of BDNF conjugated to a blood–brain barrier drug targeting system. *Stroke* **32**, 1378–1384 (2001).
19. Hefti, F. Pharmacology of neurotrophic factors. *Annu. Rev. Pharmacol. Toxicol.* **37**, 239–267 (1997).
20. Beck, T., Lindholm, D., Castren, E. & Wree, A. Brain-derived neurotrophic factor protects against ischemic cell damage in rat hippocampus. *J. Cereb. Blood Flow Metab.* **14**, 689–692 (1994).
21. Yamashita, K., Wiessner, C., Lindholm, D., Thoenen, H. & Hossmann, K. Post-occlusion treatment with BDNF reduces infarct size in a model of permanent occlusion of the middle cerebral artery in rat. *Metab. Brain Dis.* **12**, 271–280 (1997).
22. Wong, A. J. *et al.* Increased expression of the epidermal growth factor receptor gene in malignant gliomas is invariably associated with gene amplification. *Proc. Natl Acad. Sci. USA* **84**, 6899–6903 (1987).
23. Nishikawa, R. *et al.* A mutant epidermal growth factor receptor common in human glioma confers enhanced tumorigenicity. *Proc. Natl Acad. Sci. USA* **91**, 7727–7731 (1994).
24. Kurihara, A., Deguchi, Y. & Pardridge, W. M. Epidermal growth factor radiopharmaceuticals: ^{111}In chelation, conjugation to a blood–brain barrier delivery vector via a biotin–polyethylene linker, pharmacokinetics, and *in vivo* imaging of experimental brain tumors. *Bioconjug. Chem.* **10**, 502–511 (1999).
25. Kurihara, A. & Pardridge, W. M. Imaging brain tumors by targeting peptide radiopharmaceuticals through the blood–brain barrier. *Cancer Res.* **54**, 6159–6163 (1999).
26. Deguchi, Y., Kurihara, A. & Pardridge, W. M. Retention of biologic activity of human epidermal growth factor following conjugation to a blood–brain barrier drug delivery vector via an extended polyethyleneglycol linker. *Bioconjug. Chem.* **10**, 32–37 (1999).
27. Morris, J. C. *et al.* Cerebral amyloid deposition and diffuse plaques in 'normal' aging: evidence for presymptomatic and very mild Alzheimer's disease. *Neurology* **47**, 707–719 (1996).
28. Saito, Y., Buciak, J., Yang, J. & Pardridge, W. M. Vector-mediated delivery of [^{125}I]-labeled β-amyloid peptide Aβ$^{1–40}$ through the blood–brain barrier and binding to Alzheimer's Disease amyloid of the Aβ$^{1–40}$/vector complex. *Proc. Natl Acad. Sci. USA* **92**, 10227–10231 (1995).
29. Kurihara, A. & Pardridge, W. M. Aβ$^{1–40}$ radiopharmaceuticals for brain amyloid imaging, (111)In chelation, conjugation to poly(ethlyeneglycol)–biotin linkers, and autoradiography with Alzheimer's disease brain sections. *Bioconjug. Chem.* **11**, 380–386 (2000).
30. Lee, H. J., Zhang, Y., Zhu, C., Duff, K. & Pardridge, W. M. Imaging brain amyloid of Alzheimer's disease *in vivo* in transgenic mice with an Aβ peptide radiopharmaceutical. *J. Cereb. Blood Flow Metab.* **22**, 222–231 (2001).
31. Brown, D. *et al.* Effect of phosphorothioate of oligodeoxynucleotides of specific protein binding. *J. Biol. Chem.* **269**, 26801–26805 (1994).
32. Cossum, P. A. *et al.* Disposition of the ^{14}C-labeled phosphorothioate oligonucleotide ISIS 2015 after intravenous administration to rats. *J. Pharmacol. Exp. Ther.* **267**, 1181–1190 (1993).
33. Wu, D., Boado, R. J. & Pardridge, W. M. Pharmacokinetics and blood–brain barrier transport of [^{3}H]-biotinylated phosphorothioate oligodeoxynucleotide conjugated to a vector-mediated drug delivery system. *J. Pharmacol. Exp. Ther.* **276**, 206–211 (1996).
34. Pardridge, W. M., Boado, R. J. & Kang, Y.-S. Vector-mediated delivery of a polyamide ('peptide') nucleic acid analogue through the blood–brain barrier *in vivo*. *Proc. Natl Acad. Sci. USA* **92**, 5592–5596 (1995).
35. Hanvey, J. C. *et al.* Antisense and antigene properties of peptide nucleic acids. *Science* **258**, 1481–1486 (1992).
36. Shi, N., Boado, R. J. & Pardridge, W. M. Antisense imaging of gene expression in the brain *in vivo*. *Proc. Natl Acad. Sci. USA* **97**, 14709–14714 (2000).
37. Kajiwara, K. *et al.* Humoral immune responses to adenovirus vectors in the brain. *J. Neuroimmunol.* **103**, 8–15 (2000).
38. Herrlinger, U. *et al.* Pre-existing herpes simplex virus 1 (HSV-1) immunity decreases but does not abolish, gene transfer to experimental brain tumors by a HSV-1 vector. *Gene Ther.* **5**, 809–819 (1998).
39. Driesse, M. J. *et al.* Intracerebral injection of adenovirus harboring the *HSVtk* gene combined with ganciclovir administration: toxicity study in nonhuman primates. *Gene Ther.* **5**, 1122–1129 (1998).
40. Lawrence, M. S. *et al.* Inflammatory responses and their impact on β-galactosidase transgene expression following adenovirus vector delivery to the primate caudate nucleus. *Gene Ther.* **6**, 1368–1379 (1999).
A single injection of adenovirus into the primate brain causes local inflammation that leads to demyelination.
41. Kramm, C. M. *et al.* Herpes vector-mediated delivery of marker genes to disseminated central nervous system tumors. *Human Gene Ther.* **7**, 291–300 (1996).
42. McMenamin, M. M. *et al.* A γ34.5 mutant of herpes simplex 1 causes severe inflammation in the brain. *Neurosci.* **83**, 1225–1237 (1998).
Even replication-deficient strains of the herpes simplex virus are toxic to the brain, causing local inflammation, increased antigen-presenting cells and perivascular lymphocyte cuffing.
43. Hofland, H. E. J. *et al. In vivo* gene transfer by intravenous administration of stable cationic lipid/DNA complex. *Pharm. Res.* **14**, 742–749 (1997).
44. Plank, C., Tang, M. X., Wolfe, A. R. & Szoka, F. C. Jr. Branched cationic peptides for gene delivery: role of type and number of cationic residues in formation and *in vitro* activity of DNA polyplexes. *Hum. Gene Ther.* **10**, 319–332 (1999).
45. Osaka, G. *et al.* Pharmacokinetics, tissue distribution, and expression efficiency of plasmid [^{33}P]DNA following intravenous administration of DNA/cationic lipid complexes in mice: use of a novel radionuclide approach. *J. Pharm. Sci.* **85**, 612–618 (1996).
46. Shi, N. & Pardridge, W. M. Non-invasive gene targeting to the brain. *Proc. Natl Acad. Sci. USA* **97**, 7567–7572 (2000).
47. Shi, N., Boado, R. J. & Pardridge, W. M. Receptor-mediated gene targeting to tissues in the rat *in vivo*. *Pharm. Res.* **18**, 1091–1095 (2001).
48. Cruz, M. T., Simoes, S., Pires, P. P. C., Nir, S. & Lima, M. C. Kinetic analysis of the initial steps involved in lipoplex–cell interactions: effect of various factors that influence transfection activity. *Biochim. Biophys. Acta* **1510**, 136–151 (2001).
49. Zhang, Y., Lee, H. J., Boado, R. J. & Pardridge, W. M. Receptor-mediated delivery of an antisense gene to human brain cancer cells. *J. Gene Med.* (in the press).
50. Papahadjopoulos, D. *et al.* Sterically stabilized liposomes: improvements in pharmacokinetics and antitumor therapeutic efficacy. *Proc. Natl Acad. Sci. USA* **88**, 11460–11464 (1991).
This classical study shows that the conjugation of PEG to the surface of liposomes greatly prolongs the blood residence time and optimizes the pharmacokinetics.
51. Shi, N., Zhang, Y., Boado, R. J., Zhu, C. & Pardridge, W. M. Brain-specific expression of an exogenous gene following intravenous administration. *Proc. Natl Acad. Sci. USA* **98**, 12754–12759 (2001).
52. Lee, H. J., Engelhardt, B., Lesley, J., Bickel, U. & Pardridge, W. M. Targeting rat anti-mouse transferrin receptor monoclonal antibodies through the blood–brain barrier. *J. Pharmacol. Exp. Ther.* **292**, 1048–1052 (2000).
53. Pardridge, W. M., Kang, Y.-S., Buciak, J. L. & Yang, J. Human insulin receptor monoclonal antibody undergoes high affinity binding to human brain capillaries *in vitro* and rapid transcytosis through the blood–brain barrier *in vivo* in the primate. *Pharm. Res.* **12**, 807–816 (1995).
54. Coloma, M. J. *et al.* Transport across the primate blood–brain barrier of a genetically engineered chimeric monoclonal antibody to the human insulin receptor. *Pharm. Res.* **17**, 266–274 (2000).
This study describes the genetic engineering of a brain transport vector and shows targeting to the primate brain *in vivo*. The genetically engineered vector could be used to target drugs or genes to the human brain.
55. Pardridge *et al.* Blood–brain barrier: interface between internal medicine and the brain. *Ann. Intern. Med.* **105**, 82–95 (1986).
56. Duvernoy, H., Delon, S. & Vannson, J. L. The vascularization of the human cerebellar cortex. *Brain Res. Bull.* **11**, 419–480 (1983).
57. Cornford, E. M., Hyman, S., Cornford, M. E. & Caron, M. J. GLUT1 glucose transporter activity in human brain injury. *J. Neurotrauma* **13**, 523–536 (1996).
58. Brownlees, J. & Williams, C. H. Peptidases, peptides, and the mammalian blood–brain barrier. *J. Neurochem.* **60**, 793–803 (1993).
59. Tsuji, A. & Tamai, I. Carrier-mediated or specialized transport of drugs across the blood–brain barrier. *Adv. Drug Deliv. Rev.* **26**, 277–290 (1999).
60. Takasawa, K., Terasaki, T., Suzuki, H. & Sugiyama, Y. *In vivo* evidence for carrier-mediated efflux transport of 3′-azido-3′-deoxythymidine and 2′,3′-dideoxyinosine across the blood–brain barrier via a probenecid-sensitive transport system. *J. Pharmacol. Exp. Ther.* **281**, 369–375 (1997).
61. Pardridge, W. M. Receptor-mediated peptide transport through the blood–brain barrier. *Endocr. Rev.* **7**, 314–330 (1986).
62. Krewson, C. E., Klarman, M. L. & Saltzman, W. M. Distribution of nerve growth factor following direct delivery to brain interstitium. *Brain Res.* **680**, 196–206 (1995).
63. Yan, Q. *et al.* Distribution of intracerebral ventricularly administered neurotrophins in rat brain and its correlation with Trk receptor expression. *Exp. Neurol.* **127**, 23–36 (1994).

Online links

DATABASES

The following terms in this article are linked online to:
LocusLink: http://www.ncbi.nlm.nih.gov/LocusLink/
BDNF | CNT2 | EGF | EGFR | GFAP | GLUT1 | insulin | insulin receptor | LAT1 | leptin receptor | α_2-macroglobulin | MCT1 | NGF | OATP2 | scavenger receptor | TF | TFR | Tfr (mouse) | Tfr (rat) | TRKB
OMIM: http://www.ncbi.nlm.nih.gov/Omim/
Alzheimer's disease | Parkinson's disease

FURTHER INFORMATION

Alliance for Aging Research:
http://www.agingresearch.org/advocacy/default.htm
American Heart Association:
http://www.americanheart.org/presenter.jhtml?identifier=1200026
BT-CGAP: http://cgap.nci.nih.gov/Tissues/LibraryFinder
Encyclopedia of Life Sciences: http://www.els.net/
Blood–brain barrier
Access to this interactive links box is free online.

Neuron, Vol. 36, 555–558, November 14, 2002, Copyright ©2002 by Cell Press

Drug and Gene Delivery to the Brain: The Vascular Route

Minireview

William M. Pardridge[1]
Department of Medicine
School of Medicine
University of California, Los Angeles
Los Angeles, California 90024

Brain drug development of either small molecule or large molecule (recombinant proteins, gene medicines) neurotherapeutics has been limited, owing to the restrictive transport properties of the brain microvasculature, which forms the blood-brain barrier (BBB) in vivo. Widespread drug delivery to the brain, while not feasible via craniotomy and intracerebral injection, is possible if the drug is delivered to brain via the transvascular route through the BBB. Novel brain drug delivery and drug targeting strategies can be developed from an understanding of the molecular and cellular biology of the brain microvascular and BBB transport processes.

Introduction

Brain drug delivery is the rate-limiting step in the translation of progress in the molecular neurosciences into clinically effective neurotherapeutics for patients with disorders of the central nervous system (CNS). Progress in brain drug delivery has lagged behind other areas in the molecular neurosciences, because of the difficulties posed by the blood-brain barrier (BBB). The brains of all vertebrates are perfused by a dense microvascular network, which is formed by the capillary endothelial cells within the brain (Bar, 1980).

The density of the microvasculature of the brain is illustrated with the India ink injection study in the adult rat brain shown in Figure 1A. The capillary network in the brain is so intricate that no neuron or glial cell is more than 20 μm from a neighboring capillary. Therefore, every neuron is virtually perfused by its own microvessel. Once a circulating neurotherapeutic crosses the brain microvascular wall, the drug or gene is immediately delivered to the "doorstep" of every neuron within the brain.

Brain Barrier Systems. In addition to the brain microvascular endothelial barrier, which forms the BBB, there are other barrier systems within the CNS, including the arachnoid epithelial membrane, which covers the surface of the brain, and the choroid plexus epithelium, which forms the blood-cerebrospinal fluid (CSF) barrier. In humans, there are approximately 400 miles of capillaries perfusing the brain, and the surface area of the brain microvascular endothelium is approximately 20 m^2 (Pardridge, 2001), which is 1000-fold greater than the surface area of either the blood-CSF barrier or the arachnoid membrane (Dohrmann, 1970). Therefore, the quantitatively important barrier system within the brain is the BBB at the capillary endothelium (Figure 1A). Despite the vast surface area of the human BBB, the thickness of the BBB is very thin, and the total intracellular volume of the brain capillary endothelium is only 5 ml in the entire human brain and 1 μl in the rat brain. The thickness of the brain capillary endothelial cell is about 200–300 nm. This very thin cellular barrier has some of the most restrictive permeability properties of any biological membrane (Oldendorf, 1971).

Multifunctional Basis of BBB to Drugs. Drug entry into brain from blood is restricted at the BBB through multiple mechanisms, including a physical endothelial barrier, an enzymatic BBB, and an efflux barrier. This multifunctionality of the BBB arises from the multicellularity of the brain microvasculature, which is formed by the triad of brain capillary endothelial cells, capillary pericytes, and perivascular astrocyte foot processes (Pardridge, 2001). The endothelium and pericyte share a common microvascular basement membrane, and 99% of the brain surface of the capillary basement membrane is invested by the end-feet of processes extending from astrocyte cell bodies originating within brain parenchyma.

Endothelial Tight Junctions. Capillaries perfusing peripheral organs have porous endothelial walls. Peripheral capillaries have open interendothelial junctional spaces and active pinocytosis, which form a paracellular route and a transcellular route, respectively, for the free diffusion of molecules from the blood to the organ interstitium. However, in the vertebrate brain, the capillary endothelial cells express epithelial-like high resistance tight junctions, which eliminate the paracellular pathway, and have minimal pinocytosis, which eliminates the nonspecific transcellular route of molecular transport from blood to brain (Brightman, 1977). The combination of the very high resistance endothelial tight junctions and the minimal endothelial pinocytosis forms a physical barrier to drug entry into brain from blood.

Enzymatic BBB. There is an "enzymatic BBB" to circulating drugs, in addition to the physical barrier formed by the endothelial tight junctions. The capillary endothelial cells, the capillary pericytes, and the astrocyte foot processes all express a variety of ecto-enzymes on the cellular plasma membranes, including aminopeptidases, carboxypeptidases, endopeptidases, cholinesterases, and others, which inactivate many drugs that may pass the endothelial barrier. For example, circulating adenosine enters brain from blood via the BBB concentrative nucleoside transporter type 2 (CNT2) but does not have pharmacological effects in the brain, owing to rapid inactivation at the BBB by adenosine metabolizing enzymes (Pardridge, 2001). Conversely, the enzymatic BBB may serve to activate pro-drugs. Circulating L-DOPA enters brain via the BBB large neutral amino acid transporter type 1 (LAT1) and is rapidly converted to dopamine, the pharmacologically active form of the drug, by microvascular aromatic amino acid decarboxylase (AAAD).

Active Efflux Barrier. Certain drugs may cross the endothelial barrier via free diffusion and undergo influx from the blood to the brain compartment. However, this influx can be immediately followed by active efflux from

[1]Correspondence: wpardridge@mednet.ucla.edu

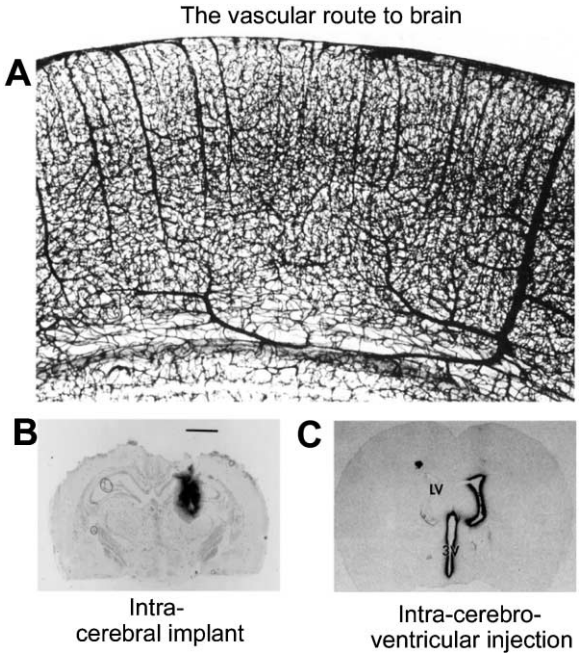

Figure 1. Transvascular and Transcranial Drug Delivery to the Brain

(A) India ink injection in adult rats shows the dense microvascular network within the brain (Bar, 1980). These brain capillaries form the BBB, and the delivery of drugs or genes across the BBB is the only pathway that enables widespread distribution of the drug to all cells within the brain.

(B) Film autoradiogram of rat brain 48 hr after the intracerebral (IC) implantation of a biodegradable polymer containing [^{125}I]-nerve growth factor (NGF) (Krewson et al., 1995). The distance bar is 2.5 mm, and the diameter of the polymer was 2 mm; therefore, there is minimal diffusion of the NGF into brain away from the IC implant.

(C) Film autoradiogram of rat brain 24 hr after the ICV injection of [^{125}I]-BDNF (Yan et al., 1994). The neurotrophin does not distribute into brain beyond the ipsilateral ependymal surface.

brain back to blood if the drug is a substrate for one of many different active efflux transporters (AET) expressed within the brain microvasculature. P-glycoprotein is the model AET at the BBB (Tsuji and Tamai, 1999), but there are many other efflux systems, such as organic anion transporting polypeptide type 2 (oatp2) (Asaba et al., 2000). One strategy to increase drug uptake into brain is the development of "co-drugs" (Pardridge, 2001). Co-drugs are inhibitors of BBB AET systems and are coadministered with the pharmacologically active drug that is an AET substrate. This is analogous to the administration of an AAAD-inhibitor with L-DOPA to prevent early degradation of the drug. In this case, the AAAD-inhibitor should be a drug that does not cross the BBB and selectively inhibits AAAD in the periphery.

Owing to these unique barrier properties of the microvascular endothelial barrier in the vertebrate brain, circulating molecules in the blood gain access to brain interstitial space via only one of two transport mechanisms:

- Lipid-mediated free diffusion of small molecules
- Catalyzed transport of small or large molecules

Free Diffusion of Small Molecules. Certain small molecules can traverse the BBB nonspecifically via lipid-mediated transport. A misconception with respect to small molecule transport across the BBB is that if a molecule is "small," then BBB transport is unrestricted. Only small molecules that are (1) lipid soluble and (2) have a molecular weight $<$500 Da threshold cross the BBB in pharmacologically significant amounts (Pardridge, 2001). Virtually all drugs presently in CNS clinical practice are small molecules that have these dual molecular characteristics. Similarly, if a small molecule is water soluble or has a molecular weight $>$500 Da, the drug may not cross biological barriers in pharmacologically significant amounts and have reduced absorption, as predicted by the "Rule of 5" (Lipinski et al., 1997). The adverse effect of molecular weight on membrane permeation is not observed if the molecular weight of the drug is $<$400 Daltons (Habgood et al., 2000). However, if the molecular weight of the drug causes the surface area of the drug to exceed 50–100 angstroms^2, then membrane permeation of the drug will not increase in proportion to the increase in lipid solubility of the drug (Fischer et al., 1998). The dependence of drug permeation through biological membranes on either molecular volume or molecular weight is not predicted by measurements of drug partitioning in solvents, because drug diffusion through solvents is not identical to drug diffusion across biological membranes (Lieb and Stein, 1986). Lipid mediation of small molecules through biological membranes requires molecular movement through channels within the lipid bilayer, and these channels have a finite size (references can be found in Pardridge, 2001). In summary, there are multiple impediments to small molecule transport across the BBB, and the following characteristics are associated with reduced BBB transport and reduced in vivo CNS pharmacologic activity:

- Molecular weight $>$500 Daltons
- Sum of hydrogen bond donor/acceptor groups $>$10
- Substrate for BBB enzyme system
- Substrate for BBB active efflux transporter
- Avid plasma protein binding of the drug

The above factors make it difficult to design a small molecule drug with effective CNS activity. Current small molecule neuropharmaceuticals only effectively treat a few CNS disorders, including pain, epilepsy, insomnia, and affective disorders (Ajay et al., 1999), and the majority of CNS disorders have thus far proven refractory to conventional small molecule therapy. A principal reason for this failure of conventional drug therapy of the brain is that $>$98% of all small molecule drug candidates do not cross the BBB, and no BBB drug targeting technology is used by the pharmaceutical industry (Pardridge, 2001).

Catalyzed Transport via CMT and RMT Systems. Small water-soluble nutrients and vitamins traverse the BBB rapidly via carrier-mediated transport (CMT). The CMT systems generally mediate the blood-to-brain transport of nutrients and include the GLUT1 glucose transporter, the LAT1 large neutral amino acid transporter, the MCT1 monocarboxylic acid transporter, the CNT2 nucleoside transporter, and many other small molecule transporters

(references can be found in Pardridge, 2001). The CMT systems are portals of entry of small molecule drugs that have a molecular structure similar to endogenous nutrients. L-DOPA, a neutral amino acid, gains access to the brain via CMT on the BBB large neutral amino acid transporter. In contrast, the conjugation of glucose to a peptide does not mediate transport via the BBB GLUT1 carrier (Witt et al., 2001), because the GLUT1 transporter does not recognize the peptide structure. In addition to the CMT systems, certain large molecule peptides or plasma proteins are selectively transported across the BBB via receptor-mediated transport (RMT) systems, including the insulin receptor, the transferrin receptor (TfR), or the leptin receptor. RMT of circulating peptides is comprised of three sequential steps: (1) receptor-mediated endocytosis of the circulating peptide at the luminal membrane of the capillary endothelium, (2) movement through the 200–300 nm of endothelial cytoplasm, and (3) exocytosis of the peptide into the brain interstitial fluid at the abluminal membrane of the capillary endothelium (Pardridge, 2001).

Brain Drug Delivery Strategies

Craniotomy-Based Drug Delivery to the Brain. Drugs or genes may be delivered to the brain via either intracerebroventricular (ICV) injection or intracerebral implantation (Shoichet and Winn, 2000). However, drug entry into brain parenchyma with either approach is limited by diffusion, and little drug diffuses into brain far from the depot site (Figures 1B and 1C). The most direct approach to drug or gene delivery to all parts of the brain is the vascular route (Figure 1A), and the transvascular brain drug delivery strategies include hyperosmolar BBB disruption, drug lipidization, protein cationization, and the chimeric peptide technology.

Hyperosmolar BBB Disruption. The intracarotid arterial infusion of hyperosmolar solutions causes a shrinking of the brain and the brain capillary endothelium, and this leads to a transient disruption of the BBB (Shoichet and Winn, 2000). BBB disruption has been used in humans for the delivery of chemotherapeutic agents to brain cancer (Dahlborg et al., 1998). The concern with BBB disruption is that this causes a generalized increase in the brain uptake of many plasma constituents. Blood proteins are toxic to brain cells (Nadal et al., 1995), and hyperosmolar BBB disruption causes chronic neuropathologic changes (Salahuddin et al., 1988).

Drug Lipidization. The BBB permeability-surface area (PS) product is an experimental measure of BBB permeability to a given drug. The BBB PS product for small molecules may be increased with lipidization via either (1) the reduction in hydrogen bonding of the drug through conjugation of lipid-soluble functional groups to water-soluble moieties on the drug, or (2) conjugation of the drug to a lipid carrier such as free fatty acid, adamantane, or dihyropyridine. A problem with drug lipidization is that the uptake of the lipidized drug by peripheral organs is also increased, and this causes a reduction in the plasma concentration of the drug. Therefore, the increased BBB transport caused by lipidization is offset by the increased uptake of the drug by peripheral tissues (Pardridge, 2001).

Protein Cationization. The cellular uptake of proteins may be increased by cationizing the protein, which triggers electrostatic interactions with anionic groups on the membrane, and this induces absorptive-mediated endocytosis into the cell (Pardridge, 2001). Proteins may be cationized via either (1) conjugation of amino groups such as hexamethylenediamine to surface carboxyl moieties, or (2) conjugation of cationic "import" peptides such as the arginine-rich tat peptide (Schwarze et al., 1999). Protein cationization has the same effect as drug lipidization. Both processes increase BBB permeability for the drug or protein but also cause a parallel increase in peripheral organ uptake and concomitant decrease in the plasma concentration of the drug or protein. Therefore, the brain uptake does not increase in proportion to the increase in BBB transport following protein cationization (Lee and Pardridge, 2001).

Chimeric Peptides. A chimeric peptide is formed when a small or large molecule drug that is normally not transported across the BBB is fused or conjugated to a BBB transport vector. The latter is comprised of an endogenous peptide, modified protein, or peptidomimetic monoclonal antibody (MAb) that undergoes RMT through the BBB on endogenous endothelial receptor systems (Pardridge, 2001). A peptidomimetic MAb transport vector binds an exofacial epitope on the BBB receptor. The MAb epitope is removed from the endogenous ligand binding site, and this binding enables the MAb to "piggyback" across the BBB on the endogenous RMT system, as demonstrated by electron microscopy of brain following the in vivo perfusion of anti-receptor MAb-gold conjugates. The MAb acts as a transport vector and can deliver to the brain any attached drug or gene. A panel of species-specific peptidomimetic MAbs has been developed to allow for transport of drugs or genes into the brain of either animal models or humans (references can be found in Pardridge, 2001).

Brain Drug Delivery of Large Molecule Drugs

Large molecule drugs are peptides, recombinant proteins, antisense agents, and gene medicines. It is widely believed that the BBB transport of large molecule drugs is not possible, and large molecule drug development programs are frequently terminated in favor of small molecule drug discovery. However, recombinant proteins, antisense drugs, and non-viral gene medicines can be delivered to the brain with brain drug targeting technology.

Recombinant Proteins. Neurotrophins could be used for a wide variety of brain diseases, but these recombinant proteins do not cross the BBB in pharmacologically significant amounts. Consequently, virtually all current neurotrophin CNS drug development programs are focused on the discovery of small molecule peptidomimetics. However, most small molecule peptidomimetics will not have molecular characteristics that pass the stringent criteria discussed above for effective BBB transport. Therefore, the small molecule peptidomimetic would benefit from reformulation with a BBB drug delivery strategy to be pharmacologically active in the brain. The development of a small molecule drug that crosses the BBB can be just as difficult as the development of a large molecule drug that is transported across the BBB. Therefore, one alternative is to reformulate the large molecule drug with a BBB drug delivery strategy. This has been done with the chimeric peptide technology, wherein a nontransportable peptide is conjugated to a BBB transport vector, which functions as a molecu-

THE JOURNAL OF GENE MEDICINE
J Gene Med 2003; **5**: 157–163.
Published online 20 September 2002 in Wiley InterScience (www.interscience.wiley.com). **DOI:** 10.1002/jgm.333

RESEARCH ARTICLE

Marked enhancement in gene expression by targeting the human insulin receptor

Yun Zhang
Ruben J. Boado
William M. Pardridge*

[1]*Department of Medicine, UCLA School of Medicine, Los Angeles, CA 90024, USA*

*Correspondence to:
Dr. William M. Pardridge, UCLA Warren Hall 13-164, 900 Veteran Avenue, Los Angeles, CA 90024, USA.
E-mail:
wpardridge@mednet.ucla.edu

Received: 21 May 2002
Revised: 31 July 2002
Accepted: 2 August 2002

Abstract

Background Exogenous genes can be delivered to cells without viral vectors using an "artificial virus" comprised of nonviral plasmid DNA encapsulated in the interior of 85 nm pegylated immunoliposomes (PIL). The liposomes are targeted to cells with receptor-specific targeting ligands such as receptor-specific peptidomimetic monoclonal antibodies.

Methods The levels of luciferase gene expression in human or rat glioma cells are measured after targeting the PIL-encapsulated plasmid DNA via the human insulin receptor, the human epidermal growth factor receptor, or the rat transferrin receptor. The luciferase expression plasmids were either derived from pCEP4, which contains the Epstein-Barr nuclear antigen-1/oriP replication system, or from pGL2, which lacks this system for episomal replication of plasmid DNA.

Results Depending on the plasmid construct used and the receptor targeted, the peak luciferase gene expression varied more than 200-fold from 1.8 ± 0.1 to 419 ± 31 pg luciferase per mg cell protein. With the same plasmid, the peak level of gene expression following delivery to the cell via the human insulin receptor was 100–200-fold higher than gene expression following delivery via either the epidermal growth factor receptor or the transferrin receptor. There was no gene expression if the targeting ligand on the PIL was replaced with a nonspecific isotype control antibody.

Conclusions The extent to which an exogenous gene is expressed within a cell via a nonviral, receptor-mediated gene transfer technology is determined by the receptor specificity of the targeting ligand. The highest levels of gene expression are obtained after targeting the insulin receptor, and this may derive from the nuclear targeting properties of this receptor system.

Keywords insulin receptor; transferrin receptor; EGF receptor; luciferase; gene therapy

Introduction

Exogenous genes can be targeted to cells with either viral or nonviral delivery systems. Nonviral gene delivery systems include cationic liposomes or complexes of receptor ligands/polycations/plasmid DNA. *In vivo* applications of nonviral gene delivery technologies have been limited owing to the aggregation in serum of either cationic liposomes or polycation complexes of plasmid DNA [1,2]. An alternative to nonviral gene transfer technology is the use of an "artificial virus", wherein nonviral plasmid DNA is encapsulated in

the *interior* of neutral/slightly anionic liposomes [3–5]. These nanocontainers are targeted to cells with receptor-specific ligands conjugated to the exterior surface of the liposome. Liposomes, *per se*, are unstable *in vivo* owing to coating of the liposome surface with serum protein [6], which triggers rapid uptake by cells lining the reticulo-endothelial system (RES). RES uptake can be inhibited and the blood circulation time can be prolonged if the surface of the liposome is conjugated with several thousand strands of polyethylene glycol (PEG) [7]. The tips of about 1–2% of the PEG strands are conjugated with a receptor-specific targeting ligand or a peptidomimetic monoclonal antibody (MAb) to form a pegylated immunoliposome (PIL) [8]. The structure of a PIL is shown in Figure 1. The super-coiled plasmid DNA is encapsulated in the interior of an 85–100 nm liposome that interacts with a targeted receptor (R) through receptor-specific peptidomimetic MAb molecules that are conjugated to the tips of PEG polymers attached to the surface of the liposome. This construct has the advantages of a viral delivery system in that the DNA is encapsulated in the interior of a nanocontainer, which protects the DNA from the ubiquitous endonucleases of the body. As with a viral vector, surface proteins on the nanocontainer trigger uptake of the complex by the target cells. However, unlike a viral vector, the artificial virus is not immunogenic, since genetically engineered or "humanized" Mab's may be incorporated in the PIL for therapeutic applications in humans. The organ specificity of gene expression *in vivo* is regulated through the incorporation of promoter elements within the plasmid, which restrict expression of the exogenous gene to the target organ [5]. The persistence of gene expression of the plasmid DNA can be enhanced by promoting episomal replication via the incorporation of the Epstein-Barr nuclear antigen (EBNA)-1 trans element and the oriP cis element, which enables one round of replication of the plasmid with each cell mitosis [9].

The extent to which the exogenous gene is expressed in the target cell is controlled, in part, by the MAb or targeting ligand that is conjugated to the PIL (Figure 1). Any receptor system that undergoes endocytosis into the cell is a potential conduit for the cellular delivery of the PIL carrying the exogenous gene. The transferrin receptor (TfR) has been targeted for gene transfer in *vivo* in rats and mice [3–5]. For gene transfer to human cells, the human insulin receptor (HIR) has been targeted with a MAb to this receptor, both *in vitro* in cell culture [10] and *in vivo* in intracranial human glial tumors in scid mice [11]. These earlier studies showed that the level of luciferase gene expression following gene transfer in rodents with the TfRMAb was much lower than the level of luciferase gene expression following gene transfer in human cells with the HIRMAb [5,10]. It is possible that certain receptors deliver the PIL complex into compartments of the cell that favor expression of the transgene. Therefore, the purpose of the present study was to examine luciferase gene expression in cultured glioma cells following targeting of the PIL to the cell via different receptors that bind and endocytose the target ligand. The PIL is targeted to the cell with peptidomimetic MAb's to the HIR, the human epidermal growth factor receptor (EGFR), and the rat TfR (Figure 1). The present studies also compare the level of luciferase gene expression in human glioma cells targeted by the HIRMAb, wherein the plasmid DNA formulation is constructed with or without the EBNA-1/oriP replication system. The overall goal of these studies is to optimize the component parts of the PIL gene transfer system so as to enable maximal levels of exogenous gene expression in target cells.

Materials and methods

Materials

U87 human brain glioma cells (ATCC HTB 14) and the 528 hybridoma (ATCC HB 8509) were obtained from the American Type Culture Collection (Rockville, MD, USA). RG2 glioma cells were obtained from Dr. Keith L. Black (UCLA Dept. of Surgery/Neurosurgery). Clone 753 is a luciferase expression plasmid derived from pGL2, and clone 790 is a luciferase expression plasmid derived from pCEP4, as described previously [12]. The luciferase gene in both plasmids is under the influence of the SV40 promoter (Table 1). The SV40 3′-untranslated region (UTR) of either plasmid contains a 200 nucleotide insert taken from the 3'-UTR of the bovine Glut1 glucose transporter mRNA (Table 1), which contains an mRNA cis element that enhances mRNA stability, as described previously [12]. Clone 790 contains the EBNA-1/oriP elements, whereas clone 753 lacks these elements

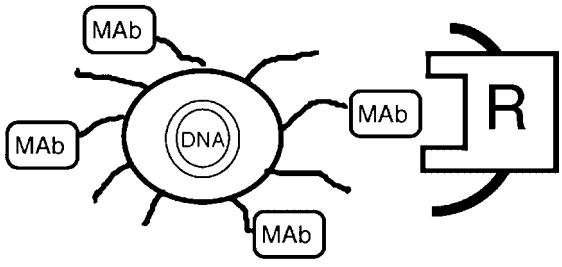

MAb	Receptor
83-14	human IR
528	human EGFR
OX26	rat TfR

Figure 1. Plasmid DNA is encapsulated in the interior of a pegylated immunoliposome (PIL) which is modified with a targeting monoclonal antibody (MAb). The targeting MAb binds to a receptor (R) on the cell membrane that triggers endocytosis of the PIL into the target cell. Three different MAbs were used in these studies: the murine 83-14 MAb to the human insulin receptor (HIR), the murine 528 MAb to the human epidermal growth factor (EGFR), and the murine OX26 MAb to the rat transferrin receptor (TfR). PIL was also prepared with the mouse IgG2a isotype control antibody

Table 1. Luciferase expression plasmids

Element	Plasmid 753	Plasmid 790
SV40 promoter	+	+
SV40/Glut1 3′-UTR	+	+
EBNA-1/oriP	−	+
Plasmid origin	pGL2	pCEP4
Size (kb)	6.0	10.6

From Ref. 12.

(Table 1). The sources of all other materials have been described previously [3–5].

Plasmid DNA preparation and radiolabeling

Luciferase expression plasmid DNA was purified from *Escherichia coli* with the Maxiprep procedure for either clone 753 or clone 790 (Qiagen, Chatsworth, CA, USA), and DNA was labeled with [$\alpha-^{32}$P]dCTP by the nick translation system as described previously [3].

Pegylated immunoliposome synthesis and plasmid DNA encapsulation

Pegylated liposomes were prepared from 1-palmitoyl-2-oleoyl-*sn*-glycerol-3-phosphocholine, didodecyldimethylammonium bromide, distearoylphosphatidylethanolamine (DSPE)-PEG^{2000}, and DSPE-PEG^{2000}-maleimide, exactly as described previously [10]. The encapsulation of either clone 753 or clone 790 plasmid DNA within the interior of pegylated liposomes, and nuclease removal of exteriorized DNA, were performed as described previously [3–5]. In a typical preparation, 200 μg of plasmid DNA, 20 μmol of lipid, and 3 mg of MAb were used as starting reagents. The DNA encapsulation in the PIL after nuclease treatment was $20 \pm 1\%$ (mean $\pm$ S.E., $n = 7$ syntheses). Following nuclease treatment, there is no exteriorized plasmid DNA in the liposome formulation, and the degraded DNA is removed by gel filtration of the PIL prior to addition to cells, as described previously [3–5]. The encapsulation of the plasmid DNA within the interior of the nuclease-treated liposome has been verified by agarose gel electrophoresis [3]. The w/w ratio of MAb/DNA in the PIL is 20 : 1. In a typical experiment, the medium concentration of the DNA encapsulated in the PIL is 0.8 μg/ml and the medium concentration of the MAb attached to the PIL is 16 μg/ml, or 100 nM.

The 83-14 murine MAb to the human IR, the 528 murine MAb to the human EGFR, and the OX26 murine MAb to the rat TfR were purified by protein G affinity chromatography from serum-free hybridoma-conditioned media as described previously [13]. Purified mouse IgG2a (mIgG2a), the isotype control antibody, was obtained from Sigma. The antibody (84-14, 528, OX26, or mIgG2a) was individually thiolated with 2-iminothiolane (Traut's reagent), and the thiolated antibody was conjugated to the maleimide-grafted pegylated liposome as described previously [8]. The PIL with the encapsulated DNA was purified by Sepharose CL-4B column chromatography as described previously [8]. The average number of MAb molecules conjugated per liposome was 55 ± 6 (mean $\pm$ S.E., $n = 7$ syntheses). With this approach, the MAb is randomly conjugated to the tip of the PEG tail and may be attached at either the Fab or the Fc portion of the antibody molecule. The attachment of the MAb to the liposome has been verified by electron microscopy [11].

Liposomes prepared with the 83-14 MAb were designated HIRMAb-PIL, liposomes prepared with the OX26 MAb were designated TfR MAb-PIL, liposomes prepared with the 528 MAb were designated EGFR MAb-PIL, and liposomes prepared with the mIgG2a isotype control antibody were designated mIgG2a-PIL. The HIRMAb-PIL encapsulated with either clone 790 or clone 753 plasmid DNA is designated HIRMAb-PIL/790 or HIRMAb-PIL/753, respectively. The targeting MAb's are species-specific. Therefore, gene delivery to rat RG-2 cells is mediated by the murine OX26 MAb to the rat TfR, and gene delivery to human U87 cells is mediated by either the murine 83-14 MAb to the HIR or the murine 528 MAb to the human EGFR (Figure 1).

Luciferase gene expression *in vitro*

Prior to addition to tissue culture medium, the PIL was sterilized with a 0.22-μm Millex GV filter (Millipore Co., Bedford, MA, USA) as described previously [10]. U87 or RG2 cells were grown on 35-mm collagen-treated dishes. When the cells reached 50–60% confluence, the medium was removed by aspiration, and 2.5 ml of fresh MEM or DMEM medium containing 10% fetal bovine serum (FBS) were added to the U87 or RG2 cells, respectively. Sterile aliquots of HIR-PIL, TfR-PIL, EGFR-PIL, or mIgG2a-PIL containing 2 μg of either clone 790 or clone 753 plasmid DNA were added to the U87 or RG2 cells plated in 35-mm Petri dishes, and the cells were incubated up to 21 days in 2.5 ml/dish of medium with 10% FBS at 37 °C without subsequent addition of PIL/DNA after day 0. For U87 cells treated with HIR-PIL/790, the medium was changed at 3, 6, 8, 11, 14, 16, and 18 days and the cells were trypsinized and sub-cultured at 3, 8, 14 and 18 days. For RG2 cells treated with TfR MAb-PIL/790 and U87 cells treated with either HIRMAb-PIL/753 or EGFR MAb-PIL/790, the medium was changed at 3, 5, and 7 days and the cells were trypsinized and sub-cultured at 5 days. In some experiments, the medium added at day 0 containing clone 753 encapsulated in the HIRMAb-PIL was supplemented with 100 μg/mL of unconjugated HIRMAb, which was present in a 6-fold molar excess over the HIRMAb conjugated to the PIL. At the end of each incubation, cell extracts were prepared and luciferase activity was measured as described previously [10], and data reported as pg luciferase activity per mg cell protein. Based on the standard curve, 1 pg of luciferase was

equivalent to 14 312 ± 2679 relative light units (RLU), which is the mean ± S.E. of five assays.

Results

The level of luciferase gene expression using the 790 luciferase expression plasmid (Table 1) was measured in either human U87 glioma cells targeted with the HIR MAb-PIL, or rat RG2 glioma cells targeted with the TfR MAb-PIL (Figure 2). The maximum level of luciferase gene expression is 419 ± 31 pg/mg protein in the human U87 cells at 7 days after a single application of the HIRMAb-PIL/790 formulation at day 0 (Figure 2A). The peak luciferase gene expression in these cells was observed at 7 days, even though the U87 cells were typsinized and sub-cultured at 3 days of incubation (Figure 2A). In contrast, the peak level of luciferase gene expression in the rat RG2 cells, 4.1 ± 0.5 pg/mg protein, was 100-fold less following targeting of the clone 790 plasmid to these cells with the TfR MAb-PIL (Figure 2B). Luciferase gene expression in the human cells targeted with clone 790 DNA encapsulated in the HIRMAb-PIL was measureable for up to 21 days of incubation, while luciferase gene expression in the rat cells targeted with clone 790 DNA encapsulated in the TfR MAb-PIL was minimal by 10 days (Figure 2).

The high level of luciferase gene expression in the human cells targeted with the HIRMAb-PIL could be a dual function of (a) targeting the insulin receptor as opposed to the transferrin receptor and (b) the selective activation of the EBNA-1/oriP system in human cells relative to rodent cells. Therefore, luciferase gene expression was measured in the human U87 glioma cells targeted with the HIRMAb-PIL carrying the clone 753 plasmid DNA (Figure 3A). Clone 753 is similar to clone 790 except the EBNA-1/oriP system is absent in clone 753 (Table 1). The maximum level of luciferase gene expression in the U87 cells targeted with the HIRMAb-PIL/753 is 36 ± 1 pg/mg protein (Figure 3A), which is >10-fold lower than the peak gene expression achieved with the HIRMAb-PIL/790 formulation in these cells (Figure 2A). These results suggest that the very high level of luciferase gene expression shown in Figure 2A is a combined effect of targeting via the insulin receptor and the use of the EBNA-1/oriP system. To further examine the role of the targeted receptor, the clone 790 plasmid DNA was encapsulated within the EGFR MAb-PIL, and applied to the human U87 cells (Figure 3B). With the EGFR MAb-PIL/790 formulation, the luciferase gene expression was the lowest, and peaked at 1.8 ± 0.1 pg/mg protein at 3 days of incubation (Figure 3B).

The expression of the luciferase gene encapsulated within the PIL was strictly a function of the targeting specificity of the MAb, as there was no measurable gene expression with clone 753 plasmid DNA encapsulated in mIgG2a-PIL, which targets no specific cell membrane receptor (Table 2). If 100 μg/ml unconjugated HIRMAb

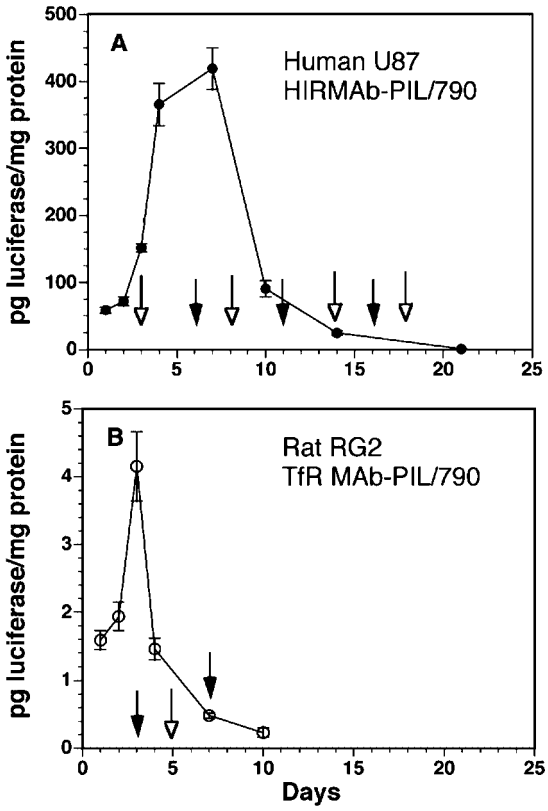

Figure 2. Luciferase gene expression in either human U87 glioma cells targeted with the HIR MAb-PIL (A) or rat RG2 glioma cells targeted with the TfR MAb-PIL gene delivery system is shown relative to the incubation time following a single addition of the PIL to the medium at day 0. The 83-14 MAb was used in the studies shown in (A) and the OX26 MAb was used in the studies reported in (B). Clone 790 plasmid DNA (Table 1) was used in both studies. The culture medium was replaced at days denoted by the closed arrows, and the cells were trypsinized and sub-cultured on days denoted by the open arrows. Data are mean ± S.D. (n = 3 dishes/time point)

were added to the medium in parallel with the HIRMAb-PIL, the peak level of luciferase gene expression was reduced by 33% (Table 2).

Discussion

The results of these studies are consistent with the following conclusions. First, targeting the human insulin

Table 2. Luciferase gene expression in human U87 glioma cells

PIL	Competing MAb	Luciferase Activity (pg/mg$_p$) 1 day	3 days	5 days
mIgG$_{2a}$-PIL	–	<0.1	<0.1	<0.1
HIRMAb-PIL	–	7.0 ± 0.9	36.2 ± 1.6	2.1 ± 0.2
HIRMAb-PIL	HIRMAb (100 μg/mL)	6.2 ± 0.3	24.3 ± 4.2	1.2 ± 0.1

Mean ± S.E. (n = 3 dishes/time point). Clone 753 (Table 1) used for all studies. There was no detectable luciferase activity in the cells incubated with the clone 753 plasmid DNA encapsulated in the mIgG$_{2a}$-PIL. The PIL was added at day 0, and the medium was changed to fresh medium (containing no DNA or PIL) at 3 days of incubation.

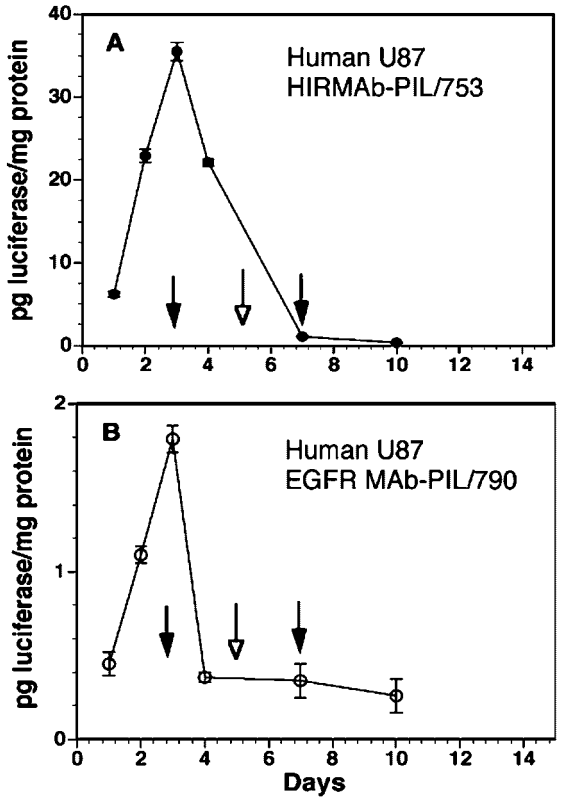

Figure 3. Luciferase gene expression in human U87 glioma cells targeted either with the HIR MAb-PIL carrying the clone 753 plasmid (A) or the EGFR MAb-PIL carrying the clone 790 plasmid (B). The PIL carrying the luciferase gene was applied only at time 0 and the culture medium was replaced at days denoted by the closed arrows. The cells were trypsinized and sub-cultured at day 5 (open arrows). Data are mean ± S.D. (n = 3 dishes/time point)

receptor results in a >100-fold increase in luciferase gene expression relative to targeting via the rat TfR or the human EGFR (Figures 2 and 3). Second, the use of the EBNA-1/oriP replication system allows for an increased persistence of gene expression in human cells, providing the plasmid is adequately delivered to the target cells (Figure 2A). Third, the targeting specificity of the PIL gene delivery system is determined solely by the targeting MAb, as there is no gene expression in cells exposed to the mIgG2a-PIL (Table 2).

The extent to which an exogenous gene is expressed in a target cell is a function of the delivery of the target gene across both the plasma membrane barrier and the nuclear membrane barrier. An exogenous gene will not be expressed if the initial plasma membrane barrier is not circumvented. However, once inside the cell, a critical step in limiting gene expression is transfer across the nuclear membrane [14,15]. Although there is no evidence that either the TfR or the EGFR delivers ligand to the nuclear compartment, there is evidence that the insulin receptor delivers ligand to the nuclear compartment. Both gold/silver enhancement electron microscopy [16] and autoradiographic electron microscopy [17] have demonstrated delivery of insulin to the nuclear compartment via the insulin receptor. Similarly, the HIRMAb also rapidly enters the nuclear compartment of human U87 cells, as demonstrated by confocal microscopy of these cells exposed to fluoresceinated HIRMAb [10]. Moreover, if plasmid DNA is fluoresceinated and then encapsulated in the interior of the HIR MAb-PIL, the plasmid DNA is localized within intranuclear vesicles at 3 h of incubation of U87 cells [10]. By 24 h of incubation, the majority of the fluoresceinated DNA within the cell is localized to the nuclear compartment of U87 cells targeted with the HIRMAb-PIL delivery system [10]. These combined studies suggest that targeting the insulin receptor system provides the highest level of expression of an exogenous gene in the cell because this receptor system targets ligands not only across the plasma membrane barrier, but also across the nuclear membrane barrier. Other receptor systems such as the basic fibroblast growth factor (bFGF) receptor system may also selectively target ligand across both the plasma membrane and the nuclear membrane barriers [18].

The present studies, in conjunction with previously reported confocal microscopy [10], show that the extent to which a given receptor-specific MAb undergoes endocytosis into the cell determines the final level of expression of the endogenous gene. If the targeting MAb, such as the mIgG2a isotype control, does not enter the cell, then there is no expression of the gene packaged in the PIL (Table 2). The receptor-mediated uptake of the MAb by the cell is initiated by ligand binding to the exofacial receptor binding site, and this binding is saturable by low-nM concentrations of ligand [19–21]. Receptor binding is followed by endocytosis, and receptor-mediated endocytosis of either the endogenous ligand or a peptidomimetic MAb, such as the HIRMAb, is non-saturable [19–21]. When the cells are exposed to the HIRMAb-PIL, the medium concentration of PIL-conjugated HIRMAb is 16 μg/ml or 100 nM (Methods), which is about 100-fold higher than the binding K_D of the HIR for either insulin or the HIRMAb [19–21]. The addition of 600 nM unconjugated HIRMAb exerts only a modest inhibitory effect on luciferase gene expression mediated by the HIRMAb-PIL (Table 2), because the medium concentration of the HIRMAb in the form of the PIL is 100 nM (Methods), which is also in the high-nM range. The relative insensitivity of the receptor-mediated gene delivery system to high-nM concentrations of competing ligand in the medium arises from the non-saturability of the insulin receptor endocytosis pathway [19–21].

The EBNA-1/oriP system plays a prominent role in controlling the level of gene expression in the target cells, providing the plasmid DNA is adequately delivered to the nuclear compartment. Both the 753 plasmid and the 790 plasmid were targeted to human U87 cells with the HIRMAb-PIL gene delivery system. These plasmids are similar with the exception that the clone 790 contains the EBNA-1/oriP system whereas clone 753 lacks these elements (Table 1). The EBNA-1 trans element produces a homodimeric protein that binds the oriP cis element and allows for one round of replication

for each mitotic division [9]. The EBNA-1/oriP system is selectively active in humans and primates and is less active in rodents [22], and this species specificity is corroborated by findings of the present study. The level of luciferase gene expression is low and peaks at 4.1 ± 0.5 pg/mg protein in the rat RG2 cells that are targeted with clone 790 using the TfR MAb-PIL gene delivery system (Figure 2B). This level of luciferase gene expression is comparable to that found *in vivo* in the mouse following the intravenous administration of the TfR MAb-PIL formulation [5]. Conversely, when the clone 790 plasmid is delivered to U87 cells via the HIRMAb-PIL, there is a >100-fold increase in luciferase gene expression, and gene expression continues to increase with time in these cells despite trypsinization and sub-culture of the cells at 3 days of incubation (Figure 2A). These results indicate the plasmid DNA replicates with early cell division subsequent to delivery to the nuclear compartment by the HIRMAb. In contrast, the level of luciferase gene expression decreases in the U87 cells exposed to the HIRMAb-PIL carrying the clone 753 plasmid after sub-culture of the cells (Figure 3A), because this plasmid lacks the EBNA-1/oriP system (Table 1), and the capability of episomal replication [22].

The level of luciferase gene expression in human U87 cells targeted with clone 790 and the HIRMAb-PIL system peaks at 419 ± 31 pg/mg protein at 7 days after a single addition of the formulation to the medium at day 0 (Figure 2A). In contrast, the level of luciferase gene expression in liver or spleen of mice injected with a luciferase gene incorporated in a lentiviral gene delivery system ranges from 3–11 pg/mg protein [23], assuming 180 mg protein/g tissue. These values of luciferase gene expression with a lentiviral vector *in vivo* are comparable to the levels of gene expression achieved with the nonviral PIL gene delivery system in mice *in vivo*, which target either the TfR or HIR [5,11].

In summary, the present studies provide evidence that the choice of the targeting ligand is an important factor in determining the level of expression of an exogenous gene that is delivered to cells with an artificial virus that accesses a receptor-mediated endocytosis system (Figure 1). The insulin receptor is a preferred pathway for delivery of exogenous genes to cells, owing to the nuclear targeting characteristics of the insulin receptor system [10]. In addition, the expression of the exogenous gene in human cells is augmented by the addition of the EBNA-1/oriP cis/trans elements that allow for episomal replication of the plasmid DNA. These findings suggest that the organ specificity and duration of trans-gene expression can be regulated by (a) the receptor-specificity of the targeting ligand attached to the PIL (Figure 1), and (b) gene elements incorporated within the plasmid that enable episomal replication of the plasmid DNA (Table 1). The tissue specificity of exogenous gene expression *in vivo* can be further regulated with the use of tissue-specific gene promoters [5]. The persistence of the expression of the trans-gene within the target cell after a single administration is sufficient to achieve pharmacological effects with weekly intravenous gene therapy using the nonviral PIL gene targeting technology [11].

Acknowledgements

This work was supported by grants from the University of California, Davis/Medical Investigation of Neurodevelopmental Disorders Institute Research Program, and the U.S. Dept. of Defense.

References

1. Garnett MC. Gene-delivery systems using cationic polymers. *Crit Rev Ther Drug Carrier Systems* 1999; **16**: 147–207.
2. Kwoh DY, Coffin DC, Lollo CP, *et al*. Stabilization of poly-L-lysine/DNA polyplexes for in vivo gene delivery to the liver. *Biochim Biophys Acta* 1999; **1444**: 171–190.
3. Shi N, Pardridge WM. Non-invasive gene targeting to the brain. *Proc Natl Acad Sci U S A* 2000; **97**: 7567–7572.
4. Shi N, Boado RJ, Pardridge WM. Receptor-mediated gene targeting to tissues in the rat in vivo. *Pharm Res* 2001; **18**: 1091–1095.
5. Shi N, Zhang Y, Boado RJ, Zhu C, Pardridge WM. Brain-specific expression of an exogenous gene following intravenous administration. *Proc Natl Acad Sci U S A* 2001; **98**: 12 754–12 759.
6. Chonn A, Semple SC, Cullis PR. Association of blood proteins with large unilamellar liposomes in vivo. *J Biol Chem* 1992; **267**: 18 759–18 765.
7. Papahadjopoulos D, Allen TM, Gabizon A, *et al*. Sterically stabilized liposomes: improvements in pharmacokinetics and antitumor therapeutic efficacy. *Proc Natl Acad Sci U S A* 1991; **88**: 11 460–11 464.
8. Huwyler J, Wu D, Pardridge WM. Brain drug delivery of small molecules using immunoliposomes. *Proc Natl Acad Sci U S A* 1996; **93**: 14 164–14 169.
9. Haan KM, Aiyar A, Longnecker R. Establishment of latent Epstein-Barr virus infection and stable episomal maintenance in murine B-cell lines. 2001; *J Virol* **75**: 3016–3020.
10. Zhang Y, Lee HJ, Boado RJ, Pardridge WM. Receptor-mediated delivery of an antisense gene to human brain cancer cells. *J Gene Med* 2002; **4**: 183–194.
11. Zhang Y, Zhu C, Pardridge WM. Antisense gene therapy of brain cancer with an artificial virus gene delivery system. *Mol Ther* 2002; **6**: 67–72.
12. Boado RJ, Pardridge WM. Ten nucleotide cis element in the 3′-untranslated region of the GLUT1 glucose transporter mRNA increases gene expression via mRNA stabilization. *Mol Brain Res* 1998; **59**: 109–113.
13. Kang YS, Pardridge WM. Use of neutral-avidin improves pharmacokinetics and brain delivery of biotin bound to an avidin-monoclonal antibody conjugate. *J Pharmol Exp Ther* 1994; **269**: 344–350.
14. Pollard H, Remy J-S, Loussouarn G, Demolombe S, Behr J-P, Escande D. Polyethylenimine but not cationic lipids promotes transgene delivery to the nucleus in mammalian cells. *J Biol Chem* 1998; **273**: 7507–7511.
15. Tachibana R, Harashima H, Shinohara Y, Kiwada H. Quantitative studies on the nuclear transport of plasmid DNA and gene expression employing nonviral vectors. *Adv Drug Del Rev* 2001; **52**: 219–225.
16. Shah N, Zhang S, Harada S, Smith RM, Jarett L. Electron microscopic visualization of insulin translocation into the cytoplasm and nuclei of intact H35 hepatoma cells using covalently linked nanogold-insulin. *Endocrinology* 1995; **136**: 2825–2835.
17. Podlecki DA, Smith RM, Kao M, *et al*. Nuclear translocation of the insulin receptor. A possible mediator of insulin's long term effects. *J Biol Chem* 1987; **262**: 3362–3368.
18. He D, Casscells W, Engler D. Nuclear accumulation of exogenous DNA fragments in viable cells mediated by FGF-2 and DNA release upon cellular injury. *Exp Cell Res* 2001; **265**: 31–45.

19. Pardridge WM, Eisenberg J, Yang J. Human blood-brain barrier insulin receptor. *J Neurochem* 1985; **44**: 1771–1778.
20. Paccaud J-P, Siddle K, Carpentier J-L. Internalization of the human insulin receptor. *J Biol Chem* 1992; **267**: 13101–13106.
21. Pardridge WM, Kang Y-S, Buciak JL, Yang J. Human insulin receptor monoclonal antibody undergoes high affinity binding to human brain capillaries in vitro and rapid transcytosis through the blood-brain barrier in vivo in the primate. *Pharm Res* 1995; **12**: 807–815.
22. Makrides S. Components of vectors for gene transfer and expression in mammalian cells. *Protein Expr Purif* 1999; **17**: 181–202.
23. Peng KW, Pham L, Ye H, *et al*. Organ distribution of gene expression after intravenous infusion of targeted and untargeted lentiviral vectors. *Gene Ther* 2001; **8**: 1456–1463.

HUMAN GENE THERAPY 14:1–12 (January 1, 2003)

Intravenous Nonviral Gene Therapy Causes Normalization of Striatal Tyrosine Hydroxylase and Reversal of Motor Impairment in Experimental Parkinsonism

YUN ZHANG, FREDERIC CALON, CHUNNI ZHU, RUBEN J. BOADO, and WILLIAM M. PARDRIDGE

ABSTRACT

Brain gene-targeting technology is used to reversibly normalize tyrosine hydroxylase (TH) activity in the striatum of adult rats, using the experimental 6-hydroxydopamine model of Parkinson's disease. The TH expression plasmid is encapsulated inside an 85-nm PEGylated immunoliposome (PIL) that is targeted with either the OX26 murine monoclonal antibody (MAb) to the rat transferrin receptor (TfR) or with the mouse IgG2a isotype control antibody. TfRMAb–PIL, or mIgG2a–PIL, is injected intravenously at a dose of 10 μg of plasmid DNA per rat. TfRMAb–PIL, but not mIgG2a–PIL, enters the brain via the transvascular route. The targeting TfRMAb enables the nanocontainer carrying the gene to undergo both receptor-mediated transcytosis across the blood–brain barrier (BBB) and receptor-mediated endocytosis into neurons behind the BBB by accessing the TfR. With this approach, the striatal TH activity ipsilateral to the intracerebral injection of the neurotoxin was normalized and increased from 738 ± 179 to 5486 ± 899 pmol/hr per milligram of protein. The TH enzyme activity measurements were corroborated by TH immunocytochemistry, which showed that the entire striatum was immunoreactive for TH after intravenous gene therapy. The normalization of striatal biochemistry was associated with a reversal of apomorphine-induced rotation behavior. Lesioned animals treated with the apomorphine exhibited 20 ± 5 and 6 ± 2 rotations/min, respectively, after intravenous administration of the TH plasmid encapsulated in mIgG2a–PIL and TfRMAb–PIL. These studies demonstrate that it is possible to normalize brain enzyme activity by intravenous administration and nonviral gene transfer.

OVERVIEW SUMMARY

Parkinson's disease (PD) results from neurodegeneration in the nigral–striatal pathway of the brain, leading to a deficiency in the striatum of tyrosine hydroxylase (TH), the rate-limiting enzyme in dopamine synthesis. One strategy for gene therapy of PD is the restoration of striatal TH activity. The present work uses the experimental 6-hydroxydopamine model of PD, which causes a 90% reduction in striatal TH enzyme activity ipsilateral to the intracerebral toxin injection. Lesioned rats are treated with a nonviral TH expression plasmid administered intravenously. The TH gene is encapsulated in an "artificial virus" composed of 85-nm PEGylated immunoliposomes targeted to the brain with a monoclonal antibody to the rat transferrin receptor. The targeted nonviral gene transfer enables delivery of the therapeutic gene across the blood–brain barrier and across the neuronal plasma membrane. Three days after a single intravenous administration of the TH gene, the striatal TH activity is normalized in association with a 70% reduction in apomorphine-induced rotation behavior.

INTRODUCTION

GENE THERAPY of Parkinson's disease (PD) aims to prevent striatal neurodegeneration and restore striatal tyrosine hydroxylase (TH) enzyme activity (Mouradian and Chase, 1997; Mandel *et al.*, 1999). Striatal TH enzyme activity is partially restored in experimental models of PD by intracerebral injection of viral vectors encoding the TH gene (During *et al.*, 1994; Kaplitt *et al.*, 1994; Mandel *et al.*, 1998). However, viral vectors must be administered intracerebrally via penetration of the skull bone. The viruses cannot be administered intravenously

Department of Medicine, University of California, Los Angeles School of Medicine, Los Angeles, CA 90024.

because the viruses do not cross the brain capillary endothelial wall, which forms the blood–brain barrier (BBB) *in vivo*. The intracerebral injection of the viral vector causes transduction of a small part of the striatum at the tip of the injection needle. Higher fractions of the striatum may be transduced by multiple injections of high viral titers in either rat brain (Leone *et al.*, 2000; Kirik *et al.*, 2002) or primate brain (Bankiewicz *et al.*, 2000; Kordower *et al.*, 2000).

The entire volume of the striatum may be transduced after transvascular delivery of the therapeutic gene subsequent to intravenous administration of the gene. The transvascular route to the striatum would be possible with the development of a gene-targeting system that is capable of transport across the BBB. Gene-targeting technology has been developed that enables widespread expression within the brain of nonviral plasmid DNA after intravenous administration (Shi *et al.*, 2000, 2001a,b). Plasmid DNA encoding the therapeutic gene is encapsulated inside a nanocontainer composed of a PEGylated immunoliposome (PIL), which is targeted across both the BBB and the neuronal cell membrane by receptor-specific monoclonal antibodies (MAbs). Delivery of the therapeutic gene across the BBB has the potential to transduce virtually every cell of the striatum, because every neuron in the brain is perfused by its own blood vessel. With the PIL gene-targeting system, it is possible to deliver an exogenous gene throughout the entire CNS after intravenous administration. Gene expression can be restricted to the brain by the use of brain-specific promoters (Shi *et al.*, 2001a). Prior work with this gene-targeting technology yielded a therapeutic result in an experimental brain cancer model, with a 100% increase in survival time for the animals treated by intravenous antisense gene therapy (Zhang *et al.*, 2002a). The present studies attempt to normalize the striatal TH activity and motor impairment in the experimental 6-hydroxydopamine model of PD in the rat. The full-length rat TH cDNA is incorporated in a pGL2-derived expression plasmid that is driven by the simian virus 40 (SV40) promoter and contains a cis stabilizing element in the 3′-untranslated region (UTR) of the mRNA. The plasmid DNA is encapsulated in the interior of the PIL, which is targeted to brain with the murine OX26 MAb to the rat transferrin receptor (TfR). Owing to the expression of the TfR at both the rodent and human BBB (Jefferies *et al.*, 1984; Pardridge *et al.*, 1987) and the neuronal plasma membrane (Mash *et al.*, 1991), TfRMAb-targeted PIL undergoes receptor-mediated transcytosis across the BBB followed by receptor-mediated endocytosis into neurons behind the BBB.

MATERIALS AND METHODS

Materials

1-Palmitoyl-2-oleoyl-*sn*-glycerol-3-phosphocholine(POPC) and didodecyldimethylammonium bromide (DDAB) were purchased from Avanti-Polar Lipids (Alabaster, AL). Distearoylphosphatidylethanolamine (DSPE)–PEG 2000 was obtained from Shearwater Polymers (Huntsville, AL), where PEG 2000 is 2000-Da polyethylene glycol. DSPE–PEG 2000–maleimide (MAL) was custom synthesized by Shearwater Polymers. [α-^{32}P]dCTP (3000 Ci/mmol) and L-[3,5-^{3}H]tyrosine (51.5 Ci/mmol) were from NEN Life Science Products (Boston, MA). *N*-Succinimidyl[2,3-^{3}H]propionate ([^{3}H]NSP, 101 Ci/mmol) and protein G–Sepharose CL-4B were purchased from Amersham Pharmacia Biotech (Arlington Heights, IL). The nick translation system was from Life Technologies (Rockville, MA). 6-Hydroxydopomine (6-OHDA), apomorphine, pargyline, catalase, (6*R*)-5,6,7,8-tetrahydrobiopterin (BH_4), β-NADPH, L-tyrosine, charcoal, the mouse MAb against rat tyrosine hydroxylase, horse serum, mouse IgG1 isotype control, and glycerol–gelatin were purchased from Sigma (St. Louis, MO); 2-iminothiolane (Traut's reagent) and bicinchoninic acid (BCA) protein assay reagents were obtained from Pierce (Rockford, IL). Mouse myeloma ascites containing mouse IgG2a (mIgG2a) isotype control was from the Cappel Division of ICN Pharmaceuticals (Aurora, OH). The anti-transferrin receptor monoclonal antibody (TfRMAb) used in these studies is the murine OX26 MAb to the rat TfR, which is a mouse IgG2a. The OX26 MAb is specific for the rat TfR, and is not active in human cells. The anti-insulin receptor MAb used for gene targeting to human cells is the murine 83-14 MAb to the human insulin receptor (HIR). TfRMAb, HIRMAb, and mIgG2a were individually purified by protein G affinity chromatography from hybridoma-generated ascites. COS-1 cells were obtained from the American Type Culture Collection (Manassas, VA). The biotinylated horse anti-mouse IgG, Vectastain ABC kit, 3-amino-9-ethylcarbazole (AEC) substrate kit, peroxidase kit, and hematoxylin QS counterstain were purchased from Vector Laboratories (Burlingame, CA). Optimal cutting temperature (O.C.T.) compound (Tissue-Tek) was purchased from Sakura FineTek (Torrance, CA). LipofectAMINE was obtained from Invitrogen (San Diego, CA).

Construction of tyrosine hydroxylase expression plasmids

The complete open reading frame (ORF) of rat (r) TH in the pBabe plasmid was obtained from D. Bredesen (Buck Center, Novato, CA) (Anton *et al.*, 1994). The rat TH ORF was isolated by double digestion with *Dra*I and *Acc*65I, which cleaved at sites located 26 nucleotides upstream and 13 nucleotides downstream of the rat TH ORF, respectively. The ~1.5-kb rTH fragment was purified by gel electrophoresis followed by centrifugation with a Spin-X filter unit (Costar; Corning, Acton, MA). The DNA was blunt ended with Klenow DNA polymerase, and subcloned in Bluescript (pBS; Stratagene, San Diego, CA) at the *Eco*RV site to form a plasmid named pBS-rTH. The identity of rat TH and its orientation in pBS-rTH were determined by DNA sequencing, using M13 forward and reverse primers. The rat TH cDNA was subcloned in pGL2 promoter-derived mammalian expression vectors described previously and designated clones 734 and 753 (Dwyer *et al.*, 1996). The pGL2 promoter plasmid was obtained from Promega (Madison, WI), and the pGL2-derived clones are driven by the SV40 promoter; clone 753 contains a 200-nucleotide cis element taken from nucleotides 2100–2300 of the bovine GLUT1 mRNA 3′-untranslated region (UTR), which causes stabilization of the mRNA (Boado and Pardridge, 1998). pBS-TH was linearized with *Not*I and blunt ended with Klenow DNA polymerase. The 1.5-kb rat TH was released with *Hin*dIII and purified by gel electrophoresis and Spin-X centrifugation. In par-

allel, the luciferase reporter gene in clones 734 and 753 was deleted with *Hin*dIII and *Eco*NI (blunt) and purified. The rat TH DNA fragment was ligated into clones 734 and 753 with T4 DNA ligase and *Escherichia coli* DH5α was transformed. Positive clones were investigated by restriction endonuclease mapping using *Pst*I, which releases the TH insert, and DNA sequencing, using the pGL2-1 sequencing primer (Promega). The pGL2-rTH expression vector derived from clone 734 was designated clone 878, and the pGL2-rTH expression vector containing the GLUT1 cis-stabilizing sequence, and derived from clone 753, was designated clone 877. The SV40-rTH expression cassettes were released from clones 877 and 878 and further subcloned in the pCEP4 expression vector to form clones 908 and 883, respectively. The pCEP4 vectors contain the Epstein–Barr virus replication origin (oriP) and nuclear antigen (EBNA-1), which enable extrachromosomal replication in human cells. Clones 877 and 878 were digested with *Xho*I, *Sal*I, and *Sca*I to release the ~2.9-kb SV40-rTH fragments. In parallel, the pCEP4 vector was digested with *Sal*I and *Xho*I to release the CMV-cassette and purified as previously described (Boado and Pardridge, 1998). The SV40-rTH expression cassettes were ligated into pCEP4. Positive clones were identified by restriction endonuclease mapping with *Nru*I and *Hin*dIII, and confirmed by DNA sequencing as previously described for GLUT1 reporter genes (Boado and Pardridge, 1998). All four TH expression plasmids (877, 878, 883, and 908) are driven by the SV40 promoter. Clones 877 and 908 contain the GLUT1 3′-UTR cis stabilizing element, and clones 883 and 908 contain the EBNA-1/oriP cis/trans elements for extrachromosomal replication in human cells. The pGL2-derived TH clones, 877 and 878, are approximately 6.0 kb in size, and the pCEP4-derived TH clones, 883 and 908, are approximately 11.0 kb in size (Boado and Pardridge, 1998). Maxiprep DNA was purified and plasmid DNA was ^{32}P labeled as described previously (Zhang *et al.*, 2002b).

Expression of the TH gene in cell culture was first evaluated by LipofectAMINE transfection of either C6 rat glial cells or COS-1 cells, which were cultivated in Dulbecco's modified Eagle's medium (DMEM) with 10% calf serum or in DMEM with high glucose (4.5 g/liter) and 10% fetal bovine serum (FBS), respectively. Plasmid DNA was amplified with a QIAfilter plasmid Maxiprep kit (Qiagen, Chatsworth, CA) and COS-1 or C6 glial cells were transfected with LipofectAMINE as described previously (Shusta *et al.*, 2002). Cells were seeded on 60- or 100-mm dishes at a density of 80,000 cells/cm^2 and the LipofectAMINE–plasmid DNA (10:1, w/w) was added in medium without serum for 4 hr. The complex was then removed, and fresh medium with serum was added and the cells were incubated for 48 hr before extraction and measurement of TH enzyme activity as described below.

PEGylated liposome synthesis and plasmid DNA encapsulation

POPC (18.8 μmol), DDAB (0.4 μmol), DSPE–PEG 2000 (0.6 μmol), and DSPE-PEG 2000-maleimide (0.2 μmol) were dissolved in chloroform followed by evaporation, as described previously (Zhang *et al.*, 2002b). The lipids were dispersed in 0.2 ml of 0.05 *M* Tris-HCl buffer (pH 7.0) and vortexed for 1 min followed by 2 min of bath sonication. Supercoiled DNA was ^{32}P labeled with [α-^{32}P]dCTP by nick translation as described previously (Shi *et al.*, 2000). Unlabeled plasmid DNA (250 μg) and 1 μCi of ^{32}P-labeled plasmid DNA were added to the lipids. The dispersion was frozen in ethanol–dry ice for 5 min and thawed at room temperature for 25 min, and this freeze–thaw cycle was repeated five times to produce large vesicles with the DNA loosely entrapped inside. The large vesicles were converted into small (85-nm-diameter) liposomes by extrusion. The liposome dispersion was diluted to a lipid concentration of 40 m*M*, followed by extrusion five times each through two stacks each of 200- and 100-nm pore size polycarbonate membranes, by using a hand-held LipoFast-Basic extruder (Avestin, Ottawa, Canada), as described previously (Shi *et al.*, 2001a). The mean vesicle diameters were determined by quasielastic light scattering by using a Microtrac ultrafine particle analyzer (Leeds-Northrup, St. Petersburg, FL), as described previously (Huwyler *et al.*, 1996).

Approximately half of the DNA is interiorized in the small liposomes and about half is exteriorized. The plasmid DNA absorbed to the exterior of the liposomes was quantitatively removed by nuclease digestion (Shi *et al.*, 2000). For digestion of the unencapsulated DNA, 5 units of pancreatic endonuclease I and 5 units of exonuclease III were added in 5 m*M* $MgCl_2$ to the liposome–DNA mixture after extrusion (Monnard *et al.*, 1997). After incubation at 37°C for 1 hr, the reaction was stopped by adding 20 m*M* EDTA. The extent to which the nuclease digestion removed the exteriorized plasmid DNA was determined by agarose gel electrophoresis and ethidium bromide staining of aliquots taken before and after nuclease treatment, as described previously (Shi *et al.*, 2000). The entrapped plasmid DNA is completely resistant to high local concentrations of nuclease. The DNA encapsulated within the PEGylated liposome is designated PEGylated liposome–DNA.

MAb conjugation to the PEGylated liposome–DNA

TfRMAb, HIRMAb, or mIgG2a was thiolated and individually conjugated to the MAL moiety of the PEGylated liposome–DNA to produce a PEGylated immunoliposome (PIL) with the desired receptor (R) specificity. PIL conjugated with the OX26 MAb is designated TfRMAb–PIL and PIL conjugated with the mIgG2a isotype control is designated mIgG2a–PIL. Either MAb or mIgG2a was radiolabeled with [^{3}H]NSP as described previously (Pardridge *et al.*, 1992). ^{3}H-Labeled MAb had a specific activity of >0.11 μCi/μg and a trichloroacetic acid (TCA) precipitability of >97%. The MAb (3.0 mg, 20 nmol) was thiolated with a 40:1 molar excess of 2-iminothiolane (Traut's reagent), as described previously (Huwyler *et al.*, 1996). The thiolated MAb, which contained a trace amount of ^{3}H-labeled MAb, was conjugated to the PEGylated liposome overnight and unconjugated MAb (and oligonucleotides produced by nuclease treatment) were separated from the PIL by Sepharose CL-4B column chromatography as described previously (Shi *et al.*, 2000). The number of MAb molecules conjugated per liposome was calculated from the total ^{3}H-labeled MAb counts per minute in the liposome pool and the specific activity of the labeled MAb, assuming 100,000 lipid molecules per liposome, as described previously (Zhang *et al.*, 2002b). The average number of MAb molecules conjugated per liposome was 52 ± 8 (mean ± SD, n = 4 syn-

theses). The final percentage entrapment of 250 μg of plasmid DNA in the liposome preparation was computed from the ^{32}P radioactivity and was 35.6 ± 2.1% (mean ± SD, $n = 4$ synthesis), or 89 μg of plasmid DNA

The PIL solution was sterilized for use in tissue culture by passage through a 0.22-μm pore size Millex-GV filter (Millipore, Bedford, MA). The PIL is not structurally altered by this filtration step (Zhang *et al.*, 2002b).

Electron microscopy

IgG-conjugated PIL carrying plasmid DNA was examined with a conjugate of 10-nm gold and a goat anti-mouse secondary antibody (G7652; Sigma). A 5-μl aliquot of the 83-14–PIL (5×10^{12} liposome-conjugated MAbs) was incubated with 72 μl of IgG–gold conjugate (1×10^{12} gold particles) for 1 hr in 0.05 *M* Tris-buffered saline, pH 6.9, with 0.7% bovine serum albumin, 5% FBS, and 12% glycerol in a total volume of 125 μl. Gold-conjugated secondary antibody bound to the PIL was separated from unbound gold conjugate by passage through a 0.7 × 10 cm column of Sepharose CL-4B (Bio-Rad, Hercules, CA). An aliquot (10 μl) of the eluate was applied to Formvar-coated 2000 mesh copper grids, washed twice with 0.05 *M* Tris–0.15 *M* NaCl, pH 7.4, counterstained with 2% uranyl acetate for 1 min, and then examined directly by electron microscopy using a JEOL JEM-100CX II electron microscope at 80 kV. Negatives, taken at a magnification of ×29,000, were scanned and enlarged in Adobe Photoshop 5.5 on a G4 Power Macintosh.

TH gene expression in cultured brain cells with the PIL gene-targeting system

Human U87 glioma cells or rat RG-2 glioma cells were plated on 60-mm collagen-treated dishes with minimal essential medium (MEM) or with F12 Ham's medium containing 10% FBS, respectively. When the cells reached 60% confluence, the medium was removed by aspiration, and 6 ml of fresh medium containing 10% FBS was added to the cells, followed by the addition of 142 μl of HIRMAb–PIL carrying clone 877 DNA (4 μg of plasmid DNA per dish) or TfRMAb–PIL carrying clone 877 DNA (4 μg of plasmid DNA per dish). The cells were incubated for 2, 4, or 6 days, with three dishes at each time point, for measurement of TH enzyme activity. This time course was based on prior work describing the temporal changes in gene expression in cultured cells exposed to TfRMA-targeted PEGylated liposomes (Zhang *et al.*, 2003).

6-Hydroxydopamine model

Adult male Sprague-Dawley rats (supplied by Harlan Breeders, Indianapolis, IN) weighing 200–250 g were anesthetized with ketamine (50 mg/kg) and xylazine (4 mg/kg) intraperitoneally. Animals received unilateral 6-OHDA injections into the right medial forebrain bundle (Armstrong *et al.*, 2002; Meshul *et al.*, 2002). Each animal received pargyline 30–60 min before surgery (50 mg/kg in normal saline, administered intraperitoneally). After pargyline administration, 4 μl of 6-OHDA (2 μg/μl; prepared freshly in ascorbic acid [0.2 μg/μl]) was injected over a 4-min period with a 10-μl Hamilton syringe, using the following stereotaxic coordinates: −4.4 mm anterior to the bregma, −1.0 mm lateral to the bregma, and 7.8 mm below the dura. The syringe needle was left in place for 2 min after the injection to allow for diffusion of the toxin. Three weeks after the lesion had been made, rats were tested for apomorphine-induced contralateral turning, using apomorphine (0.5 mg/kg) injected intraperitoneally. Full (360°), contralateral rotations only were counted over 20 min, starting 5 min after apomorphine administration, and rats turning more than 120 times in 20 min, or 6 rotations/min (rpm), were treated 1 week later by TH gene therapy. Rats were individually identified so that the rotations per minute 1 week before and 3 days after treatment could be compared for each rat.

For each experiment, successfully lesioned rats were divided into two groups: (1) control group—each rat received 10 μg of clone 877 DNA encapsulated in mIgG2a–PIL; (2) treatment group—each rat received 1, 5, or 10 μg of clone 877 DNA encapsulated in TfRMAb–PIL. PIL was administered via the femoral vein; 3 days later the rats were tested for apomorphine-induced rotation behavior and then killed. In each group, rat brains were removed and used for either TH immunocytochemistry assays or TH biochemistry assays. A time–response study was performed, wherein animals were not killed until 6 and 9 days after the single intravenous injection of clone 877 DNA encapsulated in TfRMAb–PIL. A dose–response study was also performed, wherein animals were killed 3 days after the single intravenous injection of clone 877 DNA encapsulated in TfRMAb–PIL at a dose of 1, 5, or 10 μg of DNA per rat. In these animals, the brain was removed for measurement of TH enzyme activity in the contralateral and ispsilateral striatum.

Tyrosine hydroxylase assay

The TH activity assay was performed according to Reinhard *et al.* (1986) and Horellou *et al.* (1989), with modifications. TH converts L-[3,5-^{3}H]tyrosine to both ^3H_2O and L-dopa in a 1:1 stoichiometric relationship, and the two metabolites are separated by charcoal, which selectively binds the amino acids. For cultured cells, at the end of incubation, the growth medium was removed. The cells were washed three times with cold wash buffer (5 m*M* potassium phosphate buffer), and then 400 μl of sonication buffer (wash buffer with 0.2% Triton X-100) was added to each dish. The cells were collected and, after a short vortex, the cells were sonicated for 30 sec with a Branson Ultrasonics (Danbury, CT) sonifier cell disruptor model 185. The cell homogenate was centrifuged at 10,000 × *g* for 10 min at 4°C, and the supernatant was removed for TH assays. For TH assays in rat organs, the liver, the frontal cortex, and the dorsal striatum in both lesioned (ipsilateral) and nonlesioned (contralateral) sides of brain were frozen in dry ice. The tissue was transferred to a chilled glass tissue grinder containing 0.5 ml of cold wash buffer, and was homogenized with 10–15 strokes at 4°C followed by centrifugation at 10,000 × *g* for 20 min, and the supernatant was removed for TH assays.

The tissue supernatants (200 μl) were added to 100 μl of assay buffer [final concentration 0.5 m*M* NADPH, 1 m*M* BH_4, 2600 units of catalase, 20 μM $Fe(NH_4)_2(SO_4)_2$, 10 μM L-tyrosine, L-[^{3}H]tyrosine [40–50 μCi/ml], 50 m*M* potassium phos-

phate] to start the incubation at 37°C for 45 min. The reaction was stopped by the addition of 1 ml of 7.5% charcoal in 1.0 *M* HCl. The mixture was vortexed for 2 sec and centrifuged at 500 × *g* for 10 min. The supernatant was counted for the radioactivity of the ^3H_2O product, using a Packard (Meriden, CT) Tri-Carb 2100TR liquid scintillation analyzer. The supernatant radioactivity was measured in parallel with assays blanks, and all assay measurements were at least 10-fold above the assay blank. The protein concentration in the cell extract was determined with the BCA protein assay reagent. The counts per minute were converted to picomoles of L-dopa on the basis of the [^{3}H]tyrosine specific activity, and the results were expressed as picomoles of L-dopa per hour per milligram protein.

Immunocytochemistry

Tyrosine hydroxylase immunocytochemistry was performed by the avidin–biotin complex (ABC) immunoperoxidase method (Vector Laboratories). Brains were removed immediately after sacrifice, cut through the striatum into coronal slabs, embedded in O.C.T. medium, and frozen in dry ice powder. Frozen sections (20 μm) of rat brain were cut on a Mikron HM505E cryostat, and were fixed in 4% paraformaldehyde for 20 min at 4°C. Endogenous peroxidase was blocked with 0.3% H_2O_2 in 0.3% horse serum–phosphate-buffered saline (PBS) for 30 min. Nonspecific binding of proteins was blocked with 10% horse serum in 0.1% Triton X-100–PBS for 30 min. Sections were then incubated in either mouse anti-TH MAb (0.2 μg/ml) or mouse IgG1 isotype control (0.2 μg/ml) overnight at 4°C. After wash in PBS, sections were incubated in biotinylated horse anti-mouse IgG for 30 min and then in ABC for 30 min. After development in AEC, sections were mounted with glycerol–gelatin with or without light counterstaining with hematoxylin.

Statistical analyses

Statistically significant differences in TH enzyme activity in different brain regions and treatment groups were determined by analysis of variance (ANOVA) with the Bonferroni correction, using program 7D of the BMDP Statistical Software package developed by the UCLA Biomedical Computing Series. A p value of <0.05 was considered significant.

RESULTS

Evaluation of TH expression plasmid activity in COS cells and C6 glioma cells transfected with LipofectAMINE

The four TH expression plasmids were combined with the LipofectAMINE and individually added to either COS-1 or C6 rat glioma cells, and TH enzyme activity was measured 48 hr later (Fig. 1). A similar pattern of TH gene expression was observed in both cell lines, although the TH enzyme activity in COS-1 cells was 10-fold greater than in C6 cells, consistent with the selective activation of genes driven by the SV40 promoter in COS-1 cells. In either cell line, pGL2-derived plasmid 877 produced the highest level of TH enzyme activity. Therefore, clone 877 was selected for subsequent encapsulation in TfRMAb–PIL for *in vivo* gene therapy in rats with experimentally induced PD.

Transfection of cultured cells with the PIL gene-targeting system

The encapsulation of clone 877 plasmid DNA within the PIL gene-targeting system is depicted in Fig. 2A. The targeting MAb molecules tethered to the tips of the PEG strands on the

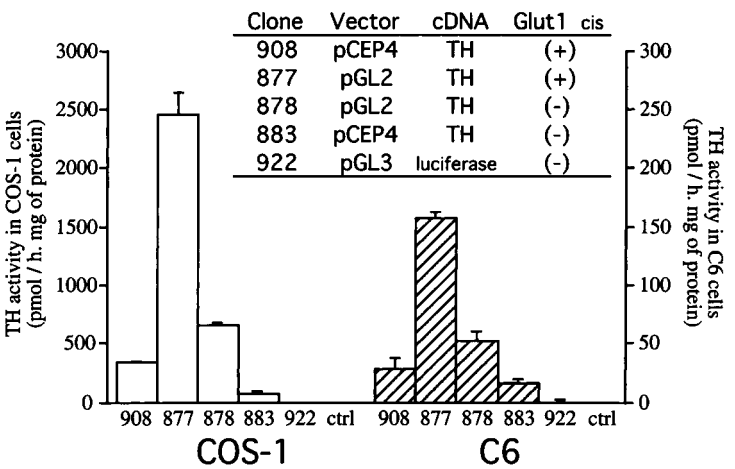

FIG. 1. Tyrosine hydroxylase (TH) activity in either COS-1 cells or C6 rat glioma cells transfected with one of five different expression plasmids in cell culture with LipofectAMINE. Clones 883 and 908 are derived from pCEP4, which contains EBNA1/oriP elements, and clones 877 and 878 are derived from pGL2, which lacks the EBNA1/oriP elements. Clones 877 and 908 contain a 200-base pair cis element taken from the 3′-untranslated region (UTR) of the GLUT1 glucose transporter mRNA, and this cis element causes stabilization of the transcript (Boado and Pardridge, 1998). Clone 922 is a pGL3 luciferase expression plasmid and this clone produced no measurable TH enzyme activity in either cell line (control, ctrl). Data represent means ± SE (n = 4 dishes per point).

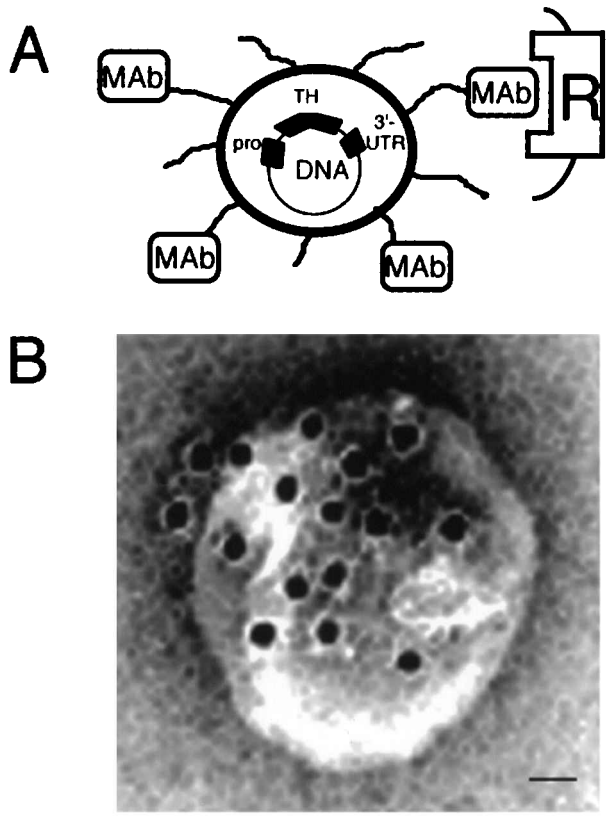

FIG. 2. (**A**) Plasmid DNA encapsulated in the interior of the PEGylated immunoliposome (PIL) with a receptor (R)-specific targeting monoclonal antibody (MAb). The targeting MAb is conjugated to 1–2% of the polyethylene glycol (PEG) strands that project from the surface of the liposome. There are about 2000 strands of 2000-Da PEG conjugated to the liposome surface. The PEG strands inhibit uptake of the PIL by the reticuloendothelial systems *in vivo* and prolong the blood residence time of the PIL *in vivo* (Shi *et al.*, 2000). The tyrosine hydroxylase (TH) gene is driven by an SV40 promoter (pro) and contains a cis-stabilizing element in the 3′-untranslated region (UTR). (**B**) Transmission electron microscopy of a PIL. The mouse IgG molecules tethered to the tips of the 2000-*Da* polyethylene glycol (PEG) are bound by a conjugate of 10-nm gold and an anti-mouse secondary antibody. The position of the gold particles illustrates the relationship of the PEG-extended MAb and the liposome. Magnification bar: 20 nm.

PIL are visualized by electron microscopy, using an anti-mouse secondary antibody conjugated with 10-nm gold (Fig. 2B). Because the targeting MAb molecules are species specific (Zhang *et al.*, 2002c), clone 877 plasmid DNA was targeted to human U87 glioma cells, with the PIL conjugated with 83-14 MAb to the human insulin receptor (HIR). Conversely, rat RG-2 glioma cells were transduced with the PIL conjugated with OX26 murine MAb to the rat transferrin receptor (rTfR). Clone 877 plasmid DNA was encapsulated in either TfRMAb–PIL or HIRMAb–PIL and 4 μg of plasmid DNA was applied to each 60-mm culture dish containing either RG-2 or U87 cells, respectively. The level of TH enzyme activity in either U87 cells or RG-2 cells increased with time of incubation and peaked 4 days after the single application of the PIL formulation at time 0 (Fig. 3). TH enzyme activity in rat RG-2 cells targeted with the OX26–PIL system was comparable to the TH enzyme activity in C6 glioma cells targeted with LipofectAMINE (Figs. 1 and 3). The TH enzyme activity in human U87 glioma cells targeted with the HIRMAb–PIL delivery system was comparable to TH enzyme activity produced with LipofectAMINE in COS-1 cells (Figs. 1 and 3).

TH enzyme activity in liver of control rats treated by intravenous gene therapy

TfRMAb–PIL targeting of the TH gene was initially examined in a TfR-rich peripheral organ, liver, of control rats so as to identify the time course of gene expression. Each control rat was administered 10 μg of clone 877 plasmid DNA encapsulated in TfRMAb–PIL and hepatic TH enzyme activity was measured 0, 1, 2, and 3 days after the single intravenous administration (Table 1). The TH activity in control rat liver increased >30-fold above basal levels by 3 days after gene administration. Therefore, 72 hr was chosen as the time point for measuring brain TH activity after intravenous TH gene therapy in rats with experimentally induced PD.

TH enzyme activity and immunoreactive TH levels in rat brain with experimentally induced parkinsonism treated by intravenous TH gene therapy

Three weeks after the intracerebral injection of 6-hydroxydopamine, rats were treated with apomorphine and rotation behavior was examined. Those rats that demonstrated contralat-

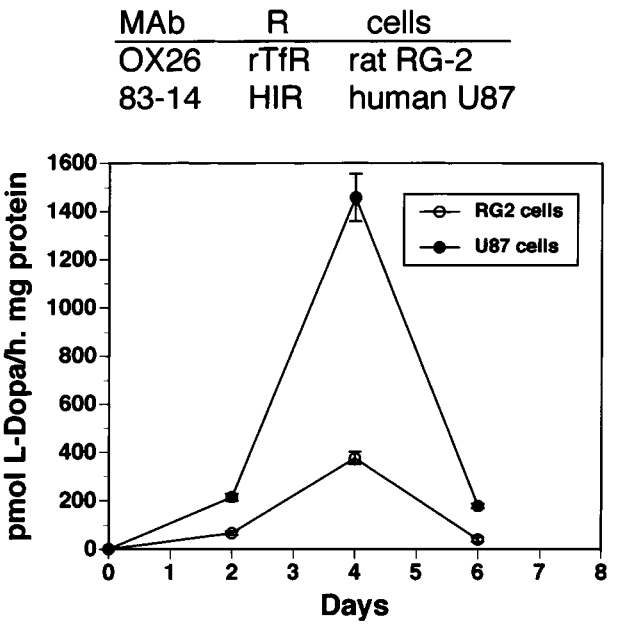

FIG. 3. Tyrosine hydroxylase activity is plotted relative to the days of incubation in cell culture of either rat RG-2 cells or human U87 glioma cells exposed to clone 877 plasmid DNA encapsulated in PIL. PIL was targeted to rat RG-2 cells with the OX26 murine MAb to the rat transferrin receptor (rTfR), and PIL was targeted to human U87 cells with the 83-14 murine MAb to the human insulin receptor (HIR). Data represent means ± SE (n = 4 dishes per point).

Table 1. Tyrosine Hydroxylase Activity in Liver After Intravenous Injection of Clone 877 Plasmid DNA Encapsulated in TfRMAb–PIL in Control Rats[a]

Day post administration	*TH activity (pmol L-dopa/hr per mg protein)*
0	3.0 ± 0.3
1	18.2 ± 1.8
2	33.2 ± 2.7
3	103.7 ± 9.1

[a]Values represent means ± SD (n = 3 rats per time point).

eral rotation in response to apomorphine were selected for subsequent treatment with the PIL gene-targeting system 1 week later. Rats with experimentally induced PD were treated either with clone 877 plasmid DNA encapsulated in PIL targeted with TfRMAb (designated TfRMAb–PIL) or with clone 877 plasmid DNA encapsulated in PIL targeted with mouse IgG2a isotype control antibody (designated mIgG2a–PIL). Plasmid DNA was injected intravenously at a dose of 10 μg of DNA per rat, and animals were killed 72 hr after the single intravenous injection for measurement of either TH enzyme activity in dorsal striatal or cortical homogenates or immunoreactive TH levels by immunocytochemistry. TH enzyme activity in the dorsal striatum ipsilateral to the 6-hydroxydopamine injection was reduced 87% compared with TH enzyme activity in the contralateral striatum, and TH enzyme activity was completely normalized in rats treated with clone 877 DNA encapsulated within TfR–PIL (Table 2). In contrast, intravenous administration of clone 877 DNA encapsulated in mIgG2a–PIL resulted in no increase in TH enzyme activity in the ipsilateral striatum (Table 2). TH enzyme activity in the cortex was only 2% relative to the contralateral striatum and there was no change in cortical TH enzyme activity in the lesioned animals treated with TfRMAb–PIL (Table 2).

The level of immunoreactive TH was measured by immunocytochemistry and there was a complete loss of immunoreactive TH in the dorsal striatum ipsilateral to the neurotoxin injection, although residual immunoreactive TH was detected in the ventral striatum and olfactory tubercle below the anterior commissure in some rats (Fig. 4D and F). The administration of clone 877 encapsulated within mIgG2a–PIL resulted in no increase in the level of immunoreactive TH in the striatum (Fig. 4D–F). However, the level of immunoreactive TH was normalized in the entire striate body 3 days after an intravenous injection of clone 877 DNA encapsulated within PIL targeted to brain by TfRMAb (Fig. 4A–C).

Reversal of motor impairment after TH gene therapy

Apomorphine-induced contralateral rotation was quantified in individual rats 1 week before and 3 days after a single intravenous injection of clone 877 TH expression plasmid encapsulated in either mIgG2a–PIL (Fig. 5A) or TfRMAb–PIL (Fig. 5B). Contralateral rotations were counted for 20 min after the intraperitoneal injection of apomorphine. Total rotations in a 20-min period 3 days after treatment are plotted in Fig. 5C. The mean rotations per minute (rpm) for the animals treated with mIgG2a–PIL was 20 ± 5 (range, 13–26 rpm per animal). In contrast, the animals treated with clone 877 TH expression plasmid encapsulated within TfRMAb–PIL demonstrated a 70% reduction in rotation to 6 ± 2 rpm (mean ± SD) with a range of 3–9 rpm per individual rat.

Time–response study

The persistence of TH gene expression in the striatum ipsilateral to the lesion was determined by measurement of striatal TH enzyme activity 6 and 9 days after a single intravenous injection of clone 877 plasmid DNA (10 μg/rat) encapsulated in TfRMAb–PIL, and these data were compared with the TH measurements at 3 days. As shown in Fig. 6, striatal TH activity peaked at 3 days and had decreased by 50% by 6 days after injection. By 9 days after injection, TH activity in the ipsilateral striatum of rats treated with TfRMAb–PIL was comparable to the control levels in the lesioned striatum of animals treated with mIgG2a–PIL (Table 2).

Dose–response study

TH enzyme activity in the striatum either contralateral or ipsilateral to the lesion was measured 3 days after a single intravenous injection of clone 877 plasmid DNA encapsulated in TfRMAb–PIL at a dose of 1, 5, or 10 μg/rat (Fig. 7). TH activity in the ipsilateral striatum was proportional to the dose of plasmid DNA administered via TfRMAb–PIL, and no increases in striatal TH was observed with the 1-μg/rat dose (Fig. 7).

Table 2. Tyrosine Hydroxylase Activity in Rat Brain Lesioned with 6-Hydroxydopamine, 3 Days After Intravenous Injection of Clone 877 Plasmid DNA Encapsulated in Either TfRMAb–PIL or mIgG2a–PIL[a]

	TH activity (pmol L-dopa/hr per mg protein)	
Region	*TfRMAb–PIL*	*mIgG2a–PIL*
Ipsilateral striatum	5486 ± 899[b]	738 ± 179
Contralateral striatum	5875 ± 550[b]	5101 ± 443[b]
Ipsilateral cortex	159 ± 27	101 ± 7
Contralateral cortex	121 ± 39	108 ± 51

[a]Values represent means ± SD (n = 5 rats in each group).
[b]$p < 0.01$ difference from ipsilateral striatum treated with mIgG2a–PIL (one-way ANOVA, Bonferroni correction).

DISCUSSION

The results of these studies are consistent with the following conclusions. First, striatal TH enzyme activity is normalized by intravenous injection of nonviral TH expression plasmid encapsulated inside a PIL targeted by a TfRMAb to neurons (Table 2). Second, normalization of TH enzyme activity in the striatum is paralleled by normalization of the level of immunoreactive TH protein, as measured by immunocytochemistry (Fig. 4). Third, the specificity of the gene-targeting system is a function of the MAb, because the only difference between TfRMAb–PIL and mIgG2a–PIL is the receptor specificity of the targeting MAb conjugated to the PEGylated liposome (Fig. 2A). Both TfRMAb–PIL and mIgG2a–PIL carry the clone 877 TH expression plasmid. Fourth, there is no change in TH enzyme activity in cortex and no measurable immunoreactive cortical TH as determined by immunocytochemistry performed after the intravenous injection of TH expression plasmid encapsulated in TfRMAb–PIL (Table 2 and Fig. 4). Fifth, there is a reversal of apomorphine-induced rotation behavior after intravenous TH gene therapy, with a 70% reduction in drug-induced rotation (Fig. 5). Sixth, the normalization of TH activity in brain after the single administration of a plasmid-based TH gene is time dependent, and the peak activity declines 50% by 6 days (Fig. 6). Seventh, the effect of gene therapy is dose dependent, as minimal, intermediate, and maximal effects on striatal TH activity are observed, respectively, after intravenous administration to each rat of 1, 5, and 10 μg of TH plasmid delivered with TfRMAb–PIL (Fig. 7).

Normalization of TH enzyme activity in the ipsilateral striatum (Table 2) is consistent with the detection of immunoreactive TH throughout the ipsilateral striatum of rats treated with TfRMAb–PIL (Fig. 4). For treatment of human PD, it may be necessary to transduce at least 50% of the striate body, because the threshold of PD symptoms occurs with a 50% loss of nigral–striatal neurons (Booij *et al.*, 2001). The transduction of 50–100% of the striatum with a therapeutic gene is possible after delivery of the gene to brain via the transvascular route. All neurons in the brain are perfused by their own capillaries and PIL carrying the therapeutic gene is delivered to the "doorstep" of virtually every neuron in the brain after transport across the BBB (Pardridge, 2002).

Transduction of cell lines with retroviral vectors carrying the TH gene increases TH enzyme activity to approximately 1600 pmol/hr per 10^6 cells (Leff *et al.*, 1998). This is comparable to the TH enzyme activity in COS-1 cells transduced with LipofectAMINE and clone 877 (Fig. 1), as 10^6 cells in culture is equivalent to 1 mg of protein. A similar level of TH enzyme activity is also generated in human U87 glioma cells with the HIRMAb–PIL gene-targeting system (Fig. 3). Therefore, the level of transduction of a target cell by the PIL gene-targeting system is comparable to levels achieved with either cationic lipids or viral vectors.

Cellular targeting of the PIL gene delivery system is a function only of the receptor specificity of the targeting MAb (Shi *et al.*, 2001a,b). TfRMAb–PIL and mIgG2a–PIL have identical formulations, except that the mouse IgG2a isotype control antibody does not recognize the rat TfR. TfRMAb triggers receptor-mediated transcytosis of the PIL nanocontainer across the BBB *in vivo*. Once in the brain interstitial space, the PIL undergoes receptor-mediated endocytosis into brain cells expressing the TfR. The TfR is widely expressed on neurons throughout the CNS (Mash *et al.*, 1991). Once inside brain cells, the fusogenic lipids of the liposome cause release of the plasmid DNA, which is then transported into the nuclear compartment for expression of the transgene. The rapid intranuclear delivery of DNA to cells by the PIL gene-targeting system has been demonstrated by confocal microscopy of fluoresceinated DNA encapsulated in PIL (Zhang *et al.*, 2002b).

TH enzyme activity is not increased in the cortex of brain after intravenous administration of TH expression plasmid encapsulated within TfRMAb–PIL (Table 2 and Fig. 4). A similar finding was made in the human TH transgenic mouse model, which shows increased TH enzyme activity in the striatum, but only minor changes in the frontal cortex (Kaneda *et al.*, 1991). The inability to mount a measurable increase in TH enzyme activity in the cortex is attributed to the absence of TH cofactor in this region of the brain (Shimoji *et al.*, 1999). The TH enzyme has an obligatory cofactor, tetrahydrobiopterin (BH_4), and the TH enzyme is not active in the absence of local production of the BH_4 cofactor (Hwang *et al.*, 1998). Studies performed in knockout mice show that the level of TH protein, measured by either enzyme activity or Western blotting, is diminished in animals lacking BH_4 (Sumi-Ichinose *et al.*, 2001). Both *in situ* hybridization and immunocytochemistry demonstrate that only monoaminergic neurons in the brain express the enzyme that is rate limiting for BH_4 synthesis, that is, GTP-cyclohydrolase (GTPCH), and there is no measurable GTPCH produced in the cortex (Nagatsu *et al.*, 1997; Hwang *et al.*, 1998). Although mRNA for GTPCH exists at a low level in the striatum (Hirayama *et al.*, 1993), the GTPCH protein is produced in nerve endings terminating in the striatum (Hwang *et al.*, 1998). GTPCH is produced in cell bodies of multiple regions of the brain outside the striatum, particularly serotoninergic systems (Lentz and Kapatos, 1996). These neurons terminate in the striatum (Hwang *et al.*, 1998), and enable the striatal production of BH_4, a diffusible small molecule, within the lesioned striatum. Both GTPCH and BH_4 levels in the striatum of 6-hydroxydopamine-lesioned rat are still one-third the concentrations in nonlesioned animals (Levine *et al.*, 1981). This residual GTPCH in the striatum provides the BH_4 cofactor for TH enzyme produced by the exogenous TH gene delivered to the brain. In contrast, GTPCH is not produced in the neocortex, and it is not possible to increase TH enzyme activity in this region of the brain by administration of exogenous TH gene (Table 2). This is advantageous for the treatment of PD, because it is not desirable to augment dopamine production in cortical structures. TH enzyme activity is increased in rat glioma cells targeted with TfRMAb–PIL or in human U87 glial cancer cells targeted with HIRMAb–PIL (Fig. 3). These findings are consistent with prior studies showing that both cultured rat glioma cells and cancer cell lines produce the GTPCH enzyme (Nussler *et al.*, 1996; Vann *et al.*, 2002). A modest increase in rat liver TH activity is observed in control rats (Table 1), and this is consistent with the expression of GTPCH in liver (Nagatsu *et al.*, 1997). However, TH enzyme activity in rat liver is reduced by 98% compared with striatal TH enzyme activity (Tables 1 and 2).

Reversal of apomorphine-induced rotational behavior in the 6-hydroxydopamine lesioned rat is not seen in all studies involving transduction of the striatum with TH genes, using vi-

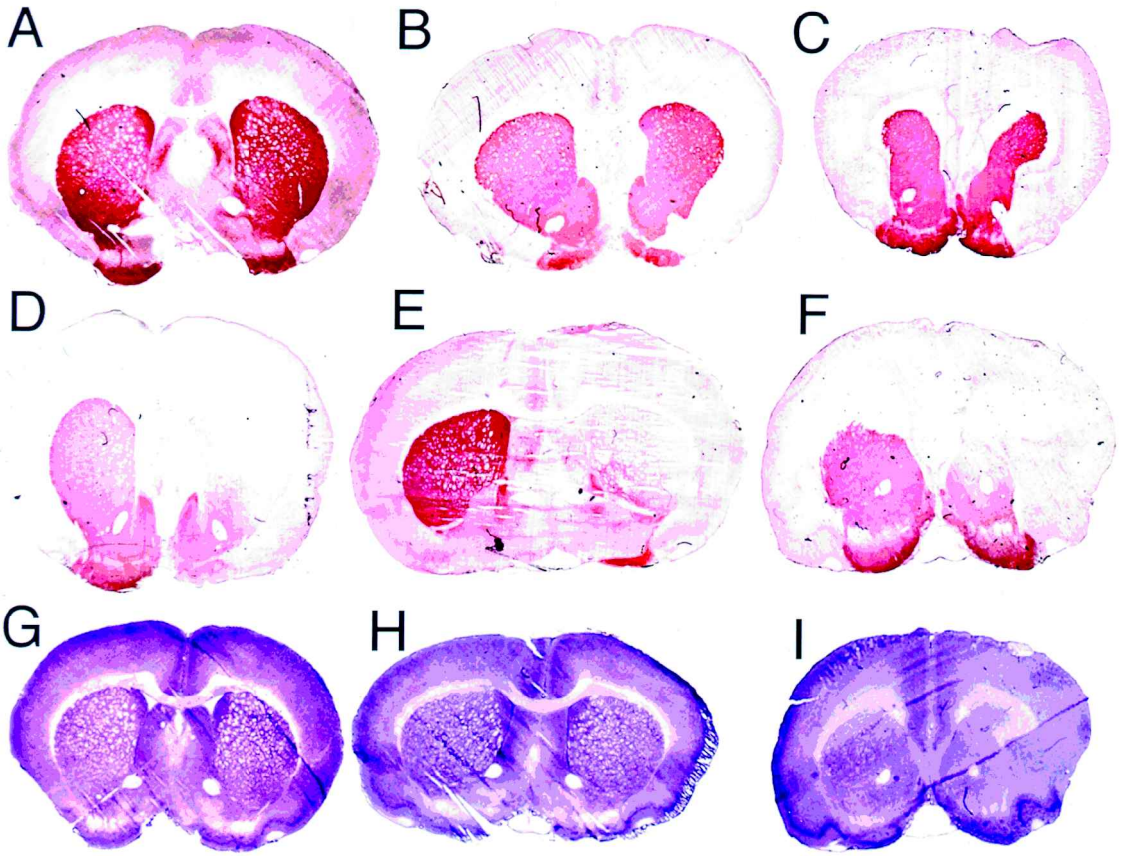

FIG. 4. Tyrosine hydroxylase immunocytochemistry of rat brain removed 72 hr after a single intravenous injection of 10 μg per rat of clone 877 plasmid DNA encapsulated in PIL targeted with either the TfRMAb (**A–C**) or with the mouse IgG2a isotype control (**D–F**). Coronal sections are shown for three different rats from each of the two treatment groups. The 6-hydroxydopamine was injected into the medial forebrain bundle of the right hemisphere, which corresponds to right side of the figure. (**G–I**) Coronal sections of brain stained with hematoxylin. (**G**), (**H**), and (**I**) correspond to (**A**), (**E**), and (**F**), respectively. Immunoreactive TH is completely abolished in both the caudal and ventral striatum in the rat shown in (**E**), whereas there is residual immunoreactive TH in the ventral striatum and olfactory tubercle in the rats shown in (**D**) and (**F**).

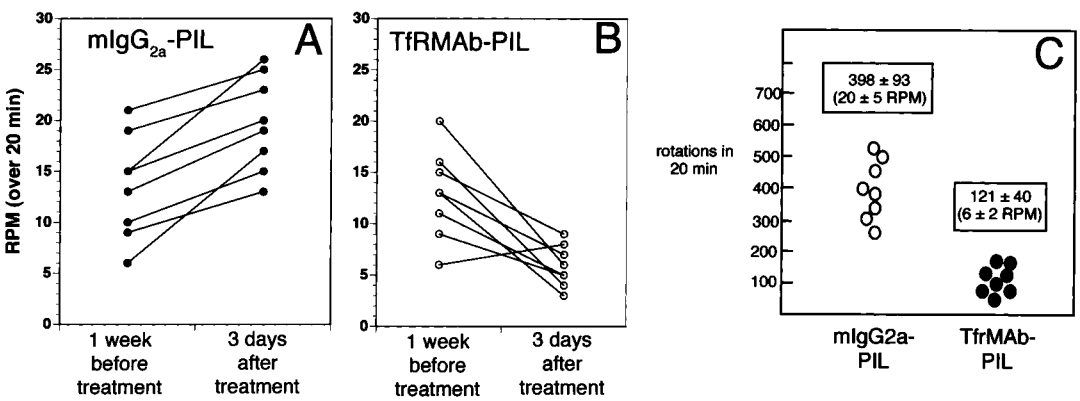

FIG. 5. (**A**) Apomorphine-induced rotations per minute (rpm) over a 20-min period, measured in individual rats 1 week before treatment and 3 days after a single intravenous injection of, per rat, 10 μg of clone 877 plasmid DNA encapsulated in PIL targeted with the mouse IgG2a isotype control antibody. (**B**) Apomorphine-induced rotations per minute over a 20-min period measured in individual rats 1 week before treatment and 3 days after a single intravenous injection of, per rat, 10 μg of clone 877 plasmid DNA encapsulated in PIL targeted with TfRMAb. (**C**) Comparison of the total rotations in the two groups 3 days after treatment. The average rotations per minute is 20 ± 5 and 6 ± 2 (mean $\pm$ SD) in animals treated with mIgG2a–PIL and TfRMAb–PIL, respectively. The difference in rotation between the two groups is significant at the $p < 0.005$ level (Student t test). The rotation behavior in all animals was measured 3 weeks after 6-hydroxydopamine injection, which corresponds to 1 week before PIL treatment, and 4 weeks after toxin injection, which corresponds to 3 days after treatment with the PIL.

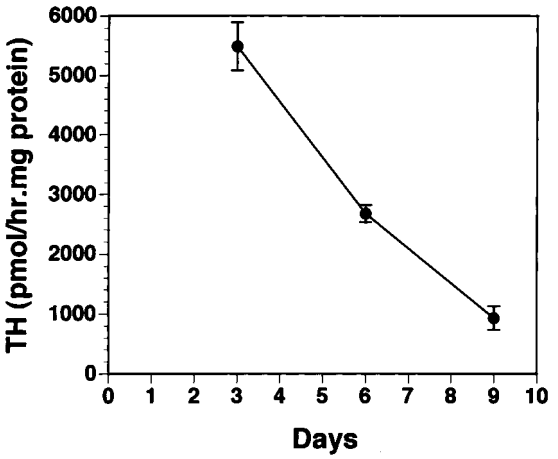

FIG. 6. The striatal tyrosine hydroxylase (TH) activity ipsilateral to the 6-hydroxydopamine lesion is plotted versus time after a single intravenous injection of, per rat, 10 μg of clone 877 plasmid DNA encapsulated in TfRMAb–PIL on day 0. Data represent means ± SD (n = 3 rats per point). The TH activity on the lesioned side 9 days after treatment with TfRMAb–PIL is comparable to the TH activity in the lesioned striatum of rats treated with mIgG2a–PIL (Table 2). The 3-day data are from Table 2.

ral vectors (Mandel *et al.*, 1998; Kirik *et al.*, 2002). Reversal of the aberrant rotational behavior in this model may require transduction of a significant volume of striatum with the TH therapeutic gene, and this may not be possible with a single intrastriatal injection of a viral vector (Kirik *et al.*, 2002). In contrast, transvascular delivery of the TH gene to brain enables complete normalization of TH enzyme activity in the striatum (Table 2) and normalization of the level of immunoreactive TH in the entire striate body (Fig. 4). These findings are consistent with reversal of apomorphine-induced rotational behavior after a single intravenous administration of the TH gene packaged in the PIL gene delivery system (Fig. 5C). Apomorphine-induced rotation 3 days after treatment with mIgG2a–PIL is increased 50% relative to drug-induced rotation 1 week before treatment (Fig. 5A), and this observation is consistent with the known pharmacodynamics of the 6-hydroxydopamine model. Apomorphine-induced rotations increase 50% by 4 weeks after 6-hydroxydopamine injection as compared with rotations observed 3 weeks after injection (Meshul *et al.*, 2002). The comparison of the two treatment groups 4 weeks after toxin injection is shown in Fig. 5C, and these data show a 70% reduction in rotation behavior after treatment with TfRMAb-targeted PIL.

Normalization of striatal TH activity after a single intravenous administration of TH gene encapsulated in targeted PIL is transient, and the level of TH activity in brain is reduced 50% by 6 days and reduced >90% by 9 days (Fig. 6). This time course in rat brain TH activity parallels prior work, which showed the rat brain activity of β-galactosidase was decreased 50% by 6 days after a single intravenous injection of expression plasmid encapsulated in targeted PIL (Shi *et al.*, 2001b). The organ level of the plasmid DNA, as determined by Southern blotting, was also 50% decreased at 6 days after a single intravenous administration of PIL (Shi *et al.*, 2001b), which suggests that gene expression declines with time owing to degradation of plasmid DNA within the target tissue. Reversible gene expression by PIL gene-targeting technology is consistent with expression of the gene episomally, without integration of the plasmid DNA within the host genome. Conversely, the expression of exogenous genes is long-lasting after the transfection of brain cells with either retrovirus (Kordower *et al.*, 2000) or adeno-associated virus (Kaplitt *et al.*, 1994), as these viral vectors randomly and stably integrate into the host genome. The long-term effects of such stable and random integration are not known (Cavazzana-Calvo *et al.*, 2000). Although gene expression is reversible with nonviral, plasmid-based gene therapy, sustained pharmacologic effects can be achieved with repeat administration of the gene medicine. Weekly intravenous administration of plasmid DNA encoding antisense RNA against the human epidermal growth factor receptor caused a 100% increase in survival time for mice with intracranial brain cancer (Zhang *et al.*, 2002a).

A linear dose response is observed as the striatal TH activity ipsilateral to the 6-hydroxydopamine injection is increased in proportion to the dose of TH expression plasmid targeted to brain by TfRMAb–PIL. A maximal effect is observed in rats receiving a 10-μg dose, whereas the 1-μg/rat dose is ineffective, and an intermediate response is obtained with the 5-μg/rat dose (Fig. 7). A per-rat dose of 10 μg of the 6.0-kb clone 877 plasmid delivers 1.2×10^9 plasmid molecules per gram of brain, because 0.07% of the injected PIL dose is delivered to 1 g of rat brain (Shi and Pardridge, 2000). Given 10^8 cells per gram of brain, the 10-μg/rat dose delivers approximately 12 plasmid DNA molecules per brain cell. Conversely, only one plasmid molecule per brain cell is delivered with the 1-μg/rat dose, and this dose has no pharmacologic effect on TH activity in brain (Fig. 7). These findings suggest a relatively high efficiency of transfection of brain cells *in vivo* by the PIL gene-targeting technology, and that pharmacological effects in brain are achieved with the delivery of only 5–10 plasmid DNA molecules per brain cell.

TH enzyme activity in rat liver is also increased by the intravenous administration of clone 877 plasmid DNA encapsulated in TfRMAb–PIL, although the enzyme activity in liver at 3 days (Table 1) is <2% of striatal enzyme activity (Table 2).

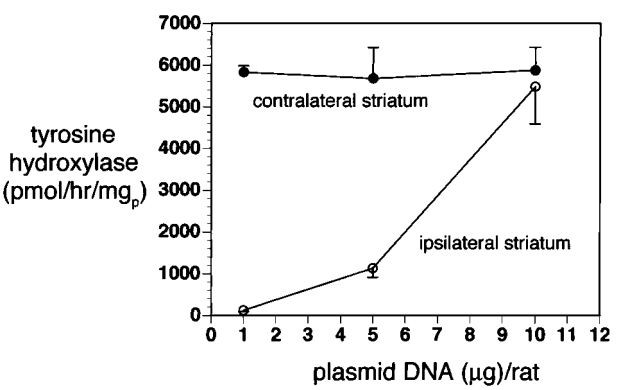

FIG. 7. The striatal tyrosine hydroxylase (TH) activity either ipsilateral or contralateral to the 6-hydroxydopamine lesion is plotted versus the dose of clone 877 plasmid DNA encapsulated in TfRMAb–PIL. Data represent means ± SD (n = 3 rats per point). Striatal TH was measured 3 days after the single intravenous administration of DNA.

The TH gene is expressed in liver because (1) the TfR is highly expressed in this organ (Shi *et al.*, 2001b), and (2) clone 877 plasmid is under the influence of the widely expressed SV40 promoter (see Materials and Methods). However, if the SV40 promoter is replaced with a brain-specific promoter, such as the 5′-flanking sequence of the glial fibrillary acidic protein gene, then extracerebral gene expression is eliminated (Shi *et al.*, 2001a). Therefore, the tissue specificity of expression of the exogenous gene can be controlled by the combined use of gene-targeting technology and tissue-specific gene promoters.

In summary, the intracerebral injection of 6-hydroxydopamine into the medial forebrain bundle caused a 90% decrease in ipsilateral TH enzyme activity and immunoreactive TH in the ipsilateral striatum. TH enzyme activity and immunoreactive TH in the striatum were normalized by a single intravenous injection of a nonviral TH expression plasmid encapsulated in the interior of PIL and targeted to neurons by a TfRMAb. Normalization of striatal TH enzyme activity was associated with a 70% reduction in apomorphine-induœd rotation behavior. The pharmacological effect in brain is both time and dose dependent. This work shows that it is possible to achieve pharmacological effects in target tissues by nonviral gene transfer after intravenous administration of the gene.

ACKNOWLEDGMENTS

This work was supported by a grant from the Neurotoxin Exposure Treatment Research Program of the U.S. Department of Defense. F.C. was supported by the Canadian Institutes of Health Research.

REFERENCES

ANTON, R., KORDOWER, J.H., MAIDMENT, N.T., MANASTER, J.S., KANE, D.J., RABIZADEH, S., SCHUELLER, S.B., YANG, J., RABIZADEH, S., EDWARDS, R.H., MARKHAM, C.H., and BREDESEN, D.E. (1994). Neural-targeted gene therapy for rodent and primate hemiparkinsonism. Exp. Neurol. **127,** 207–218.

ARMSTRONG, R.J.E., HURELBRINK, C.B., TYERS, P., RATCLIFFE, E.L., RICHARDS, A., DUNNETT, S.B., ROSSER, A.E., and BARKER, R.A. (2002). The potential for circuit reconstruction by expanded neural precursor cells explored through porcine xenografts in a rat model of Parkinson's disease. Exp. Neurol. **175,** 98–111.

BANKIEWICZ, K.S., EBERLING, J.L., KOHUTNICKA, M., JAGUST, W., PIVIROTTO, P., BRINGAS, J., CUNINGHAM, J., BUDINGER, T.F., and HARVEY-WHITE, J. (2000). Convection-enhanced delivery of AAV vector in parkinsonian monkeys: In vivo detection of gene expression and restoration of dopaminergic function using pro-drug approach. Exp. Neurol. **164,** 2–14.

BOADO, R.J., and PARDRIDGE, W.M. (1998). Ten nucleotide cis element in the 3′-untranslated region of GLUT1 glucose transporter mRNA increases gene expression via mRNA stabilization. Mol. Brain Res. **59,** 109–113.

BOOIJ, J., BERGMANS, P., WINOGRODZKA, A., SPEELMAN, J.D., and WOLTERS, E.C. (2001). Imaging of dopamine transporters with [^{123}I]FP-CIT SPECT does not suggest a significant effect of age on the symptomatic threshold of disease in Parkinson's disease. Synapse **39,** 101–108.

CAVAZZANA-CALVO, M., HACEIN-BEY, S., DE SAINT BASILE, G., YVON, E., NUSBAUM, P., SELZ, F., HUE, C., CERTAIN, S., CASANOVA, J.L., BOUSSO, P., DEIST, F.L., and FISCHER, A. (2000). Gene therapy of human severe combined immunodeficiency (SCID)-X1 disease. Science **288,** 669–672.

DURING, M.J., NAEGELE, J.R., O'MALLEY, K.L., and GELLER, A.I. (1994). Long-term behavioral recovery in parkinsonian rats by an HSV vector expressing tyrosine hydroxylase. Science **266,** 1399–1403.

DWYER, K.J., BOADO, R.J., and PARDRIDGE, W.M. (1996). Cis-element/cytoplasmic protein interactions within the 3′-untranslated region of GLUT1 glucose transporter mRNA. J. Neurochem. **66,** 449–458.

HIRAYAMA, K., LENTZ, S.I., and KAPATOS, G. (1993). Tetrahydrobiopterin cofactor biosynthesis: GTP cyclohydrolase I mRNA expression in rat brain and superior cervical ganglia. J. Neurochem. **61,** 1006–1014.

HORELLOU, P., GUIBERT, B., LEVIEL, V., and MALLET, J. (1989). Retroviral transfer of a human tyrosine hydroxylase cDNA in various cell lines: Regulated release of dopamine in mouse anterior pituitary AtT-20 cells. Proc. Natl. Acad. Sci. U.S.A. **86,** 7233–7237.

HUWYLER, J., WU, D., and PARDRIDGE, W.M. (1996). Brain drug delivery of small molecules using immunoliposomes. Proc. Natl. Acad. Sci. U.S.A. **93,** 14164–14169.

HWANG, O., BAKER, H., GROSS, S., and JOH, T.H. (1998). Localization of GTP cyclohydrolase in monaminergic but not nitric oxide-producing cells. Synapse **28,** 140–153.

JEFFERIES, W.A., BRANDON, M.R., HUNT, S.V., WILLIAMS, A.F., GATTERS, K.C., and MASON, D.Y. (1984). Transferrin receptor on endothelium of brain capillaries. Nature **312,** 162–163.

KANEDA, N., SASAOKA, T., KOBAYASHI, K., KIUCHI, K., NAGATSU, I., KUROSAWA, Y., FUJITA, K., YOKOYAMA, M., NOMURA, T., KATSUKI, M., and NAGATSU, T. (1991). Tissue-specific and high-level expression of the human tyrosine hydroxylase gene in transgenic mice. Neuron **6,** 583–594.

KAPLITT, M.G., LEONE, P., SAMULSKI, R.J., XIAO, X., PFAFF, D.W., O'MALLEY, K.L., and DURING, M.J. (1994). Long-term gene expression and phenotypic correction using adeno-associated virus vectors in the mammalian brain. Nat. Genet. **8,** 148–154.

KIRIK, D., GEORGIEVSKA, B., BURGER, C., WINKLER, C., MUZYCZKA, N., MANDEL, R.J., and BJORKLUND, A. (2002). Reversal of motor impairments in parkinsonian rats by continuous intrastriatal delivery of L-dopa using rAAV-mediated gene transfer. Proc. Natl. Acad. Sci. U.S.A. **99,** 4708–4713.

KORDOWER, J.H., EMBORG, M.E., BLOCH, J., MA, S.Y., CHU, Y., LEVENTHAL, L., MCBRIDE, J., CHEN, E.-Y., PALFI, S., ROITBERG, B.Z., BROWN, W.D., HOLDEN, J.E., PYZALSKI, R., TAYLOR, M.D., CARVEY, P., LING, Z., TRONO, D., HANTRAYE, P., DEGLON, N., and AEBISCHER, P. (2000). Neurodegeneration prevented by lentiviral vector deliver of GDNF in primate models of Parkinson's disease. Science **290,** 767–773.

LEFF, S.E., RENDAHL, K.G., SPRATT, S.K., KANG, U.J., and MANDEL, R.J. (1998). In vivo L-DOPA production by genetically modified primary rat fibroblast or 9L gliosarcoma cell grafts via coexpression of GTP cyclohydrolase I with tyrosine hydroxylase. Exp. Neurol. **154,** 249–264.

LENTZ, S.I., and KAPATOS, G. (1996). Tetrahydrobiopterin biosynthesis in the rat brain: Heterogeneity of GTP cyclohydrolase I mRNA expression in monoamine-containing neurons. Neurochem. Int. **28,** 569–582.

LEONE, P., MCPHEE, S.W.J., JANSON, C.G., DAVIDSON, B.L., FREESE, A., and DURING, M.J. (2000). Multi-site partitioned delivery of human tyrosine hydroxylase gene with phenotypic recovery in parkinsonian rats. Neuroreport **2,** 1145–1151.

LEVINE, R.A., MILLER, L.P., and LOVENBERG, W. (1981). Tetrahydrobiopterin in striatum: Localization in dopamine nerve terminals and role in catecholamine synthesis. Science **214,** 919–921.

MANDEL, R.J., RENDAHL, K.G., SPRATT, S.K., SNYDER, R.O., COHEN, L.K., and LEFF, S.E. (1998). Characterization of intrastriatal recombinant adeno-associated virus-mediated gene transfer of human tyrosine hydroxylase and human GTP-cyclohydrolase I in rat model of Parkinson's disease. J. Neurosci. **18,** 4271–4284.

MANDEL, R.J., RENDAHL, K.G., SNYDER, R.O., and LEFF, S.E. (1999). Progress in direct striatal delivery of L-dopa via gene therapy for treatment of Parkinson's disease using recombinant adeno-associated viral vectors. Exp. Neurol. **159,** 47–64.

MASH, D.C., PABLO, J., BUCK, B.E., SANCHEZ-RAMOS, J., and WEINER, W.J. (1991). Distribution and number of transferrin receptors in Parkinson's disease and in MPTP-treated mice. Exp. Neurol. **114,** 73–81.

MESHUL, C.K., KAMEL, D., MOORE, C., KAY, T.S., and KRENTZ, L. (2002). Nicotine alters striatal glutamate function and decreases the apomorphine-induced contralateral rotations in 6-OHDA-lesioned rats. Exp. Neurol. **175,** 257–274.

MONNARD, P.-A., OBERHOLZER, T., and LUISI, P. (1997). Entrapment of nucleic acids in liposomes. Biochim. Biophys. Acta **1329,** 39–50.

MOURADIAN, M.M., and CHASE, T.N. (1997). Gene therapy for Parkinson's disease: An approach to the prevention or palliation of levodopa-associated motor complications. Exp. Neurol. **144,** 51–57.

NAGATSU, I., ARAI, R., SAKAI, M., YAMAWAKI, Y., TAKEUCHI, T., KARASAWA, N., and NAGATSU, T. (1997). Immunohistochemical colocalization of GTP cyclohydrolase I in the nigrostriatal system with tyrosine hydroxylase. Neurosci. Lett. **224,** 185–188.

NUSSLER, A.K., LIU, Z.-Z., HATAKEYAMA, K., GELLER, D.A., BILLIAR, T.R., and MORRIS, S.M., JR. (1996). A cohort of supporting metabolic enzymes is coinduced with nitric oxide synthase in human tumor cell lines. Cancer Lett. **103,** 79–84.

PARDRIDGE, W. (2002). Drug and gene targeting to the brain with molecular Trojan horses. Nat. Rev. Drug Discov. **1,** 131–139.

PARDRIDGE, W.M., EISENBERG, J., and YANG, J. (1987). Human blood–brain barrier transferrin receptor. Metabolism **36,** 892–895.

PARDRIDGE, W.M., BUCIAK, J.L., and YOSHIKAWA, T. (1992). Transport of recombinant CD4 through the rat blood–brain barrier in vivo. J. Pharmacol. Exp. Ther. **261,** 1175–1180.

REINHARD, J.F., SMITH, G.K., and NICHOL, C.A. (1986). A rapid and sensitive assay for tyrosine-3-monooxygenase based upon the release of ^3H_2O and adsorption of [^{3}H]-tyrosine by charcoal. Life Sci. **39,** 2185–2189.

SHI, N., and PARDRIDGE, W.M. (2000). Noninvasive gene targeting to the brain. Proc. Natl. Acad. Sci. U.S.A. **97,** 7567–7572.

SHI, N., ZHANG, Y., BOADO, R.J., ZHU, C., and PARDRIDGE, W.M. (2001a). Brain-specific expression of an exogenous gene following intravenous administration. Proc. Natl. Acad. Sci. U.S.A. **98,** 12754–12759.

SHI, N., BOADO, R.J., and PARDRIDGE, W.M. (2001b). Receptor-mediated gene targeting to tissues in the rat in vivo. Pharm. Res. **18,** 1091–1095.

SHIMOJI, M., HIRAYAMA, K., HYLAND, K., and KAPATOS, G. (1999). GTP cyclohydrolase I gene expression in the brains of male and female hph-1 mice. J. Neurochem. **72,** 757–764.

SHUSTA, E.V., BOADO, R.J., and PARDRIDGE, W.M. (2002). Vascular proteomics and subtractive antibody expression cloning. Mol. Cell. Proteomics **1,** 75–82.

SUMI-ICHINOSE, C., URANO, F., KURODA, R., OHYE, T., KOJIMA, M., TAZAWA, M., SHIRAISHI, H., YASUMICHI, H., NAGATSU, T., NOMURA, T., and ICHINOSE, H. (2001). Catecholamines and serotonin are differently regulated by tetrahydrobiopterin. J. Biol. Chem. **276,** 41150–41160.

VANN, L.R., PAYNE, S.G., EDSALL, L.C., TWITTY, S., SPIEGEL, S., and MILSTIEN, S. (2002). Involvement of sphingosine kinase in TNF-α-stimulated tetrahydrobiopterin biosynthesis in C6 glioma cells. J. Biol. Chem. **277,** 12649–12656.

ZHANG, Y., ZHU, C., and PARDRIDGE, W.M. (2002a). Antisense gene therapy of brain cancer with an artificial virus gene delivery system. Mol. Ther. **6,** 67–72.

ZHANG, Y., LEE, H.J., BOADO, R.J., and PARDRIDGE, W.M. (2002b). Receptor-mediated delivery of an antisense gene to human brain cancer cells. J. Gene Med. **4,** 183–194.

ZHANG, Y., BOADO, R.J., and PARDRIDGE, W.M. (2003). Marked enhancement in gene expression by targeting the human insulin receptor. J. Gene Med. **5,** in press.

Address reprint requests to:
Dr. William M. Pardridge
UCLA
Warren Hall 13-164
900 Veteran Avenue
Los Angeles, CA 90024

E-mail: wpardridge@mednet.ucla.edu

Received for publication September 18, 2002; accepted after revision November 13, 2002.

Published online: December 2, 2002.

doi:10.1016/S1525-0016(02)00018-7

Global Non-Viral Gene Transfer to the Primate Brain Following Intravenous Administration

Yun Zhang, Felix Schlachetzki,* and William M. Pardridge†

Dept. of Medicine, UCLA School of Medicine, Los Angeles, CA 90024
**Present address: Dept. of Neurology, University of Regensburg, Regensburg, Germany*

†To whom correspondence should be addressed: Dr. William M. Pardridge, UCLA Warren Hall 13-164, 900 Veteran Avenue, Los Angeles, CA 90024. Phone: (310) 825-8858. Fax: (310) 206-5163. E-mail: Wpardridge@mednet.ucla.edu.

Expression plasmids encoding either luciferase or β-galactosidase were encapsulated in the interior of an "artificial virus" comprised of an 85 nm pegylated immunoliposome, which was targeted to the rhesus monkey brain *in vivo* with a monoclonal antibody (MAb) to the human insulin receptor (HIR). The HIRMAb enables the liposome carrying the exogenous gene to undergo transcytosis across the blood-brain barrier and endocytosis across the neuronal plasma membrane following intravenous injection. The level of luciferase gene expression in the brain was 50-fold higher in the rhesus monkey as compared to the rat. Widespread neuronal expression of the β-galactosidase gene in primate brain was demonstrated by both histochemistry and confocal microscopy. This approach makes feasible reversible adult transgenics in 24 hours.

Key Words: gene therapy, insulin receptor, liposomes, non-viral gene transfer, blood-brain barrier

INTRODUCTION

Many diseases of the central nervous system (CNS) are candidates for treatment by gene therapy [1], and for most of these disorders, it is necessary to achieve widespread expression of the exogenous gene throughout the entire CNS. Global, neuronal gene expression in the brain is possible with trans-vascular delivery of the gene following intravenous administration. The cerebral microvasculature, which forms the blood-brain barrier (BBB) *in vivo*, is a very dense network, comprising approximately 400 miles in the human brain. Since virtually every neuron in the brain is perfused by its own blood vessel, the delivery of the gene across the BBB targets the gene to the "doorstep" of every neuron in the brain. Subsequent to transport across the BBB, it is also necessary for the exogenous gene to undergo uptake into brain cells via endocytosis across the brain cell plasma membrane (BCM).

The widespread expression of exogenous genes in rodent brain has been recently demonstrated using non-viral gene transfer technology and pegylated immunoliposomes (PIL). In this approach, the non-viral plasmid DNA is encapsulated in the interior of an 85 nm liposome [2]. The liposome has the same size as many viral vectors, and like a viral vector, the liposome houses the plasmid DNA in the interior of a nanocontainer to prevent degradation of the DNA by endonucleases [3], which are ubiquitous *in vivo*. The blood residence time of the liposome is prolonged by conjugating several thousand strands of 2000 Dalton polyetheylene glycol (PEG) to the surface of the liposome [2]. The PEG strands reduce adsorption of serum proteins to the liposome surface, which minimizes uptake of the nanocontainer by the cells lining the reticulo-endothelial system *in vivo* [4]. The pegylated liposome can be targeted to brain cells by tethering to the tips of 1–2% of the PEG strands a receptor-specific targeting ligand, such as a peptidomimetic monoclonal antibody (MAb). The MAb attaches to a receptor expressed on both the BBB and the BCM to enable sequential receptor-mediated transcytosis across the BBB and receptor-mediated endocytosis across the BCM (Figure 1). The targeting MAb acts as molecular Trojan horse to ferry the PIL across biological barriers in the brain via endogenous transport systems [5]. The targeting MAb's are species-specific. Endogenous genes are delivered to mouse brain with the rat 8D3 MAb to the mouse transferrin receptor (TfR) [6], and to rat brain with the murine OX26 MAb to the rat TfR [2,7]. In addition to the targeting specificity of the MAb, tissue-specific gene expression is influenced by the gene promoter. Exogenous genes driven by the SV40 promoter, and targeted to rodent tissues with a TfRMAb are expressed in brain [6,7] or retina [8], as well as peripheral tissues that also express the TfR. However, the SV40 promoter is widely expressed *in vivo* [9]. Replacement of the

1525-0016/03 $30.00

doi:10.1016/S1525-0016(02)00018-7

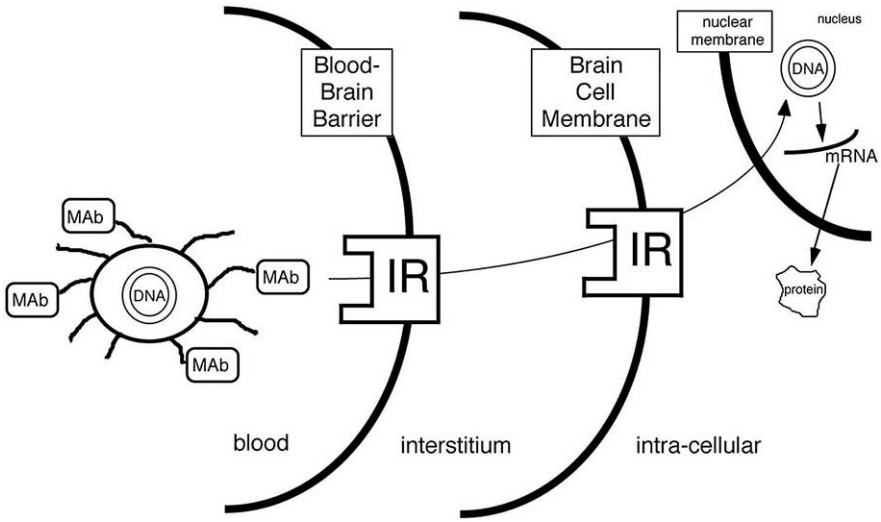

FIG. 1. The plasmid DNA is encapsulated in the interior of an 85 nm pegylated immunoliposome (PIL). The surface of the liposome is conjugated with several thousand strands of 2000 Dalton polyethyleneglycol (PEG), and the tips of 1–2% of the PEG strands is tethered with a targeting ligand, such as a insulin receptor (IR)-specific monoclonal antibody (MAb). The MAb-conjugated PIL undergoes receptor-mediated transcytosis across the blood-brain barrier and receptor-mediated endocytosis across the brain cell plasma membrane and enters the nuclear compartment [12].

SV40 promoter with a brain specific promoter eliminates exogenous gene expression in peripheral TfR-rich organs following intravenous administration [6]. Successful gene therapy of the brain is feasible with intravenous administration of the gene formulated with the PIL gene targeting technology. The survival time is increased 100% in mice with intra-cranial human brain cancer following weekly injections of the targeted PIL carrying plasmid DNA that expresses antisense mRNA to the human epidermal growth factor [10].

The 8D3 or OX26 anti-TfRMAb's are specific for mice and rats, respectively, and are not active in primates or humans [5]. Drug or gene targeting to the brain of Old World primates such as the rhesus monkey is possible with the murine 83-14 MAb to the human insulin receptor (HIR). The rate of transport of the HIRMAb across the primate BBB is nearly 10-fold greater than the rate of transport of an anti-human TfRMAb across the primate BBB *in vivo* [5]. The high activity of the HIRMAb was demonstrated recently with respect to gene targeting to cultured human or rat glioma cells. In these studies, a luciferase expression plasmid was targeted to human glial cells with HIRMAb-conjugated PIL and to rat glial cells with TfRMAb-conjugated PIL [11]. The level of gene expression was $>$ 10-fold greater in human cells targeted with the HIRMAb as compared to rat cells targeted with the TfRMAb.

The purpose of the present study is to evaluate the targeting of exogenous genes to primate brain *in vivo* using the PIL gene targeting technology and the HIRMAb as the targeting ligand. This MAb acts as a molecular Trojan horse to ferry the liposome across the BBB and the BCM in the primate brain *in vivo* (Figure 1). Expression plasmids driven by the SV40 promoter and encoding luciferase or bacterial β-galactosidase were encapsulated in the HIRMAb-PIL and injected intravenously into the adult Rhesus monkey. The animal was sacrificed 48 hours later and brain expression of the luciferase and β-galactosidase genes in the primate brain was measured. Since luciferase measurements are quantitative, the level of luciferase gene expression in the primate brain targeted with the HIRMAb-PIL was compared to luciferase gene expression in rat brain targeted with the TfRMAb-PIL.

RESULTS

The level of luciferase gene expression in hemispheric gray matter in the primate is high and approximately 10 pg luciferase per mg of brain protein (Figure 2A). The level of luciferase gene expression in the Rhesus monkey brain targeted with the HIRMAb-PIL is nearly 50-fold greater than the level of luciferase gene expression in rat brain targeted with the TfRMAb-PIL (Figure 2B). The luciferase gene, driven by the SV40 promoter, is also expressed in insulin receptor-rich or TfR-rich organs in the monkey and rat, respectively, such as liver, spleen, and lung (Figure 2) with minimal gene expression in kidney or heart in these species (Figure 2). Luciferase gene expression in primate skeletal muscle was also low, 0.13 $\pm$ 0.02 pg luciferase per mg protein. Luciferase gene expression in hemispheric white matter of the primate brain was 3.2 $\pm$ 0.3 pg luciferase per mg protein, which is 3-fold lower than luciferase gene expression in gray matter of primate brain (Figure 2A). The level of luciferase gene expression in primate cerebellar gray matter and white matter was 7.0 $\pm$ 1.6 and 4.0 $\pm$ 0.4 pg luciferase per mg protein, respectively.

The expression of the β-galactosidase gene in primate brain was examined with both histochemistry and confocal microscopy. The histochemistry of frozen sections of primate brain removed 48 hours after the single intravenous injection of the gene shows diffuse and wide-

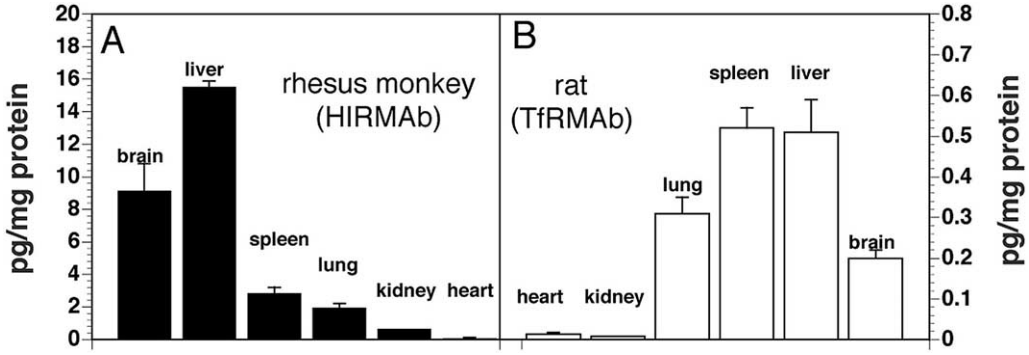

FIG. 2. Luciferase gene expression in the brain and other organs of the adult rhesus monkey (A) and adult rat (B) measured at 48 hours after a single intravenous injection of the PIL carrying the plasmid DNA. Data are mean ± SE. The plasmid DNA encoding the luciferase gene used in either species is clone 790, which is driven by the SV40 promoter [11,12]. The PIL carrying the DNA was targeted to primate organs with the 83-14 HIRMAb and to rat organs with the OX26 TfRMAb.

spread expression of β-galactosidase in primate brain (Figure 3A, 3C). In contrast, β-galactosidase histochemistry of control or un-injected primate brain shows no β-galactosidase activity (Figure 3B). The gray and white matter tracts of the brain are delineated in the histochemistry, consistent with a greater level of β-galactosidase gene expression in gray matter relative to white matter. Light micrographs of the primate brain β-galactosidase histo-

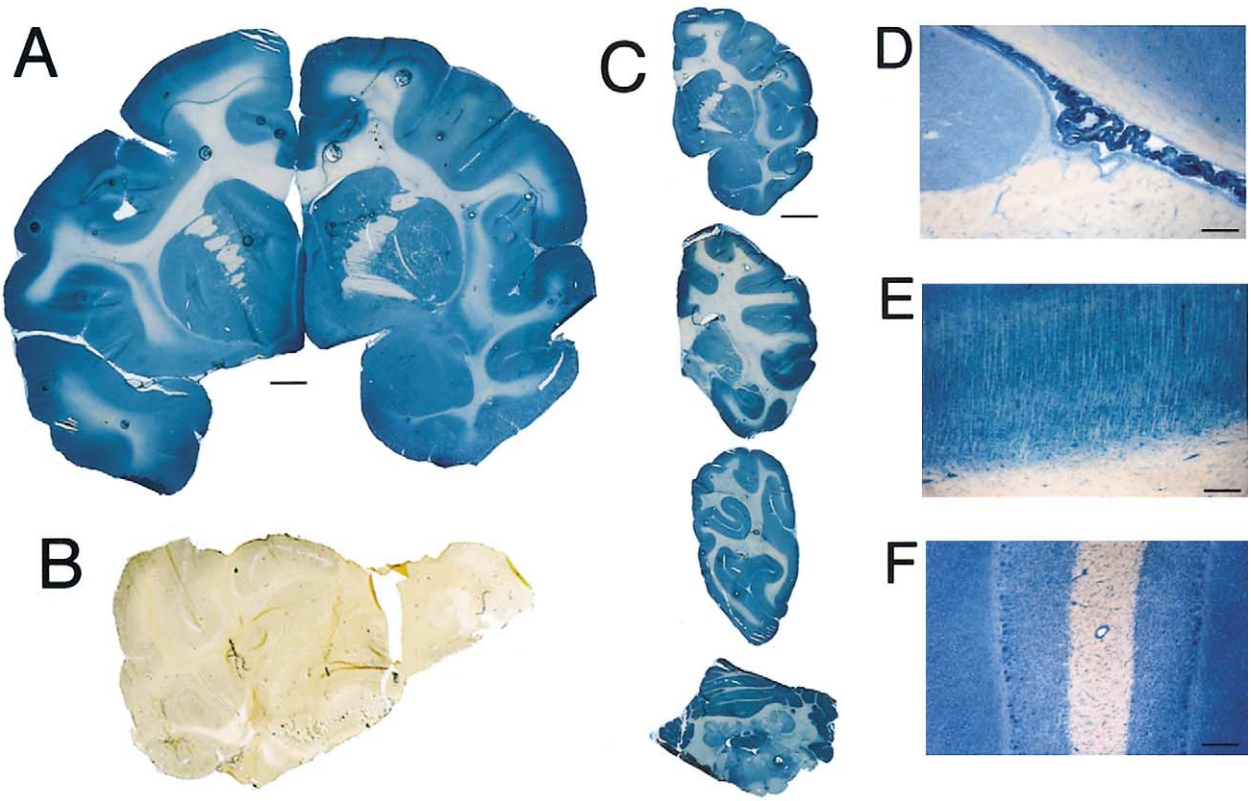

FIG. 3. β-Galactosidase histochemistry of brain removed from either the HIRMAb-PIL injected rhesus monkey (A, C, D, E, and F) or the control, uninjected rhesus monkey (B). The plasmid DNA encapsulated in the PIL is the pSV-β-galactosidase expression plasmid driven by the SV40 promoter. Panel A is a reconstruction of the 2 halves of a coronal section of the forebrain. Panel C shows half-coronal sections through the primate cerebrum and a full coronal section through the cerebellum; the sections from top to bottom are taken from the rostral to caudal parts of brain. Panels D, E, and F are light micrographs of choroid plexus, occipital cortex, and cerebellum, respectively. All specimens are β-galactosidase histochemistry without counter-staining. The magnification in panels A and B is the same and the magnification bar in panel A is 3 mm; the magnification bar in panel C is 8 mm; the magnification bars in panels D–F are 155 μm.

doi:10.1016/S1525-0016(02)00018-7

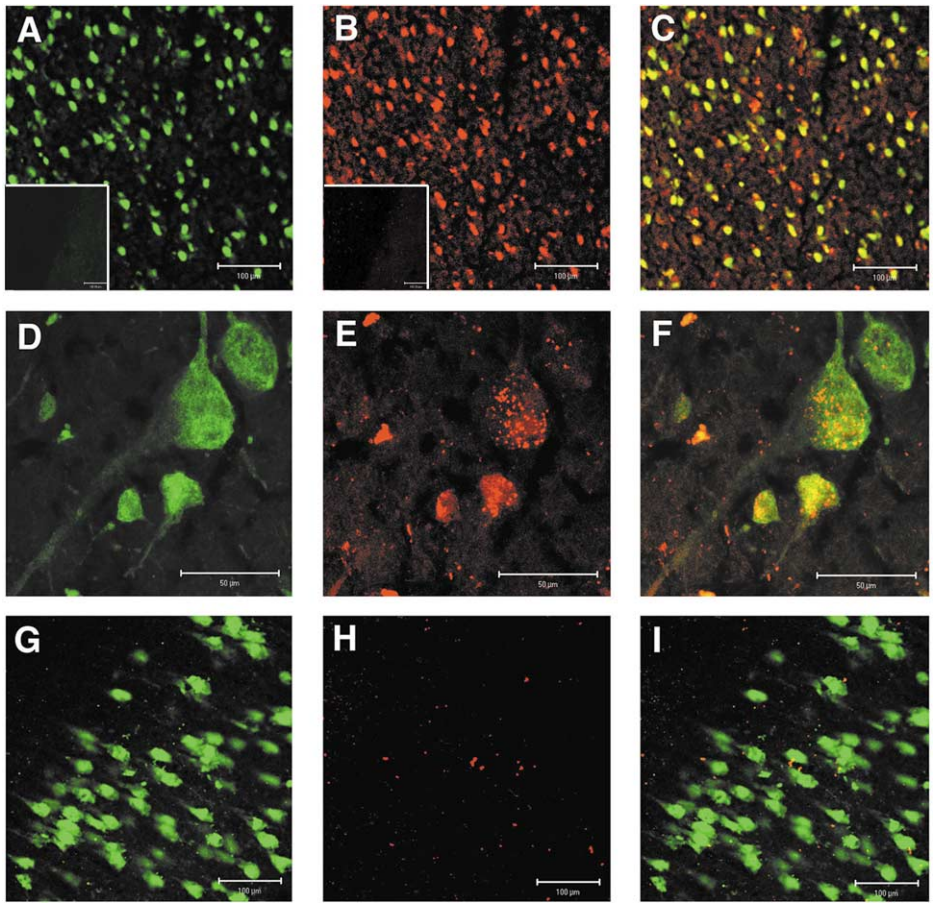

FIG. 4. Confocal immunofluorescent imaging of β-galactosidase expression in neurons of the gene injected (A–F) and the uninjected control rhesus monkey brain (G–I). Immunoreactive neuronal nuclei (NeuN) are stained with a mouse anti-neuN primary antibody and a fluorescein-labeled secondary antibody, as shown in panels A, D, and G. Immunoreactive β-galactosidase is stained with a rabbit anti-bacterial β-galactosidase primary antibody and a rhodamine-labeled secondary antibody, as shown in panels B, E, and H. The respective superimposed yellow images reveal co-localization of the neuN and β-galactosidase in neurons (C, F). Primate brain was also immunolabeled with the isotype control mouse IgG_1 or rabbit IgG, which showed no specific staining as shown in the insets of panels A and B, respectively. Scale bars in panels A–C and G–I are 100 μm; scale bars in panels D–F (oil immersion) are 50 μm. Neurons from the primate supplementary motor cortex are shown in panels A–C, and larger neurons from the primate primary motor cortex are shown in panels G–H.

chemistry are shown in Panels D–F of Figure 3. The choroid plexus bordered by gray matter and white matter is shown in Figure 3D. Gene expression is visible within the choroid plexus epithelium, the ependymal lining of the ventricle, and the capillary endothelium of adjacent white matter (Figure 3D). The β-galactosidase gene expression within the neurons of the occipital cortex is visible and reveals the columnar organization of the occipital cortex of the primate brain (Figure 3E). Dense gene expression in the molecular and granular layers of the cerebellum, as well as the intermediate Purkinje cells, are visible in Figure 3F. Owing to the reduced level of gene expression in the cerebellar white matter, the β-galactosidase enzyme activity is detected in the capillary endothelium within the white matter of the cerebellum (Figure 3F).

Confocal microscopy confirmed neuronal expression of the β-galactosidase gene, as there is overlap of immunoreactive neuN and β-galactosidase in primate brain (Figure 4). Immunostaining of neuN is shown in Figure 4A and 4D in the gene-injected monkey and in Figure 4G for the un-njected control monkey. Immunoreactive β-galactosidase is detected in the brain of the gene injected monkey (Figure 4B and 4E), but not in the brain of the un-injected control monkey (Figure 4H). The overlap of the immunoreactive neuN and β-galactosidase is shown in Figure 4C and 4F. Control staining with the either mouse IgG_1 or rabbit IgG were negative as shown in the insets of Figures 4A and 4B, respectively.

Histochemistry of primate peripheral organs demonstrated tissue specific expression of the β-galactosidase gene (Figure 5), similar to luciferase gene expression (Figure 2B). Diffuse trans-hepatic gene expression was observed in primate liver (Figure 5A) and light microscopy shows the gene is expressed in hepatocytes (Figure 5B). Diffuse gene expression is observed in spleen (Figure 5C), and light microscopy shows a higher level of gene expression in red pulp as compared to white pulp (Figure 5D). No detectable β-galactosidase gene expression is observed in heart, skeletal muscle, or fat in the primate (Figure 5E–J).

DISCUSSION

The results of these studies are consistent with the following conclusions. First, the PIL gene targeting technology

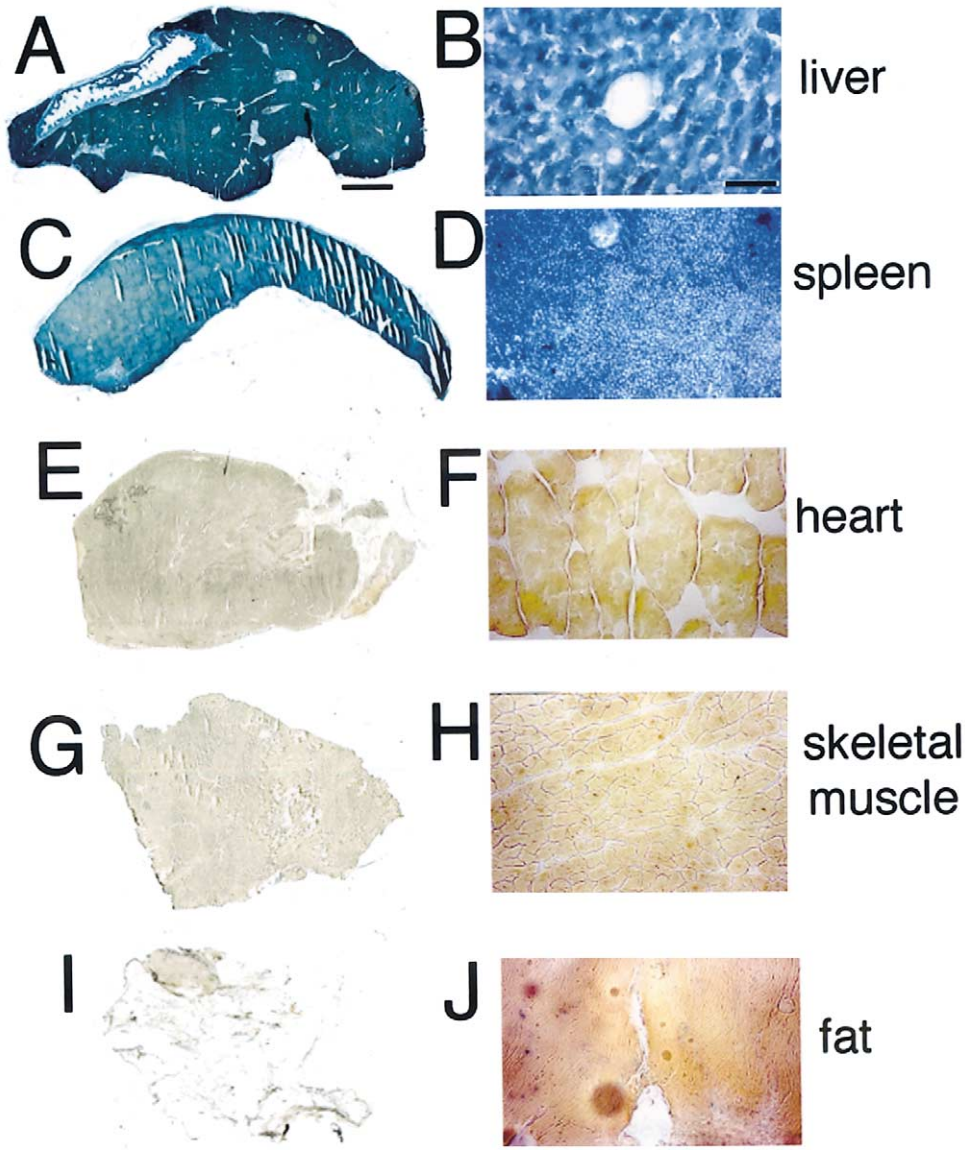

FIG. 5. β-Galactosidase histochemistry of rhesus monkey organs removed 48 hours after intravenous injection of the pSV-β-galactosidase expression plasmid encapsulated in the HIRMAb-PIL, including liver (A,B), spleen (C, D), heart (E, F), biceps skeletal muscle (G, H), and omental fat (I, J). Magnification in panels A, C, E, G, and I is the same and the magnification bar in panel A is 5 mm. Magnification in panels B, D, F, H, and J is the same and the magnification bar in panel B is 65 μm. The β-galactosidase gene is diffusely expressed in primate liver and spleen, whereas there is no detectable gene expression in heart, skeletal muscle, or fat. No sections are counter-stained.

enables diffuse, widespread expression of exogenous genes in the primate brain (Figure 3). Second, the level of gene expression in the monkey brain targeted with the HIRMAb-PIL is 50-fold greater than gene expression in the rat brain targeted with the TfRMAb-PIL (Figure 2). Third, the exogenous gene is expressed in neurons in the primate brain as shown by co-labeling primate brain sections with antibodies against the neuN neuronal specific antigen and bacterial β-galactosidase (Figure 4). Fourth, the exogenous gene is expressed in primate peripheral tissues expressing the insulin receptor, which have a permeable microvasculature, such as liver or spleen, but not in peripheral tissues which are perfused by a microvasculature with a continuous endothelium, such as heart, skeletal muscle, kidney, or fat (Figures 2, 5).

The PIL is targeted to brain of rats or monkeys because both the brain cell membrane, and the brain microvascular endothelium, which forms the BBB *in vivo,* are enriched in either insulin receptor (IR) or TfR [5]. However, the extent to which a given gene is expressed is a function of the activity of the targeting antibody and the targeted receptor. The present studies show that the level of gene expression in the primate brain targeted with the HIRMAb-PIL is nearly 50-fold greater than the level of gene expression in the rat brain targeted with the TfRMAb-PIL (Figure 2). This finding parallels recent observations that the level of gene expression in cultured human glial cells targeted with the HIRMAb-PIL is >10-fold greater than the gene expression in cultured rat glial cells targeted with the TfRMAb-PIL [11]. The higher levels of

doi:10.1016/S1525-0016(02)00018-7

gene expression following targeting of the insulin receptor may be due to the property of this receptor to target the nuclear compartment [11]. Confocal microscopy of cultured human glial cells shows the HIRMAb-PIL rapidly delivers fluoresceinated plasmid DNA to the nucleus of the cell [12].

The delivery of the exogenous gene to the primate brain is global (Figure 3). Gene expression is higher in gray matter as compared to white matter, based on the β-galactosidase histochemistry (Figure 3). The level of luciferase activity in gray matter is 2–3-fold higher than in primate white matter (Results), and these findings are consistent with the approximate 3-fold greater vascular density of gray matter relative to white matter [13]. Within the gray matter regions of brain, the majority of the neurons within a field express the exogenous gene, as shown by the microscopy of either the occipital cortex (Figure 3E) or the cerebellar cortex (Figure 3F). The PIL gene targeting technology enables the global transduction of the majority of neurons throughout the entire brain, and this is possible because the gene is delivered to brain via the trans-vascular route.

In addition to brain, the PIL-targeted gene is expressed in liver and spleen (Figure 5). These organs are perfused by a leaky sinusodal vasculature, which allows rapid transvascular egress of the PIL into the organ interstitium, and the parenchymal cells in liver or spleen are enriched in IR or TfR [7]. Despite the high expression of the IR on parenchymal cells, gene expression in heart, skeletal muscle, fat, or kidney is minimal (Figures 2, 5), because these organs are perfused by capillaries with continuous endothelium. Unlike the brain, where the IR is expressed on the microvascular endothelial barrier (Figure 1), the IR is not expressed on the endothelium in peripheral organs. The PIL cannot readily enter the extravascular space of these peripheral organs in the absence of endothelial transport mechanisms that enable the receptor-mediated transcytosis across the microvascular endothelial barrier. A similar transport restriction across myocardial capillaries occurs for adenoviral vectors following the intra-coronary infusion of the virus [14]. Both adenovirus and the PIL are about 85 nm in diameter, which is too large to freely traverse the small pore system of the endothelium of continuous capillaries.

Gene expression in primate lung is moderate and less than brain, liver, or spleen (Figure 2A). The modest lung expression of the gene illustrates the marked differences between the PIL gene transfer technology and conventional non-viral gene transfer approaches, which use DNA/cationic liposomes. Cationic liposomes, even pegylated cationic liposomes, are taken up by lung at rates log orders greater than liver or spleen [15]. Cationic liposome/DNA complexes aggregate in physiological saline [16], and these aggregates deposit in the first vascular bed encountered after an intravenous injection, which is the pulmonary circulation. In contrast, the PIL does not aggregate in saline or serum and has prolonged blood residence times [2].

The expression of the exogenous gene in primate peripheral tissues such as liver or spleen is observed because either the luciferase or the β-galactosidase expression plasmids used in these studies is under the influence of the SV40 promoter [17]. If the widely expressed SV40 promoter is replaced with a brain specific promoter such as the 5′-flanking sequence from the human glial fibrillary acidic protein (GFAP) gene, then transgene expression in maintained in brain, but is eliminated in peripheral tissues such as liver or spleen [6]. In addition to the promoter, the targeting MAb conjugated to the PIL restricts the specificity of tissue gene expression. If the targeting MAb is replaced with an isotype IgG control antibody, then there is no gene expression in any organ in rats or mice following intravenous administration of the gene encapsulated in the PIL [2,6,7].

The levels of luciferase gene expression in primate brain, liver, or spleen following an intravenous injection of the HIR-PIL (Figure 2) are comparable to the levels of luciferase gene expression in mice following the intravenous injection of HIV-1-based lentivirus encoding the luciferase gene. The luciferase activity in liver and spleen of mice subjected to multiple intravenous infusions with 10^8 viral units is 2000 and 600 pg luciferase per gram tissue, and there is no luciferase expression in brain [18]. Peripheral organs contain 180 mg protein per gram tissue. Therefore, the luciferase activity in liver and spleen of the lentivirus-injected mice is 11 and 3 pg luciferase per mg protein, and these values are comparable to the luciferase levels generated in primate brain, liver, or spleen with non-viral gene transfer of a luciferase expression plasmid (Figure 2).

In summary, these studies show that it is possible to achieve widespread expression of exogenous genes throughout the primate brain following a single intravenous injection of a non-viral formulation of the gene. The PIL gene targeting technology enables adult transgenics of the brain within 24 hours. The only other way to achieve an experimental result such as that shown in Figure 3 is with the engineering and breeding of transgenic primates producing bacterial β-galactosidase within the brain. The PIL acts as an artificial virus carrying exogenous genes across the biological barriers in brain (Figure 1). The component of the PIL that is potentially immunogenic is the targeting antibody. However, the immunogenicity of the antibody can be reduced or eliminated with genetic engineering and the production of "humanized" monoclonal antibodies. The chimeric form of the murine 83-14 HIRMAb has been produced, and has equal affinity for the HIR as the original murine antibody [19]. Therefore, the technology is now available to deliver therapeutic genes to the human brain with an intravenous administration without the use of viral vectors. The plasmid DNA is episomally expressed in cells and must be given on repeat

occasions depending on the persistence of the transgene. In rats, the gene expression in brain decreases approximately 50% at 6 days following a single intravenous administration of a PIL encapsulated plasmid expressing either β-galactosidase [7] or tyrosine hydroxylase [20]. In mice with intra-cranial experimental brain cancer, therapeutic results were achieved with intravenous administrations of the gene medicine given once per week [10]. In rats with experimental Parkinson's disease, striatal tyrosine hydroxylase is normalized at 3–6 days following the single intravenous injection of the gene, whereas gene expression is minimal at 9 days after administration [20]. Therefore, the persistence of the plasmid expression *in vivo* in the brain is sufficient to allow for the intended pharmacological response, which is reversible owing to the episomal nature of plasmid gene expression [21]. The persistence of plasmid gene expression is enhanced with the administration of either linearized mini-genes [21] or genomic DNA [22]. Therefore, it is possible to prolong the duration of gene expression derived from non-viral, plasmid-based gene therapy.

EXPERIMENTAL PROCEDURES

Materials. POPC (1-palmitoyl-2-oleoyl-*sn*-glycerol-3-phosphocholine) and DDAB (didodecyldimethylammonium bromide) were purchased from Avanti-Polar Lipids Inc. (Alabaster, AL). Distearoylphosphatidylethanolamine (DSPE)-PEG 2000 was obtained from Shearwater Polymers (Huntsville, AL). DSPE-PEG 2000-maleimide was custom synthesized by Shearwater Polymers. [α-^{32}P]dCTP (3000 Ci/mmol) was from NEN Life Science Product Inc. (Boston, MA). The nick translation system was from Life Technologies Inc. (Rockville, MA). 5-Bromo-4-chloro-3-indoyl-β-D-galactoside (X-gal), IGEPAL CA-630 and all other chemicals were purchased from Sigma Chemical Co. (St. Louis, MO). The luciferase reagent and recombinant luciferase were obtained from Promega; 2-iminothiolane (Traut's reagent) and bicinchoninic acid (BCA) protein assay reagents were obtained from Pierce Chemical Co. (Rockford, IL). The 83-14 murine MAb to the HIR, and the OX26 murine MAb to the rat TfR were purified by protein G affinity chromatography from serum-free hybridoma-conditioned media as described previously [12]. The luciferase expression plasmid is designated clone 790 and is derived from the pCEP4 plasmid under the control of the SV40 promoter as described previously [17]. The pSV-β-galactosidase expression plasmid driven by the SV40 promoter is designated clone 756 as described previously [2,6], and was purchased from Promega (Madison, WI).

Pegylated immunoliposome synthesis. Pegylated immunoliposomes (PILs) were synthesized with a total of 20 μmol of lipids, including 18.8 μmol of POPC, 0.4 μmol of DDAB, 0.6 μmol of DSPE-PEG, and 0.2 μmol of DSPE-PEG-maleimide, as described previously [6,7]. The PIL lipid contains 2% cationic lipid (DDAB) and 8% anionic lipid (DSPE-PEG), and has a net anionic charge [7]. Clone 756 plasmid DNA or clone 790 plasmid DNA was produced by Maxiprep (Qiagen, Chatsworth, CA). The supercoiled plasmid DNA (200 μg) and 1 μCi of ^{32}P-nick translated plasmid DNA were encapsulated in the pegylated liposomes by serial extrusion resulting in liposomes of 85 nm diameter [2]. The exteriorized DNA was removed by nuclease digestion [23], as described previously [2]. The 83-14 HIRMAb or OX26 TfRMAb, containing a trace amount of 3H-labeled antibody, was individually thiolated with Traut's reagent and the thiolated MAb was conjugated to the pegylated liposome overnight at room temperature as described previously [6,12]. The unconjugated MAb, and the degraded exteriorized DNA were separated from the DNA encapsulated within the PIL by elution through a 1.6 × 18 cm column of Sepharose CL-4B in 0.05 M Hepes, pH = 7.0, as described previously [6,12]. The average number of MAb molecules conjugated per liposome was 43 ± 2 (mean ± SE, n = 3 syntheses). The final percentage entrapment of 200 μg of plasmid DNA in the liposome preparation was computed from the ^{32}P radioactivity and was 35 ± 7.5% (mean ± SE, n = 3 synthesis). The PIL conjugated with the HIRMAb is designated HIRMAb-PIL and the PIL conjugated with the TfRMAb is designated TfRMAb-PIL. Clone 790 DNA was encapsulated in either HIRMAb-PIL or OX26-PIL for injection into primates or rats, respectively. Clone 756 was encapsulated in HIRMAb-PIL for primate injection. The HIRMAb-PIL carrying either the clone 756 or clone 790 plasmid DNA was sterilized before injection into the primate with a 0.22 μm filter (Millipore Co., Bedford, MA) as described previously [12].

In vivo gene administration. A 10 year-old 6 kg female Rhesus monkey was purchased from Covance (Alice, TX). The animal was anesthetized with 10 mg/kg ketamine intra-muscular, and 5 ml of sterile HIRMAb-PIL containing 70 μg of each of clone 756 and clone 790 plasmid DNA was injected into the monkey via the saphenous vein with a 18-g catheter. The total dose of HIRMAb that was conjugated to the PIL and administered to the primate was 1.8 mg. Adult male Spraque-Dawley rats weighing 250g were injected via the femoral vein with OX26-PIL carrying clone 790 plasmid DNA at a dose of 5 μg of PIL-encapsulated plasmid DNA per rat. The dose of PIL encapsulated plasmid DNA was 12 and 20 μg/kg, respectively, for the primate and rat. Both species were sacrificed at 48 hours post-injection. The brain and peripheral organs [liver, spleen, heart, skeletal muscle (biceps), and omental fat] were removed immediately after euthanasia. The primate brain weighing approximately 100g was divided into 4 coronal sections, and each section was divided into the left and right hemispheres. The brain slabs and peripheral organs were frozen in powdered dry ice for 30 min, embedded in OCT and re-frozen for cryostat sectioning.

β-galactosidase histochemistry. Frozen sections of 20-μm thickness were cut on a Mikron cryostat and fixed with 0.2% glutaraldehyde in 0.1 M NaH_2PO_4(pH = 7.0) for 1 hour. Because an entire coronal section of the primate brain was too large to section on the cryostat, each coronal slab was sectioned as coronal hemisphere slices. The sections were washed with 0.1 M NaH_2PO_4(pH = 7.0) three times, and incubated overnight at 37 C in X-gal staining solution (20 mM potassium-ferrocyanide, 20 mM potassium-ferricyanide, 2 mM $MgCl_2$, 0.02% IGEPAL CA-630, 0.01% Na deoxycholate, and 1 mg/ml of X-gal in 0.1 M NaH_2PO_4) at pH = 7.3. Prior to coverslipping, the sections were scanned with a UMAX PowerLookIII scanner with transparency adapter, and the image was cropped in Adobe Photoshop 5.5 on a G4 Power Macintosh computer. Sections were not counter-stained. Control or un-injected rhesus monkey brain was stained in parallel with the brain obtained from the gene-injected animal. The control rhesus monkey brain was frozen as coronal slabs in Tissue Tek OCT embedding medium immediately after euthanasia by Sierra Biomedical/Charles River (Sparks, NV).

Luciferase measurements. Primate tissue samples were taken from the frontal and occipital poles of the cerebrum, as well as from cerebellum, liver, lung, heart, kidney, spleen, and skeletal muscle (biceps). The tissues were homogenized in 4 volumes of lysis buffer for measurements of organ luciferase activity, as described previously [12]. Luciferase activity in rat brain, liver, lung, heart, kidney and spleen were measured in the same way. The data are reported as pg luciferase activity per mg cell protein. Based on the standard curve, 1 pg of luciferase was equivalent to 14,312 ± 2,679 relative light units (RLU), which is the mean ± S.E. of 5 assays [11]. No luciferase enzyme activity was detectabel in brain from the control, uninjected monkey.

Confocal microscopy. Frozen sections were fixed for 20 min in 2% paraformaldehyde in 0.1 M Na_2HPO_4, pH = 7.4 at 4C. The slides were blocked in 0.01 M PBS buffer with 0.1% Triton X, and 10% goat serum. Primary antibodies were mouse anti-neuronal nuclei (neuN) monoclonal antibody (Chemicon Int., Temecula, CA), rabbit anti E.coli β-galactosidase polyclonal antibody (Biodesign Int., Saco, ME), mouse IgG1 isotype control, and rabbit IgG control at a concentration of 6.7 μg/ml in PBS, pH = 7.4, 0.1% Triton X-100, and 3% bovine serum albumin. Secondary antibodies

doi:10.1016/S1525-0016(02)00018-7

used were 488-goat anti-mouse IgG (fluorescein channel) and 594-goat anti-rabbit IgG (rhodamine channel) (Molecular Probes, Eugene, OR) at a concentration of 6.7 μg/ml in PBS, pH = 7.4, 0.1% Triton X-100, and 1% goat serum. Confocal imaging was performed with a Zeiss LSM 5 PASCAL confocal microscope with dual argon and helium/neon lasers equipped with Zeiss LSM software for image reconstruction. All sections were scanned in multitrack mode to avoid overlap of the fluorescein and rhodamine channels.

ACKNOWLEDGMENTS

Dr. Ruben Boado provided valuable discussions. Drs. Dafang Wu, Hwa Jeong Lee, and Chunni Zhu provided assistance in the primate experiment. This work was supported by a grant from the University of California, Davis/Medical Investigation of Neural Developmental Disorders Institute Research Program, and the Neurotoxin Exposure Treatment Research Program of the U.S. Dept. of Defense. Felix Schlachetzki was supported by a grant from the Ernst Schering Research Foundation (Berlin, Germany).

RECEIVED FOR PUBLICATION SEPTEMBER 12; ACCEPTED NOVEMBER 5, 2002.

REFERENCES

1. Martin, J. B. (1995). Gene therapy and pharmacological treatment of inherited neurological disorders. *Trends Biotechnol* **13:** 28–35.
2. Shi, N., and Pardridge, W. M. (2000). Non-invasive gene targeting to the brain. *Proc. Natl. Acad. Sci. USA* **97:** 7567–7572.
3. Mok, K. W. C., Lam, A. M. I., and Cullis, P. R. (1999). Stabilized plasmid-lipid particles: factors influencing plasmid entrapment and transfection properties. *Biochem. Biophys. Acta* **1419:** 137–150.
4. Semple, S. C., Chonn, A., and Cullis, P. R. (1998). Interactions of liposomes and lipid-based carrier systems with blood proteins: relation to clearance behaviour in vivo. *Adv. Drug Deliv. Rev.* **32:** 3–17.
5. Pardridge, W. M. (2001). *Brain Drug Targeting; The Future of Brain Development*. Cambridge University Press, Cambridge, United Kingdom, 1–370.
6. Shi, N., Zhang, Y., Boado, R. J., Zhu, C., and Pardridge, W. M. (2001). Brain-specific expression of an exogenous gene following intravenous administration. *Proc. Natl. Acad. Sci. USA* **98:** 12754–12759.
7. Shi, N., Boado, R. J., and Pardridge, W. M. (2001). Receptor-mediated gene targeting to tissues in the rat in vivo. *Pharm. Res.* **18:** 1091–1095.
8. Zhu, C., Zhang, Y., and Pardridge, W. M. (2002). Widespread expression of an exogenous gene in the eye following intravenous administration. *Invest. Ophthalmol. Vis. Sci.* **43:** 3075–3080.
9. Strayer, D. S. (1996). SV40 as an effective gene transfer vector in vivo. *J. Biol. Chem.* **271:** 24741–24746.
10. Zhang, Y., Zhu, C., and Pardridge, W. M. (2002). Antisense gene therapy of brain cancer with an artificial virus gene delivery system. *Mol. Ther.* **6:** 67–72.
11. Zhang, Y., Boado, R. J., Pardridge, W. M. (2003). Marked enhancement in gene expression by targeting the human insulin receptor. *J. Gene Med.,* in press.
12. Zhang, Y., Lee, H. J., Boado, R. J., and Pardridge, W. M. (2002). Receptor-mediated delivery of an antisense gene to human brain cancer cells. *J. Gene Med.* **4:** 183–194.
13. Lierse, W., and Horstmann, E. (1959). Quantitative anatomy of the cerebral vascular bed with especial emphasis on homogeneity and inhomogeneity in small parts of the gray and white matter. *Acta. Neurol.* **14:** 15–19.
14. Nevo, N., Chossat, N., Gagnach, W., Logeart, D., Mercadier, J.-J., and Michel, J.-B. (2001). Increasing endothelial cell permeability improves the efficiency of myocyte adenoviral vector infection. *J. Gene Med.* **3:** 42–50.
15. Hong, K., Zheng, W., Baker, A., and Papahadjopoulos, D. (1997). Stabilization of cationic liposome-plasmid DNA complexes by polyamines and poly(ethlene glycol)-phospholipid conjugates for efficient in vivo gene delivery. *FEBS Lett.* **400:** 233–237.
16. Plank, C., Tang, M. X., Wolfe, A. R., and Szoka, F. C. Jr. (1999). Branched cationic peptides for gene delivery: role of type and number of cationic residues in formation and in vitro activity of DNA polyplexes. *Hum. Gene Ther.* **10:** 319–332.
17. Boado, R. J., and Pardridge, W. M. (1998). Ten nucleotide cis element in the 3′-untranslated region of the GLUT1 glucose transporter mRNA increases gene expression via mRNA stabilization. *Mol. Brain Res.* **59:** 109–113.
18. Peng, K.-W., Pham, L., Ye, H., Zufferey, R., Trono, D., Cosset, F.-L., and Russell, S. J. (2001). Organ distribution of gene expression after intravenous infusion of targeted and untargeted lentiviral vectors. *Gene Ther.* **8:** 1456–1463.
19. Coloma, M. J., Lee, H. J., Kurihara, A., Landaw, E. M., Boado, R. J., Morrison, S. L., and Pardridge, W. M. (2000). Transport across the primate blood-brain barrier of a genetically engineered chimeric monoclonal antibody to the human insulin receptor. *Pharm. Res.* **17:** 266–274.
20. Zhang, Y., Calon, F., Zhu, C., Boado, R. J., Pardridge, W. M. (2003). Intravenous non-viral gene therapy causes normalization of striatal tyrosine hydroxylase and reversal of motor impairment in experimental Parkinsonism. *Human Gene Therapy* **14:** 1–12.
21. Chen, Z.-Y., Yant, S. R., He, C.-Y., Meuse, L., Shen, S., and Kay, M. A. (2001). Linear DNAs concatemerize in vivo and result in sustained transgene expression in mouse liver. *Mol. Ther.* **3:** 403–410.
22. Stoll, S. M., Sclimenti, C. R., Baba, E. J., Meuse, L., Kay, M. A., and Calos, M. P. (2002). Epstein-Barr virus/human vector provides high-level, long-term expression of α_1-antitrypsin in mice. *Mol. Ther.* **4:** 122–129.
23. Monnard, P.-A., Oberholzer, T., and Luisi, P. L. (1997). Entrapment of nucleic acids in liposomes. *Biochem. Biophys. Acta* **1329:** 39–50.

Absence of Toxicity of Chronic Weekly Intravenous Gene Therapy with Pegylated Immunoliposomes

Yu-feng Zhang,[1] Ruben J. Boado,[1] and William M. Pardridge[1,2]

Received April 29, 2003; accepted July 16, 2003

Purpose. Plasmid DNA-based gene therapy involves episomal gene expression and must be given on a chronic basis. Therefore, the purpose of the present study was to examine for toxic side effects of the chronic weekly intravenous administration of plasmid DNA delivered with a nonviral gene transfer method using pegylated immunoliposomes (PIL).

Methods. A 7-kb expression plasmid encoding for rat tyrosine hydroxylase (TH) was encapsulated in PILs targeted with either the murine OX26 monoclonal antibody (MAb) to the rat transferrin receptor (TfR) or with the mouse IgG2a isotype control antibody. Rats were treated with weekly intravenous injections of 5 μg/rat/week of the TH expression plasmid DNA encapsulated in either the TfRMAb-targeted PIL or the mouse IgG2a-targeted PIL for a total period of 6 weeks. A third control group of rats was treated with saline.

Results. The animals treated with either saline, the TfRMAb-PIL, or the mouse IgG2a-PIL had no measurable differences with respect to body weights, 14 serum chemistries, or organ histology of brain, liver, spleen, kidney, heart, or lung. Immunocytochemistry showed no evidence of inflammation in brain. The delivery to brain of the TH expression plasmid was confirmed with Southern blotting.

Conclusions. The PIL nonviral gene transfer method causes no toxic side effects following chronic weekly intravenous administration in rats.

KEY WORDS: gene therapy; brain; liposomes; nonviral gene transfer; inflammation.

INTRODUCTION

An important issue with either viral or nonviral gene delivery systems is organ toxicity associated with the delivery vector (1). In the case of either adenovirus or Herpes simplex virus, the preexisting immunity to these viruses causes an inflammatory reaction (2,3). A single injection of either adenovirus or Herpes simplex virus into the brain causes inflammation leading to demyelination (4,5). More than 90% of the human population has a preexisting immunity to adeno-associated virus (6). Therefore, there is a need to establish nonviral gene transfer technology with minimal toxicity. The principal forms of nonviral gene transfer include the use of complexes of DNA/cationic polymers or the hydrodynamic injection method. Cationic polyplexes have a relatively narrow therapeutic index. A nitrogen/phosphate (N/P) ratio of 6–10 is necessary for gene expression in the lung following the intravenous injection of the cationic polymer/plasmid DNA complexes, whereas an N/P ratio >20 is lethal (7). The hydrodynamic method involves the rapid intravenous injection of a volume of saline greater than the existing blood volume of the animal. This results in transitory right heart failure and hepatic congestion causing a selective expression of plasmid DNA in the liver (8). This gene delivery method results in an increase in liver enzymes, and the mortality with this method can be as high as 40% depending on the salt solution injected (8).

An alternative form of nonviral gene transfer involves the use of pegylated immunoliposomes (PIL). In this formulation, the nonviral plasmid DNA is encapsulated in the interior of an 85-nm liposome that has a net anionic charge (9). The surface of the liposome is pegylated with several thousand strands of 2000-Da polyethyleneglycol (PEG). The pegylated liposome is then targeted to distant sites by conjugating a transporting ligand to the tips of 1–2% of the PEG strands. Peptidomimetic monoclonal antibodies (MAb) to either the transferrin receptor (TfR) or the insulin receptor (IR) have been used to target PILs carrying expression plasmids to distant sites following intravenous injection (9,10). The PILs do not aggregate in saline and have prolonged blood residence times (11). PILs have been administered intravenously to mice on a weekly basis for the treatment of brain cancer (12), and PILs have been given to rats for the treatment of experimental Parkinson's disease (13). PILs targeted with the TfRMAb have been used to deliver nonviral plasmid DNA to brain. Because of the expression of the TfR on both the blood–brain barrier (BBB) and the neuronal plasma membrane, the TfRMAb-targeted PIL delivers the plasmid DNA to brain as well as other organs rich in TfR, such as liver and spleen (9,14). However, to date, there has been no evaluation of the potential toxicity of repeat intravenous administration of PILs.

The purpose of the present study was to examine the potential toxicity of repeat weekly intravenous administration of PIL-encapsulated plasmid DNA that was targeted to tissues in the rat with either the murine OX26 MAb to the rat TfR, or PILs targeted with the corresponding mouse IgG2a isotype control antibody. The plasmid DNA used in the present studies is the clone 877 DNA, which encodes for rat tyrosine hydroxylase (TH), as described previously (13). The delivery of the TH expression plasmid to brain with the TfRMAb-targeted PIL results in a normalization of striatal TH enzyme activity in brain of rats lesioned with a neurotoxin (13). For the present toxicity study, the TH expression plasmid DNA was encapsulated in either the TfRMAb-PIL or the mIgG2a-targeted PIL and was injected weekly for 6 weeks at a dose of 5 μg/rat of PIL-encapsulated plasmid DNA. Body weights of the animals were determined during the treatment period, and at the end of the 6-week treatment, blood was obtained for measurement of 14 parameters of serum chemistry reflecting liver and renal function. Major organs were removed at the end of the treatment period for pathologic analysis. In addition, brain was examined in detail with immunocytochemistry using antibodies to multiple antigens that reflect underlying tissue inflammation. Immunocytochemistry of brain was performed with the mouse OX1 MAb to rat leukocytes, the mouse OX2 MAb to the rat class II multiple histocompatibility complex (MHC) antigen, the mouse OX18

[1] Department of Medicine, UCLA, Los Angeles, CA 90024.
[2] To whom correspondence should be addressed. (email: wpardridge@mednet.ucla.edu)

0724-8741/03/1100-1779/0 © 2003 Plenum Publishing Corporation

MAb to the rat class I MHC antigen, the mouse OX35 MAb to the rat lymphocyte CD4 receptor, and the mouse OX42 MAb to the rat macrophage. Finally, the present studies used Southern blotting to confirm distribution of the TH expression plasmid in brain following targeting with the TfRMAb-PIL.

METHODS

Materials

1-Palmitoyl-2-oleoyl-*sn*-glycerol-3-phosphocholine (POPC) and didodecyldimethylammonium bromide (DDAB) were purchased from Avanti-Polar Lipids Inc. (Alabaster, AL). Distearoylphosphatidylethanolamine (DSPE)-PEG^{2000} was obtained from Shearwater Polymers (Huntsville, AL), where PEG^{2000} is polyethylene glycol (PEG) of 2000 Daltons. DSPE-PEG^{2000}-maleimide was custom-synthesized by Shearwater Polymers. The LiposoFAST-Basic extruder and polycarbonate filters were from Avestin (Ottawa, Canada). [α-^{32}P]dCTP (3000 Ci/mmol) was from NEN Life Science Products Inc. (Boston, MA). *N*-Succinimidyl[2,3-^{3}H]propionate ([^{3}H]NSP, 101 Ci/mmol), Sepharose CL-4B, and Protein G-Sepharose CL-4B were from Amersham Pharmacia Biotech (Arlington Heights, IL). The nick translation system was purchased from Invitrogen Life Technologies (Carlsbad, CA). Exonuclease III was purchased from Promega (Madison, WI); 2-iminothiolane (Traut's reagent) was obtained from Pierce Chemical Co. (Rockford, IL). Mouse myeloma ascites containing IgG2a (κ) (mIgG2a), pancreatic DNase I with a specific activity of 2000 Kunitz units/mg, horse serum, mouse IgG1 isotype, mouse anti–glia fibrillary acidic protein (GFAP) monoclonal antibody (MAb), and glycerol-gelatin were from Sigma Chemical Co. (St. Louis, MO). The antitransferrin receptor monoclonal antibody (TfRMAb) used in these studies is the murine OX26 MAb to the rat TfR, which is a mouse IgG2a. TfRMAb and mIgG2a were individually purified by protein G affinity chromatography from hybridoma-generated ascites. The biotinylated horse anti-mouse IgG, Vectastain ABC kit, and 3-amino-9-ethylcarbazole (AEC) substrate kit were purchased from Vector Laboratories (Burlingame, CA). Mouse antirat class I multiple histocompatibility complex (MHC) monoclonal antibody (OX18), mouse antirat leukocyte CD45 (OX-1), mouse antirat lymphocyte CD4 (OX-35), mouse antirat class II MHC (OX-6), and mouse antirat macrophage CD11b (OX42) were purchased from Serotec (Raleigh, NC). Optimal cutting temperature (O.C.T.) compound (Tissue-Tek) was purchased from Sakura FineTek (Torrance, CA). Adult male Sprague-Dawley rats (weighing from 180–220 g) were obtained from Harlan Breeders (Indianapolis, IN).

Plasmid DNA Preparation and Radiolabeling

The tyrosine hydroxylase expression plasmid, driven by the SV40 promotor and designated clone 877, was constructed as described previously (13). Clone 877 plasmid DNA was purified from *E. coli* with the Plasmid Maxi Kit and desalted per the manufacturer's instructions (Qiagen, Chatsworth, CA). The size of the DNA was confirmed by 0.8% agarose gel electrophoresis. DNA was labeled with [^{32}P]dCTP using nick translation. The specific activity of [^{32}P]DNA was 15–20 μCi/μg. The trichloroacetic acid precipitability was 99%.

PEGylated Liposome Synthesis and Plasmid Encapsulation

POPC (18.8 μmol), DDAB (0.6 μmol), DSPE-PEG^{2000} (0.6 μmol), and DSPE-PEG^{2000}-maleimide (0.2 μmol) were dissolved in chloroform, followed by evaporation, as described previously (14). The lipids were dispersed in 0.2 ml of 0.05 M Tris-HCl buffer (pH 7.0) and vortexed for 1 min, followed by 2 min of bath sonication. Supercoiled DNA (200 μg) and 1 μCi of [^{32}P]DNA were added to the lipids. The dispersion was frozen in ethanol/dry ice for 5 min and thawed at room temperature for 25 min, and this freeze–thaw cycle was repeated five times to produce large vesicles with the DNA loosely entrapped inside. The large vesicles were converted into small (85-nm-diameter) liposomes by extrusion. The liposome dispersion was diluted to a lipid concentration of 40 mM, followed by extrusion five times each through two stacks each of 200- and 100-nm pore size polycarbonate membranes with a hand-held LiposoFAST-Basic extruder as described previously (11). The mean vesicle diameters were determined by quasielastic light scattering using a Microtrac Ultrafine Particle Analyzer (Leeds-Northrup, St. Petersburg, FL) as described previously (11).

The plasmid adsorbed to the exterior of the liposomes was removed by nuclease digestion, and 6 U of pancreatic endonuclease I and 33 U of exonuclease III were added in 5 mM $MgCl_2$ to the liposome/DNA mixture after extrusion. After incubation at 37°C for 1 h, the reaction was stopped by adding 20 mM EDTA. The nuclease digestion removed any exteriorized plasmid DNA, as demonstrated by agarose gel electrophoresis and ethidium bromide staining of aliquots taken before and after nuclease treatment, as described previously (11). The formulation before antibody conjugation is designated a pegylated liposome (PL), and the formulation after antibody conjugation is called a pegylated immunoliposome (PIL).

MAb Conjugation to the PEGylated Liposome Encapsulated with DNA

TfRMAb or mIgG2a was thiolated and individually conjugated to the maleimide moiety of the PEGylated liposome to produce the PIL with the desired receptor specificity. PIL conjugated with the OX26 MAb is designated TfRMAb-PIL, and PIL conjugated with the mIgG2a isotype control is designated mIgG2a-PIL. Either MAb or mIgG2a was radiolabeled with [^{3}H]NSP as described previously (15). [^{3}H]MAb had a specific activity of >0.11 μCi/μg and a TCA precipitability of >97%. The MAb (3.0 mg, 20 nmol) was thiolated with 40:1 molar excess of 2-iminothiolane (Traut's reagent), as described previously (15). The thiolated MAb, which contained a trace amount of ^{3}H-labeled MAb, was conjugated overnight to the PEGylated liposome with encapsulated plasmid DNA containing a trace amount of [^{32}P]DNA. The unconjugated MAb and the oligonucleotides produced by nuclease treatment were separated from the PIL by Sepharose CL-4B column chromatography as described previously (11). The number of MAb molecules conjugated per liposome was calculated from the total ^{3}H-labeled MAb radioactivity in the liposome pool and the specific activity of the labeled MAb,

assuming 100,000 lipid molecules per liposome, as described previously (15). The average number of MAb molecules conjugated per liposome was 57 ± 12 (mean ± SD, n = 4 syntheses). The final percentage entrapment of 200 μg of plasmid DNA in the liposome preparation was computed from the ^{32}P radioactivity and was 30 ± 2% (mean ± SD, n = 4 syntheses), or 60 μg of plasmid DNA.

Chronic Intravenous Administration of PIL-Encapsulated DNA

Adult male Sprague-Dawley rats weighing 200–220 g were anesthetized with ketamine (50 mg/kg) and xylazine (4 mg/kg) intraperitoneally. Animals were divided into three groups. PIL or saline was injected i.v. via femoral vein with a 30-g needle. The first group was injected with TfRMAb-PIL carrying clone 877 plasmid DNA at a dose of 5 μg per rat. The second group was injected with mIgG2a-PIL carrying clone 877 plasmid DNA at a dose of 5 μg per rat. The third group was injected with saline. The average intravenous injection volume for all treatments was 300 μL. These intravenous treatments were given once a week for 6 consecutive weeks. Each week before injection, the body weight for each rat was measured. At 3 days following the sixth injection, the rats were anesthetized, and blood was collected from the vena cava. Serum was stored at –20°C for serum chemistry measurements by autoanalyzer in the UCLA Medical Center Clinical Laboratory. The rats were then sacrificed, and organs were removed for immunocytochemistry.

Immunocytochemistry

Immunocytochemistry was performed by the avidin–biotin complex (ABC) immunoperoxidase method (Vector Laboratories). Brains were removed immediately after sacrifice, and cut into three sagittal slabs. One slab was immersion fixed in cold 4% paraformaldehyde in 0.01 M phosphate-buffered saline (PBS) for 24 h at 4°C. The second slab was fixed in cold 100% methanol for 24 h at –20°C. These slabs were cryoprotected in 20% sucrose in 0.1 M phosphate-buffered water, pH 7.4 (PBW), for 24 h at 4°C, and 30% sucrose in PBW for 24 h at 4°C. Brains were embedded in O.C.T. medium and frozen in dry ice powder. Frozen sections (20 μm) of rat brain were cut on a Mikron HM505E cryostat. Endogenous peroxidase was blocked with 0.3% H_2O_2 in 0.3% horse serum–phosphate-buffered saline (PBS) for 30 min. Nonspecific binding of proteins was blocked with 10% horse serum in PBS for 30 min. Sections were then incubated in primary antibodies overnight at 4°C. Based on either results provided by the manufacturer or on pilot studies, the fixative (methanol or paraformaldehyde) was chosen to preserve the target antigenicity in the fixed tissue. For methanol-fixed brain sections, OX1 (5 μg/ml), OX18 (5 μg/ml), or OX35 (5 μg/ml) was used as the primary antibody; for paraformaldehyde-fixed brain sections, OX6 (5 μg/ml), OX42 (5 μg/ml), or mouse anti-GFAP MAb (1 μg/ml) was used as the primary antibody. Identical concentrations of isotype control antibody were also used as primary antibody. Mouse IgG1 was used as the isotype control antibody for OX18, OX1, OX6, and GFAP, and mouse IgG2a was used as the isotype control antibody for OX35 and OX42. After incubation and wash in PBS, sections were incubated in biotinylated horse antimouse IgG for 30 min. After development in AEC, sections were mounted with glycerol-gelatin and examined by light microscopy.

Hematoxylin and Eosin Staining of Rat Organs

The third sagittal slab of brain, as well as liver, spleen, kidney, heart, and lung of each rat were removed and immersion fixed in 10% formalin in 0.1 M phosphate buffer for 48 h at 4°C. The fixed organs were embedded in paraffin and stained with hematoxylin and eosin and examined by light microscopy.

Southern Blotting

Plasmid DNA was isolated with the Hirt procedure (16) from rat brain 3 days following the intravenous injection of saline, clone 877 encapsulated in TfRMAb-PIL, or clone 877 encapsulated in mIgG2a-PIL. Rat brain (100 mg) was homogenized in 2 ml lysis buffer (20 mM Tris pH 7.5, 10 mM EDTA, 1% SDS) containing 15 μg/ml DNase-free RNase A using a Polytron PT-MR 3000 homogenizer (Littau, Switzerland) at full speed for 10 s Samples were incubated for 30 min at 37°C. Proteinase K was added to a final concentration of 1 mg/ml and samples incubated for 2 h at 37°C. Nuclear DNA was precipitated overnight at 4°C in the presence of 1.1 M NaCl. Samples were centrifuged at 14,000 rpm and 4°C for 30 min. Supernatants were extracted with phenol:chloroform, and plasmid DNA precipitated with ethanol in the presence of 10 μg glycogen carrier. Aliquots of precipitated material were resolved by gel electrophoresis in 0.8% agarose and blotted onto a GeneScreen Plus membrane (14). To prevent hybridization with the endogenous rat TH genomic DNA, membranes were hybridized with [^{32}P]pGL2 clone 734 (17), which contains the clone 877 backbone but without the rat TH cDNA insert (13). Southern blot hybridization was performed as previously reported (14). Autoradiograms were developed with Kodak X-Omat Blue film and intensifying screens for 24 h at –70°C. Films were scanned with a Umax PowerLook III scanner, and images imported and cropped in Adobe Photoshop 5.5 on a G4 Power Macintosh.

Statistical Analysis

Statistical differences at the $p < 0.05$ level among different groups were evaluated by analysis of variance with Bonferroni correction.

RESULTS

The animals were divided into three groups depending on whether the rat was treated with weekly intravenous injections of (a) saline, (b) the TH expression plasmid encapsulated in mouse IgG2a targeted PILs, or (c) the TH expression plasmid encapsulated in the OX26 TfRMAb-targeted PILs. The body weights of the animals in the three treatment groups are shown in Fig. 1, and there was no significant difference between the body weights of the animals in the three groups throughout the treatment period.

The results of the chemistry analysis of the serum taken 3 days after the sixth weekly injection are shown in Table I. There are no significant differences in any of the 14 different serum chemistries for any of the three treatment groups

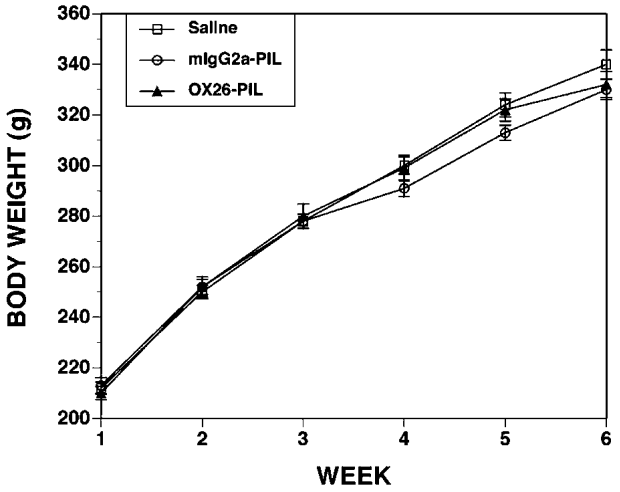

Fig. 1. The body weight of each rat in the three treatment groups was measured weekly during the course of treatment, and the mean ± SE (n = 6 rats per group) is shown. The OX26-PIL is the TfRMAb-targeted PIL, and the mIgG2a-PIL is the PIL targeted with the non-specific mouse IgG2a, which is the isotype control antibody for the OX26 MAb.

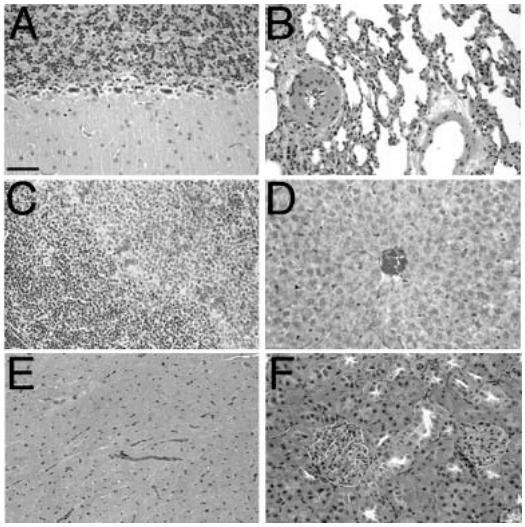

Fig. 2. Hematoxylin and eosin staining of formalin fixed cerebellum (A), lung (B), spleen (C), liver (D), heart (E), and kidney (F), removed 3 days after the sixth weekly intravenous injection of the TH expression plasmid encapsulated in the OX26 TfRMAb-targeted PIL. The magnification is the same in all panels, and the *magnification bar* in panel A is 37 μm.

(Table I). The organ histology in the rats sacrificed 3 days following the sixth weekly treatment is shown in Fig. 2 for brain cerebellum (Fig. 2A), lung (Fig. 2B), spleen (Fig. 2C), liver (Fig. 2D), heart (Fig. 2E), and kidney (Fig. 2F). The histology shown in Fig. 2 is for organs removed from rats treated with the TfRMAb-PIL. The organ histology of these animals was normal (Fig. 2) and was no different from the histology of organs taken from animals treated with either saline or the mIgG2a-PIL.

The results of the brain immunocytochemistry are given in Table II. No OX1-immunoreactive leukocytes were found in brain in any of the three treatment groups, although there was immunopositive choroidal endothelium staining in all groups (Table II). There was an occasional OX6-immunoreactive class II antigen-presenting cell in the meningial surface of all three treatment groups with no evidence of any parenchymal infiltration of class II immunopositive cells in any of the treatment groups (Table II). OX18 immunoreactivity indicative of the class I MHC antigen was found on capillary endothelium and in focal subependymal microglia, and the same staining pattern was found in all three treatment groups (Table II). OX35-immunoreactive CD4 lymphocytes were rare in brain with the same pattern in all three treatment groups (Table II). OX42-immunoreactive microglia were found diffusely in the parenchyma throughout the cerebrum and cerebellum, with an identical pattern in all treatment groups (Table II). Immunoreactive GFAP astrocytes were found diffusely throughout the cerebrum and cerebellum, with the same pattern in all three treatment groups (Table II). There was no immunoreactivity in brain with the nonspecific mouse IgG1 (mIgG1), which is the isotype control antibody for the OX1, OX18, OX6, and the GFAP antibodies (Table II). There was no immunocytochemical staining of brain using the nonspecific mouse IgG2a (mIgG2a), which is the isotype control antibody for the OX35 and OX42 antibodies (Table II).

Table I. Summary of Serum Chemistry

Assay	Units	Saline	mIgG2a-PIL	OX26-PIL
Sodium	mM	143 ± 1	142 ± 1	140 ± 1
Potassium	mM	4.4 ± 0.1	4.6 ± 0.1	4.6 ± 0.2
Chloride	mM	100 ± 1	100 ± 1	100 ± 1
CO_2	mM	29 ± 1	29 ± 1	27 ± 1
Glucose	mg/dl	168 ± 8	160 ± 6	163 ± 4
Creatinine	mg/dl	0.45 ± 0.03	0.40 ± 0.01	0.45 ± 0.02
Urea nitrogen	mg/dl	19 ± 1	21 ± 2	18 ± 1
Total protein	g/dl	5.2 ± 0.1	5.3 ± 0.1	5.3 ± 0.1
Albumin	g/dl	1.4 ± 0.1	1.4 ± 0.1	1.4 ± 0.1
Bilirubin, total	mg/dl	0.35 ± 0.03	0.25 ± 0.05	0.33 ± 0.02
Alk phos	U/L	231 ± 27	212 ± 25	281 ± 11
AST (SGOT)	U/L	65 ± 5	59 ± 2	74 ± 6
ALT (SGPT)	U/L	54 ± 2	52 ± 3	59 ± 1
Calcium	mg/dl	9.4 ± 0.1	9.5 ± 0.2	9.2 ± 0.1

Data are mean ± SE (n = 6 rats in each of the three treatment groups).

The delivery of the TH expression plasmid to brain was verified with Southern blotting as shown in Fig. 3 (Lane 3). No signal was detected in the saline-treated animals (Lane 1, Fig. 3) because these animals were not administered DNA. No hybridization signal was detected in the brain of animals treated with the expression plasmid encapsulated in the mIgG2a-PIL (Lane 2, Fig. 3) because this isotype control antibody was unable to target the PIL across the BBB and into brain cells.

DISCUSSION

These studies show that the repeat weekly intravenous administration of the PIL-based gene therapy in rats for 6 weeks causes no measurable toxicity in brain or peripheral tissues. In addition, these studies show that the chronic weekly intravenous administration of a TH expression plasmid encapsulated in TfRMAb-PILs causes no inflammation within the target organ, the central nervous system (CNS).

Table II. Summary of Immunocytochemistry

Antibody	Parameter	Fixative	Findings
OX1	Leukocytes	Methanol	Positive choroidal endothelium Same pattern in all 3 treatment groups
OX6	Class II MHC	Para.[a]	Occasional positive cell in meninges Same pattern in all 3 treatment groups
OX18	Class I MHC	Methanol	Weak staining of capillary endothelium Focal subependymal microglia Same pattern in all 3 treatment groups
OX35	CD4-lymphocytes	Methanol	Minimal staining of brain and equal to mouse IgG2a control Same pattern in all 3 treatment groups
OX42	Macrophages	Para.	Diffuse immunoreactive microglia throughout cerebrum and cerebellum Same pattern in all 3 treatment groups
GFAP	Astrocytes	Para.	Diffuse immunoreactive astrocytes throughout cerebrum and cerebellum Same pattern in all 3 treatment groups
Mouse IgG1	Control	Methanol	No reaction (control for OX1, OX18)
		Para.	No reaction (control for OX6, GFAP)
Mouse IgG2a	Control	Methanol, Para.	No reaction (control for OX35) No reaction (control for OX42)

Para., paraformaldehyde.

There is no general systemic toxicity following weekly PIL administration based on the observation that the body weights of the animals increase over the 6 week treatment period at the same rate for all 3 treatment groups (Fig. 1). The PIL targets the plasmid DNA to TfR-rich organs such as the brain, liver, or spleen (9,14). The serum chemistries show normal hepatic function tests and an absence of an increase in serum bilirubin or liver enzymes (Table I). In contrast, the intravenous injection of adenovirus in primates results in increased liver enzymes secondary to hepatic inflammation caused by reaction to the immunogenic viral vector (18). There is no change in serum electrolytes or other renal function tests (Table I). The normal serum chemistry is paralleled by the normal organ histology for liver, speen, kidney, heart, lung, and brain (Fig. 2). The serum chemistry and organ histology were examined at 3 days following the sixth weekly injection because prior work has shown the TH gene expression following PIL injection is maximal at this time (13).

The intracerebral injection of viral vectors, such as adenovirus or Herpes simplex virus, leads to inflammation of the brain, as evidenced by perivascular cuffing with lymphocytes and increased immunoreactivity for class I and class I MHC antigens in brain (2–5). Therefore, the present studies performed a detailed immunocytochemical analysis of brain to examine for any evidence of inflammation in the brain following the chronic delivery to brain of a TH expression plasmid encapsulated in a TfRMAb-targeted PIL. The brain immunocytochemistry of the animals treated weekly with the TfRMAb-targeted PIL was compared to that of control groups of rats treated weekly with either saline or with mIgG2a-targeted PILs. There is an identical pattern of immunoreactivity in rat brain using OX1, OX6, OX18, OX35, OX42, and GFAP antibodies in immunocytochemical analysis of brain for all three treatment groups (Table II). In these studies, the brain was fixed with either methanol or paraformaldehyde, depending on which was the optimal fixative for each antigen (Methods), to preserve antigen recognition in the fixed brain. Chronic delivery of TfRMAb-targeted PILs to brain caused (a) no elevations in parenchymal class I (OX18) or II MHC (OX6), (b) no elevations in parenchymal infiltration by lymphocytes (OX35), leukocytes (OX1), or macrophages (OX42), and (c) no elevations in parenchymal gliosis (GFAP).

In summary, these studies demonstrate that nonviral expression plasmids can be delivered to organs with the PIL gene transfer method without toxic side effects when administered at a PIL-encapsulated plasmid DNA dose of 25 μg/kg. The chronic weekly intravenous administration of this dose of plasmid DNA encoding for rat TH and encapsulated in TfRMAb-targeted PILs causes no evidence of toxicity in ei-

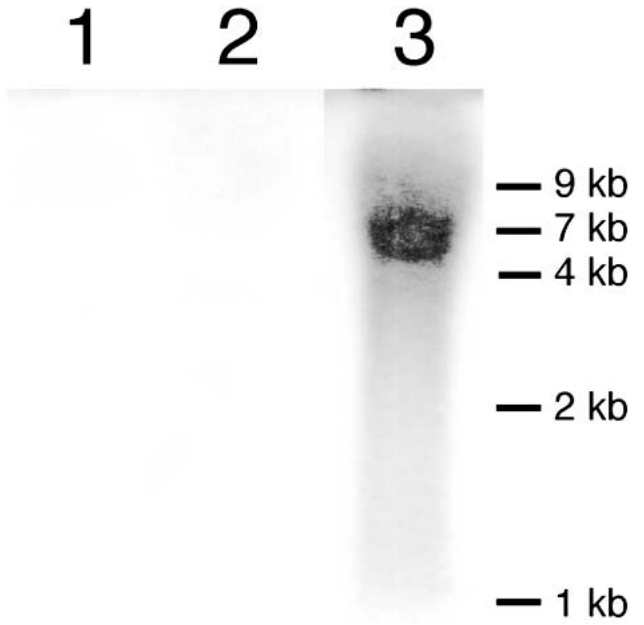

Fig. 3. Southern blot analysis of rat brain with [^{32}P]pGL2 clone 734. Lane 1, brain isolated from a saline-treated rat; lane 2, brain isolated from a rat injected with the TH expression plasmid encapsulated in the mIgG2a-targeted PIL; and lane 3, brain isolated from a rat injected with the TH expression plasmid encapsulated in the TfRMAb-targeted PIL. The migration of the DNA standards is indicated in the figure. The expected ~7-kb plasmid DNA corresponding to the size of the TH expression plasmid is seen only in the brain of the rats treated with the TfRMab-targeted PIL (lane 3).

ther the target organ, brain, or in peripheral tissues, such as liver, spleen, kidney, heart, or lung. It is possible that toxic effects may be observed at higher doses, but the dose used in this study in rats was chosen because this dose is therapeutic in rats (13). Moreover, a much higher dose, 200 μg/kg, of PIL-encapsulated plasmid DNA has been administered weekly to mice without evidence of toxicity (12). The need for high dosing of plasmid DNA with the PIL gene-targeting method is unlikely because a dose of 12 μg/kg of PIL-encapsulated plasmid DNA in adult primates results in levels of gene expression that are 50-fold higher than in rodents (10). The finding of a lack of toxicity following chronic PIL administration is important because the PIL gene transfer method delivers to the target organ a nonviral plasmid that directs gene expression for only a finite duration (12,13). The expression plasmid is transcribed episomally and is not permanently or randomly integrated into the host genome. Therefore, in order to sustain a pharmacologic effect with plasmid DNA-based gene therapy, it is necessary to administer the gene medicine on a chronic basis. The frequency of the administration is a function of the persistence of plasmid expression in the target organ. Long-term gene expression is possible with viral vectors that permanently integrate into the host genome, but this approach is associated with the risk of insertional mutagenesis (1). An alternative approach to gene therapy is chronic treatment with episomal-based plasmid DNA that is formulated in such a way that the DNA is able to target distant sites following intravenous administration. Prior work has shown that the PIL gene-targeting method enables widespread expression of the exogenous gene in distant sites such as brain in mice, rats, and rhesus monkeys (9–11). The present studies show that PIL-based gene therapy can be given chronically without the development of tissue toxicity in either the target organ, brain, or in peripheral tissues.

ACKNOWLEDGMENTS

This work was supported by a grant from the Neurotoxin Exposure Treatment Research Program of the U.S. Department of Defense. Dr. Felix Schlachetzki assisted with the immunocytochemistry.

REFERENCES

1. S. Hacein-Bey-Abina, C. von Kalle, M. Schmidt, F. LeDeist, N. Wulffraat, E. McIntyre, I. Radford, J. L. Villeval, C. C. Fraser, M. Cavazzana-Calvo, and A. Fischer. A serious adverse event after successful gene therapy for X-linked severe combined immunodeficiency. *N. Engl. J. Med.* **348**:255–256 (2003).
2. M. M. McMenamin, A. P. Byrnes, H. M. Charlton, R. S. Coffin, D. S. Latchman, and M. J. A. Wood. A γ34.5 mutant of herpes simplex 1 causes severe inflammation in the brain. *Neuroscience* **83**:1225–1237 (1998).
3. Y. Stallwood, K. D. Fisher, P. H. Gallimore, and V. Mautner. Netralisation of adenovirus infectivity by ascitic fluid from ovarian cancer patients. *Gene Ther.* **7**:637–643 (2000).
4. R. A. Dewey, G. Morrissey, C. M. Cowsill, D. Stone, F. Bolognani, N. J. F. Dodd, T. D. Southgate, D. Klatzmann, H. Lassmann, M. G. Castro, and P. R. Lowenstein. Chronic brain inflammation and persistent herpes simplex virus 1 thymidine kinase expression in survivors of syngeneic glioma treated by adenovirus-mediated gene therapy: Implications for clinical trials. *Nature Med.* **5**:1256–1263 (1999).
5. M. J. A. Wood, H. M. Charlton, K. J. Wood, K. Kajiwara, and A. P. Byrnes. Immune responses to adenovirus vectors in the nervous system. *Trends Neurosci.* **19**:497–501 (1996).
6. N. Chirmule, K. J. Propert, S. A. Magosin, Y. Qian, R. Qian, and J. M. Wilson. Immune responses to adenovirus and adeno-associated virus in humans. *Gene Ther.* **6**:1574–1583 (1999).
7. S. M. Zou, P. Erbacher, J. S. Remy, and J. P. Behr. Systemic linear polyethylenimine (L-PEI)-mediated gene delivery in the mouse. *J. Gene Med.* **2**:128–134 (2000).
8. G. Zhang, V. Budker, and J. A. Wolff. High levels of foreign gene expression in hepatocytes after tail vein injections of naked plasmid DNA. *Hum. Gene Ther.* **10**:1735–1737 (1999).
9. N. Shi, Y. Zhang, R. J. Boado, C. Zhu, and W. M. Pardridge. Brain-specific expression of an exogenous gene following intravenous administration. *Proc. Natl. Acad. Sci. USA* **98**:12754–12759 (2001).
10. Y. Zhang, F. Schlachetzki, and W. M. Pardridge. Global non-viral gene transfer to the primate brain following intravenous administration. *Mol. Ther.* **7**:11–18 (2003).
11. N. Shi and W. M. Pardridge. Noninvasive gene targeting to the brain. *Proc. Natl. Acad. Sci. USA* **97**:7567–7572 (2000).
12. Y. Zhang, C. Zhu, and W. M. Pardridge. Antisense gene therapy of brain cancer with an artificial virus gene delivery system. *Mol. Ther.* **6**:67–72 (2002).
13. Y. Zhang, F. Calon, C. Zhu, R. J. Boado, and W. M. Pardridge. Intravenous nonviral gene therapy causes normalization of striatal tyrosine hydroxylase and reversal of motor impairment in experimental parkinsonism. *Hum. Gene Ther.* **14**:1–12 (2003).
14. N. Shi, R. J. Boado, and W. M. Pardridge. Receptor mediated gene targeting to tissues *in vivo* following intravenous administration of pegylated immunoliposomes. *Pharm. Res.* **18**:1091–1095 (2001).

15. J. Huwyler, D. Wu, and W. M. Pardridge. Brain drug delivery of small molecules using immunoliposomes. *Proc. Natl. Acad. Sci. USA* **93**:14164–14169 (1996).
16. D. Duan, P. Sharma, J. Yang, Y. Yue, L. Dudus, Y. Zhang, K. J. Fisher, and J. F. Engelhardt. Circular intermediates of recombinant adeno-associated virus have defined structural characteristics responsible for long-term episomal persistence in muscle tissue. *J. Virology* **72**:8568–8577 (1998).
17. R. J. Boado and W. M. Pardridge. Ten nucleotide cis element in the 3′-untranslated region of the GLUT1 glucose transporter mRNA increases gene expression via mRNA stabilization. *Molec. Brain Res.* **59**:109–113 (1998).
18. J. N. Lozier, G. Csako, T. H. Mondoro, D. M. Krizek, M. E. Metzger, R. Costello, J. G. Vostal, M. E. Rick, R. E. Donahue, and R. A. Morgan. Toxicity of a first-generation adenoviral vector in rhesus macaques. *Hum. Gene Ther.* **13**:113–124 (2002).

Molecular Vision 2003; 9:465-72 <http://www.molvis.org/molvis/v9/a59>
Received 25 June 2003 | Accepted 23 September 2003 | Published 3 October 2003

Organ-specific gene expression in the rhesus monkey eye following intravenous non-viral gene transfer

Yun Zhang,[1] Felix Schlachetzki,[1,2] Jian Yi Li,[1] Ruben J. Boado,[1] William M. Pardridge[1]

[1]Department of Medicine, UCLA, Los Angeles, CA; [2]Department of Neurology, University of Regensburg, Regensburg, Germany

Purpose: The transfer of exogenous genes to the entire retina and other ocular structures is possible with a vascular route of gene delivery using a non-viral gene transfer method. The present studies examine the extent to which either β-galactosidase or luciferase expression plasmids are targeted to the retina in the adult rhesus monkey following intravenous administration. In addition, these studies examine the pattern of organ expression of the transgene in the rhesus monkey depending on whether the plasmid is under the influence of a widely expressed promoter, the SV40 promoter, or an ocular-specific promoter, the opsin promoter.

Methods: The plasmid DNA with either the SV40 or opsin promoter is encapsulated in the interior of 85 nm pegylated immunoliposomes (PILs), which are targeted across the blood-retinal barrier and into ocular cells with a monoclonal antibody to the human insulin receptor. Following a single intravenous injection of the PIL carrying the transgene, the animals were sacrificed 2, 7, or 14 days later for the measurement of β-galactosidase or luciferase gene expression in the monkey eye and peripheral organs.

Results: Histochemistry showed expression of the β-galactosidase gene throughout the entire primate retina including the photoreceptor cells with either an SV40 or a bovine opsin promoter. Whereas the SV40 promoter enables gene expression in other organs of the primate (brain, liver, spleen), the opsin promoter restricted trans-gene expression to the primate eye, as there was no gene expressed in other organs. The retinal luciferase activity at 2 days after administration was 9.6±0.4 pg luciferase/mg protein, and at 14 days after administration was still comparable to maximal levels of luciferase gene expression in the mouse or rat. Confocal microscopy with antibodies to the insulin receptor and to β-galactosidase demonstrated co-localization in the retina, with high expression of the trans-gene and the insulin receptor in the inner segments of the photoreceptor cells.

Conclusions: The PIL non-viral gene transfer technology makes possible adult transgenics in 24 h. Ectopic expression of exogenous genes in organs other than the target organ is made possible with the use of organ specific promoters, and gene expression in the primate is restricted to the eye when the trans-gene is under the influence of the opsin promoter. Plasmid-based gene expression is still in the therapeutic range for 2-3 weeks after a single intravenous administration. Exogenous genes are expressed throughout the entire primate retina following the delivery of the gene to the eye via a trans-vascular route.

Many forms of blindness are potentially treatable with retinal gene therapy [1,2]. The retinal photoreceptor cells can be transduced with sub-retinal injections of viruses such as adeno-associated virus (AAV) [3]. The portion of the human retina that is transduced with a sub-retinal injection is localized to the injection site [4,5]. Conversely, global expression of an exogenous gene throughout the human retina may be possible with a transvascular route to the eye following intravenous administration. However, viral vectors do not cross the blood-retinal barrier (BRB). In mice a non-viral gene delivery system comprised of pegylated immunoliposomes (PIL) can be targeted across the BRB following intravenous administration, and this leads to expression of an exogenous gene in the eye [6]. In this approach, the therapeutic gene is incorporated in non-viral plasmid DNA, which is encapsulated in the interior of 85 nm anionic liposomes [7,8]. The surface of the liposome is conjugated with several thousand strands of polyethylene glycol (PEG), which stabilizes the liposome in the circulation, minimizes liposome uptake by the reticulo-endothelial system, and enables a sustained circulation time of the liposome in the blood. The tips of 1-2% of the PEG strands are conjugated with a targeting ligand such as a peptidomimetic monoclonal antibody (MAb). The targeting ligand binds to specific receptors expressed at both the BRB and the plasma membrane of retina and ocular cells to trigger receptor-mediated transcytosis across the BRB and receptor-mediated endocytosis into cells of the eye [6].

Exogenous genes have been targeted to the mouse eye and retinal pigmented epithelium (RPE) with PILs formulated with a MAb to the mouse transferrin receptor (TfR) [6]. This resulted in widespread expression of the exogenous gene throughout the RPE, but there was no measureable gene expression in the photoreceptor cells of the mouse retina [6]. The absence of gene expression in the photoreceptor layer is attributed to the minimal expression of TfR on the plasma membranes in the outer nuclear layer (ONL) of the retina [9,10]. The reduced expression of the TfR in the ONL is con-

Correspondence to: Dr. William M. Pardridge, UCLA, Warren Hall 13-164, 900 Veteran Avenue, Los Angeles, CA, 90024; Phone: (310) 825-8858; FAX: (310) 206-5163; email: wpardridge@mednet.ucla.edu

sistent with very low concentrations of iron and ferritin in this region of the retina [10]. Conversely, the cells of the ONL express high levels of the insulin receptor (IR) [11,12] and a targeting ligand that accesses the IR could deliver genes to the ONL. The 83-14 murine MAb to the human insulin receptor (HIR) is rapidly transported across the blood-brain barrier (BBB) of Old World primates, owing to high expression of the IR on the primate BBB [13]. Gene transfer with the HIRMAb-targeted PIL enables the global delivery of exogenous genes to the brain of the rhesus monkey following intravenous injection [14]. The IR is also expressed at the BRB [11,12]. Therefore, the present studies determine the extent to which endogenous genes are expressed in the Rhesus monkey retina following a single intravenous injection of non-viral plasmid DNA encapsulated in a PIL that is targeted to the HIR. Owing to the genetic similarity between humans and Old World monkeys such as the Rhesus monkey [15], the 83-14 HIRMAb cross-reacts with the Rhesus monkey IR [13]. In the present studies, plasmids encoding either β-galactosidase or luciferase are administered by peripheral venous injection, and gene expression in the primate retina is measured with the luciferase assay, β-galactosidase histochemistry, and confocal microscopy using antibodies directed against β-galactosidase and the HIR. The β-galactosidase expression plasmid, under the influence of the SV40 promoter, is alternatively designated pSV-β-galactosidase or clone 756, as described previously [14]. The luciferase expression plasmid, under the influence of the SV40 promoter, was derived from the pCEP4 plasmid, and is designated clone 790 as described previously [14].

A second goal of the present work was to examine the organ specificity of gene expression with the PIL gene transfer approach. If the exogenous gene is under the influence of a widely expressed promoter, such as the SV40 promoter, then the gene is expressed in multiple organs of the primate, including brain, liver, and spleen, following the intravenous injection of HIRMAb-targeted PILs [14]. In the present study, a β-galactosidase expression plasmid under the influence of the bovine opsin promoter, is injected into the primate following encapsulation in HIRMAb-targeted PILs. The opsin-β-galactosidase plasmid is designated pLacF, as described by Zack et al [16].

METHODS

Materials: POPC (1-palmitoyl-2-oleoyl-*sn*-glycerol-3-phosphocholine) and DDAB (didodecyldimethylammonium bromide) were purchased from Avanti-Polar Lipids Inc. (Alabaster, AL), and distearoylphosphatidylethanolamine (DSPE)-PEG 2000 was obtained from Shearwater Polymers (Huntsville, AL). DSPE-PEG 2000-maleimide was custom synthesized by Shearwater Polymers. [α-^{32}P]dCTP (3000 Ci/mmol) was from NEN Life Science Product Inc. (Boston, MA). The nick translation system was from Invitrogen (San Diego, CA). 5-Bromo-4-chloro-3-indoyl-β-D-galactoside (X-gal), IGEPAL CA-630 and all other chemicals were purchased from Sigma Chemical Co. (St. Louis, MO). The 2-iminothiolane (Traut's reagent) and bicinchoninic acid (BCA) protein assay reagents were obtained from Pierce Chemical Co. (Rockford, IL). The 83-14 murine MAb to the HIR was purified by protein G affinity chromatography from hybridoma generated ascites. The luciferase expression plasmid is designated clone 790 and is derived from the pCEP4 plasmid under the control of the SV40 promoter as described previously [17]. The pSV-β-galactosidase expression plasmid driven by the SV40 promoter is designated clone 756 as described previously [7]. The pLacF expression plasmid under the influence of the bovine rhodopsin promoter was provided by Dr. Don Zack of Johns Hopkins University, and was described previously [16], and is designated clone 933. This 8 kb plasmid includes nucleotides -2174 to +70 of the bovine rhodopsin gene. The presence of this portion of the bovine rhodopsin promoter within the plasmid was confirmed by DNA sequencing using a M13 reverse sequencing primer followed by custom sequencing primers. Digestion of the rhodopsin/β-galactosidase plasmid with BamHI released the 3.0 kb insert from the 5.0 kb vector backbone.

Pegylated immunoliposome synthesis: Pegylated immunoliposomes (PILs) were synthesized from a total of 20 μmol of lipids, including 18.6 μmol of POPC, 0.6 μmol of DDAB, 0.6 μmol of DSPE-PEG, and 0.2 μmol of DSPE-PEG-maleimide [7,8]. Clone 756 plasmid DNA, clone 790 plasmid DNA, or pLacF plasmid DNA was produced by Maxiprep (Qiagen; Chatsworth, CA), and the supercoiled plasmid DNA (200 μg) and 1 μCi of ^{32}P-nick translated plasmid DNA were encapsulated in the pegylated liposomes by serial extrusion through filters of 400, 200, and 100 nm pore size, which forms liposomes of 85 nm diameter [18]. The exteriorized DNA was quantitatively removed by exhaustive nuclease digestion, as described previously [18]. The 83-14 MAb containing a trace amount of ^{3}H-labeled antibody, was thiolated with Traut's reagent and the thiolated MAb was conjugated to the pegylated liposome overnight at room temperature as described previously [7,19]. The unconjugated MAb, and the degraded exteriorized DNA were separated from the DNA encapsulated within the PIL by elution through a 1.6x18 cm column of Sepharose CL-4B in 0.05 M Hepes, pH 7.0, as described previously [7,19]. The average number of MAb molecules conjugated per liposome was 43±2 (mean±SE, n=3 syntheses). The final percentage entrapment of 200 μg of plasmid DNA in the liposome preparation was computed from the ^{32}P radioactivity and was 35±7.5% (mean±SE, n=3 syntheses). The PIL conjugated with the HIRMAb is designated HIRMAb-PIL. The HIRMAb-PIL carrying either plasmid DNA was sterilized before injection into the primate with a 0.22 μm filter (Millipore Co., Bedford, MA) as described previously [19].

Intravenous gene administration in Rhesus monkeys: Three healthy 5-10 year old, 5-6 kg female Rhesus monkeys were purchased from Covance (Alice, TX) and used in this study. In addition, a fourth rhesus monkey was sacrificed for removal of control tissues from an uninjected primate. Animal care guidelines were comparable to those published by the Institute for Laboratory Animal Research (Guide for the Care and Use of Laboratory Animals) and the US Public Health

Service (Public Health Service Policy on Human Care and Use of Laboratory Animals). The animals were anesthetized with 10 mg/kg ketamine intra-muscular, and 5 ml of sterile HIRMAb-PIL containing 70 μg of plasmid DNA was injected into the monkey via the saphenous vein with a 18-g catheter. The total dose of HIRMAb that was conjugated to the PIL and administered to each monkey was 1.8 mg or 300 μg/kg of antibody. The injection dose of PIL encapsulated plasmid DNA was 12 μg/kg. The eyes were enucleated immediately after euthanasia. In addition, the brain, liver, spleen, lung, heart, kidney, triceps skeletal muscle and omental fat were removed. The conjunctiva, orbital connective and muscular tissues, and vitreous body were removed from the eye. One eye was used for measurement of luciferase activity and the other eye was frozen in powdered dry ice for 30 min, embedded in OCT and re-frozen for cryostat sectioning. Eyes were also removed from a control rhesus monkey (Sierra Biomedical/Charles River; Sparks, NV), not injected with gene, and these eyes were frozen in OCT embedding medium immediately after euthanasia, and processed in parallel with the eyes from the gene injected monkey.

The experimental design involved the injection of either 1 or 2 plasmids in the same animal, so as to minimize the number of terminal primate experiments. Monkey 1 was injected on day 0 with both clone 756 (the SV40 driven β-galactosidase plasmid), and clone 790 (the SV40 driven luciferase plasmid), and sacrificed at 2 days after injection. For the monkey 1 experiment, the clone 756 or clone 790 plasmid DNA was individually encapsulated in separate preparations of HIRMAb-targeted PILs and co-injected into the primate, similar to the experimental design used previously [14]. Monkey 2 was injected with clone 790 on day 0, and injected with clone 933, the pLacF (the rhodopsin promoter driven β-galactosidase plasmid), on day 5, and sacrificed on day 7. Monkey 3 was injected with clone 790 on day 0 and sacrificed on day 14. Monkey 4 was the control, uninjected primate.

β-Galactosidase histochemistry: Frozen sections of 20 μm thickness were cut on a Mikron cryostat and fixed with 0.2% glutaraldehyde in 0.1 M NaH_2PO_4 for 1 h. The sections were washed with 0.1 M NaH_2PO_4 three times, and incubated overnight at 37 °C in X-gal staining solution (20 mM potassium-ferrocyanide, 20 mM potassium-ferricyanide, 2 mM

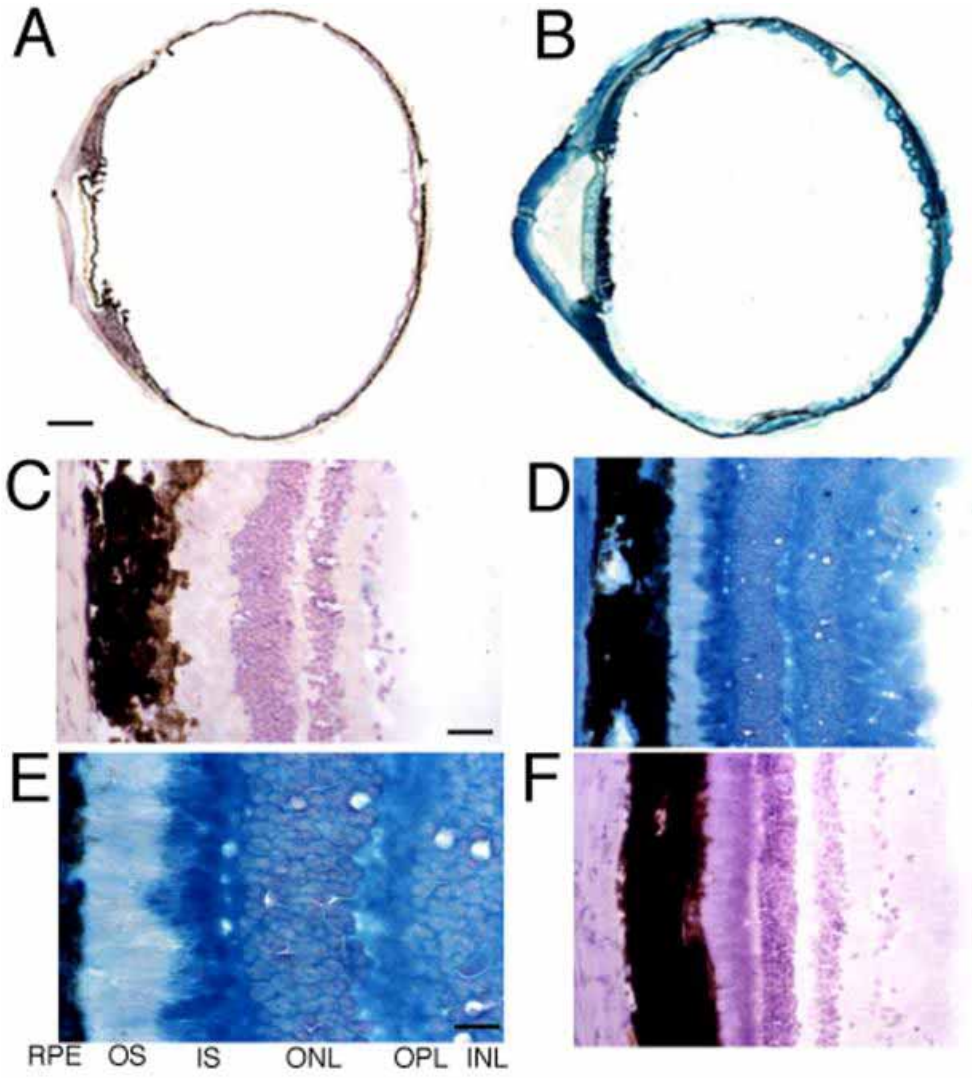

Figure 1. β-Galactosidase histochemistry of primate eyes. β-galactosidase histochemistry in control, un-injected Rhesus monkey eye (Panels **A** and **C**) and gene-injected Rhesus monkey eye (Panels **B**, **D**, **E**, and **F**). Panels **A**-**E** show β-galactosidase histochemistry followed by counter-staining with hematoxylin, whereas Panel **F** shows the retina only counter-stained with hematoxylin. Magnification in Panels **A** and **B** is the same; the magnification bar in Panel **A** represents 2 mm. The magnification in Panels **C**, **D**, and **F** is the same; the magnification bar in Panel **C** represents 32 μm. The magnification bar in Panel **E** represents 13 μm. Abbreviations in Panel **E**: INL, inner nuclear layer; OPL, outer plexiform layer; ONL, outer nuclear layer; IS inner segments; OS, outer segments; RPE, retinal pigmented epithelium. All specimens shown in Panels **B**, **D**-**F** were taken 48 h after the intravenous administration of clone 756, the pSV40-β-galactosidase plasmid, in monkey 1 (see Methods).

$MgCl_2$, 0.02% IGEPAL CA-630, 0.01% Na deoxycholate, and 1 mg/ml X-gal in 0.1 M NaH_2PO_4) at pH 7.3. Prior to coverslipping, the sections were scanned with a UMAX PowerLookIII scanner with transparency adapter, and the image was cropped in Adobe Photoshop 5.5 on a G4 Power Macintosh computer. Control or un-injected rhesus monkey eye was stained in parallel with the eye obtained from the gene-injected animal. Specimens were examined with and without hematoxylin counter-staining.

Confocal Imaging: Frozen sections (20 μm) of either gene-injected and control monkey eyes were fixed for 5 min in 100% acetone at room temperature (RT). Following air drying, all sections were washed in 0.01 M PBS buffer and non-specific binding was blocked using 10% goat serum in 0.01 M PBS with 0.1% Triton X-100, pH 7.4 for 60 min at RT. Primary antibodies were the 83-14 mouse anti-human insulin receptor, rabbit anti E. coli β-galactosidase polyclonal antibody (Biodesign Int., Saco, ME), mouse IgG2a isotype control, or rabbit IgG, 5 μg/ml, in 3% bovine serum albumin, 0.01 M PBS with 0.1% Triton X-100, pH 7.4; all primary antibodies were used at 5 μg/ml. Incubation time was 48 h at 4 °C in a humidified chamber. Secondary antibodies used were 594 Goat anti-mouse IgG and 488 goat anti-rabbit IgG (Molecular Probes; Eugene, OR), 5 μg/ml, in 1% goat serum, 0.01 M PBS, 0.1% Triton X-100, pH 7.4. Incubation time was 1 h at RT. Confocal imaging was performed with a Zeiss LSM 5 PASCAL confocal microscope with dual argon and helium/neon lasers equipped with Zeiss LSM software for image reconstruction (Zeiss, Jena, Germany). All sections were scanned in multitrack mode to avoid overlap of the fluorescein (excitation at 488 nm) and rhodamine (excitation at 543 nm) channels employing the Plan-Neofluar 40x/0.75 objective. Pinhole size was 126 μm in both channels, and detector gain, amplifier gain and amplifier offset was identical for the gene-injected and control retina. Two scanning lines were integrated for a 512x512 image matrix. By integrating 4 serial tomographic images stack sizes of 230.3x230.3x4.8 μm dimension were created. 2D images were visualized by integrating 4 serial tomographs by maximum intensity projection.

Luciferase measurements: Primate retina was homogenized in 4 volumes of lysis buffer for measurement of luciferase activity, as described previously [19]. The data are reported as pg luciferase activity per mg cell protein. Based on the standard curve, 1 pg of luciferase was equivalent to 14,312±2,679 relative light units (RLU), which is the mean±S.E. of 5 assays.

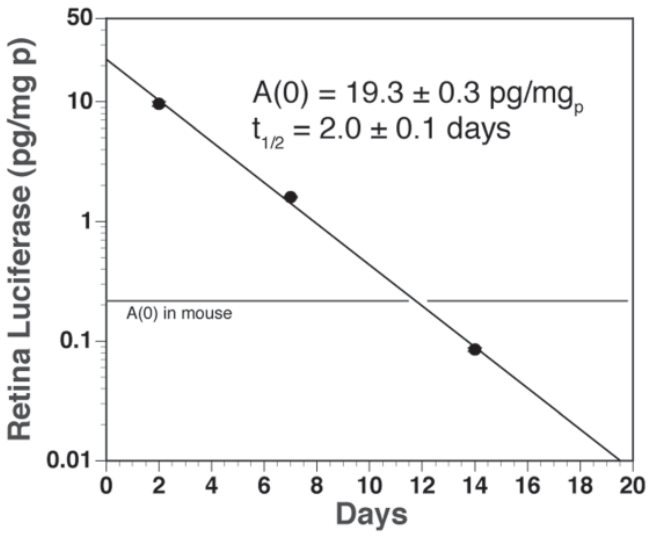

Figure 2. Luciferase gene expression in the primate eye. Retinal luciferase activity in 3 rhesus monkeys sacrificed at 2, 7, or 14 days after intravenous administration of clone 790 in monkeys 1, 2, and 3, respectively (see Methods). The data were fit to a single-exponential equation to yield the slope/half-time ($t_{1/2}$) and the intercept, [A(0)]. The horizontal line shows the A(0) of luciferase activity in control mouse brain, 0.22±0.08 pg/mg [20], which indicates the level of gene expression in the monkey retina is still above the therapeutic level for at least 2 weeks after injection. The luciferase expression plasmid was under the influence of the SV40 promoter in these studies. The diagonal line through the data points was drawn by eye. Error bars representing the stardard deviation are shown over each closed circle.

RESULTS

Histochemistry of the retina obtained from a control, un-injected Rhesus monkey shows no measurable β-galactosidase histochemical product (Figure 1A). In contrast, there is global β-galactosidase histochemical product in the primate retina and eye obtained 48 h after the single intravenous injection of the pSV-β-galactosidase plasmid encapsulated in the HIRMAb-PIL (Figure 1B). Exogenous gene expression is detected in multiple structures of the eye including the entire retina, the epithelium of the cornea, the ciliary body, and the iris. Higher magnification of the retina shows no evidence of histochemical product in the eye obtained from the un-injected monkey (Figure 1C), although there is gene expression in most layers of the retina in the gene-injected Rhesus monkey (Figure 1D). There is abundant histochemical product in the cell bodies of the ONL as well as the inner segments (IS) and some measurable histochemical product in the outer segments (OS) of the photoreceptor cells (Figure 1E). Other layers of the retina that are positive for β-galactosidase gene expression include the inner plexiform layer (IPL), the inner nuclear layer (INL), the outer plexiform layer (OPL) and the ganglion cell layer (GCL); see Figure 1D,E. There is no structural damage to the retina caused by the PIL administration as shown by the counter-staining of the primate retina (Figure 1F).

The luciferase gene was also expressed in the retina, and the retinal luciferase activity at 48 h was 9.6 ±0.4 pg luciferase/mg protein (mean±S.E., n=3 replicates). This is equivalent to $1.4x10^5$ relative light units (RLU)/mg protein (Methods). No luciferase enzyme activity was detected in the retina of the control, uninjected monkey. The retina luciferase activity was also measured in primates at 7 and 14 days after injection, and the retinal luciferase activity decayed exponentially (Figure 2). The half-time of luciferase gene expression decay was 2.0±0.1 days and the extrapolated Y-intercept [A(0)], which

gives the maximal retinal luciferase level, was 19.3±0.1 pg per mg protein (Figure 2). The horizontal line in Figure 2 is the luciferase A(0) in the mouse [20], which corresponds to the primate retina luciferase activity at 12 days after a single intravenous injection (Figure 2).

Confocal microscopy shows diffuse expression of the IR in the retina of the gene-injected primate with high levels in the IS, OPL, IPL, and intermediate levels of expression in the INL and ONL cell bodies (Figure 3A). The same pattern of retinal expression of the IR is seen in the control monkey (Figure 3D). There is diffuse immunoreactive β-galactosidase in the gene-injected monkey with high levels in the IS, OPL, and IPL (Figure 3B). There is no immunoreactive β-galactosidase in the un-injected control monkey, as the faint autofluorescence seen over the RPE, OPL, and rod outer segments (Figure 3E, left lower corner) was also detected with control rabbit IgG (Figure 3H). The IR/β-galactosidase overlap images for the gene-injected monkey and un-injected control monkey are shown in Figure 3C,F, respectively. There is a co-localization of β-galactosidase and IR in the gene injected monkey with minimal overlap signal in the un-injected monkey (Figure 3F).

The organ specificity of β-galactosidase gene expression was examined in the primate at 2 days following the intravenous injection of the pLacF plasmid driven by the bovine opsin promoter. Although there was abundant gene expression in multiple structures of the eye (Figure 4A), there was no gene expression in monkey brain, heart, lung, fat, spleen, or liver (Figure 4C-H). The negative histochemical reaction in these multiple peripheral tissues was not assay related, because the histochemistry was done in parallel with the primate eye (Figure 4A,I) as well as the primate kidney (Figure 4B,J). Control kidney from un-injected animals contains β-galactosidase that is active at neutral pH and is histochemically active in the β-galactosidase assay [7]. Therefore, the histochemistry of kidney tissues serves as a positive control for the β-galactosidase assay. The pattern of cellular gene expression in the layers of the primate retina following administration of the opsin promoter plasmid (Figure 4I) is comparable to that found with the SV40 promoter plasmid as shown in Figure 1E. β-galactosidase gene expression under the influence of the opsin promoter was observed in multiple layers of the retina including the ONL, and the IS and OS of the photoreceptor cells (Figure 4I).

DISCUSSION

The results of these studies support the following conclusions. First, exogenous plasmid-based genes may be targeted to nearly all structures of the primate eye using the PIL gene targeting system and a HIRMAb as the targeting ligand (Figure 1). Second, the IR is expressed in the cell bodies of the ONL (Figure 3A), which enables global expression of exogenous genes in the photoreceptor cells and particularly IS (Figure 1E and Figure 3B). Third, β-galactosidase gene expression in the rhesus monkey is restricted to the eye when the trans-gene is under the influence of a ocular-specific promoter such as the opsin

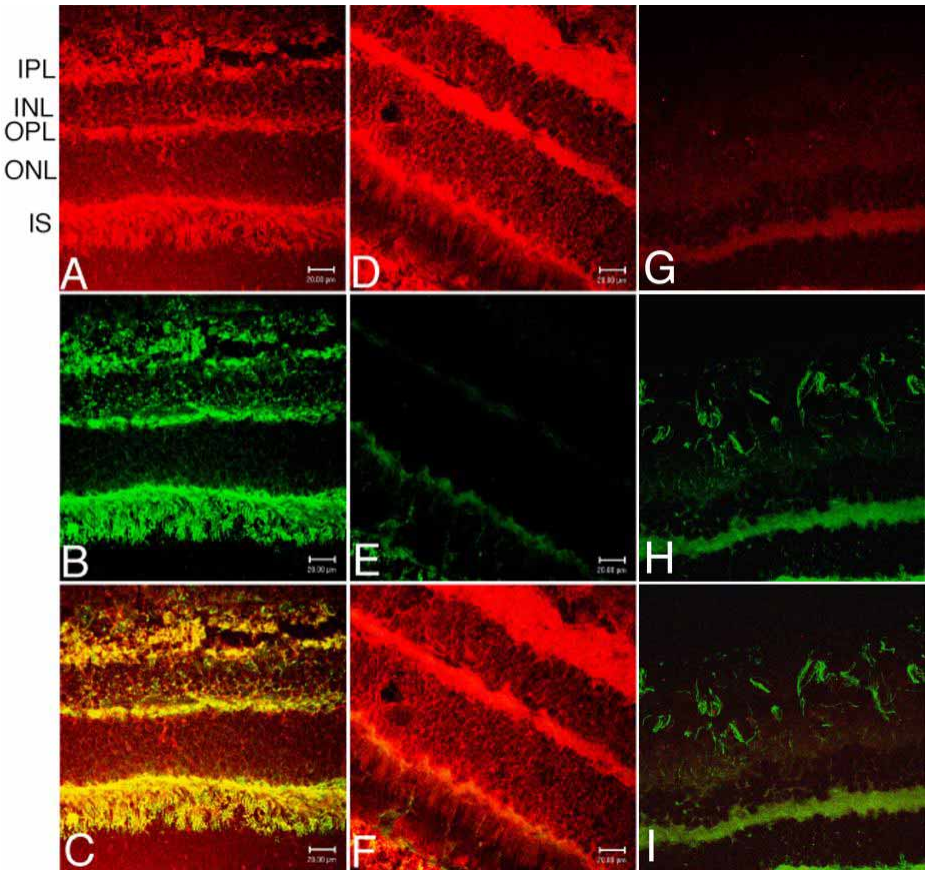

Figure 3. Confocal microscopy of the primte retina. Confocal microscopy of the retina from the gene-injected monkey (**A**-**C**, **G**-**I**) and from the control, un-injected monkey (**D**-**F**). Immunoreactive insulin receptor, stained with rhodamine-labeled secondary antibody, is shown in Panels **A** and **D**. Immunoreactive β-galactosidase, stained with the fluorescein-labeled secondary antibody, is shown in Panels **B** and **E**. Staining with the pre-immune mouse IgG or the rabbit IgG is shown in Panels **G** and **H**. The respective superimposed images are shown in panels **C**, **F**, and **I**. The yellow image in panel **C** shows co-localization of the β-galactosidase and human insulin receptor in the retina of the gene-injected monkey, including the photoreceptor cells. Scale bar: 20 μm. Abbreviations in Panel **A**: IPL, inner plexiform layer; INL, inner nuclear layer; OPL, outer plexiform layer; ONL, outer nuclear layer; IS, inner segments. All specimens shown in Panels **A**-**C** were taken 48 h after the intravenous administration of clone 756, the pSV40-β-galactosidase plasmid in monkey 1 (see Methods).

promoter (Figure 4). Fourth, the expression of a reporter gene in the monkey eye declines following a single intravenous injection of plasmid and decays exponentially with a $t_{1/2}$ of 2.0±0.1 days (Figure 2).

The nearly global expression of the exogenous gene delivered to the primate eye via the HIRMAb targeted PIL is shown by the β-galactosidase histochemistry (Figure 1B). There is gene expression in the retina, the cornea, the ciliary body, and the iris, and this global expression in the eye is observed with either the SV40 promoter (Figure 1B) or the bovine opsin promoter (Figure 4A). The sites of β-galactosidase gene expression parallel the sites of expression of the insulin receptor. The IR is expressed in the human eye in the epithelium and endothelium of the cornea, the lens capsular epithelium, and multiple cells within the retina including the inner segments, the ONL, the RPE, GCL, and Müller cells [11,12]. In addition to the widespread expression within the eye of the IR, this receptor is also useful for gene targeting to the nucleus. The IR serves to deliver ligand to the nucleus; prior work has shown that the IR delivers to the nucleus the majority of plasmid DNA taken up by the cell [19,21]. The mechanism of gene delivery to the eye is receptor-mediated, and not a nonspecific breakdown of the BRB caused by the PIL injection. Prior work has shown that when the β-galactosidase expression plasmid is encapsulated in a PIL targeted with an isotype control antibody that does not recognize any receptor, then there is no β-galactosidase gene expression observed either in the eye [6], or in any other organ [7,8]. There is normal cellular architecture in the retina following PIL administration (Figure 1F).

The present studies target genes to the primate eye with the HIRMAb and demonstrate gene expression in the primate photoreceptor cells (Figures 1, 3 and 4). In contrast, prior work in mice targeted genes to the retina with the TfRMAb, and no expression of the β-galactosidase gene in the photoreceptor cells of the mouse retina was observed [6]. This observation correlates with the known tissue-specific expression of the TfR within the retina. The TfR is produced in the RPE, IS, OPL, INL, and GCL, but is minimally expressed in the cell bodies of the ONL [9,10]. The low expression of TfR in the ONL is consistent with the very low stores of either iron or ferritin in the ONL [10]. The TfR is expressed on the IS of the photoreceptor cells [6], but PIL entry into the photoreceptor cell at the IS apparently cannot support gene expression [6]. There may be minimal retrograde transport of the PIL from the IS to the cell body of the photoreceptor cell in the ONL. While the TfR is minimally expressed in the cell bodies of the ONL [10], the insulin receptor is expressed in this region of the retina in both humans and rats [11,12]. The present studies demonstrate that the ONL of the primate retina is also a site of abundant insulin receptor expression as shown by confocal microscopy (Figure 3A,D). In parallel with the expression of insulin receptor at the ONL, the β-galactosidase gene is expressed in the photoreceptor cells of the monkey (Figure 1E). The β-galactosidase gene expression is more prominent in the inner segments relative to the outer segments, although β-galactosidase activity in the outer segments is visible by histochemistry (Figure 1E and Figure 4I).

The organ specificity of gene expression is a function of two variables: (a) the organ specificity of the targeting MAb attached to the PIL, and (b) the organ specificity of the pro-

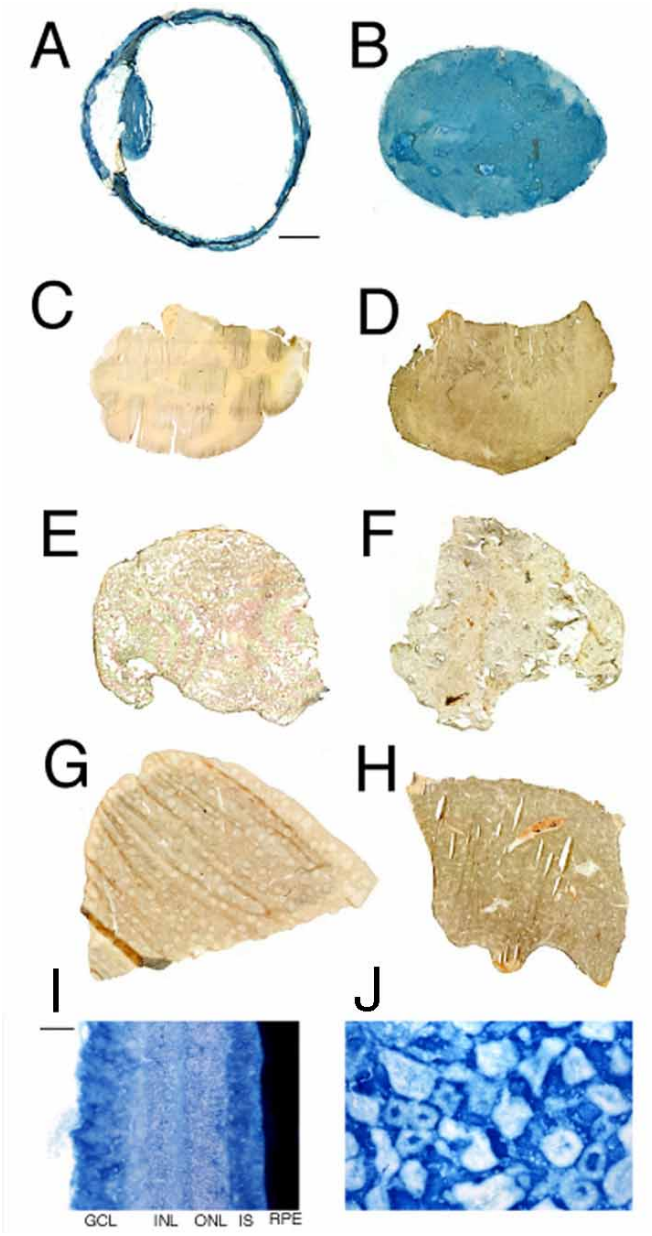

Figure 4. β-Galactosidase histochemistry of primate organs. Organ β-galactosidase histochemistry for Rhesus monkey eye (**A** and **I**), kidney (**B** and **J**), brain (**C**), heart (**D**), lung (**E**), omental fat (**F**), spleen (**G**), and liver (**H**). Skeletal muscle was also examined (not shown), and like the heart showed no histochemical reaction. The organs were removed from the animal sacrificed at 48 h after an intravenous injection of the opsin promoter-driven pLacF plasmid encapsulated in HIRMAb-targeted PILs, which corresponds to monkey 2 (see Methods). The magnification is the same for panels **A**-**H**; the magnification bar in Panel **A** represents 3 mm. The magnification is the same for panels **I**-**J**; the magnification bar in Panel **I** represents 12 μm.

moter incorporated in the expression plasmid. In prior work in the rhesus monkey, the pSV-β-galactosidase expression plasmid was under the influence of the widely expressed SV40 promoter. Therefore, gene expression was observed in multiple organs of the primate including brain, liver, and spleen [14]. However, the present studies show that the expression of the β-galactosidase gene is restricted to the eye when the β-galactosidase expression plasmid is under the influence of the bovine opsin promoter (Figure 4). The pLacF β-galactosidase expression plasmid is driven by the 2 kb of the 5'-flanking sequence (FS) of the bovine opsin gene [16]. Under the restriction of the opsin promoter, there is no expression in brain, liver, spleen or other organs following the intravenous administration of HIRMAb-targeted PILs in the rhesus monkey (Figure 4). This observation in the primate of organ-specific gene expression with organ-specific promoters parallels prior work in the mouse and rat [7,8]. Genes driven by the SV40 promoter and encapsulated in TfRMAb-targeted PILs are expressed in multiple TfR-rich peripheral organs including brain, liver, and spleen [7]. However, a different pattern of gene expression is observed if the exogenous gene is driven by a brain-specific promoter such as the 2 kb of the 5'-FS of the glial fibrillary acidic protein (GFAP) gene. If the SV40 promoter is replaced with the GFAP promoter, then gene expression in the brain and eye is preserved [6,7], whereas trans-gene expression in peripheral tissues such as liver or spleen is eliminated [7]. The finding of eye-specific gene expression in the monkey with the pLacF plasmid (Figure 4) parallels prior work with transgenic mice produced with the pLacF gene. Gene expression is confined to the eye in either the germ cell transgenic mouse [16], or the adult rhesus monkey made acutely transgenic with the PIL gene transfer technology (Figure 4).

The bovine opsin promoter restricts transgene expression to the eye, but does not restrict gene expression to the photoreceptor cells in the monkey (Figure 4A). A similar finding was made in transgenic mice produced with the pLacF construct, as these transgenic mice expressed the β-galactosidase gene in the photoreceptor cells, as well as the iris and ciliary body, and the brain [16]. One possible explanation for the diffuse expression of the reporter gene in the eye is selective expression in the photoreceptor cells followed by secretion and diffusion to other parts of the eye. However, this explanation appears unlikely since prior work has shown selective localization of the β-galactosidase enzyme in retinal structures without secretion and diffusion to other parts of the eye [6]. A more likely explanation for the broad spectrum of opsin promoter driven gene expression in the eye is that the other ocular structures are embryologically related to the neural retina. Transfection of iris or ciliary body with the photoreceptor cell specific *Crx* homeobox gene results in the synthesis of rhodopsin in these extra-retinal ocular structures [22]. The restriction of gene expression to the photoreceptor cells may require regulatory gene elements in addition to the 5'-FS of the gene. In the case of brain GFAP gene expression, the 5'-FS confers brain specificity, but does not restrict gene expression within the brain to astrocytes. Astrocyte specific gene expression requires the coordinate interaction of gene elements in both the 5'-FS and the 3'-FS of the GFAP gene [23,24].

The luciferase gene expression decays exponentially with a half-time of 2.0±0.1 days, and the peak luciferase expression, A(0) is 19.3±0.3 pg/mg (Figure 2). The peak luciferase gene expression is 50-fold higher than the A(0) in rodent brain [14,20], and the rodent A(0) is shown by the horizontal line in Figure 2. The higher peak level of gene expression in the primate, relative to the rodent, is attributed to the much higher activity of the HIRMAb as a targeting ligand, as compared to the TfRMAb [21]. The HIRMAb is used to target PILs to primate brain [14], whereas the TfRMAb is used to target PILs to rodent brain [6-8]. The level of gene expression achieved with the TfRMAb is sufficient to cause the desired pharmacological effect. The intravenous administration of TfRMAb-targeted PILs produces a 100% increase in survival time in mice with experimental brain cancer treated with EGFR antisense gene therapy [20], or a 100% normalization of striatal enzyme activity in rats with experimental Parkinsonism treated with tyrosine hydroxylase gene therapy [25]. Therefore, the mouse A(0) shown in Figure 2 represents levels of gene expression that yield therapeutic effects. Owing to the very high initial level of gene expression in the primate with the HIRMAb, the level of retinal gene expression is still in the therapeutic range for more than 2 weeks after a single intravenous injection (Figure 2). Therefore, primates may require repeat administration of gene therapy at intervals of 3-4 weeks.

In summary, these studies show it is possible to achieve global expression of an exogenous gene in photoreceptor cells of the primate retina following a non-invasive, intravenous administration of a non-viral form of the gene. The plasmid replicates episomally and gene expression is reversible (Figure 2). Southern blotting shows no integration of the plasmid DNA into host chromosomal DNA following PIL gene delivery [8]. Similarly, plasmid DNA delivered to organs in vivo with the hydrodynamics injection method is not integrated in the host chromosome [26]. Owing to the transient nature of plasmid-based gene expression, it is necessary to administer the PIL formulation at regular intervals to sustain a therapeutic effect, and this has been done for the treatment of mice with brain cancer [20]. The chronic weekly intravenous administration of PIL encapsulated genes causes no change in organ histology, serum chemistry, or body weights, and causes no inflammation in the central nervous system [27]. Repeat intravenous administration of the PIL formulation is possible, because the only antigenic component of the liposome is the targeting ligand. The immunogenicity of the targeting MAb can be reduced or eliminated with genetic engineering and "humanization" of the original murine MAb. The murine 83-14 HIRMAb has been genetically engineered to produce the chimeric form of this antibody, and the chimeric HIRMAb has an identical affinity for the HIR as the original murine antibody [28]. The chimeric HIRMAb rapidly crosses the primate BBB in vivo [28], and the present studies provide evidence that the HIRMAb also crosses the primate BRB and distributes to the retina and to multiple ocular structures.

ACKNOWLEDGEMENTS

Dafang Wu, Hwa Jeong Lee, Chunni Zhu, Toyofumi Suzuki, and Yufeng Zhang of the UCLA Department of Medicine provided assistance in the primate experiments. This work was supported by grants from the University of California, Davis/ Medical Investigation of Neurodevelopmental Disorders Institute Research Program, and the Neurotoxin Exposure Treatment Research Program of the U. S. Department of Defense. Felix Schlachetzki was supported by a grant from the Ernst Schering Research Foundation (Berlin, Germany). This work was presented in part at the Annual Meeting of the Association for Research in Vision and Ophthalmology (ARVO-2003), Fort Lauderdale, FL, May, 2003.

REFERENCES

1. Hauswirth WW, Beaufrere L. Ocular gene therapy: quo vadis? Invest Ophthalmol Vis Sci 2000; 41:2821-6.
2. Dejneka NS, Bennett J. Gene therapy and retinitis pigmentosa: advances and future challenges. Bioessays 2001; 23:662-8.
3. Hauswirth WW, McInnes RR. Retinal gene therapy 1998: summary of a workshop. Mol Vis 1998; 4:11 .
4. Bennett J, Maguire AM, Cideciyan AV, Schnell M, Glover E, Anand V, Aleman TS, Chirmule N, Gupta AR, Huang Y, Gao GP, Nyberg WC, Tazelaar J, Hughes J, Wilson JM, Jacobson SG. Stable transgene expression in rod photoreceptors after recombinant adeno-associated virus-mediated gene transfer to monkey retina. Proc Natl Acad Sci U S A 1999; 96:9920-5.
5. Flannery JG, Zolotukhin S, Vaquero MI, LaVail MM, Muzyczka N, Hauswirth WW. Efficient photoreceptor-targeted gene expression in vivo by recombinant adeno-associated virus. Proc Natl Acad Sci U S A 1997; 94:6916-21.
6. Zhu C, Zhang Y, Pardridge WM. Widespread expression of an exogenous gene in the eye after intravenous administration. Invest Ophthalmol Vis Sci 2002; 43:3075-80.
7. Shi N, Zhang Y, Zhu C, Boado RJ, Pardridge WM. Brain-specific expression of an exogenous gene after i.v. administration. Proc Natl Acad Sci U S A 2001; 98:12754-9.
8. Shi N, Boado RJ, Pardridge WM. Receptor-mediated gene targeting to tissues in vivo following intravenous administration of pegylated immunoliposomes. Pharm Res 2001; 18:1091-5.
9. Davis AA, Hunt RC. Transferrin is made and bound by photoreceptor cells. J Cell Physiol 1993; 156:280-5.
10. Yefimova MG, Jeanny JC, Guillonneau X, Keller N, Nguyen-Legros J, Sergeant C, Guillou F, Courtois Y. Iron, ferritin, transferrin, and transferrin receptor in the adult rat retina. Invest Ophthalmol Vis Sci 2000; 41:2343-51.
11. Naeser P. Insulin receptors in human ocular tissues. Immunohistochemical demonstration in normal and diabetic eyes. Ups J Med Sci 1997; 102:35-40.
12. Gosbell AD, Favilla I, Baxter KM, Jablonski P. Insulin receptor and insulin receptor substrate-I in rat retinae [published erratum in: Clin Experiment Ophthalmol 2000; 28:443]. Clin Experiment Ophthalmol 2000; 28:212-5.
13. Pardridge WM, Kang YS, Buciak JL, Yang J. Human insulin receptor monoclonal antibody undergoes high affinity binding to human brain capillaries in vitro and rapid transcytosis through the blood-brain barrier in vivo in the primate. Pharm Res 1995; 12:807-16.
14. Zhang Y, Schlachetzki F, Pardridge WM. Global non-viral gene transfer to the primate brain following intravenous administration. Mol Ther 2003; 7:11-8.
15. Ford SM. Systematics of the new world monkeys. In: Erwin J, Swindler DR, editors. Comparative primate biology I: Systematics, evolution, and anatomy. New York: Alan R. Liss; 1986. p. 23-135.
16. Zack DJ, Bennett J, Wang Y, Davenport C, Klaunberg B, Gearhart J, Nathans J. Unusual topography of bovine rhodopsin promoter-lacZ fusion gene expression in transgenic mouse retinas. Neuron 1991; 6:187-99.
17. Boado RJ, Pardridge WM. Ten nucleotide cis element in the 3'-untranslated region of the GLUT1 glucose transporter mRNA increases gene expression via mRNA stabilization. Brain Res Mol Brain Res 1998; 59:109-13.
18. Shi N, Pardridge WM. Noninvasive gene targeting to the brain. Proc Natl Acad Sci U S A 2000; 97:7567-72.
19. Zhang Y, Jeong Lee H, Boado RJ, Pardridge WM. Receptor-mediated delivery of an antisense gene to human brain cancer cells. J Gene Med 2002; 4:183-94.
20. Zhang Y, Zhu C, Pardridge WM. Antisense gene therapy of brain cancer with an artificial virus gene delivery system. Mol Ther 2002; 6:67-72.
21. Zhang Y, Boado RJ, Pardridge WM. Marked enhancement in gene expression by targeting the human insulin receptor. J Gene Med 2003; 5:157-63.
22. Haruta M, Kosaka M, Kanegae Y, Saito I, Inoue T, Kageyama R, Nishida A, Honda Y, Takahashi M. Induction of photoreceptor-specific phenotypes in adult mammalian iris tissue. Nat Neurosci 2001; 4:1163-4.
23. Kaneko R, Sueoka N. Tissue-specific versus cell type-specific expression of the glial fibrillary acidic protein. Proc Natl Acad Sci U S A 1993; 90:4698-702.
24. Galou M, Pournin S, Ensergueix D, Ridet JL, Tchelingerian JL, Lossouarn L, Privat A, Babinet C, Dupouey P. Normal and pathological expression of GFAP promoter elements in transgenic mice. Glia 1994; 12:281-93.
25. Zhang Y, Calon F, Zhu C, Boado RJ, Pardridge WM. Intravenous nonviral gene therapy causes normalization of striatal tyrosine hydroxylase and reversal of motor impairment in experimental parkinsonism. Hum Gene Ther 2003; 14:1-12.
26. Stoll SM, Sclimenti CR, Baba EJ, Meuse L, Kay MA, Calos MP. Epstein-Barr virus/human vector provides high-level long-term expression of alpha1-antitrypsin in mice. Mol Ther 2001; 4:122-9.
27. Zhang YF, Boado RJ, Pardridge WM. Absence of toxicity of chronic weekly intravenous gene therapy with pegylated immunoliposomes. Pharm Res. In press 2003.
28. Coloma MJ, Lee HJ, Kurihara A, Landaw EM, Boado RJ, Morrison SL, Pardridge WM. Transport across the primate blood-brain barrier of a genetically engineered chimeric monoclonal antibody to the human insulin receptor. Pharm Res 2000; 17:266-74.

The print version of this article was created on 3 Oct 2003. This reflects all typographical corrections and errata to the article through that date. Details of any changes may be found in the online version of the article.

[32] Gene Targeting *In Vivo* with Pegylated Immunoliposomes

By WILLIAM M. PARDRIDGE

Introduction

Targeting therapeutic genes to tissues in cell culture or *in vivo* has been performed in the past with one of three different technologies: (1) viral vectors, (2) cationic liposomes, and (3) plasmid DNA complexed to conjugates of a polycationic protein and a receptor ligand (asialoglycoproteins, transferrin, or folic acid). Viral vectors, such as adenovirus or herpes simplex virus, generate inflammatory responses as a result of the preexisting immunity of virtually all humans to either virus.[1,2] The single injection of either virus into animal or human brain results in a local, inflammatory reaction leading to demyelination.[3–12] The principal nonviral form of gene delivery uses complexes of cationic liposomes and DNA. However, the *in vivo* application of cationic liposomes is limited by the aggregation of

[1] U. Herrlinger, C. M. Kramm, K. S. Aboody-Guterman, J. S. Silver, K. Ikeda, K. M. Johnston, P. A. Pechan, R. F. Barth, D. Finkelstein, E. A. Chiocca, D. N. Louis, and X. O. Breakefield, *Gene Ther.* **5,** 809 (1998).
[2] Y. Stallwood, K. D. Fisher, P. H. Gallimore, and V. Mautner, *Gene Ther.* **7,** 637 (2000).
[3] M. S. Lawrence, H. G. Foellmer, J. D. Elsworth, J. H. Kim, C. Leranth, D. A. Kozlowski, A. L. M. Bothwell, B. L. Davidson, M. C. Bohn, and D. E. Redmond, Jr., *Gene Ther.* **6,** 1368 (1999).
[4] A. P. Byrnes, J. E. Rusby, M. J. A. Wood, and H. M. Charlton, *Neuroscience* **66,** 1015 (1995).
[5] M. M. McMenamin, A. P. Byrnes, H. M. Charlton, R. S. Coffin, D. S. Latchman, and M. J. A. Wood, *Neuroscience* **83,** 1225 (1998).
[6] C. M. Kramm, N. G. Rainov, M. Sena-Esteves, M. Chase, P. A. Pechan, E. A. Chiocca, and X. O. Breakefield, *Hum. Gene Ther.* **7,** 291 (1996).
[7] J. G. Smith, S. E. Raper, E. B. Wheeldon, D. Hackney, K. Judy, J. M. Wilson, and S. L. Eck, *Hum. Gene Ther.* **8,** 943 (1997).
[8] R. A. Dewey, G. Morrissey, C. M. Cowsill, D. Stone, F. Bolognani, N. J. Dodd, T. D. Southgate, D. Klatzmann, H. Lassmann, and M. G. Castro, *Nat. Med.* **5,** 1256 (1999).
[9] M. J. Driesse, A. J. P. E. Vincent, P. A. E. Sillevis Smitt, J. M. Kros, P. M. Hoogerbrugge, C. J. J. Avezaat, D. Valerio, and A. Bout, *Gene Ther.* **5,** 1122 (1998).
[10] M. J. Driesse, M. C. Esandi, J. M. Kros, C. J. J. Avezaat, Ch. J. Vecht, C. Zurcher, I. van der Velde, D. Valerio, A. Bout, and P. A. E. Sillevis Smitt, *Gene Ther.* **7,** 1401 (2000).
[11] M. J. A. Wood, H. M. Charlton, K. J. Wood, K. Kajiwara, and A. P. Byrnes, *Trends Neurosci.* **19,** 497 (1996).
[12] K. Kajiwara, A. P. Byrnes, Y. Ohmoto, H. M. Charlton, M. J. A. Wood, and K. J. Wood, *J. Neuroimmunology* **103,** 8 (2000).

0076-6879/03 $35.00

cationic liposome–DNA complexes in physiological saline. The cationic lipid–DNA formulations do not aggregate in water. However, once the salt content is raised to the physiological level, the complexes become electrically neutral and aggregate into multimicron structures.[13–16] Therefore, when cationic liposome–DNA complexes are injected intravenously, large aggregates form immediately and are deposited in the first vascular bed, the pulmonary circulation. Gene expression in the lung is several log orders of magnitude greater than gene expression in peripheral tissues such as the liver or spleen, and there is no gene expression in brain following the intravenous administration of cationic liposome–DNA complexes.[17–19] Aggregation also occurs with complexes of polycations and DNA; in this approach, the polycationic protein substitutes for the cationic lipid. However, aggregation in saline is observed, and there is preferential expression of the exogenous gene in the pulmonary circulation.[20] The lung is targeted by gene delivery systems composed of polycationic lipids or proteins, because the pulmonary circulation is the very first vascular bed immediately distal to an intravenous injection, and aggregates are trapped in the lung microcirculation. The instability of the gene formulation in serum has also been observed for conjugates of a receptor ligand and plasmid DNA complexed to a polycationic protein such as polylysine, and this instability is not altered by pegylation of the polylysine.[21] Presumably, the electrostatic interactions that bind the anionic DNA to the cationic protein are disrupted by serum proteins *in vivo*. Each of the traditional approaches for gene targeting *in vivo* have distinct advantages. However, each approach also has significant disadvantages that prevent the widespread application of the gene targeting technology *in vivo*.

An alternative approach to targeting therapeutic genes to tissues *in vivo* is the use of pegylated immunoliposomes (PIL), which are depicted in Fig. 1A. The PIL formulation is similar to a viral vector in that the DNA

[13] H. Matsui, L. G. Johnson, S. H. Randell, and R. C. Boucher, *J. Biol. Chem.* **272,** 1117 (1997).
[14] R. I. Mahato, A. Rolland, and E. Tomlinson, *Pharm. Res.* **14,** 853 (1997).
[15] C. Plank, M. X. Tang, A. R. Wolfe, and F. C. Szoka, Jr., *Hum. Gene Ther.* **10,** 319 (1999).
[16] T. Niidome, N. Ohmori, A. Ichinose, A. Wada, H. Mihara, T. Hirayama, and H. Aoyagi, *J. Biol. Chem.* **272,** 15307 (1997).
[17] L. G. Barron, L. S. Uyechi, and F. C. Szoka, Jr., *Gene Ther.* **6,** 1179 (1999).
[18] K. Hong, W. Zheng, A. Baker, and D. Papahadjopoulos, *FEBS Lett.* **400,** 233 (1997).
[19] G. Osaka, K. Carey, A. Cuthbertson, P. Godowski, T. Patapoff, A. Ryan, T. Gadek, and J. Mordenti, *J. Pharm. Sci.* **85,** 612 (1996).
[20] S. M. Zou, P. Erbacher, J. S. Remy, and J. P. Behr, *J. Gene Med.* **2,** 128 (2000).
[21] D. Y. Kwoh, C. C. Coffin, C. P. Lollo, J. Jovenal, M. G. Banaszczyk, P. Mullen, A. Phillips, A. Amini, J. Fabrycki, R. M. Bartholomew, S. W. Brostoff, and D. J. Carlo, *Biochim. Biophys. Acta.* **1444,** 171 (1999).

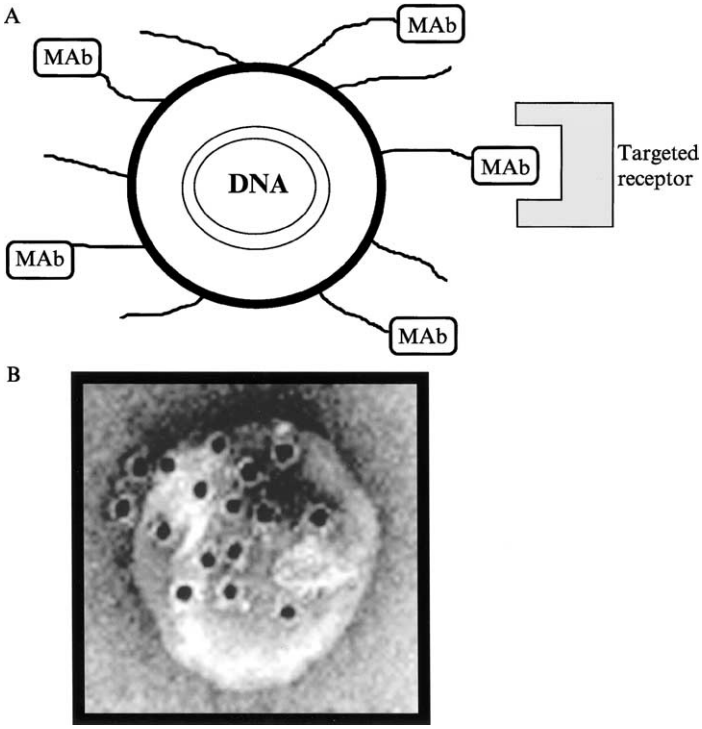

FIG. 1. (A) Diagram showing the supercoiled circular double-stranded plasmid DNA encapsulated in the interior of a pegylated immunoliposome (PIL). There are approximately 3000 strands of polyethylene glycol of 2000-Dalton molecular weight, designated PEG^{2000}, attached to the liposome surface, and 1%–2% of the PEG strands are conjugated with a targeting monoclonal antibody (MAb). For gene targeting to the brain, a MAb directed against the transferrin receptor (TfR) has been used in rats[22,23] and mice,[24] and an antibody directed against the human insulin receptor (HIR) has been used for drug targeting to human cells.[37] The targeted receptor could be the TfR, the HIR, or some other receptor. The targeting MAb must be an endocytosing antibody that enters the cell on binding to an exofacial epitope on the receptor. The MAb binding site on the receptor should be spatially removed from the binding site of the endogenous ligand, so as to not interfere with endogenous transport. (B) Transmission electron microscopy of a PIL. The mouse MAb tethered to the tips of the PEG^{2000} are bound by a conjugate of 10 nm gold and an anti-mouse secondary MAb. The gold particles are bound to the MAb conjugated to the tip of the PEG strand, which projects from the surface of the liposome. The position of the gold particles illustrates the relationship of the PEG-extended MAb and the liposome. Original magnification = 245,000.

is housed in the interior of a nanocontainer, and the PIL formulation is similar to the receptor-mediated approach in that the gene is targeted *in vivo* to a specific receptor. In the PIL formulation, a nonviral double-stranded supercoiled plasmid DNA is packaged in the *interior* of a neutral or slightly anionic liposome.[22–24] Packaging the DNA in the interior of the liposome renders the DNA resistant to the ubiquitous endonucleases that are present *in vivo* and that rapidly degrade exposed DNA.[25] The liposome is prepared from a mixture of neutral lipid, such as 1-palmitoyl-2-oleoyl-*sn*-glycerol-3-phosphocholine (POPC), cationic lipid, such as didodecyldimethylammonium bromide (DDAB), and anionic lipid, such as distearoylphosphatidylethanolamine (DSPE) conjugated to polyethylene glycol (PEG). A small amount of cationic lipid (2–3% of the total lipid) is included in the lipid formulation to stabilize the anionic DNA. The net charge of the liposome is anionic, because there is an excess of DSPE-PEG relative to DDAB (see later).

The encapsulation of DNA in the interior of a conventional liposome would not yield significant gene expression *in vivo*, because this structure would be immediately coated with serum proteins following intravenous injection. The protein-coated liposome would be rapidly removed from blood by cells lining the reticuloendothelial system (RES).[26] The blood transit time can be prolonged, and uptake by the RES can be minimized by pegylation of the surface of the liposome, wherein 2000–3000 strands of PEG of varying molecular weight (2000–5000 Da) are conjugated to the liposome lipids.[27] The 2000-D PEG is typically used and is designated PEG^{2000}, and the strands of PEG projecting from the surface of the liposome are depicted in Fig. 1A. However, DNA encapsulated in the interior of pegylated liposomes would not be specifically targeted to tissues. Organ targeting is accomplished by tethering a receptor-specific ligand to the tips of 1–2% of the PEG strands.[28] The targeting ligand might be an endogenous peptide, modified protein, or a peptidomimetic monoclonal antibody (MAb). The conjugation of the targeting MAb to the tips of the liposome-anchored PEG strands is demonstrated in Fig. 1B. The PIL was

[22] N. Shi and W. M. Pardridge, *Proc. Natl. Acad. Sci. USA* **97,** 7567 (2000).
[23] N. Shi, R. J. Boado, and W. M. Pardridge, *Pharm. Res.* **18,** 1091 (2001).
[24] N. Shi, Y. Zhang, C. Zhu, R. J. Boado, C. Zhu, and W. M. Pardridge, *Proc. Natl. Acad. Sci. USA* **98,** 12754 (2001).
[25] K. W. C. Mok, A. M. I. Lam, and P. R. Cullis, *Biochim. Biophys. Acta.* **1419,** 137 (1999).
[26] D. V. Devine and J. M. J. Marjan, *Crit. Rev. Ther. Drug Carrier Sys.* **14,** 105 (1997).
[27] D. Papahadjopoulos, T. M. Allen, A. Gabizon, E. Mayhew, K. Matthay, S. K. Huang, K. D. Lee, M. C. Woodle, D. D. Lasic, and C. Redemann, *Proc. Natl. Acad. Sci. USA* **88,** 11460 (1991).
[28] J. Huwyler, D. Wu, and W. M. Pardridge, *Proc. Natl. Acad. Sci. USA* **93,** 14164 (1996).

visualized with electron microscopy after binding to the PIL-extended MAb a secondary anti-mouse IgG that was conjugated with 10-nm gold particles.

The MAb binds an exofacial epitope on the targeted receptor (Fig. 1A), and this triggers receptor-mediated endocytosis of the PIL.[29] The targeting of genes to the intracellular compartment of cells following intravenous injection is a ''two-barrier'' gene-targeting problem. The PIL must traverse both the capillary endothelial membrane (first barrier) and then cross the plasma membrane of the tissue cell (second barrier). For gene targeting to the brain, the targeting ligand binds to a receptor (e.g., the transferrin receptor [TfR] or the insulin receptor) that is present on both the first (capillary) and second (tissue cell) barriers.[29,30] Binding to the capillary endothelial receptor triggers receptor-mediated transcytosis of the PIL across the microvascular endothelial barrier. Binding of the targeting ligand to the receptor on brain cell membranes then triggers receptor-mediated endocytosis of the PIL into the target brain cell subsequent to transport across the microvascular endothelium.

Gene targeting to tissues such as liver or spleen, which have highly porous sinusoidal capillary beds, is a one-barrier gene-targeting problem, because the PILs freely cross the sinusoidal barrier.[23] The limiting barrier is endocytosis across the plasma membrane of the parenchymal cell in liver or spleen. However, in tissues such as heart or brain, which have continuous endothelial barriers, the exodus of the PIL from the capillary compartment to the organ interstitial space is minimal in the absence of targeting of the PIL across the endothelial barrier. The endothelial barrier is tightest in the brain, and the brain capillary wall constitutes the blood–brain barrier (BBB). Gene targeting in the brain is accomplished by using a MAb to the TfR, which is expressed on both the BBB and the brain cell membrane (BCM).[22] The anti-TfR MAb is an endocytosing antibody and binds an exofacial epitope on the TfR, and this binding triggers receptor-mediated transcytosis across the endothelial barrier and receptor-mediated endocytosis into brain cells.[31] In contrast to the brain, there is minimal TfR on the capillary endothelium in heart or kidney. Consequently, the PIL does not escape the capillary compartment in the heart or kidney, and there is no gene expression in these organs when the PIL is targeted to the TfR.[22–24]

[29] J. Huwyler, J. Yang, and W. M. Pardridge, *J. Pharmacol. Exp. Ther.* **282,** 1541 (1997).
[30] J. Huwyler and W. M. Pardridge, *J. Neurochem.* **70** 883 (1998).
[31] W. M. Pardridge, ''Brain Drug Targeting; The Future of Brain Drug Development.'' Cambridge University Press, Cambridge, 2001.

TABLE I
SPECIES-SPECIFIC PEPTIDOMIMETIC MONOCLONAL ANTIBODIES FOR GENE TARGETING TO THE BRAIN

Species to be targeted	Targeting ligand	Reference
Mouse	8D3 rat MAb to mouse transferrin receptor	[33]
Rat	OX26 murine MAb to rat transferrin receptor	[32]
Rhesus monkey	83–14 murine MAb to human insulin receptor	[34]
Human	Genetically engineered chimeric HIRMAb	[35]

MAb, monoclonal antibody; HIR, human insulin receptor; HIRMAb, MAb against HIR.

Peptidomimetic MAb targeting ligands tend to be species-specific, and a panel of targeting MAbs has been developed for gene targeting to the brain in different species (Table I). For gene targeting to rat brain, the OX26 murine MAb to the rat TfR is used.[32] However, the OX26 MAb is not active in mice.[33] Gene targeting to mice, including transgenic mice, is accomplished with the rat 8D3 MAb to the mouse TfR.[33] Gene targeting to the primate brain can be achieved with the murine 83–14 MAb to the human insulin receptor (HIR).[34] The HIRMAb cross-reacts with the insulin receptor at both the human BBB and the BBB of Old-World primates, such as Rhesus monkeys. The HIRMAb does not react with the insulin receptor of New-World primates, such as squirrel monkeys, because of the reduced genetic similarity between humans and New-World primates.[34] The murine HIRMAb cannot be used in humans because of immunological reactions in humans to proteins of mouse origin. However, a genetically engineered chimeric HIRMAb has been produced, and this chimeric HIRMAb has an affinity for the HIR that is identical to that of the original murine MAb.[35] The chimeric HIRMAb is avidly transported across the primate BBB *in vivo*, with 2% of the injected dose (ID) being delivered to the primate brain *in vivo* following a single intravenous injection. The chimeric HIRMAb could be used to target therapeutic genes to the brain of humans.

One goal of gene therapy is the widespread expression of the exogenous gene in the targeted organ following noninvasive administration. Because gene targeting technology was not developed, therapeutic genes were

[32] W. M. Pardridge, J. L. Buciak, and P. M. Friden, *J. Pharmacol. Exp. Ther.* **259,** 66 (1991).
[33] H. J. Lee, B. Engelhardt, J. Lesley, U. Bickel, and W. M. Pardridge, *J. Pharmacol. Exp. Ther.* **292,** 1048 (2000).
[34] W. M. Pardridge, Y. S. Kang, J. L. Buciak, and J. Yang, *Pharm. Res.* **12,** 807 (1995).
[35] M. J. Coloma, H. J. Lee, A. Kurihara, E. M. Landaw, R. J. Boado, S. L. Morrison, and W. M. Pardridge, *Pharm. Res.* **17**, 266 (2000).

delivered to the brain with neurosurgical approaches such as craniotomy. In addition to being highly invasive, craniotomy is not a useful approach to gene delivery to the brain, because the effective treatment volume following direct injection into the brain is only the volume at the tip of the injection needle or <1 mm^3. Instead, what is desired is the widespread expression of a therapeutic gene throughout the brain or any organ, and this can only be accomplished by targeting the therapeutic gene through the organ capillary bed. In the human brain, there are 400 miles of capillaries, and the surface area of the brain endothelial barrier is about 20 m^2. Therefore, if an exogenous gene is targeted through the capillary wall, there is immediate distribution of the gene throughout the entire organ volume.

Another goal of gene targeting is tissue-specific expression of the exogenous gene following intravenous administration. One might anticipate that the only way the expression of an exogenous gene might be restricted to a particular organ is to physically inject the gene into the organ. However, tissue-specific gene expression can be achieved with noninvasive intravenous routes of administration through the combined use of (1) gene-targeting technology and (2) tissue-specific gene promoters.[24] Many expression plasmids are driven by the SV40 promoter, which is widely expressed in most tissues. The intravenous injection of a β-galactosidase expression plasmid that is driven by the SV40 promoter, and packaged in the interior of OX26-PIL, results in the expression of the exogenous gene in multiple TfR-rich organs, including brain, liver, and spleen.[22–24] There is no measurable gene expression in TfR-poor organs, such as the kidney or heart.[22–24] The SV40 promoter was then replaced with a brain-specific promoter, taken from the 5′-flanking sequence (FS) of the human glial fibrillary acidic protein (GFAP) gene. The β-galactosidase gene, under the influence of the GFAP promoter, was packaged in the interior of 8D3-PIL and injected intravenously in mice.[24] Under these conditions, there was expression of the exogenous gene only in the brain, with no detectable gene expression in peripheral tissues including the liver or spleen. A gene can be delivered to peripheral tissues rich in the targeted receptor, but there will not be significant expression if the gene is driven by a tissue-specific promoter that is not transcriptionally active in a given tissue. This promoter will be activated only by specific trans-acting factors, which are expressed in a tissue-specific pattern. Therefore, the limiting factor in achieving tissue-specific gene expression *in vivo* with the PIL gene–targeting technology is the choice of the promoter-driving gene expression and the tissue specificity of that promoter.

Before using the gene targeting technology described in the following, the investigator needs to obtain access to the following items that are

not readily commercially available. First, if a peptidomimetic MAb is used as the targeting ligand (Table I), 10 to 100-mg quantities of the MAb may be required. This necessitates that the hybridoma secreting the MAb be available and that milligram quantities of the MAb be produced by either propagating liters of hybridoma-conditioned media or by the ascites method. Second, the targeted gene may be a commercially available reporter gene such as luciferase or β-galactosidase. However, if the targeted gene is a therapeutic gene, appropriate expression plasmids must be designed. Important elements in the design of the expression plasmid are the tissue specificity of the 5′-promoter or 3′-enhancer elements and the activity of elements that promote persistence of the gene by means of a extrachromosomal replication.[31] Third, a bifunctional PEG derivative is required (Fig. 2A), and these often must be obtained by custom synthesis.[22,28]

Methods

Maxiprep of Plasmid DNA

A typical PIL formulation starts with encapsulation of 150 μg of plasmid DNA, and this amount of plasmid DNA can be routinely isolated with the QIAfilter Plasmid Maxi kit from Qiagen, Inc. (Valencia, CA). The *Escherichia coli*, or other suitable host, that has been transformed with the plasmid DNA is removed from the freezer, and an aliquot is used to inoculate 150 ml of LB medium. The liquid culture is incubated at 37° with vigorous shaking (200 rpm) for 20–24 hours using a rotary water-bath shaker. The bacterial pellet is harvested in 250-ml plastic bottles at 6000 *g* for 15 min at 4° and is resuspended in 10 ml of ice-cold resuspension buffer P1 (0.05 M TRIS, pH 8.0, 10 m*M* EDTA). The P1 buffer contains 100 μg/ml of RNase A. Ten milliliters of lysis buffer P2 (0.2 M NaOH, 1% SDS) is added, and the suspension is mixed gently but thoroughly and incubated at room temperature for 5 min. Vortexing should be avoided, because this could shear the DNA. Ten milliliters of cold neutralization buffer P3 (3 M potassium acetate, pH 5.5) is added to the lysate, and the lysate is poured into the barrel of the QIAfilter cartridge and incubated at room temperature for 10 min. This 10-min incubation at room temperature is necessary for optimal performance of the QIAfilter maxi cartridge. The cartridge should not be agitated at this time. Ten milliliters of equilibration buffer QBT (0.75 M NaCl, 50 m*M* MOPS, pH 7.0, 15% isopropanol, 0.15% Triton X-100) is added and allowed to elute from the column by gravity. This is filtered until all lysate is passed from the QIAfilter cartridge, one should not apply force. Approximately 25 ml of lysate is

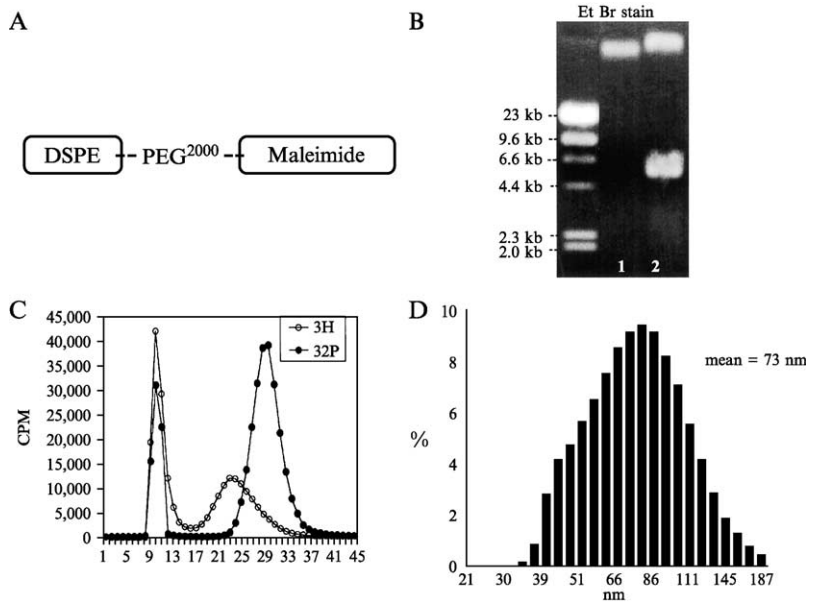

FIG. 2. (A) The structure of the bifunctional PEG^{2000} that contains a distearoylphosphatidylethanolamine (DSPE) moiety at one end, for incorporation into a liposome surface, and a maleimide moiety at the opposite tip of the PEG strand, to enable conjugation to a thiolated monoclonal antibody. (B) DNA encapsulated within pegylated liposomes before (lane 2) and after (lane 1) nuclease treatment is resolved with 0.8% agarose gel electrophoresis followed by ethidium bromide (Et Br) staining. DNA molecular weight size standards are shown on the left side. Before nuclease digestion, approximately 50% of the DNA associated with the pegylated liposome is bound to the exterior of the liposome (lane 2), and this is quantitatively removed by the nuclease treatment (lane 1).[22] (C) The conjugation of the MAb to the pegylated liposome carrying the encapsulated plasmid DNA following nuclease digestion is demonstrated by Sepharose CL-4B gel filtration chromatography. A trace amount of the encapsulated plasmid DNA was radiolabeled with ^{32}P, and a trace amount of the targeting MAb was radiolabeled with ^{3}H. This study shows comigration in the first peak off the column of the MAb, which is conjugated to the PEG^{2000} strand, and the plasmid DNA, which is encapsulated in the interior of the liposome. The unconjugated MAb and the exteriorized, digested DNA elute from the column at later elution volumes.[37] (D) The mean diameter of pegylated immunoliposomes with encapsulated plasmid DNA is 73 nm as determined by quasielastic light scattering.[22]

generally recovered after filtration. The Qiagen-tip is washed with wash buffer QC (1 M NaCl, 50 m*M* MOPS, pH 7.0, 15% isopropanol) and the DNA is with eluted 15 ml of elution buffer QF (1.25 M NaCl, 50 m*M* MOPS, pH 8.5, 15% isopropanol), the eluate is collected in 50-ml Nalgene Oak Ridge centrifuge tubes (polycarbonate centrifuge tubes should not be

used). The DNA is precipitated by adding 10.5 ml (0.7 volumes) of room temperature 2-propanol to the eluted DNA. This is centrifuged at 15,000 *g* for 30 min at 4° and the supernatant is carefully decanted. All solutions should be kept at room temperature to minimize salt precipitation, although centrifugation is carried out at 4° to prevent overheating of the sample. The DNA pellet is washed with 5 ml of room temperature 70% ethanol and centrifuged at 15,000*g* for 10 min at 4°. The supernatant is carefully decanted the pellet is air-dried for 5–10 min, and the DNA is dissolved in a suitable volume of TE buffer (0.01 M TRIS, pH = 8.0, 0.1 m*M* ethylenediamine tetraacetic acid [EDTA]). The concentration of the DNA is determined by measurement of the A_{260}. An A_{260} of 1.0 is equivalent to a DNA concentration of 50 μg/ml. Overdrying the pellet will make the DNA difficult to redissolve. DNA dissolves best under alkaline conditions and is not easily dissolved in acidic buffers because of protonation of the phosphate groups. A typical Maxiprep procedure should generate 750–1250 μg of DNA, which is enough for several PIL preparations.

Labeling of Plasmid DNA by Nick Translation

A small aliquot of the plasmid DNA should be ^{32}P-labeled by nick translation, so that the encapsulation of the DNA in the interior of the PIL can be confirmed and quantitated. The Nick Translation kit is obtained from Life Technologies, Inc. (Gaithersburg, MD) and contains the DNA polymerase I–DNaseI mixture, deoxynucleotide triphosphates (dNTP) minus deoxycytidine triphosphate (dCTP), and stop buffer. Sephadex-G25 (fine) spin columns are obtained from Roche (Indianapolis, IN). To a 1.5-ml microfuge tube, 5 μl of the dNTP mixture, 1 μl of plasmid DNA (1–2 μg), 4 μl (40 μCi) ^{32}P-dCTP, and 35 μl of distilled water are added. Following the manufacturer's instructions, the DNA polymerase I/DNase I is added, the mixture is incubated for 60 min at 15°, and the reaction is stopped with addition of EDTA stop buffer. The unincorporated nucleotides are removed with a G25 spin column, and the percent of radioactivity that is precipitated by trichloroacetic acid (TCA) should be measured. An aliquot of radioactivity is removed, 2.5% bovine serum albumin (BSA) is added as a carrier, and the DNA is precipitated by the addition of 10% cold TCA. More than 95% of the radioactivity should be precipitated by TCA. If this is not observed, there may have been problems with the gel filtration spin column and removal of unreacted radiolabeled dCTP. There can be degradation of the plasmid DNA during this procedure, and the TCA precipitability will not detect partial degradation. Plasmid DNA degradation is best assessed with agarose gel electrophoresis (see later) and film autoradiography.

Liposome Formation and DNA Encapsulation

POPC (MW = 760 D) and DDAB (MW = 631 D) are obtained from Avanti Polar Lipids (Alabaster, AL). The DSPE-PEG^{2000} (MW = 2748 D) is obtained from Shearwater Polymers as a catalog item. A bifunctional PEG^{2000} derivative with a DSPE moiety at one terminus and a maleimide (MAL) moiety at the other end is custom synthesized by Shearwater Polymers (MW = 2955 D). If stored properly, the DSPE-PEG^{2000}–MAL reagent is stable for at least a year. The LipoFast™-Basic extruder and the 400-, 200-, 100-, and 50-nm pore-sized polycarbonate membranes are obtained from Avestin (Ottawa, Canada). A total of 20 μmol of lipids is typically used for a PIL preparation involving the encapsulation of 150–250 μg of plasmid DNA. To a test tube containing 1 ml of chloroform, 97 μl of 146 mg/ml of POPC in chloroform (18.6 μmol), 60 μl of 10 m*M* DDAB (0.6 μmol, 3% final concentration), 100 μl of 16.4 mg/ml DSPE-PEG^{2000} (0.6 μmol, 3% final concentration), and 120 μl of 5 mg/ml DSPE-PEG^{2000}–maleimide (0.2 μmol, 1% final concentration) are added. Although DSPE is an electrically neutral lipid, DSPE-PEG or DSPE-PEG-maleimide are anionic lipids. The total concentration of anionic lipids in the formulation is 4%, and the total concentration of cationic lipids is 3%, so the net charge of the liposome is anionic. Lipids are stored under a nitrogen atmosphere. Following mixing of the lipids, the chloroform is evaporated under a stream of nitrogen while it is vortexed to produce a thin-layer lipid film. This should be performed continuously without interruption, and the lipid film should dry well and sit at room temperature for at least 30 min before going to the next step. Then, 0.2 ml of 0.05 M TRIS, pH = 7.4 is added to produce a total lipid concentration of approximately 100 m*M*. This solution is vortexed three to four times and sonicated for 2 min with a bath sonicator; it is vortexed again for approximately 1 min. Then, 150 μg of plasmid DNA and 2 μCi of ^{32}P-DNA in a total volume of approximately 300 μl is added, and the total ^{32}P radioactivity is determined. This CPM is designated ''A'' and is used for subsequent calculations (see later). An ethanol–dry ice bath is prepared, and the lipids undergo a freeze–thaw cycle for a total of 10 times with placement in the ice bath for 5 min followed by thawing at 40° for 1.5–2 min. Before the freeze–thaw cycles, if air bubbles are visible in the lipid solution, the solution should be allowed to sit, or an additional two to three freeze–thaw cycles should be performed, so as to eliminate the air bubbles, because these inhibit DNA encapsulation. At this point, 0.05 M HEPES, pH = 7.0, is added to a final volume of 500 μl (40 m*M* lipid), and the solution is mixed well by tapping. Two stacked 400-nm polycarbonate filters are inserted into a washed extruder and the liposome and DNA mixture is forced through the extruder; the

extrusion is repeated seven times. Then, the mixture is forced five times through the extruder containing two stacked 200-nm polycarbonate filters. Finally, the lipids should be forced three to four times through two stacked polycarbonate filters with a pore size of 100 nm. Depending on the results of the liposome sizing experiments, it may be preferable to extrude the solution through an additional two stacked polycarbonate filters with a pore size of 50 nm, so that the mean diameter of the PIL is less than 100 nm. There is a tradeoff, because smaller size liposomes are presumably transcytosed easier but encapsulate DNA less efficiently. A compromise is achieved by preparing liposomes with diameters in the range of 75–100 nm. At this point, approximately half of the DNA has been interiorized in the liposome, and half remains absorbed to the surface of the liposome. The exterior bound DNA can interfere with conjugation of the thiolated targeting ligand to the maleimide moiety on the DSPE-PEG^{2000}–MAL. Therefore, the exteriorized DNA is removed by nuclease digestion.[36]

Nuclease Digestion

Pancreatic endonuclease I is obtained from Sigma (St. Louis, MO), and exonuclease III is obtained from GIBCO-BRL. The extruded pegylated liposome–DNA mixture is added to a 1.5-ml microfuge tube followed by addition of 3 μl (6 units) of DNAse I, 0.5 μL (33 units) of exonuclease III, and 5 μl of 500 m*M* $MgCl_2$ to yield a final $MgCl_2$ concentration of 5 m*M*. The solution is incubated at 37° for 60 min, and the nuclease reaction is stopped by the addition of 20 μl of 0.5 M EDTA, pH = 8.0 (to yield a final EDTA concentration of 20 m*M*). The ^{32}P should be counted (designated ''B''). The ratio of the [''B''/''A''] radioactivity allows for calculation of the loss of DNA (and lipid) because of the dead volume of the extruder. The targeting ligand or MAb should be thiolated in parallel with the nuclease digestion step, and the PIL should be formed by overnight conjugation by mixing the nuclease-treated pegylated liposomes and the thiolated MAb. The efficacy of the nuclease treatment can be assessed with 0.8% agarose gel electrophoresis and ethidium bromide staining (Fig. 2B).

Monoclonal Antibody Thiolation

To a glass tube, 3.0 mg of MAb (300 μl of a 10 mg/ml solution or 20 nmol of MAb) is added followed by addition of 2 μCi of either ^{3}H-labeled MAb or ^{125}I-labeled MAb (10–20 μl of a stock solution of 100–200 μCi/ml) (The MAb can be labeled with ^{125}I and chloramine T or

[36] P. A. Monnard, T. Oberholzer, and P. Luisi, *Biochim. Biophys. Acta.* **1329,** 39 (1997).

labeled with ^{3}H-*N*-succinimidyl propionate). An appropriate volume of 0.15 M sodium borate, pH = 8.5, 0.1 m*M* EDTA, is added to yield a final sodium borate concentration of approximately 0.05 M. Then, 12.2 μl of 9.1 mg/ml of fresh Traut's reagent (2-iminothiolane) is added. The solution is incubated at room temperature for 60 min, and the ^{3}H or ^{125}I radioactivity is counted (designated ''X''). The unreacted Traut's reagent is removed from the thiolated MAb using a Centriprep-30 concentration filter (Amicon, Millipore, Billerica, MA). The mixture is added to the concentrator, and the volume is brought to 20 ml with 0.05 M HEPES, pH = 7.4, and 0.1 m*M* EDTA (HE buffer), and the volume is reduced to 2 ml by centrifugation at 2700 rpm for approximately 60 min at 4°. This cycle is repeated one more time with a final reduction of the volume to approximately 1 ml. An aliquot should be removed for counting radioactivity to determine whether there is significant loss of the MAb during the Centriprep-30 buffer exchange. The loss of MAb at this step does not alter calculations of MAb conjugation, because the latter is based on the specific activity of the MAb, which is the μCi of radiolabeled MAb per milligram of unlabeled MAb added at the beginning of the MAb thiolation. The thiolated MAb is transferred to a small bottle that can be capped with a rubber stopper, and the liposome–DNA mixture is added to the thiolated MAb and mixed gently. The bottle is capped with an air-tight stopper, and the air phase is flushed with nitrogen and rocked slowly overnight at room temperature.

Pegylated Immunoliposome Purification with Gel Filtration Chromatography

The next day the conjugated PIL is applied to a 1.5 × 20-cm column of Sephacryl CL-4B and eluted with 0.05 M HEPES, pH = 7.0, and 1-ml fractions are collected with a flow rate of 1 ml/min controlled by a chromatography pump. For all tubes off the column, take 100 μl and count in 10 ml of Ultima-gold (Packard) for either ^{3}H/^{32}P or ^{125}I/^{32}P in a liquid scintillation counting (LSC) spectrometer. The DNA is labeled with ^{32}P, and the MAb is labeled with either ^{125}I or ^{3}H. For ^{3}H/^{32}P counting, count ^{3}H in a window of 0–16 keV and count ^{32}P in a window of 16–1700 keV; there is no ^{3}H spillover in the ^{32}P channel, and there is about 2% spillover of ^{32}P into the ^{3}H channel. This spillover correction should be performed when needed. For simultaneous counting of ^{125}I/^{32}P, count ^{125}I in a window of 0–100 keV and count ^{32}P in a window of 100–1700 keV; there is no ^{125}I spillover in the ^{32}P channel, and there is about a 26% spillover of ^{32}P into the ^{125}I channel, and this spillover correction should be performed. For either the radiolabeled DNA or the radiolabeled MAb, there will be two peaks off the CL-4B column. The first peak is the PIL elution, and there

should be an exact comigration of the radiolabeled DNA encapsulated in the interior of the PIL and the radiolabeled MAb conjugated to the tips of the PEG strands (Fig. 2C). At a later elution time, the unconjugated radiolabeled MAb should be detected followed by degraded DNA and free nucleotides generated in the nuclease treatment step (Fig. 2C). The DNA and MAb radioactivity in the first (PIL) peak should be determined, and the DNA counts are designated ''C'' and the MAb radioactivity is designated ''Y.'' It is also useful to check the TCA precipitability of the PIL, and this radioactivity should be more than 95% precipitable by TCA. The diameter of the PIL can be determined with quasielastic light-scattering methods[27] and should be $\leq$100 nm (Fig. 2D).

Calculations

The two principal parameters that are used to assess the quality of the PIL formulation are (1) the amount of DNA encapsulated in the interior of the PIL and (2) the number of MAb molecules conjugated to the PIL. A typical DNA encapsulation is 20%, and 35–65 MAb molecules are usually conjugated per PIL. For calculation of the number of MAb molecules conjugated per PIL, it is assumed that there are 100,000 lipid molecules in a 100-nm diameter liposome.[28] Given this parameter, it can be calculated that there are 1.2×10^{14} liposome particles in 20 μmol of lipid. The mole of conjugated MAb is determined from the total CPM in the first peak off the CL-4B column (Y) divided by the MAb-specific activity (CPM/mol). The MAb-specific activity is the total CPM in fraction X divided by 20 nmol of initial MAb. The number of MAb molecules conjugated in peak ''Y'' is divided by the number of liposomes (1.2×10^{14}) and corrected for the loss of lipid in the dead space of the extruder (Z), where

$$Z = 1 - (B/A)$$

The loss of lipid with the extruder step is assumed to be equal to the loss of DNA. The percent of DNA encapsulated in the liposomes is determined from [''C''/''A''] $\times$ 100, and the fractional encapsulation is multiplied by the total micrograms of initial DNA (e.g., 150 μg) to determine the total micrograms of encapsulated DNA. If the number of MAb molecules conjugated per liposome is <10–15, and/or the percent of DNA encapsulation is <10%, the synthesis of the PIL should probably be repeated.

Sterilization of Pegylated Immunoliposome for Tissue Culture Experiments

If the PIL is used for tissue culture, the TRIS and HEPES buffers should be sterilized by extrusion through a 0.22-μm Millipore (Billerica, MA) filter. All the plastic and glass tubes and pipet tips should be autoclaved before the

experiment. Once the PIL is ready for addition to cultured cells, the PIL is sterilized by extrusion through a 0.22-μm Millipore filter unit (SLGV R25 LS, Millipore Corp.). The recovery of either the DNA or the MAb is >95% after filtration sterilization.[37] If this sterilized PIL is reapplied to the CL-4B column, all of the DNA and MAb elute in the first PIL peak, indicating the Millipore filtration does not disrupt the PIL.[37]

Organ Luciferase Measurements

At various days after a single intravenous injection of the PIL carrying a luciferase expression plasmid, the animal is killed, and the brain or other organs are removed. The organs (about 0.5 g) are homogenized in 2 ml of lysis buffer (0.1 M potassium phosphate, pH = 7.8, 1% Triton X-100, 1 m*M* dithiothreitol, and 2 m*M* EDTA) using a Polytron homogenizer. The homogenate is centrifuged at 14,000 rpm for 10 min at 4°, and the supernatant is subsequently frozen for later use for measurements of tissue luciferase activity with a luminometer (Biolumat LB 9507, Berthold, Bundoora, Victoria, Australia); 100 μl of reconstituted luciferase substrate (Promega, Madison, WI) is added to 20 μl of tissue extract. The peak light emission is measured for 10 s at 20° and recorded as relative light units (RLU). Recombinant luciferase (Promega) is assayed in parallel to establish a standard curve, and the standard curve is used to convert the RLU into picograms of luciferase activity. The protein content in the tissue extract is measured with the bicinchoninic acid (BCA) protein assay reagent (Pierce Chemical Co.), and the final organ luciferase activity is expressed as picograms of luciferase per milligram of tissue protein. For studies in mice, the pGL3-control luciferase expression plasmid driven by the SV40 promoter is obtained from Promega and encapsulated in the interior of 8D3-PIL. Adult male BALB/c mice (25–30 g) are injected intravenously with the 8D3-PIL at a dose of 5 μg plasmid DNA per mouse. Organ luciferase is measured at 48 and 72 h after a single intravenous injection (Table II). These data show expression of the luciferase gene in TfR-rich organs of the mouse, such as brain, liver, spleen, and lung, with background levels of gene expression in TfR-poor organs, such as heart or kidney. The luciferase levels at 72 h in the TfR-rich organs range from 50–75% of the luciferase level at 48 h after intravenous injection (Table II). At 72 h after intravenous administration, the level of luciferase expression in brain and spleen is comparable and is about one-third the level in liver (Table II).

The luciferase expression levels in Table II demonstrate the marked differences in organ specificity of gene expression using the PIL technology,

[37] Y. Zhang, H. J. Lee, R. J. Boado, and W. M. Pardridge, *J. Gene Med.*, **4,** 183 (2002).

TABLE II
ORGAN LUCIFERASE ACTIVITY IN THE MOUSE AFTER A SINGLE INTRAVENOUS INJECTION OF pGL3-CONTROL PLASMID DNA ENCAPSULATED IN 8D3 PEGYLATED IMMUNOLIPOSOMES[24]

	Picograms luciferase/mg protein	
Organ	48 h	72 h
Brain	0.76 ± 0.09	0.50 ± 0.10
Heart	0.015 ± 0.001	0.018 ± 0.004
Liver	3.1 ± 0.5	1.4 ± 0.1
Spleen	1.1 ± 0.1	0.52 ± 0.11
Lung	0.74 ± 0.06	0.34 ± 0.09
Kidney	0.0092 ± 0.0009	0.0082 ± 0.0003

Data are mean ± SE (n = 5 mice per time point). Mice were administered a single intravenous injection of 5 μg/mouse of pGL3 plasmid DNA encapsulated in 8D3-PIL.
PIL, pegylated immunoliposome.

compared with either viral vectors or cationic liposomes. With the PIL gene targeting approach, the gene expression in the lung is comparable to brain and is less than gene expression in spleen or liver. The opposite is observed with cationic liposome–DNA formulations, wherein >99% of gene expression is observed in the lung,[17,18] <1% in liver or spleen, and 0% in brain.[19] Gene expression in the lung is principally in the pulmonary endothelial compartment[38] as a result of precipitation of the aggregated cationic liposome–DNA mixture in the lung circulation. The intravenous injection of adenoviral vectors in the mouse results in >90% of the exogenous gene expression in the liver because of rapid entrapment of adenovirus by liver cells.[39] In contrast, with the PIL drug-targeting technology, an exogenous gene is expressed in organs in a pattern that is predicted from the specificity of the targeting MAb and the tissue distribution of the targeted receptor. Luciferase expression in organs such as liver or spleen reflects the fact that these are TfR-rich organs. Expression in liver or spleen is not due to nonspecific uptake of the PIL by the RES cells in these organs. For example, when a nonspecific rat IgG is used in lieu of the rat 8D3 MAb and the exogenous gene is encapsulated in rat IgG-PIL and injected into mice, there is no gene expression in liver, spleen, or brain.[24] Similarly,

[38] H. E. J. Hofland, D. Nagy, J. J. Liu, K. Spratt, Y. L. Lee, O. Danos, and S. M. Sullivan, *Pharm. Res*. **14,** 742 (1997).
[39] K. R. Zinn, J. T. Douglas, C. A. Smyth, H. G. Liu, Q. Wu, V. N. Krasnykh, J. D. Mountz, D. T. Curiel, and J. M. Mountz, *Gene Ther*. **5,** 798 (1998).

when the OX26 MAb is replaced by a mouse IgG_{2a} isotype control antibody and IgG_{2a}-PIL is prepared, there is no expression of the exogenous gene in liver or spleen in the rat (Fig. 3). These results indicate the PIL is targeted to tissues on the basis of the receptor specificity of the targeting ligand, with minimal nonspecific uptake of the PIL by the RES.[23]

The organ luciferase activity in the mouse following the administration of 8D3-PIL is obtained with the intravenous injection of only 5 μg DNA/25 g mouse, which is 200 μg/kg (Table II). A similar level of luciferase activity is observed in rat tissues, with the pGL3-control plasmid packaged in OX26-PIL and administered at an intravenous dose of 5 μg/250 g rat, which is a dose of only 20 μg/kg. Because of the inefficiency of cationic liposomes *in vivo*, it is necessary to inject large amounts of DNA, ranging from 30–100 μg per mouse[17,18] or doses up to 5000 μg/kg. The administration of such large amounts of DNA can cause inflammation even with nonviral gene delivery systems, owing to the inflammatory response to large doses of exogenous DNA.[40] The PIL gene-targeting approach allows for tissue expression of exogenous genes following the administration of relatively low doses of systemic DNA ranging from 20–200 μg/kg. This dosage may be reduced further with advances in plasmid DNA formulation that enable persistence of gene expression.[31] The inclusion in the plasmid of the Epstein Barr nuclear antigen (EBNA)-1 gene element allows for persistence of extrachromosomal replication in human, but not rodent, cells.[37] The administration of luciferase expression plasmids carrying the EBNA-1 gene to human cells with the HIRMAb-PIL gene targeting system yields cell luciferase levels that are >100 pg/mg protein.[37] The level of luciferase gene expression in cultured cells with the HIRMAb-PIL gene-targeting system is comparable to that obtained with lipofectamine.[37]

β-Galactosidase Histochemistry

An alternative reporter gene other than luciferase is *Escherichia coli* β-galactosidase, and expression plasmids encoding for *E. coli* β-galactosidase are readily available commercially. The advantage of using β-galactosidase as a reporter gene is that histochemistry can be used to identify the cellular location of gene expression (Fig. 3). At various times after a single intravenous injection of a β-galactosidase gene encapsulated in the interior of the PIL, organs are removed and rapidly frozen in powdered dry ice and dipped in Tissue-tek OCT embedding medium. Then, 18-μm frozen sections are prepared on a cryostat and stored at -70°. The sections are

[40] J. Norman, W. Denham, D. Denham, J. Yang, G. Carter, A. Abouhamze, C. L. Tannahill, S. L. D. MacKay, and L. L. Moldawer, *Gene Ther.* **7,** 1425 (2000).

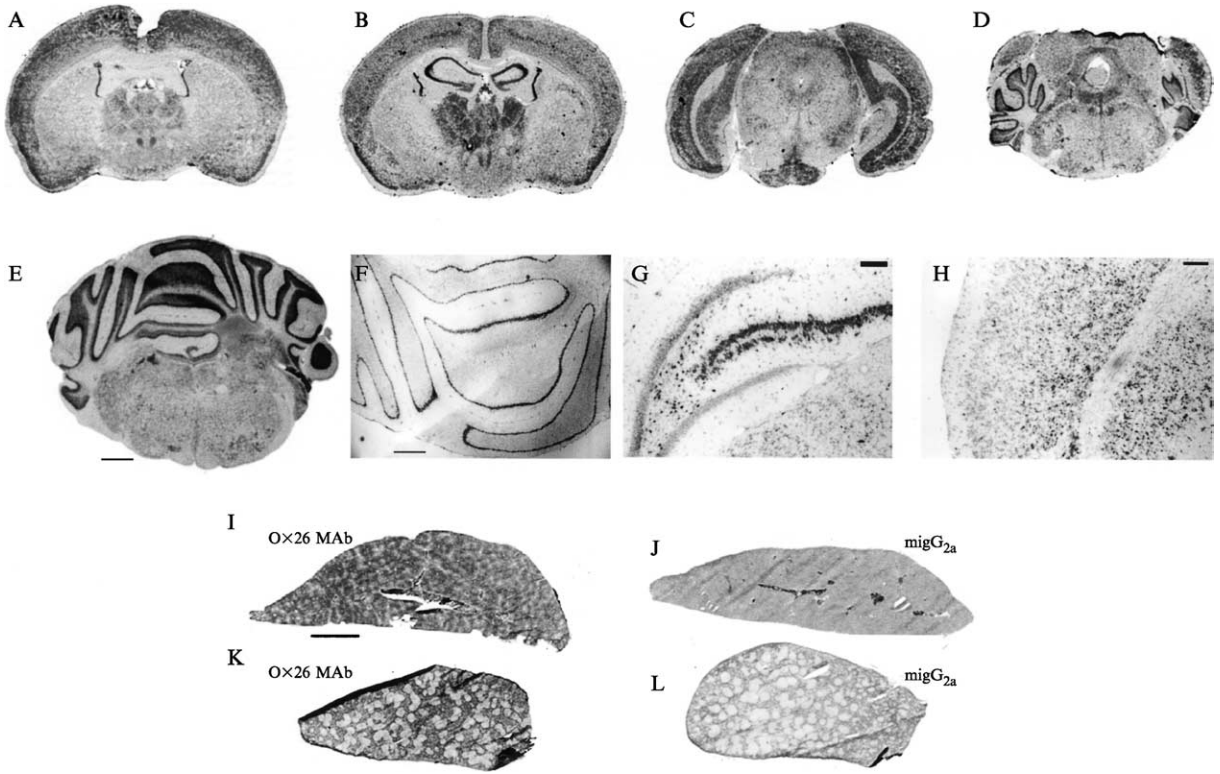

FIG. 3. β-Galactosidase histochemistry of mouse (A–H) and rat (I–L) tissues 48 h after a single intravenous injection of a β-galactosidase expression plasmid encapsulated in the interior of pegylated immunliposomes (PIL) conjugated with either the 8D3 (A–H) or OX26 (I–L) MAb.[23,24] (A–D) Coronal sections through the mouse brain at the level of the septostriatum, the rostral diencephalon, the rostral

fixed at room temperature in 0.5% glutaraldehyde/0.1 M phosphate buffer (pH = 7.0) for 5 min. The β-galactosidase histochemistry is performed with 5-bromo-4-chloro-3-indoyl-β-D-galactoside (X-gal). A kit for X-GAL histochemistry is available from Invitrogen. The slides are developed with the X-gal chromagen overnight at 37° in a humidified chamber. Before coverslipping, the air-dried slides are scanned with a 1200 dpi UMAX flatbed scanner with transluminator and cropped in Adobe Photoshop 5.5 with a G4 Power Macintosh. Scanned images are shown in Fig. 3 (A–E, I–L). After scanning, the slides are coverslipped for light microscopy (F–H of Fig. 3).

The β-galactosidase histochemistry assay should be performed with care, because it is possible to have both false-negative and false-positive results. False-negative results are obtained when there is no blue histochemical product following the overnight X-gal incubation. It is essential to use only polypropylene tubes and pipet tips with the X-gal histochemical assay. The X-gal will precipitate on polystyrene surfaces and yield false-negative results. If care is not taken to maintain the pH at 7.0, false-positive results can be obtained if the overnight incubation is performed under conditions of acidic pH. There is β-galactosidase–like enzyme activity in the mammalian lysosome that is activated at pH 4–5.[41,42] Lysosomal activity will give a false histochemical product under acidic pH conditions. False-positive results can be eliminated by maintaining the pH at 7.0 and can be tracked by performing parallel histochemistry on tissues obtained from control or uninjected mice. The endogenous β-galactosidase–like activity in rat kidney is very high and is readily detectable even at pH 7.0. Therefore, control mouse kidney should be examined in all β-galactosidase assays to confirm that there are no false-negatives results in the histochemical assay. If there is no substantial β-galactosidase histochemical activity in both the cortex and medulla of control rat or mouse kidney, the assay was

[41] D. J. Weiss, D. Liggitt, and J. G. Clark, *Histochem. J.* **31,** 231 (1999).

[42] J. Sanchez-Ramos, S. Song, M. Dailey, F. Cardozo-Pelaez, C. Hazzi, T. Stedeford, A. Willing, T. B. Freeman, S. Saporta, T. Zigova, P. R. Sanberg, and E. Y. Snyder, *Cell Transplant.* **9,** 657 (2000).

mesencephalon, and the caudal mesencephalon, respectively. Expression of the exogenous gene throughout the brain is shown. (D) A counterstained scanned image of the mouse cerebellum. Light microscopy of selected regions of the mouse brain are shown for the cerebellum (F), the hippocampus (G), and the temporoparietal cortex (H). The β-galactosidase gene is expressed widely throughout the rat liver (I) and spleen (K) following the administration of OX26 PIL. However, if the OX26 MAb is replaced on the pegylated liposome by a mouse IgG_{2a} isotype control, there is no β-galactosidase gene expression in liver (J) or spleen (L). The magnification bars are 600 μm, 250 μm, 70 μm, and 70 μm in E–H, respectively. The magnification bar in I is 2.1 mm. The only section that was counterstained is E. (See color insert.)

not performed properly. A greater histochemical reaction product is obtained with the use of 18-μm sections than with 5-μm sections, presumably because there is a $>$threefold more β-galactosidase gene product in the thicker sections. β-Galactosidase histochemistry has been performed in rats to examine the persistence of the β-Galactosidase transgene expression following a single intravenous injection of the PIL formulation. The level of β-galactosidase gene expression as determined by either histochemistry or by Southern blotting decreases approximately 50% in the rat 6 days following a single intravenous injection of a β-galactosidase plasmid driven by the SV40 promoter encapsulated in OX26-PIL.[23]

Southern Blotting

Expression of the plasmid DNA in tissues can also be confirmed by Southern blotting.[23] Genomic DNA is isolated from tissues using the Genomic Isolation kit from Qiagen, and a typical yield is approximately 1.3 μg of DNA per mg of tissue. The absorbance at 260–280 nm should be determined for quality control of the isolate. Then, 10-μg DNA aliquots are digested with 15 units of *EcoRI* for 1 h at 37° to remove the insert from the plasmid. The sample is resolved with agarose gel electrophoresis followed by blotting to a GeneScreen-plus membrane, which is then hybridized with ^{32}P-radiolabeled plasmid. Following washing, the membrane is applied to the Kodak X-Omat Blue X-ray film for 3 h at room temperature. During the agarose gel, the migration of xylene cyanol (XC) and bromophenol blue (BPB) tracking dyes are observed. The XC and BPB dyes migrate near the 4.4 and 0.6 kb DNA sizing standards, respectively.

Confocal Microscopy

The intracellular fate of the plasmid DNA following uptake of the PIL can be followed with confocal microscopy following the initial conjugation of fluorescein or an alternative fluorochrome to the plasmid DNA. For the production of fluorescein-conjugated DNA, 15 μg of plasmid DNA is labeled with fluorescein-12-dUTP using the Nick translation kit (Roche) and purified by lithium chloride–ethanol precipitation per the manufacturer's instructions. Then, 15 μg of fluorescein-labeled plasmid DNA is incorporated in a 10-μmol lipid preparation of PIL. Gene targeting to human cells is achieved with the HIRMAb (Table I). The fluoro-DNA packaged in the HIRMAb-PIL can be targeted to U87 human glioma cells in tissue culture.[37] The exogenous gene that is conjugated with the fluorescein is an expression plasmid producing antisense RNA directed against the human epidermal growth factor (EGF) receptor mRNA. The HIRMAb-PIL carrying the fluoresceinated DNA is added to U87 human glioma cells

in tissue culture following sterilization of the PIL preparation as described previously. The cells are plated on coverslips at the bottom of wells of a cluster dish, and the glioma cells are incubated for either 3 or 24 h with a total of 1 μg/dish of the fluoresceinated plasmid DNA encapsulated in the interior of HIRMAb-PIL. The incubations are performed in MEM with 10% FBS. The presence of serum does not interfere with cell uptake of the PIL, and this contrasts with the cationic lipid–DNA formulation. The activity of cationic lipids such as lipofectamine is blocked by serum, owing to the binding of the cationic lipid by serum proteins. At the end of the incubation, the media is removed by aspiration, the cells are washed with cold buffer, and fixed with 1 ml/well of 10% formalin in PBS at 4° for 20 mins. The formalin is aspirated, the cells are washed with PBS, and the coverslips containing the adhered cells are removed from the cluster dish and mounted to glass slides. Confocal microscopy is performed with the LSM 5 PASCAL microscope (Zeiss, Jena, Germany) with an argon laser. The intracellular delivery of plasmid DNA encapsulated in the PIL is demonstrated by confocal microscopy (Fig. 4). After 3 h of incubation, the fluorescein-conjugated DNA, delivered to the cell with the HIRMAb-PIL, is distributed throughout the cytoplasm and is also observed within intranuclear vesicles (Fig. 4A). After 24 h of incubation, the fluorescein-conjugated DNA is primarily sequestered within the nucleus (Fig. 4B). These confocal microscopy studies confirm that the plasmid DNA is delivered to the nucleus with the PIL gene targeting system.

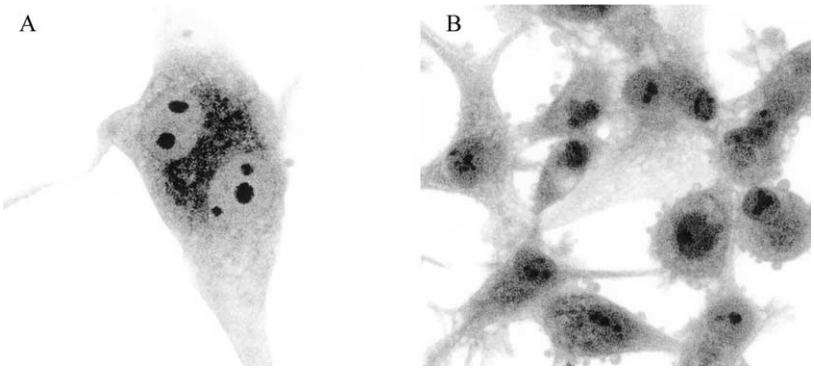

FIG. 4. Confocal microscopy of human U87 glioma cells following a 3-h (A) or 24-h (B) incubation of fluorescein-conjugated plasmid DNA (fluoro-DNA) encapsulated in HIRMAb-pegylated immunoliposomes.[37] The gray-scale confocal image was inverted in Photoshop, so that the localization of the fluoro-DNA is shown by the black areas. There is primarily cytoplasmic accumulation of the fluoro-DNA at 3 h, whereas the fluoro-DNA is largely confined in the nuclear compartment at 24 h. Fluoro-DNA entrapped within intranuclear vesicles is visible at both 3 and 24 h.

Summary

The PIL gene-targeting technology is based on an advanced molecular reformulation of the therapeutic gene (Fig. 1A). This gene-targeting technology is derived from the merger of multiple and disparate disciplines, including liposome technology, pegylation technology, monoclonal antibody technology, and molecular biology. The PIL gene-targeting technology enables the widespread expression of an exogenous gene throughout the target organ (Fig. 3) following a noninvasive, intravenous injection of a nonviral formulation. The targeting specificity of the PIL is strictly a function of the specificity of the targeting ligand or MAb conjugated to the PIL (Fig. 1A, Table I). The specificity of the tissue expression of the exogenous gene is derived from the combined influences of the specificity of the targeting ligand and the tissue specificity of the promoter that is placed at the 5′-end of the therapeutic gene. With the combined use of gene-targeting technology and tissue-specific gene promoters, it is possible to have tissue-specific gene expression widely throughout the target organ following an intravenous injection of the therapeutic gene.[24] The PIL gene targeting technology has thus far been used only for transient or extrachromasomal gene expression *in vivo* using plasmid vectors that do not integrate into the host genome. Conversely, certain viral vectors such as retroviruses or adeno-associated virus stably integrate into the host genome. Nevertheless, it is possible to trigger stable integration of an exogenous gene into genomic host DNA with nonviral expression vectors by incorporating into the plasmid certain transposons. These are 1.6–1.7 kb terminal inverted repeats, and these transposons enable genomic integration of the exogenous gene without the use of viruses.[43] The incorporation of transposon elements into expression plasmids may allow for stable integration of the exogenous gene in the host genome following the intravenous administration of a nonviral plasmid DNA that is encapsulated in a pegylated immunoliposome.

Acknowledgments

The author is indebted for many valuable discussions to Drs. Ruben Boado, Yun Zhang, Ningya Shi, Hwa Jeong Lee, and Frederic Calon. This work was supported by a grant from the UC Davis–MIND Institute and by a grant from the U. S. Department of Defense-Neurotoxin Program.

[43] Z. Izsvak, Z. Ivics, and R. H. Plasterk, *J. Mol. Biol.* **302,** 93 (2000).

HUMAN GENE THERAPY 15:339–350 (April 2004)

Normalization of Striatal Tyrosine Hydroxylase and Reversal of Motor Impairment in Experimental Parkinsonism with Intravenous Nonviral Gene Therapy and a Brain-Specific Promoter

YUN ZHANG, FELIX SCHLACHETZKI,* YU-FENG ZHANG, RUBEN J. BOADO, and WILLIAM M. PARDRIDGE

ABSTRACT

The goal of this work was to normalize striatal tyrosine hydroxylase (TH) activity with intravenous nonviral TH gene therapy and at the same time eliminate ectopic TH gene expression in peripheral organs such as liver in the rat. TH-expression plasmids, containing either the SV40 promoter or the glial fibrillary acidic protein (GFAP) gene promoter, were globally delivered to the brain across the blood-brain barrier (BBB) after intravenous administration of pegylated immunoliposomes (PILs). The GFAP-TH– or SV40-TH–expression plasmids were encapsulated in the interior of 85-nm PILs, which were targeted across both the BBB and the neuronal cell membrane with a monoclonal antibody (mAb) to the transferrin receptor (TfR). Striatal TH activity was 98% depleted with the unilateral intracerebral injection of 6-hydroxydopamine. TH in the striatum ipsilateral to the lesion was normalized 3 days after the intravenous injection of 10 μg per rat of either the SV40-TH or the GFAP-TH plasmid DNA. Whereas the SV40-TH gene caused a 10-fold increase in hepatic TH activity, there was no increase in liver TH with the GFAP-TH gene. The GFAP-TH gene therapy caused an 82% reduction in apomorphine-induced rotation in the lesioned rats. Confocal microscopy using antibodies to TH, GFAP, and neuronal nuclei (NeuN) showed the GFAP-TH gene was selectively expressed in nigra-striatal neurons, with no expression in either cortical neurons, or astrocytes. These studies demonstrate that global delivery of exogenous genes to the brain is possible with intravenous nonviral gene transfer, and that ectopic gene expression is eliminated with the use of brain-specific gene promoters.

OVERVIEW SUMMARY

Nonviral gene transfer using pegylated immunoliposomes (PILs) targets the plasmid DNA to brain with receptor-specific transport ligands, which act as a molecular Trojan horse to ferry the gene across both the blood-brain barrier and the neuronal cell membrane. Because the transport ligands may also deliver the gene to nonbrain organs, brain-specific gene expression can be achieved with the combined use of the PIL gene delivery technology and organ-specific gene promoters. The present work shows the ectopic expression of an exogenous tyrosine hydroxylase (TH) gene in peripheral tissues such as liver is eliminated, when the TH-expression plasmid is driven by a brain-specific promoter taken from the 5′-flanking sequence of the glial fibrillary acidic protein (GFAP) gene. After intravenous administration of PILs carrying the GFAP-TH–expression plasmid, striatal TH activity is completely restored in the 6-hydroxydopamine model of experimental Parkinson's disease.

INTRODUCTION

PARKINSON'S DISEASE (PD) is associated with a loss of dopaminergic neurons originating in the substantia nigra and terminating in the striatum (Mouradian and Chase, 1997; Mandel *et al.*, 1999). The rate-limiting enzyme in dopamine synthesis is tyrosine hydroxylase (TH), and one approach to the

Department of Medicine, University of California, Los Angeles, Los Angeles, CA 90024.
*Current address: Department of Neurology, University of Regensburg, 93053 Regensburg, Germany.

treatment of PD is TH replacement gene therapy. The goals of TH gene therapy in PD are (1) the delivery of the TH gene to the majority of the nigral-striatal neurons resulting in the restoration of dopaminergic neurotransmitter release in the striatum and (2) the selective expression of the TH gene in this region of brain without ectopic TH gene expression in either the cortex or in nonbrain organs. Ectopic TH gene expression could lead to unwanted increased dopaminergic activity in peripheral organs. The transduction of the majority of the nigral-striatal neurons with TH gene therapy is possible with a transvascular route to the brain. In this approach, the gene is administered intravenously followed by entry into the brain across the blood-brain barrier (BBB). Because every neuron is perfused by its own blood vessel, the gene is targeted to virtually every neuron in the brain following a transvascular delivery route (Pardridge, 2002). Prior work with a nonviral expression plasmid driven by the widely expressed SV40 promoter demonstrated normalization of striatal TH activity in the 6-hydroxydopamine (6-OHDA)–lesioned rat brain using the pegylated immunoliposome (PIL) gene targeting technology (Zhang *et al.*, 2003a). The TH expression plasmid is encapsulated in an 85-nm pegylated liposome, which is targeted across both the BBB and the neuronal cell membrane with a peptidomimetic monoclonal antibody (mAb) to the transferrin receptor (TfR) after intravenous administration. The transduction of rat brain with the TH-PIL gene therapy was confined to the nigral-striatal tract, and TH was not increased in the cortex of rat brain (Zhang *et al.*, 2003a). The lack of TH gene expression in the cortex is caused by the obligatory requirement of the TH enzyme for the biopterin cofactor (Hwang *et al.*, 1998). The rate-limiting enzyme in the biosynthetic pathway of biopterin, GTP cyclohydrolase I (GTPCH), is not expressed in cortex because the expression of this gene in brain is confined to monoaminergic neurons (Shimoji *et al.*, 1999). However, GTPCH is expressed in peripheral tissues such as liver (Nagatsu *et al.*, 1997). Consequently, intravenous TH gene therapy with the PIL technology and a widely expressed SV40 promoter led to ectopic gene expression in rat liver (Zhang *et al.*, 2003a). Ectopic expression of an exogenous TH gene under the influence of a widely expressed promoter is expected in any tissue that also expresses the GTPCH gene.

Ectopic TH gene expression can be reduced with the combined use of the PIL gene targeting technology and brain-specific promoters. The peripheral expression of a β-galactosidase expression plasmid was eliminated when the transgene was driven by the 2 kb of the 5′-flanking sequence (FS) of the human glial fibrillary acidic protein (GFAP) gene (Shi *et al.*, 2001a). Genes under the influence of the GFAP promoter are selectively expressed in brain, although the GFAP promoter enables gene expression in both neurons and astrocytes in brain (Kaneko and Sueoka, 1993; Galou *et al.*, 1994). Because astrocytes do not express GTPCH or the biopterin cofactor (Nagatsu *et al.*, 1997; Hwang *et al.*, 1998), it is possible the use of the GFAP promoter, in lieu of the SV40 promoter, may enable neuronal expression of the TH gene in brain, yet eliminate ectopic TH gene expression in nonbrain organs such as liver. Therefore, the purpose of the present studies was to produce a TH-expression plasmid under the influence of the GFAP promoter, and to treat 6-OHDA–lesioned rats with intravenous administration of the GFAP-TH plasmid DNA encapsulated in antitransferrin receptor monoclonal antibody (TfRmAb)-targeted PILs.

MATERIALS AND METHODS

Materials

POPC (1-palmitoyl-2-oleoyl-*sn*-glycerol-3-phosphocholine) and DDAB (dimethyldioctadecylammoniumbromide) were purchased from Avanti-Polar Lipids Inc. (Alabaster, AL). Distearoylphosphatidylethanolamine (DSPE)-PEG^{2000} was obtained from Shearwater Polymers (Huntsville, AL), where PEG^{2000} is 2000-Da polyethyleneglycol. DSPE-PEG^{2000}-maleimide (MAL) was custom synthesized by Shearwater Polymers. [α-^{32}P]dCTP (3000 Ci/mmol) and [3,5-^{3}H]-L-tyrosine (51.5 Ci/mmol) were from NEN Life Science Product Inc. (Boston, MA). N-succinimidyl[2,3-^{3}H]propionate (^{3}H-NSP, 101 Ci/mmol) and protein G Sepharose CL-4B were purchased from Amersham-Pharmacia Biotech (Arlington Heights, IL). The nick translation system was from Life Technologies Inc. (Rockville, MA). The 6-OHDA, apomorphine, pargyline, catalase, (6R)-5,6,7,8-tetrahydrobiopterin (BH4), β-NADPH, L-tyrosine and charcoal were purchased from Sigma (St. Louis, MO); 2-iminothiolane (Traut's reagent) and bicinchoninic acid (BCA) protein assay reagents were obtained from Pierce Chemical Co. (Rockford, IL). Mouse myeloma ascites containing mouse IgG2a (mIgG2a) isotype control was from the Cappel Division of ICN Pharmaceuticals (Aurora, OH). The TfRmAb used in this study is the murine OX26 mAb to the rat TfR, which is a mouse IgG2a. The anti-insulin receptor mAb used for gene targeting to human U87 glioma cells is the murine 83-14 mAb to the human insulin receptor (HIR). The TfRmAb, the HIRmAb, or the mIgG2a were individually purified with protein G affinity chromatography from hybridoma generated ascites, where HIRmAb is a murine mAb to the HIR. The pGfap-cLac plasmid (Brenner *et al.*, 1994; Segovia *et al.*, 1998) was provided by Dr. Jose Segovia, Centro de Investigacion y de Estudios Avanzados (San Pedro Zacatenco, Mexico). A mouse monoclonal antibody against GFAP (clone G-A-5), a mouse monoclonal anti-TH antibody, mouse IgG1 isotype control, and control rabbit IgG were purchased from Sigma. A mouse monoclonal antibody (MAB377) against neuronal nuclei (NeuN), a mouse mAb (MAB5262) antineurofilament 200-kd antibody, and an affinity purified rabbit polyclonal antibody (AB152) against TH were obtained from Chemicon (Temecula, CA). Secondary antibodies used were Alexa fluor 488 donkey anti-mouse IgG and Alexa fluor 594 donkey anti-rabbit IgG (Molecular Probes, Eugene, OR).

Construction of TH expression plasmid with GFAP promoter

The approximately 2-kb human GFAP promoter was obtained by polymerase chain reaction (PCR) amplification using the pGfap-cLac plasmid. Custom oliogdeoxynucleotide primers were designed to amplify nucleotides 1-2210 of the human GFAP promoter region (GenBank accession # M67446). The forward, ATGGCTAGCGAGCTCCCACCTCCCTCTCT G, and reverse, ATGAAGCTTGCGAGCAGCGGAGGTG ATGCG, primers contain *Nhe*I and *Hind*III sites, respectively, for directional cloning (Fig. 1A). In addition, these primers have three unrelated nucleotides on the 5′ end to facilitate restriction endonuclease digestion. Custom primers were obtained from Biosource International (Camarillo, CA). PCR amplification of the GFAP promoter was performed using 50 ng plasmid DNA

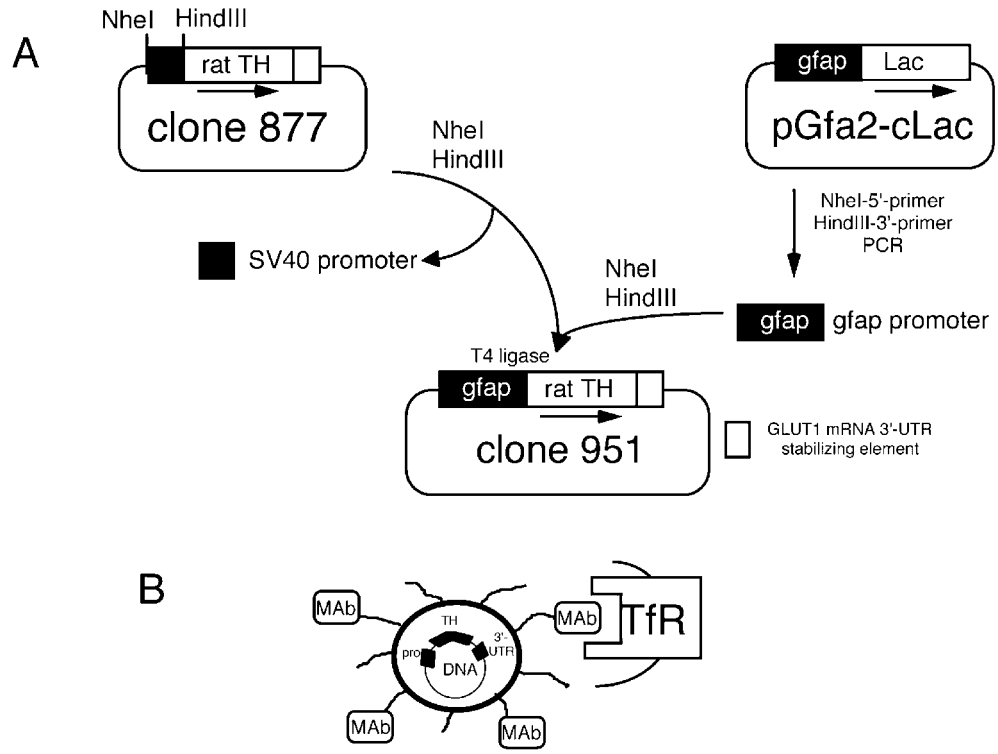

FIG. 1. **A**: Production of clone 951 from clone 877 and pGfa2-cLac. Clone 877 is an SV40 promoter (pro) rat tyrosine hydroxylase (TH) expression plasmid derived from pGL2 as described previously (Zhang *et al.*, 2003a). The pGfa2-cLac is a human glial fibrillary acidic protein (GFAP) promoter driven β-galactosidase expression plasmid (Brenner *et al.*, 1994; Segovia *et al.*, 1998). The rat SV promoter was released from clone 877 with *Nhe*I and *Hind*III, in parallel with the polymerase chain reaction (PCR) amplification of the GFAP promoter with an *Nhe*I 5′-primer and an *Hind*III 3′-primer. The SV40 promoter of clone 877 was replaced with the GFAP promoter to produce clone 951. Both clones 877 and 951 contain a 200 nucleotide sequence within the 3′ untranslated region (UTR), which is taken from the 3′-UTR of the bovine GLUT1 glucose transporter mRNA, and that optimizes gene expression via mRNA stabilization (Boado and Pardridge, 1998; Zhang *et al.*, 2003a). **B**: Diagram of a super-coiled TH expression plasmid encapsulated in an 85-nm pegylated immunoliposome (PIL) targeted to the rat transferrin receptor (TfR) with the OX26 murine monoclonal antibody (mAb).

in a total volume of 50 μl Pfu DNA polymerase buffer (Stratagene, La Jolla, CA). The reaction also contained 0.4 μM forward and reverse primers, 0.2 mM deoxynucleotide triphosphates (dNTPs), and 1 μl is equal to 2.5 U Pfu-Turbo DNA polymerase (Stratagene). The sample was denatured for 30 sec at 95°C, and amplified in 17 cycles of 30 sec at 95°C, 60 sec at 55°C (annealing), and 6 min at 68°C (extension). PCR products were resolved by agarose gel electrophoresis and a major band of approximately 2 kb corresponding to the human GFAP promoter was seen. PCR products were purified using the Qiagen PCR purification kit (Valencia, CA), and double-digested with *Nhe*I and *Hind*III for subcloning in the TH expression vector as described below.

The expression plasmid containing the complete open reading frame of the rat TH driven by the SV40 promoter is derived from the pGL2 plasmid and is designated clone 877 as described previously (Zhang *et al.*, 2003a). The SV40 promoter was deleted from clone 877 by double-digestion with *Nhe*I and *Hind*III, which cleaved at sites located upstream and downstream of the promoter, respectively (Fig. 1A). The approximately 6.0-kb rTH-vector backbone fragment was purified by gel electrophoresis followed by centrifugation with a Spin X filter unit. The approximately 2-kb GFAP promoter was prepared as described above and subcloned at the same restriction endonuclease sites to form a GFAP-TH–expression plasmid named clone 951 (Fig. 1A). Positive clones were identified by restriction endonuclease mapping (i.e., *Nhe*I and *Hind*III), and its identity confirmed by DNA sequencing using the pGL2 sequencing primer 1 (Promega, Madison, WI).

Synthesis of PILs

The GFAP-TH (clone 951) plasmid DNA or the SV40-TH (clone 877) plasmid DNA was encapsulated in PILs as described previously (Shi *et al.*, 2001a; Zhang *et al.*, 2002a, 2003a). The liposome is 85–100 nm in diameter and the surface of the liposome is conjugated with several thousand strands of 2000-Da polyethyleneglycol (PEG). The tips of approximately 1–2% of the PEG strands are conjugated with either the mouse OX26 mAb to the rat TfR or the mouse 83-14 mAb to the HIR or mIgG2a (Fig. 1B). The mIgG2a is the isotype control for either the murine OX26 or 83-14 mAb. Any plasmid DNA not encapsulated in the interior of the liposome is quantitatively removed by exhaustive nuclease treatment (Shi *et al.*,

2000). In a typical synthesis, 36–40% of the initial plasmid DNA (250 μg) was encapsulated within 20 μmol of lipid, and each liposome had a range of 69–73 mAb molecules conjugated to the PEG strands. The PIL conjugated with the OX26 TfRmAb is designated TfRmAb-PIL; the PIL conjugated with the murine 83-14 HIRmAb is designated the HIRmAb-PIL; and the PIL conjugated with the mouse IgG2a isotype control antibody is designated mIgG2a-PIL. The targeting mAbs are species specific and the HIRmAb-PIL is used for gene delivery to human cells and the TfRmAb-PIL is used for gene targeting to rat cells (Zhang *et al.*, 2003b).

TH gene expression in cultured U87 human glioma cells

Human U87 glioma cells were plated on 60-mm collagen-treated dishes with MEM containing 10% fetal bovine serum (FBS). When the cells reached 60% confluence, the medium was removed by aspiration, and 6 ml of fresh medium containing 10% FBS was added to the cells, followed by the addition of 167 μl of the HIRmAb-PIL carrying the 951 DNA (4 μg of plasmid DNA per dish). The cells were incubated for 2, 4, or 6 days, with three dishes at each time point, for measurement of TH enzyme activity. The cells were washed three times with cold wash buffer (5 m*M* potassium phosphate buffer), and then 400 μl of sonication buffer (wash buffer with 0.2 % Triton X-100) was added to each dish. The cells were collected, and after a short vortex, the cells were sonicated for 30 sec with a Branson Sonifier Cell Disruptor Model 185 (Branson Ultrasonics Corp., Danbury, CT). The cell homogenate was centrifuged at 10,000*g* for 10 min at 4°C. TH activity was measured with 200 μl of the supernatant as described previously (Zhang *et al.*, 2003a).

6-OHDA model

Adult male Sprague-Dawley rats (supplied by Harlan Breeders, Indianapolis, IN) weighing 200–230 g were anesthetized with ketamine (100 mg/kg) and xylazine (10 mg/kg) intraperitoneally. Animals received unilateral 6-OHDA injections into the right medial forebrain bundle as described previously (Zhang *et al.*, 2003a). Each animal received pargyline 30–60 min prior to surgery (50 mg/kg in normal saline intraperitoneally). After pargyline administration, 4 μl of 2 μg/μl of 6-OHDA (freshly prepared in 0.2 μg/μl ascorbic acid) was injected over a 4-min period using a 10-μl Hamilton syringe with the following stereotaxic coordinates: 4.8 mm posterior to bregma, 1.1 mm lateral to bregma, and 8.0 mm below the dura. The syringe needle was left in place for 2 min after the injection to allow for diffusion of the toxin. Three weeks after the lesion, rats were tested for apomorphine-induced contralateral turning using 0.5 mg/kg of apomorphine injected intraperitoneally. Full (360°), contralateral rotations only were counted over 20 min starting 5 min after apomorphine administration. Those rats turning more than 160 times in 20 min, or more than 8 rotations per min (RPM), were designated as having been successfully lesioned, and were treated 1 week later with TH gene therapy. In one series of experiments, the lesioned apormorphine-responsive rats were divided into two groups. The control group in which rats received 10 μg per rat of clone 951 DNA encapsulated in mIgG2a-PIL or the treatment group in which rats received 10 μg per rat of clone 951 DNA encapsulated in TfRmAb-PIL. The PIL was administered via the femoral vein; 3 days later the rats were tested for apomorphine-induced rotation behavior and then sacrificed. In each group, half of the rats were used for TH immunocytochemistry, and the other half were used for confocal microscopy. In a different series of experiments, the two groups of lesioned apomorphine-responsive rats were treated with either 10 μg per rat of clone 877 DNA encapsulated in TfRmAb-PIL or 10 μg per rat of clone 951 DNA encapsulated in TfRmAb-PIL. These animals were sacrificed 3 days later for measurement of organ TH activity by a radioenzymatic assay described previously (Zhang *et al.*, 2003a).

TH assay

The TH activity assay was performed as described previously (Zhang *et al.*, 2003a), and measures the conversion of L-[3,5-^{3}H]tyrosine to both [^{3}H]-H_2O and [^{3}H]-L-DOPA in a 1:1 stoichiometric relationship; the two metabolites are separated by charcoal, which selectively binds the amino acid. For the TH assay in rat organs, liver, heart, lung, kidney, frontal cortex, and the dorsal striatum in both lesioned (ipsilateral) and nonlesioned (contralateral) sides of brain were frozen in dry ice. The counts per minute were converted to picomoles of L-DOPA on the basis of the [^{3}H]tyrosine specific activity, and the results were expressed as picomoles of L-DOPA per hour per milligram of protein.

Immunocytochemistry and confocal microscopy

The brains were removed and placed into coronal or sagittal rat brain matrices for immunocytochemistry and confocal microscopy, respectively. For immuncytochemistry, frozen sections were prepared as described previously (Zhang *et al.*, 2003a). For confocal microscopy, brain tissue was then immersion fixed in 4% paraformaldehyde in 0.01 *M* phosphate-buffered water (PBW), pH 7.4 and stored overnight at 4°C. After brief washing in 0.01 *M* PBW the brain slabs were cryoprotected in 30% sucrose in 0.1 *M* PBW, pH 7.4 for additional 12 hr at 4°C. After brief washing in 0.01 *M* PBW, the brains were placed in cryomolds filled with OCT embedding compound and rapidly frozen in powdered dry ice.

TH immunocytochemistry was performed on coronal sections by the avidin-biotin complex (ABC) immunoperoxidase method (Vector Laboratories, Burlingame, CA). Frozen sections (20 μm) were incubated in either mouse anti-TH mAb (1 μg/ml) or mouse IgG1 isotype control (1 μg/ml) overnight at 4°C. The sections were incubated in biotinylated horse anti-mouse IgG (35 μg/ml) for 30 min. After development in 3-amino-9-ethylcarbazole (AEC), sections were scanned with a UMAX PowerLook III flatbed scanner (UMAX Technologies, Dallas, TX) with transparency adapter, and then cover-slipped.

Coronal sections (20 μm) through the level of the substantia nigra, pars reticulata were cut from both hemispheres for confocal microscopy. After 30 min drying at room temperature (20°C) slides were washed and permeabilized using 0.01 *M* PBS, pH 7.4 with 0.1% Triton-X 100 (PBST). Blocking for 1–2 hr was performed with 10% preimmune donkey serum in 0.01 *M* PBST at 20°C. Primary antibodies and all control studies with isotype IgG were used as follows: 15 μg/ml mouse mono-

clonal anti-NeuN antibody (Liu *et al.*, 1998), 10 μg/ml mouse monoclonal anti-GFAP antibody (Debus *et al.*, 1983), 2.5 μg/ml mouse monoclonal anti-TH antibody, 1 μg/ml mouse monoclonal antineurofilament 200-kd antibody (Anderton *et al.*, 1982), and 0.4 μg/ml affinity purified rabbit polyclonal anti-TH antibody (Horger *et al.*, 1998). Sections were incubated overnight at 4°C with primary antibodies diluted in 3% bovine albumin in 0.01 *M* PBST. The secondary antibody, 488 donkey anti-mouse IgG (fluorescein-labeled) and 594 donkey anti-mouse IgG (rhodamine-labeled) were used at a concentration of 5 μg/ml diluted in 0.01 *M* PBST. After extensive washing in 0.01 *M* PBS all specimens were cover-slipped and slides stored at 4°C light protected.

Confocal imaging was performed employing a Zeiss LSM 5 PASCAL confocal microscope with dual argon and helium/neon lasers equipped with Zeiss LSM software for image reconstruction (LSM 5 PASCAL, version 3.2, Jena, Germany). All sections were scanned in multitrack mode to avoid overlap of the fluorescein (excitation at 488 nm) and rhodamine (excitation at 568 nm) channels. For acquisition of three-dimensional images, up to 20 serial images with a slice thickness between 1.6–3.7 μm were used. Pinhole size for each channel was maintained as small as possible as to ensure sufficient signal-to-noise ratio and highest spatial resolution (126–145 nm). Line density ranged from 0.19–0.45 μm using these settings. Detector gain and amplifier offset were optimized to reduce artificial background for each image. No amplifier gain was used. Three-dimensional image slices were scanned with a 1024 × 1024 resolution. All scanning parameters were kept constant. Image analysis was performed for each single image slice also in the three-dimensional data stacks. Three-dimensional images were reconstructed by projecting six consecutive planar views. To ensure a more objective measure of overlap, a colocalization feature was applied that color-codes only regions in which both channels overlap at a threshold intensity level. Intensity of the fluorescent signal was measured in an arbitrary scale ranging from 0 (no signal) to 250 (highest signal) with respect to the individual image intensity profile. The intensity level was defined individually for each dataset using the integrated colocalization software and an overlap coefficient of 1 (Manders *et al.*, 1993).

Real-time PCR

The abundance of the rat TH and the control 4F2hc transcripts were determined by reverse transcriptase (RT) and real-time PCR of total RNA isolated from brain and liver tissues of saline- and PIL-injected animals. Total RNA was obtained using the RNAqueous-4PCR isolation kit (Ambion, Houston, TX). Total RNA was used to synthesize cDNA by RT with oligo dT priming and the SuperScript system for RT-PCR (Invitrogen, San Diego, CA). The real-time PCR was performed in an iCycler equipped with the optical module (BioRad, Hercules, CA), per the manufacturer's instructions using the BioRad iQ SYBR green supermix. PCR reaction was run using a modified three-step amplification protocol followed by a melting curve to confirm the production of a single PCR product. The threshold cycle number (Ct) was calculated for rat TH and rat 4Fhc using the iCycler BioRad software. The 4F2hc gene encodes the heavy chain (hc) of multiple amino acid transporters and is a common housekeeping gene that is expressed in both brain and liver (Boado *et al.*, 1999). PCR primers were designed using the Beacon Designer (Palo Alto, CA) software, and obtained from Biosource International (Camarillo, CA). The TH PCR primers (forward 5′-GCTGTCACGTCCCCAAGGTT-3′ and reverse 5′-CAGCCCGAGACAAGGAGGAG-3′) amplify a region of 220 nucleotides (nt) located at nt 449–668 of the rat TH cDNA (accession # NM_012470). The 4F2hc PCR primers (forward 5′-CCAAGGAGGAGCTATTGAAGGTA-3′ and reverse 5′-CGCCCGAACGATGATAACCA-3′) target nt 369–496 of the rat 4F2hc cDNA (accession # AB015433) to produce a DNA fragment of 128 nt.

Statistical analyses

Statistically significant differences in different treatment groups were determined by analysis of variance (ANOVA) with Bonferroni correction using program 7D of the BMDP Statistical Software package developed by the UCLA Biomedical Computing Series. A p value < 0.05 was considered significant.

RESULTS

GFAP-TH–expression plasmid activity in U87 human glioma cells targeted with the HIRmAb-PIL

Human U87 cells express GFAP (Mandil *et al.*, 2001) and also support TH gene expression in cell culture (Zhang *et al.*, 2003a). Therefore, the biologic activity of the GFAP-TH–expression plasmid (clone 951) was measured in cultured U87 cells at 2, 4, and 6 days after the single application at day 0 of the plasmid DNA encapsulated in HIRmAb-targeted PILs. Clone 951 is well expressed, and the level of TH enzyme activity in the cells is comparable whether the TH gene is under the influence of either the SV40 promoter or the GFAP promoter (Table 1).

TH enzyme activity in brain and peripheral organs in lesioned rats treated with either the SV40-TH– or the GFAP-TH–expression plasmid targeted with the TfRmAb-PIL

The intracerebral injection of 6-OHDA caused a 98% reduction in TH enzyme activity in the ipsilateral striatum compared to the contralateral or non-lesioned striatum (Table 2, saline treated rats). The TH enzyme activity in the cortex ipsilateral or contralateral to the lesion was no different, and was 98% reduced compared to the TH activity in the contralateral striatum (Table 2). The 6-OHDA–lesioned, apomorphine-responsive rats were treated with SV40-TH gene therapy using clone 877 plasmid DNA encapsulated in the TfRmAb-targeted PIL. At 3 days after the single intravenous administration of 10 μg per rat of the clone 877 plasmid DNA, the TH activity in the ipsilateral or lesioned striatum was normalized and was not significantly different from the TH enzyme activity in the contralateral striatum (Table 2). SV40-TH gene therapy caused no increase in TH in the cortex in brain, but did cause a 10-fold increase in TH enzyme activity in the liver (Table 2). In contrast, there was no increase in hepatic TH enzyme activity after intravenous administration of the GFAP-TH (clone 951) en-

Table 1. TH Activity in Cultured U87 Glioma Cells After Delivery of Either SV40 Promoter (Clone 877) or GFAP Promoter (Clone 951) TH Expression Plasmid Encapsulated in HIRmAb-Targeted PIL

	TH activity (pmol L-Dopa/hour/mg$_p$)	
Days of incubation	*Clone 877*	*clone 951*
2	214 ± 14	231 ± 10
4	1458 ± 99	1576 ± 33
6	177 ± 10	311 ± 22

Mean ± SE (n = 3 dishes per time point). Clone 877 data from Zhang *et al.* (2003a).

SE, standard error; TH, tyrosine hydroxylase; GFAP, glial fibrillary acidic protein; PIL, pegylated immunoliposomes.

capsulated in the TfRmAb-targeted PIL (Table 2). However, treatment with the GFAP-TH gene, similar to the SV40-TH gene, caused complete normalization of the TH enzyme activity in the ipsilateral striatum of the 6-OHDA–lesioned apomorphine-responsive rats (Table 2).

Reversal of motor impairment after GFAP-TH gene therapy

The lesioned rats that responded to apomorphine were separated into 2 groups and treated with clone 951 plasmid DNA (10 μg/rat) encapsulated in either mIgG2a-targeted PILs or TfRmAb-targeted PILs, and apomorphine-induced rotation behavior was measured in individual rats before and 3 days after intravenous gene therapy (Figure 2A,B). The apomorphine-induced rotation (mean RPM of 4 ± 3) in the rats treated with clone 951 encapsulated in the TfRmAb-PIL was reduced 82% compared to the apomorphine-induced roation (mean RPM of 22 ± 3) in the rats treated with clone 951 encapsulated in the mIgG2a-PIL (Figure 2C).

Neuronal expression of immunoreactive TH following GFAP-TH gene therapy

TH immunocytochemistry of coronal sections of rat brain is shown in Figure 3. There was complete normalization of the immunoreactive TH in the striatum of 6-OHDA–lesioned apomorphine-responsive rats at 3 days after a single intravenous injection of clone 951 plasmid DNA (10 μg per rat) encapsulated in the TfRmAb-targeted PIL (Fig. 3A, 3B, and 3C). However, there was minimal immunoreactive TH detected in the striatum of 6-OHDA–lesioned apomorphine-responsive rats at 3 days after a single intravenous injection of clone 951 plasmid DNA (10 μg per rat) encapsulated in the mIgG2a-targeted PIL (Fig. 3D, 3E, and 3F). The marked reduction in immunoreactive TH in the striatum of these rats correlates with the 98% reduction in striatal TH enzyme activity in the lesioned animals (Table 2).

The cellular origin of TH gene expression in the brains of lesioned rats treated with the clone 951 DNA encapsulated in TfRmAb-PILs or mIgG-PILs was examined by confocal microscopy (Fig. 4). The TH gene was selectively expressed in nerve terminals in the striatum on the side contralateral to the lesion with no overlap with NeuN immunoreactive neuronal cell bodies (Fig. 4A). Virtually all of the nerve terminals were negative for TH in the ipsilateral striatum of lesioned rats treated with clone 951 encapsulated in the mIgG2a-PIL (Fig. 4B). Conversely, the density of TH reactive nerve terminals in the ipsilateral striatum of lesioned rats treated with the clone 951 DNA encapsulated in the TfRmAb-targeted PIL was no different than in the contralateral, non-lesioned striatum (Fig. 4A and 4C). The nerve terminals in the contralateral striatum that were immunopositive for TH were generally immunonegative for the 200-kDa neurofilament protein (Fig. 4D), and there was preser-

Table 2. Tyrosine Hydroxylase in Brain and Peripheral Organs in the Rat Three Days After Intravenous Injection of Gene Therapy

Organs	*Saline (pmol/hr/mg$_p$)*	*TfRmAb-PIL/877 (pmol/hr/mg$_p$)*	*TfRmAb-PIL/951 (pmol/hr/mg$_p$)*
Ipsilateral striatum	128 ± 27	5177 ± 446*	5536 ± 395*
Contralateral striatum	6445 ± 523	5832 ± 391	5713 ± 577
Ipsilateral cortex	176 ± 30	132 ± 16	184 ± 38
Contralateral cortex	150 ± 36	150 ± 24	135 ± 25
Heart	29 ± 3	45 ± 8	31 ± 3
Liver	13 ± 2	130 ± 28*	18 ± 6
Lung	42 ± 13	74 ± 22	30 ± 6
Kidney	24 ± 2	35 ± 5	31 ± 8

*$p < 0.01$ difference from saline group (ANOVA with Bonferroni correction; n = 4 rats per group). Rats were lesioned with intracerebral injections of 6-hydroxydopamine; 3 weeks after toxin injection the rats were tested for apomorphine-induced rotation behavior; those rats resting positively to apormorphine were selected for gene therapy, which was administered intravenously 4 weeks after toxin administration; all animals were euthanized 3 days after gene administration.

ANOVA, analysis of variance.

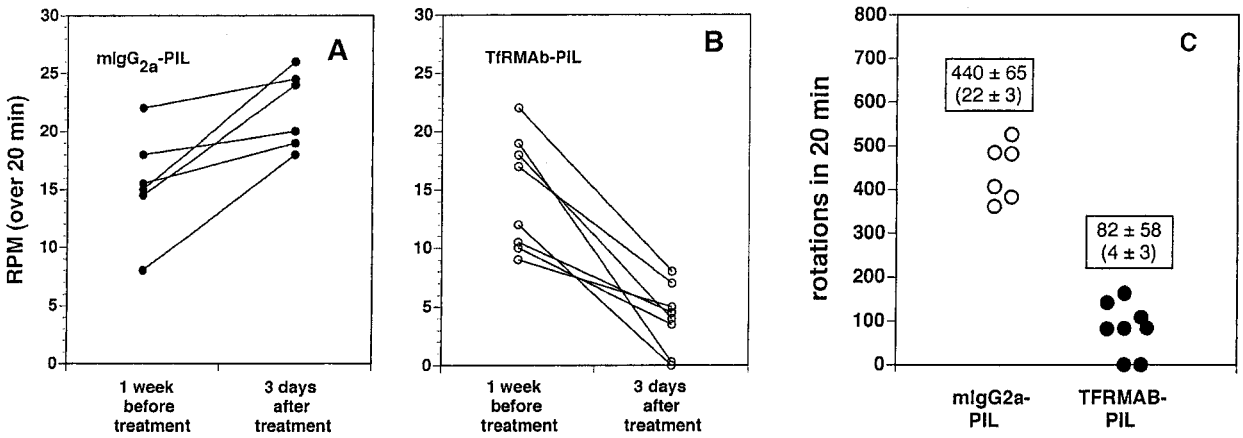

FIG. 2. **A**: Apomorphine-induced rotations per minute (RPM) over a 20-min period measured in individual rats at 1 week before treatment and at 3 days after a single intravenous injection of 10 μg per rat of clone 951 plasmid DNA encapsulated in a pegylated immunoliposome (PIL) targeted with the mouse IgG2a isotype control antibody. **B**: Apomorphine-induced RPM over a 20-min period measured in individual rats at 1 week before treatment and at 3 days after a single intravenous injection of 10 μg per rat of clone 951 plasmid DNA encapsulated in a PIL targeted with the TfRmAb. **C**: Comparison of the total rotations in the two groups at 3 days after treatment. The average RPM is 22 ± 3 and 4 ± 3 (mean ± standard deviation [SD]) in animals treated with the mIgG2a-PIL and the TfRmAb-PIL, respectively. The difference in rotation between the two groups is significant at the $p < 0.005$ level.

vation of the 200-kDa neurofilament fibers in the ipsilateral striatum of lesioned rats treated with the clone 951 encapsulated in the mIgG2a-PIL (Fig. 4E). The pattern of nerve terminals in the ipsilateral striatum of lesioned rats treated with clone 951 encapsulated in the TfRmAb-PIL was comparable to that in the contralateral striatum (Fig. 4D and 4F).

The parallel expression of immunoreactive TH, GFAP, and NeuN in the striatum and substantia nigra is shown in Figure 4 for regions of the brain ipsilateral to the lesion and in rats treated with the clone 951 plasmid DNA and encapuslated in the TfRmAb-PIL. For the striatum, separate views are shown for GFAP and TH immunostaining in Figure 4G and 4H. The overlap image in Figure 4I indicates there is no coexpression of the TH in the GFAP-positive astrocytes. Parallel immunostaining for TH and NeuN in the substantia nigra shows there is expression of immunoreactive TH in NeuN immunoreactive neuronal cell bodies (Fig. 4J, 4K, and 4L).

Measurement of TH gene expression by real-time PCR

The measurement of immunoreactive TH (Figs. 3 and 4) and TH enzyme activity (Tables 1 and 2) were corroborated by assays of TH mRNA using real-time PCR (Table 3). Rats were treated with either saline or 10 μg per rat of clone 877 plasmid

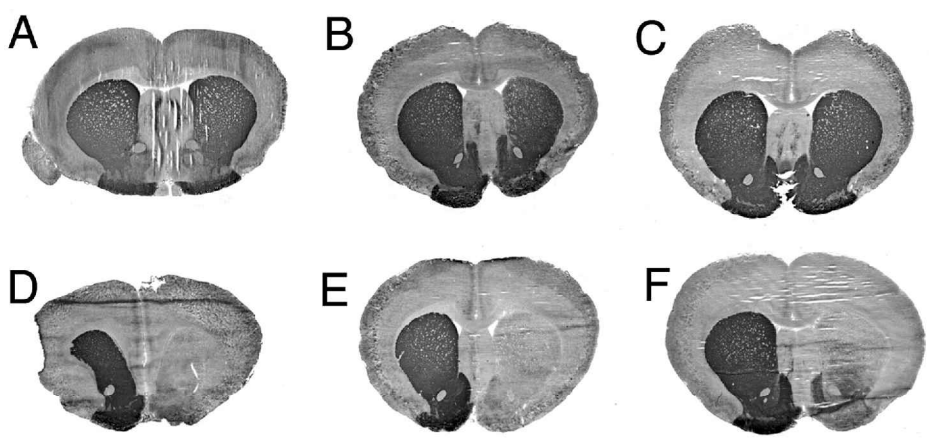

FIG. 3. Tyrosine hydroxylase immunocytochemistry of rat brain removed 72 hr after a single intravenous injection of 10 μg per rat of clone 951 plasmid DNA encapsulated in pegylated immunoliposome (PIL) targeted with either the TfRmAb (**A**, **B**, **C**) or with the mouse IgG2a isotype control (**D**, **E**, **F**). Coronal sections are shown for three different rats from each of the two treatment groups. The 6-hydroxydopamine was injected in the medial forebrain bundle of the right hemisphere, which corresponds to right side of the figure. Sections are not counterstained.

DNA encapsulated in TfRmAb-targeted PILs, and 3 days later animals were sacrificed for isolation of RNA from either cortex or liver. There was no significant increase of TH mRNA in brain cortex, although the Ct was increased from 29.0 ± 2.3 to 34.6 ± 1.3 in the livers of rats treated with TH-PIL gene therapy; this corresponds to more than a 10-fold increase in liver TH mRNA. The hepatic mRNA levels of a housekeeping gene, 4F2hc, were also measured and TH PIL gene therapy caused no change in 4F2hc mRNA concentrations in liver (Table 3).

DISCUSSION

The results of these studies are consistent with the following conclusions. First, the ectopic expression of the TH gene in peripheral tissues such as liver after intravenous gene therapy is eliminated when the TH gene is under the influence of a brain specific promoter, such as the GFAP promoter (Table 2). Second, intravenous GFAP-TH gene therapy with clone 951 (Fig. 1A) and the PIL gene targeting technology (Fig. 1B) causes a normalization of striatal TH in the 6-OHDA–lesioned rat, but this is associated with no change in cortical TH (Table 2, Fig. 3). Third, the normalization of striatal TH with intravenous GFAP-TH gene therapy is associated with an 82% reduction in apomorphine-induced rotation behavior (Fig. 2). Fourth, the GFAP-TH gene is selectively expressed in neurons, not astrocytes, of the nigral-striatal tract (Fig. 4).

The stability of the TH enzyme is linked to the availability of the biopterin cofactor, and the expression of the TH enzyme is found only in those regions of brain that express GTPCH, the rate-limiting enzyme in biopterin biosynthesis (Nagatsu *et al.*, 1995; Hwang *et al.*, 1998; Shimoji *et al.*, 1999). However, GTPCH is also expressed in some peripheral organs such as liver (Nagatsu *et al.*, 1997), which supports TH gene expression after intravenous gene therapy with an exogenous TH gene under the influence of a widely expressed promoter, such as the SV40 promoter. There is a 10-fold increase in hepatic TH activity in rats treated with clone 877, the SV40-TH, which is encapsulated in the TfRmAb-targeted PIL (Table 2). However, the ectopic expression of the TH gene in liver is eliminated with the use of a brain-specific promoter, such as the GFAP promoter (Table 2). These results parallel prior observations on β-galactosidase reporter gene expression. If the β-galactosidase gene was under the influence of the SV40 promoter, and was administered intravenously encapsulated in a TfRmAb-targeted PIL, then the gene was expressed in both brain and TfRmAb-positive peripheral organs such as liver (Shi *et al.*, 2001a,b). However, β-galactosidase gene expression in peripheral organs of the mouse was eliminated if the gene was under the influence of the GFAP promoter (Shi *et al.*, 2001a). Similarly, in the adult rhesus monkey, ocular-specific gene expression is observed after the intravenous injection of HIRmAb-targeted PILs carrying a trans-gene driven by the rhodopsin promoter (Zhang *et al.*, 2003d).

The TfRmAb-targeted PIL delivers the TH gene to hepatocytes because the hepatic microcirculation is a sinusoidal network of highly porous capillaries, which allows free access of the 85-nm PIL to the extravascular space of liver. Conversely, peripheral organs such as heart or kidney are perfused by continuous endothelial barriers that block the egress into the extravascular compartment of the circulating PIL. The endothelium of most peripheral organs do not express sufficient amounts of TfR to enable transcapillary transport of the PIL. Consequently, there is no gene expression in these organs for either TH (Table 2) or for reporter genes such as β-galactosidase or luciferase (Shi *et al.*, 2000, 2001a,b). Unlike capillaries in peripheral tissues, the capillaries of the brain express high levels of TfR (Jefferies *et al.*, 1984; Pardridge *et al.*, 1987), which can be a conduit for the delivery of genes to rodent brain (Shi *et al.*, 2001a,b). The PIL targets the TfR, which causes receptor-mediated transcytosis across the BBB followed by receptor-mediated endocytosis across the neuronal cell membrane. In addition, PILs target the nuclear membrane and the majority of intracellular DNA is confined to the nuclear compartment at 24 hr after administration (Zhang *et al.*, 2002a).

The GFAP-TH gene is expressed in neurons in the nigral-striatal tract after the intravenous administration of the clone 951 DNA encapsulated in the TfRmAb-targeted PIL, as demonstrated by confocal microscopy (Fig. 4). Conversely, neuronal TH expression is not observed in the cortex based on either measurement of TH enzyme activity (Table 2) or immuncytochemistry (Fig. 3). In addition, the confocal mi-

FIG. 4. Confocal microscopy of striatum in 6-OHDA-lesioned rats sacrificed at 3 days after intravenous injection of clone 951 plasmid DNA encapsulated in pegylated immunoliposomes (PILs) targeted either with mouse IgG2a (**B** and **E**) or with the TfRmAb (**A**, **C**, **D**, and **F**). Panels A and D are from the striatum contralateral to toxin injection, and panels B, C, E, and F are from the striatum ipsilateral to toxin injection. Panels A–C show striatum colabeled with a mouse monoclonal antibody to neuronal nuclei (NeuN) (green) and a rabbit polyclonal antibody to tyrosine hydroxylase (TH; red). Panels D–F show striatum colabeled with a mouse monoclonal antibody to the 200-kDa neurofilament protein (green) and a rabbit polyclonal antibody to TH (red). All images were taken with a 40× objective, and the magnification bar in panel A is 20 μm. All images are three-dimensional projection views of multiple planar images. The yellow color is an artifact from the three-dimensional projection as there was no overlap observed in the single planar views. Confocal microscopy of striatum (**G–I**) and substantia nigra (**J–L**) ipsilateral to the 6-OHDA lesion in rats sacrificed at 3 days after intravenous injection of clone 951 plasmid DNA encapsulated in PILs targeted with the TfRmAb. Panels G and J show immune staining (green channel) with monoclonal antibodies to glial fibrillary acidic protein (GFAP) and neuronal nuclei (NeuN), respectively. Panels H and K show immune staining (red channel) with a rabbit polyclonal antibody to TH. The overlap image of TH and GFAP in striatum is shown in panel I; the overlap image of TH and NeuN in substantia nigra is shown in panel L. Panels G–L were photographed with a 40× objective, whereas the size of panels J–L was increased with a 2× zoom. The inset of panel L is a 100× oil immersion view of colabeling of TH (red), neuronal nuclei (NeuN) (green), and the overlap (yellow) in a neuron in the substantia nigra. The magnification bars in panels G and J are 20 and 10 μm, respectively. All images are three-dimensional projection views of multiple planar images.

croscopy shows that neuronal tracts immunopositive for the 200-kDa neurofilament protein do not express TH in the striatum of the treated rat (Fig. 4F). Neuronal expression of the TH transgene in the nigro-striatal tract is also indicated by the 82% reduction in apormorphine-induced rotation behavior following intravenous administration of the GFAP-TH in the TfRmAb-PIL (Fig. 2). The ability of intravenous TH gene therapy to cause normalization of nigral-striatal TH expression in the 6-

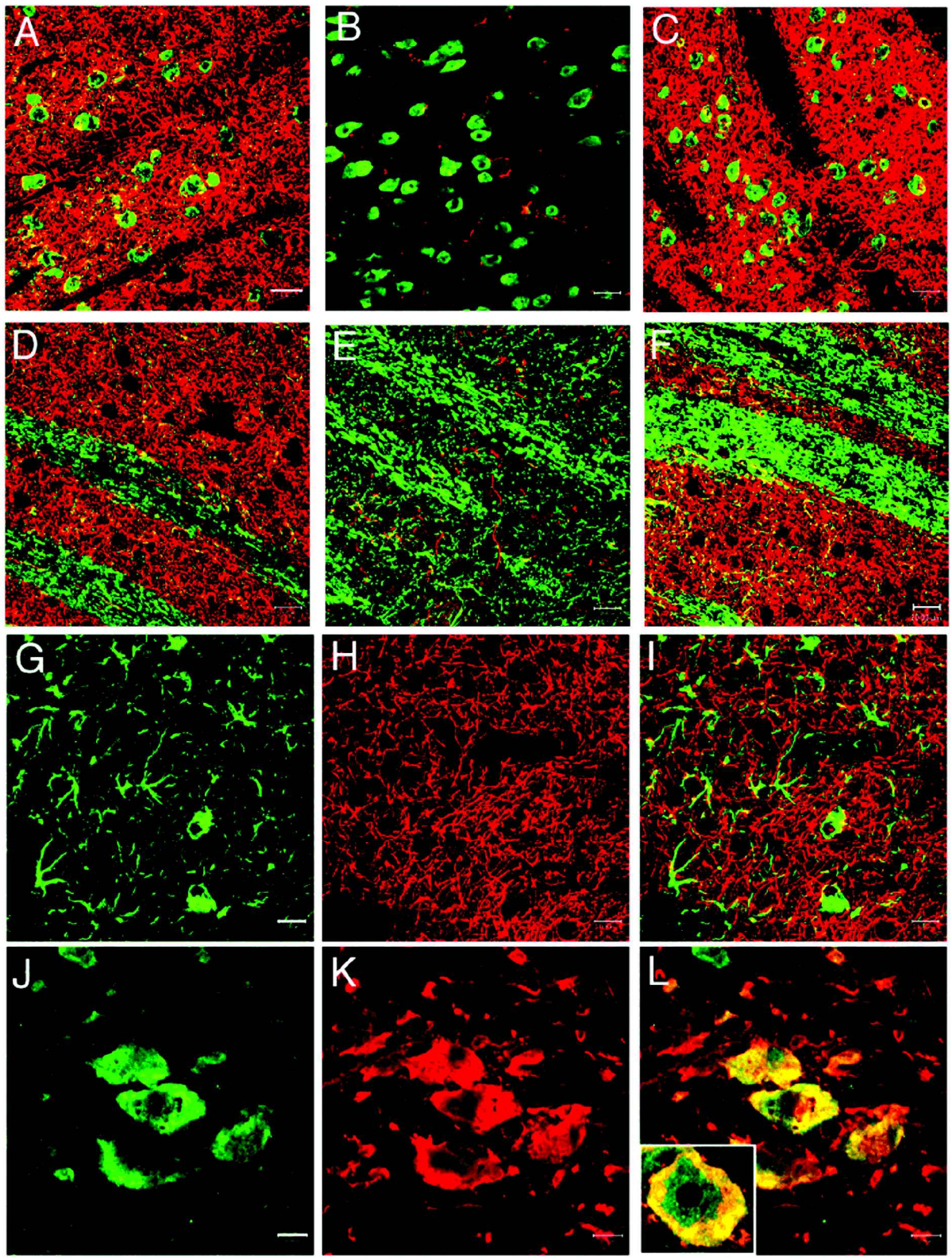

Table 3. Real-time PCR Ct for TH and 4F2hc mRNA Levels in Control, Nonlesioned Rats Treated with Either Saline or TH Gene Therapy

	Ct values					
	Saline			*TfRMAb-PIL/877*		
Organ	*TH*	*4F2hc*	*TH/4F2hc*	*TH*	*4F2hc*	*TH/4F2hc*
Brain cortex	26.3 ± 0.1	19.3 ± 0.2	1.36 ± 0.01	25.7 ± 0.1	19.4 ± 0.3	1.33 ± 0.02
Liver	34.6 ± 1.3	19.9 ± 0.2	1.74 ± 0.06	29.0 ± 2.3*	20.1 ± 0.3	1.43 ± 0.09*

Mean ± SE ($n = 3$ rats per group).
*$p < 0.05$ difference from saline values.
PCR, polymerase chain reaction; Ct, threshold cycle; TH, tyrosine hydroxylase.

OHDA–lesioned model may be related to the immediate regeneration in this pathway after neurotoxin administration. Providing that at least 25% of the nigral neurons survive the chemical lesion, which is the case for the moderate dose (8 μg) of 6-OHDA used in this study (see Materials and Methods), there is intense sprouting of surviving neurons from the substantia nigra to the striatum after the lesion (Finkelstein *et al.*, 2000; Parish *et al.*, 2002). Therefore, when the TH expression plasmid is delivered to substantia nigral neurons at 4 weeks after the lesion, the enzyme may be expressed in these cell bodies (Fig. 4L) and transported to the regenerated terminals in the striatum (Fig. 4C and 4F). In addition, the TH may be transported to the striatum via neurons that survive the chemical lesion.

The expression of the GFAP-TH gene in brain is confined to neurons with no expression in astrocytes (Fig. 4). The 5′-FS of the GFAP gene confers brain specificity of gene expression, but does not restrict gene expression to astrocytes (Kaneko and Sueoka, 1993; Galou *et al.*, 1994). Astrocyte-specific expression requires the coordinate interactions of regulatory elements in both the 5′-FS and more distal parts of the gene, including the 3′-FS (Kaneko and Sueoka, 1993). Recent work in transgenic models demonstrate that the 5′-FS of the GFAP gene enables widespread neuronal expression of transgenes in brain (Zhuo *et al.*, 2001). These findings parallel other observations that neurons secrete trans-acting factors that interact with the 5′-FS of the GFAP gene (Gomes *et al.*, 1999). The 5′-FS of the GFAP gene is completely methylated in peripheral tissues such as spleen but is hypomethylated in neurons and astrocytes (Condorelli *et al.*, 1997). In the presence of the entire GFAP gene, the neuron-suppressing elements in the 3′-FS prevent GFAP gene expression in neurons in brain in vivo (Kaneko and Sueoka, 1993). However, in the absence of the 3′-FS, the GFAP promoter can be used to direct brain-specific expression of exogenous genes in neurons (Zhuo *et al.*, 2001). The GFAP promoter also enables gene expression in astrocytes (Brenner *et al.*, 1994). However, no TH gene expression in astrocytes was detected in this study (Fig. 4G–4I). Similarly, the TH gene expression in cortical neurons was minimal (Fig. 3). Neither astrocytes or cortical neurons express the GTPCH gene, and do not produce the biopterin cofactor necessary for TH enzyme activity (Nagatsu *et al.*, 1995; Hwang *et al.*, 1998).

The absence of any increase in the cortex of immunoreactive TH (Fig. 3) or TH enzyme activity (Table 2) is paralleled by the absence of a change in TH mRNA in this region of the brain as measured by real-time PCR (Table 3). These results parallel the findings of the human TH transgenic mouse, wherein no increase in TH mRNA levels in the cortex were recorded (Kaneda *et al.*, 1991), and this is attributed, in part, to the absence of GTPCH gene expression in the cortex (Shimoji *et al.*, 1999). However, the expression of the exogenous TH gene in brain after delivery with PILs is expected in those neurons expressing the GTPCH cofactor gene. The use of a brain-specific promoter, such as the GFAP gene promoter, eliminates ectopic TH gene expression in peripheral tissues, but would not eliminate TH gene expression in cells of the brain that also express the GTPCH cofactor gene. The restriction of TH gene expression to only dopaminergic neurons is possible with the use of a trans-gene driven by the TH gene promoter that encompasses 9 kb of the 5′-FS of the gene (Min *et al.*, 1994).

The striatal TH enzyme activity is normalized with either the SV40 promoter (clone 877) or the GFAP promoter (clone 951), as shown in Table 2. In neither case are supranormal levels of TH enzyme activity observed. These observations in adult rats subjected to TH gene therapy parallel findings in TH transgenic mice. Despite a more than 50-fold increase in nigral TH mRNA levels, only minor increases in either immunoreactive TH or in TH enzyme activity in the striatum were observed (Kaneda *et al.*, 1991). These observations suggest that TH gene expression is controlled at the posttranscriptional level in the brain so that striatal TH enzyme activity is regulated within a narrow range (Min *et al.*, 1994).

In summary, the present study demonstrates transduction of the entire striatum with TH gene therapy in the 6-OHDA–lesioned rat brain. The global expression of the TH gene in the entire striatum is possible because the exogenous gene encapsulated in PILs is delivered to brain via the transvascular route across the BBB. With the transvascular approach to brain gene therapy, nearly every neuron in the brain is accessible to the exogenous gene after intravenous administration in either rodents (Shi *et al.*, 2001a,b) or primates (Zhang *et al.*, 2003c,d). Ectopic expression of the TH gene in peripheral organs such as liver is eliminated with the combined use of a brain-specific promoter and the PIL gene targeting technology. Brain TH gene expression is reversible and declines 50% at 6 days after a single intravenous administration (Zhang *et al.*, 2003a). The decline in gene expression with time is caused by degradation of

the episomal plasmid DNA based on real-time PCR measurements (unpublished observations). Therefore, long-term TH gene therapy requires repeat administration at periods determined by the persistence in brain of plasmid gene expression. PIL gene therapy has been administered intravenously on a weekly schedule and this resulted in a 100% increase in survival time in mice with intra-cranial brain cancer (Zhang *et al.*, 2002b). The period of repeat gene administration in humans may be less frequent, as the level of gene expression in the rhesus monkey is still in the therapeutic range at 2–3 weeks after a single intravenous administration (Zhang *et al.*, 2003d). Long-term weekly administration of TH expression plasmids encapsulated in TfRmAb-targeted PILs has no toxic side effects in rats and causes no change in serum chemistry, organ histology, or body weights, and induces no inflammatory reactions in brain (Zhang *et al.*, 2003e). Southern blotting shows no temporal decline in the level of plasmid persistence in brain associated with long-term weekly intravenous treatments (Zhang *et al.*, 2003e). Long-term administration of reversible, episomal-based nonviral gene therapeutics is an alternative approach that avoids problems associated with random and permanent integration in the host genome of exogenous genes. The use of the PIL gene targeting technology enables the noninvasive delivery of the exogenous gene to all target cells within the brain after intravenous administration.

ACKNOWLEDGMENTS

This work was supported by a grant from the Neurotoxin Exposure Treatment Research Program of the U.S. Department of Defense. F.S. was supported by the Ernst Schering Research Foundation.

REFERENCES

ANDERTON, B.H., BREINBURG, D., DOWNES, M.J., GREEN, P.J., TOMLINSON, B.E., ULRICH, J., WOOD, J.N., and KAHN, J. (1998). Monoclonal antibodies show that neurofibrillary tangles and neurofilaments share antigenic determinants. Nature **298,** 84–86.

BOADO, R.J., and PARDRIDGE, W.M. (1998). Ten nucleotide cis element in the 3′-untranslated region of the GLUT1 glucose transporter mRNA increases gene expression via mRNA stabilization. Mol. Brain Res. **59,** 109–113.

BOADO, R.J., LI, J.Y., NAGAYA, M., ZHANG, C., and PARDRIDGE, W.M. (1999). Selective expression of the large neutral amino acid transporter (LAT) at the blood-brain barrier. Proc. Natl. Acad. Sci. U.S.A. **96,** 12079–12084.

BRENNER, M., KISSEBERTH, W.C., SU, Y., BESNARD, F., and MESSING, A. (1994). GFAP promoter directs astrocyte-specific expression in transgenic mice. J. Neurosci. **14,** 1030–1037.

CONDORELLI, D.F., DELL'ALBANI, P., CONTICELLO, S.G., BARRESI, V., NICOLETTI, V.G., CARUSO, A., KAHN, M., VACANTI, M., ALBANESE, V., and DE VELLIS, J. (1997). A neural-specific hypomethylated domain in the 5′ flanking region of the glial fibrillary acidic protein gene. Dev. Neurosci. **19,** 446–456.

DEBUS, E., WEBER, K., and OSBORN, M. (1983). Monoclonal antibodies specific for glial fibrillary acidic (GFA) protein and for each of the neurofilament triplet polypeptides. Differentiation **25,** 193–203.

FINKELSTEIN, D.I., STANIC, D., PARISH, D., TOMAS, D., DICKSON, K., and HORNE, M.K. (2000). Axonal sprouting following lesions of the rat substantia nigra. Neuroscience **97,** 99–112.

GALOU, M., POURIN, S., ENSERGEUIX, D., RIDET, J.-L., TCHELINGERIAN, J.L., LOSSOUARN, L., PRIVAT, A., BABINET, C., and DUPOUEY, P. (1994). Normal and pathological expression of GFAP promoter elements in transgenic mice. Glia **12,** 281–293.

GOMES, F.C.A., GARCIA-ABREU, J., GALOU, M., PAULIN, D., and NETO, V.M. (1999). Neurons induce GFAP gene promoter of cultured astrocytes from transgeneic mice. Glia **26,** 97–108.

HORGER, B.A., NISHIMURA, M.C., ARMANINI, M.P., WANG, L.C., POULSEN, K.T., ROSENBLAD, C., KIRIK, D., MOFFAT, B., SIMMONS, L., JOHNSON, E., Jr., MILBRANDT, J., ROSENTHAL, A., BJORKLUND, A., VANDLEN, R.A., HYNES, M.A., and PHILLIPS, H.S. (1998). Neurturin exerts potent actions on survival and function of midbrain dopaminergic neurons. J. Neurosci. **18,** 4929–4937.

HWANG, O., BAKER, H., GROSS, S., and JOH, T.H. (1998). Localization of GTP cyclohydrolase in monaminergic but not nitric oxide-producing cells. Synapse **28,** 140–153.

JEFFERIES, W.A., BRANDON, M.R., HUNT, S.V., WILLIAMS, A.F., GATTERS, K.C., and MASON, D.Y. (1984). Transferrin receptor on endothelium of brain capillaries. Nature **312,** 162–163.

KANEDA, N., SASAOKA, T., KOBAYASHI, K., KIUCHI, K., NAGATSU, I., KUROSAWA, Y., FUJITA, K., YOKOYAMA, M., NOMURA, T., KATSUKI, M., and NAGATSU, T. (1991). Tissue-specific and high-level expression of the human tyrosine hydroxylase gene in transgenic mice. Neuron **6,** 583–594.

KANEKO, R., and SUEOKA, N. (1993). Tissue-specific versus cell type-specific expression of the glial fibrillary acidic protein. Proc. Natl. Acad. Sci. U.S.A. **90,** 4698–4702.

LIU, J., SOLWAY, K., MESSING, R.O., and SHARP, F.R. (1998). Increased neurogenesis in the dentate gyrus after transient global ischemia in gerbils. J. Neurosci. **18,** 7768–7778.

MANDEL, R.J., RENDAHL, K.G., SNYDER, R.O., and LEFF, S.E. (1999). Progress in direct striatal delivery of L-dopa via gene therapy for treatment of Parkinson's disease using recombinant adeno-associated viral vectors. Exp. Neurol. **159,** 47–64.

MANDERS, E.M., VERBEEK, F.J., and ATEN, J.A. (1993). Measurements of co-localization of objects in dual-color confocal images. J. Microscopy **169,** 375–382.

MANDIL, R., ASHKENAZI, E., BLASS, M., KRONFELD, I., KAZIMIRSKY, G., ROSENTHAL, G., UMANSKY, F., LORENZO, P.S., BLUMBERG, P.M., and BRODIE, C. (2001). Protein kinase Cα and protein kinase Cδ play opposite roles in the proliferation and apoptosis of glioma cells. Cancer Res. **61,** 4612–4619.

MIN, N., JOH, T.H., KIM, K.S., PENG, C., and SON, J.H. (1994). 5′ upstream DNA sequence of the rat tyrosine hydroxylase gene directs high-level and tissue-specific expression to catecholaminergic neurons in the central nervous system of transgenic mice. Mol. Brain Res. **27,** 281–289.

MOURADIAN, M.M., and CHASE, T.N. (1997). Gene therapy for Parkinson's disease: An approach to the prevention or palliation of levodopa-associated motor complications. Exp. Neurol. **144,** 51–57.

NAGATSU, I., ICHINOSE, H., SAKAI, M., TITANI, K., SUZUKI, M., and NAGATSU, T. (1995). Immunocytochemical localization of GTP cyclohydrolase I in the brain, adrenal gland, and liver of mice. J. Neural Transm. **102,** 175–188.

NAGATSU, I., ARAI, R., SAKAI, M., YAMAWAKI, Y., TAKEUCHI, T., KARASAWA, N., and NAGATSU, T. (1997). Immunohistochemical colocalization of GTP cyclohydrolase I in the nigrostriatal system with tyrosine hydroxylase. Neurosci. Lett. **224,** 185–188.

PARDRIDGE, W. (2002). Drug and gene delivery to the brain: The vascular route. Neuron **36,** 555–558.

PARDRIDGE, W.M., EISENBERG, J., and YANG, J. (1987). Human blood-brain barrier transferrin receptor. Metabolism **36,** 892–895.

PARISH, C.L., FINKELSTEIN, D.I., TRIPANICHKUL, W., SATOSKAR, A.R., DRAGO, J., and HORNE, M.K. (2002). The role of interleukin-1, interleukin-6, and glia in inducing growth of neuronal terminal arbors in mice. J. Neurosci. **22,** 8034–8041.

SEGOVIA, J., VERGARA, P., and BRENNER, M. (1998). Differentiation-dependent expression of transgenes in engineered astrocyte cell lines. Neurosci. Lett. **242,** 172–176.

SHI, N., and PARDRIDGE, W.M. (2000). Non-invasive gene targeting to the brain. Proc. Natl. Acad. Sci. U.S.A. **97,** 7567–7572.

SHI, N., ZHANG, Y., BOADO, R.J., ZHU, C., and PARDRIDGE, W.M. (2001a). Brain-specific expression of an exogenous gene following intravenous administration. Proc. Natl. Acad. Sci. U.S.A. **98,** 12754–12759.

SHI, N., BOADO, R.J., and PARDRIDGE, W.M. (2001b). Receptor-mediated gene targeting to tissues in the rat in vivo. Pharm. Res. **18,** 1091–1095.

SHIMOJI, M., HIRAYAMA, K., HYLAND, K., and KAPATOS, G. (1999). GTP cyclohydrolase I gene expression in the brains of male and female hph-1 mice. J. Neurochem. **72,** 757–764.

ZHANG, Y., LEE, H.J., BOADO, R.J., and PARDRIDGE, W.M. (2002a). Receptor-mediated delivery of an antisense gene to human brain cancer cells. J. Gene Med. **4,** 183–525.

ZHANG, Y., ZHU, C., and PARDRIDGE, W.M. (2002b). Antisense gene therapy of brain cancer with an artificial virus gene delivery system. Mol. Ther. **6,** 67–72.

ZHANG, Y., CALON, F., ZHU, C., BOADO, R.J., and PARDRIDGE, W.M. (2003a). Intravenous non-viral gene therapy causes normalization of striatal tyrosine hydroxylase and reversal of motor impairment in experimental Parkinsonism. Hum. Gene Ther. **14,** 1–12.

ZHANG, Y., BOADO, R.J., and PARDRIDGE, W.M. (2003b). Marked enhancement in gene expression by targeting the human insulin receptor. J. Gene Med. **5,** 157–163.

ZHANG, Y., SCHLACHETZKI, F., and PARDRIDGE, W.M. (2003c). Global non-viral gene transfer to the primate brain following intravenous administration. Mol. Ther. **7,** 11–18.

ZHANG, Y., SCHLACHETZKI, F., LI, J.Y., BOADO, R.J., and PARDRIDGE. W.M. (2003d). Organ-specific gene expression in the rhesus monkey eye following intravenous non-viral gene transfer. Mol. Vis. **9,** 465–472.

ZHANG, Y.-.F, BOADO, R.J., and PARDRIDGE, W.M. (2003e). Absence of toxicity of chronic weekly intravenous gene therapy with pegylated immunoliposomes. Pharm. Res. **20,** 1779–1785.

ZHUO, L., THES, M., ALVAREZ-MAYA, I., BRENNER, M., WILLECKE, K., and MESSING, A. (2001). hGFAP-cre transgenic mice for manipulation of glial and neuronal function in vivo. Genesis **31,** 85–94.

Address reprint requests to:
William M. Pardridge
UCLA Warren Hall 13-164
900 Veteran Avenue
Los Angeles, CA 90024

E-mail: wpardridge@mednet.ucla.edu

Received for publication October 2, 2003; accepted after revision February 26, 2004.

Published online: March 12, 2004.

Gene therapy of the brain

The trans-vascular approach

Felix Schlachetzki, MD; Yun Zhang, PhD; Ruben J. Boado, PhD; and William M. Pardridge, MD

Abstract—Many chronic neurologic diseases do not respond to small molecule therapeutics, and have no effective long-term therapy. Gene therapy offers the promise of an effective cure for both genetic and acquired brain disease. However, the limiting problem in brain gene therapy is delivery to brain followed by regulation of the expression of the transgene. Present day gene vectors do not cross the blood-brain barrier (BBB). Consequently, brain gene therapy requires craniotomy and the local injection of a viral gene vector. However, there are few brain disorders that can be effectively treated with local injection. Most applications of gene therapy require global expression in the brain of the exogenous gene, and this can only be achieved with a noninvasive delivery through the BBB—the trans-vascular route to brain. An additional consideration is the potential toxicity of all viral and nonviral approaches, which may either integrate into the host genome and cause insertional mutagenesis or cause inflammation in the brain. Nonviral, noninvasive gene therapy of the brain is now possible with the development of a new approach to targeting therapeutic genes to the brain following an IV administration. This approach utilizes genetically engineered molecular Trojan horses, which ferry the gene across the BBB and into neurons. Global and reversible expression of therapeutic genes in the human brain without surgery and without viral vectors is now possible.

NEUROLOGY 2004;62:1275–1281

Certain brain diseases such as affective disorders, chronic pain, or epilepsy respond sufficiently to conventional small molecule neurotherapeutics. However, the majority of brain diseases do not respond well to small molecule drugs, and have no effective long-term therapy. Many such conditions are candidates for gene therapy,[1] and these include both genetic (table) and acquired brain disorders. While gene therapy holds great promise for the treatment of brain disease, progress in clinical trials has been slow, and a major limiting factor is delivery of the gene to brain. Gene expression vectors do not cross the blood-brain barrier (BBB) following an IV administration, and must be given via craniotomy. However, the local injection of an exogenous gene in the brain treats <1% of the 1,200 g human brain, and it is not clear if any brain disease can be effectively treated with local intracerebral injections of the gene. Apart from how the gene is actually delivered to the brain, the other confounding factor in brain gene therapy is the use of viral vectors. The use of viruses in humans may have unwanted side effects, including permanent integration into the host genome and brain inflammation.

The delivery issue in brain gene therapy has become such a limiting factor, because the viral vectors were initially tested in cell culture, where the BBB is absent. The inability of the vector to cross the BBB necessitated craniotomy-based gene delivery, which then resulted in limited distribution of the gene in brain, because the gene is only expressed in brain at the tip of the injection needle. However, most brain diseases that are candidates for gene therapy require the gene be delivered to the majority of cells in the brain. Because every neuron is virtually perfused by its own blood vessel, the majority of cells in the brain can be transduced if the gene medicine is delivered to brain via the trans-vascular route across the BBB. Recently, a new approach to brain gene therapy has emerged that enables the trans-vascular delivery of exogenous nonviral genes to the brain. This is accomplished by targeting nanocontainers carrying genes to the brain via delivery on endogenous BBB transport systems.[2]

Craniotomy-based brain delivery. The inability to distribute effectively to brain following craniotomy-based brain delivery is illustrated in the figure, A, for an intracerebral (IC) injection, and in the figure, B, for an intracerebroventricular (ICV) injection. The autoradiogram of rat brain shown in the figure, A, was taken 48 hours after the intracerebral implantation of a 2

From the Department of Neurology (Dr. Schlachetzki), University of Regensburg, Germany; and Department of Medicine (Drs. Zhang, Boado, and Pardridge), University of California Los Angeles.

Supported by a grant of the Ernst Schering Research Foundation, Berlin, Germany (F.S.).

Received September 5, 2003. Accepted in final form December 1, 2003.

Address correspondence and reprint requests to Dr. William M. Pardridge, UCLA Warren Hall 13-164, 900 Veteran Avenue, Los Angeles, CA 90024; e-mail: wpardridge@mednet.ucla.edu

Table *CNS gene therapy candidates: Inherited diseases*

Group/disease	Gene	GenBank accession ID
Lysosomal storage disorders		
MPS-1 (Hurlers)	*IDUA*	NM_000203
MPS-II (Hunters)	*IDS*	NM_000202
MPS-IIIA (Sanfilippo A)	*SGSH*	NM_000199
MPS-IIIB (Sanfilippo B)	*NAGLU*	NM_016256
MPS-VII (Sly)	*GUSB*	NM_000181
Fabry disease	*GLA*	NM_000169
Neuronal ceroid lipofuscinosis (NCL1)	*PPT*	NM_000310
NCL2, late infantile (Jansky-Bielschowsky)	*CLN2*	NM_000391
Leukodystrophy (Canavan)	*ASPA*	NM_000049
Globoid cell dystrophy (Krabbe)	*GALC*	NM_000153
GM2 gangliosidosis I (Tay-Sachs)	*HEXA*	NM_000520
GM2 gangliosidosis II (Sandhoff)	*HEXB*	NM_000521
GM2 gangliosidosis AB	*GM2A*	NM_000405
Spongiform encephalopathy	*PRNP*	NM_000311
Transcription factor disorders		
Rett syndrome	*MeCP2*	NM_004992
Fragile-X syndrome	*FMR1*	NM_002024
	FMR2	NM_002025
Familial dysautonomia	*IKBKAP*	NM_003640
Ataxias		
Ataxia telangiectasia	*ATM*	NM_138293
Friedreich ataxia	*FRDA*	NM_000144
SCA1	*SCA1*	NM_000332
SCA2	*SCA2*	NM_002973
SCA3 (Machado-Joseph)	*SCA3*	NM_004993
Triplet repeat (CAG) disorders		
Huntington disease	*Huntingtin*	NM_002111
Spinal-bulbar muscular atrophy (Kennedy)	*SBMA*	NM_000044
Dentatorubralpallidoluysian atrophy	*DRPLA*	NM_001940
Blindness		
Retinitis pigmentosa-1	*RHO*	NM_000539
Peripherin-related retinal degeneration	*RDS*	NM_000322
Gyrate atrophy	*OAT*	NM_000274
CNS tumor		
Neurofibromatosis 1 (von Recklinghausen)	*NF1*	NM_000267
Neurofibromatosis 2	*NF2*	NM_000268
Retinoblastoma	*RB*	NM_000321

IDUA = alpha-L-iduronidase; IDS = iduronate 2-sulfatase; SGSH = N-sulfoglucosamine sulfohydrolase; NAGLU = N-acetylglucosamine-1-phosphodiester alpha-N-acetylglucosaminidase; GUSB = β-glucuronidase; GLA = α-galactosidase; PPT = palmityl-protein thioesterase; CLN2 = tripeptidyl-peptidase; ASPA = aspartoacyclase; GALC = galactosylceramidase; HEXA = hexoaminidase A; HEXB = hexoaminidase B; GM2A = GM2 ganglioside activator protein; PRNP = prion protein; MeCP2 = methyl-CpG-binding protein; FMR 1 = familial mental retardation; IKBKAP = IkappaB kinase complex-associated protein; ATM = ataxia telangiectasia mutated; FRDA = Friedreich ataxia (human frataxin); SCA = spinocerebellar ataxia; SBMA = spinal and bulbar muscular atrophy; DRPLA = dentatorubralpallidoluysian atrophy; RHO = rhodopsin; RDS = retinal degeneration, slow; OAT = ornithine aminotransferase; NF = neurofibromin; RB = retinoblastoma.

mm polymeric disc containing radiolabeled nerve growth factor (NGF).[3] The study shows that this 25,000 Dalton neurotrophic factor has not effectively distributed to brain, as the treatment volume is about the same size as the volume occupied by the implant. The distribution of a drug into brain is no better with an ICV administration, as illustrated by the autoradiogram of rat brain taken 24 hours after the ICV injec-

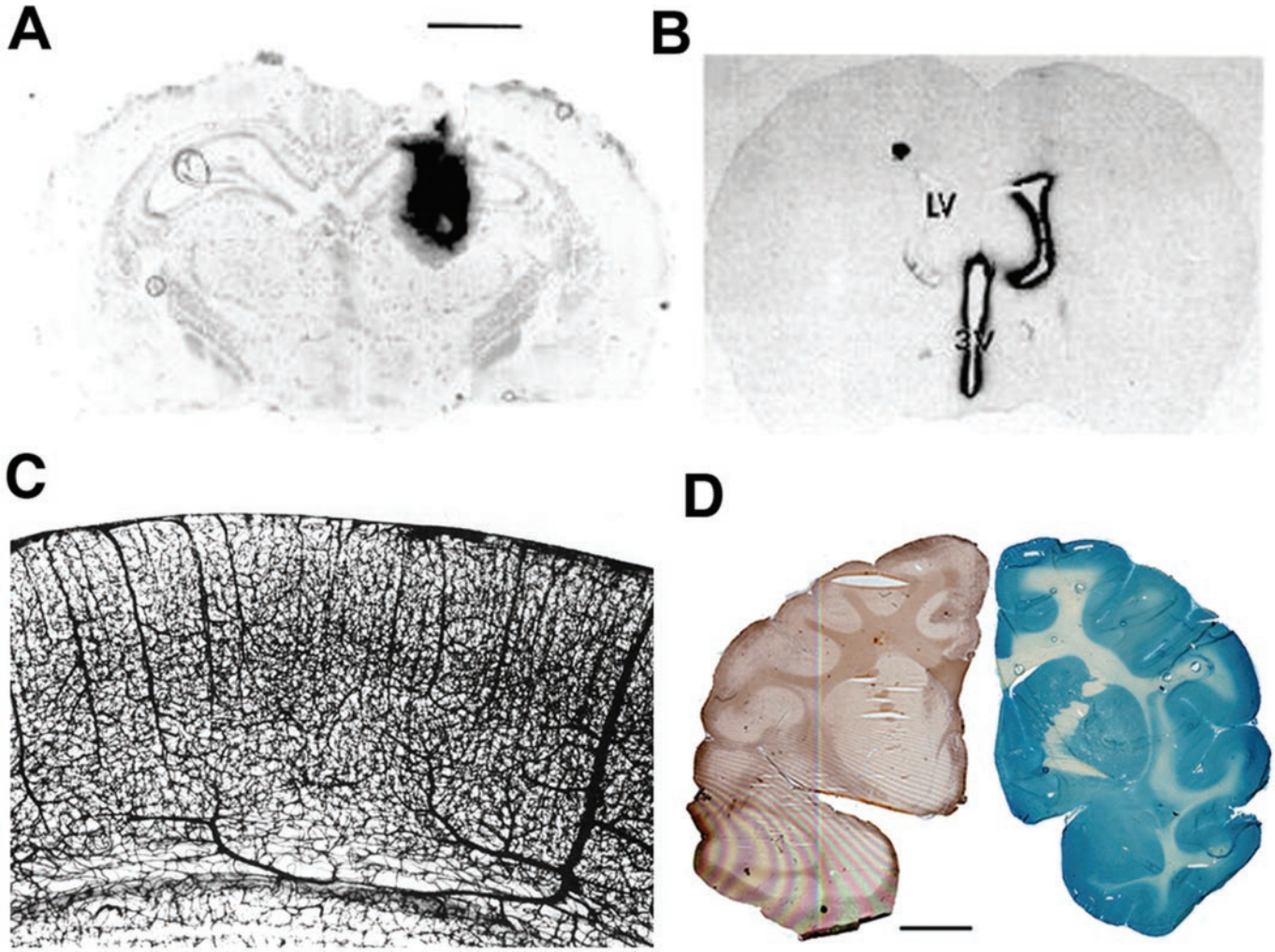

Figure. (A) Film autoradiogram of rat brain at 48 hours after the intracerebral (IC) implantation of a polymer embedded with [^{125}I]-nerve growth factor. The diameter of the polymeric disc was 2 mm and the distance bar in the figure is 2.5 mm. The study shows minimal diffusion of a drug into brain parenchyma following the IC route of administration. From Krewson et al.[3] (B) Film autoradiogram of rat brain at 24 hours after the intracerebroventricular (ICV) injection of [^{125}I]-brain derived neurotrophic factor into one lateral ventricle (LV). The drug moves into the third ventricle (3V), prior to exit into the general circulation, and does not diffuse either to the contralateral brain or beyond the ipsilateral ependymal barrier. From Yan et al.[4] (C) India ink injection study showing the complex vascular network in the rat brain. From Bar.[6] (D) Histochemistry of Rhesus monkey brain for β-galactosidase gene expression, which is indicated by the deposition of a blue chromagen. The control, uninjected primate brain is shown on the left panel. The right panel is primate brain removed 2 days after a single IV injection of the β-galactosidase expression plasmid encapsulated in a pegylated immunoliposome (PIL) targeted to brain with a monoclonal antibody (mAb) to the human insulin receptor (HIR). The HIRMAb targets the PIL across both the blood-brain barrier and the neuronal cell membrane. This study in the living primate shows it is possible to achieve adult transgenics in 24 hours with the IV injection of a nonviral formulation of an exogenous gene. From Zhang et al.[20]

tion of radiolabeled brain derived neurotrophic factor (BDNF) (see the figure, B).[4] The neurotrophin distributes only to the ipsilateral ependymal surface, and does not effectively enter into brain. The IC or ICV delivery approaches both rely on diffusion of drug or gene into brain. However, the efficacy of diffusion decreases exponentially with the distance from the implantation site. The limitations of diffusion provide the basis for a third craniotomy-based approach to brain gene delivery called convection enhanced diffusion (CED), wherein drug or gene is infused into the brain via bilateral cannulas connected to an external delivery device.[5] While CED is more effective than the diffusion-based delivery approaches, it is still not possible to deliver genes to the entire brain with this invasive approach.

The trans-vascular route to brain. The human brain is perfused by more than 100 billion capillaries, which form the BBB in vivo. Virtually every brain cell is perfused by its own blood vessel, and the passage of a gene across the capillary barrier delivers the gene to the doorstep of every neuron in the brain.[2] The complexity of the vascular tree in brain

is illustrated in the India ink stain of rat brain shown in the figure, C.[6] There are approximately 400 miles of capillaries in the human brain, and the global distribution of a gene medicine to virtually every neuron in the human brain is possible with a trans-vascular route to the brain.

Trans-vascular delivery of genes to the brain has been attempted with BBB disruption, using the intracarotid infusion of either hyperosmolar solutions or vasoactive compounds. However, this approach requires arterial access, and the disruption of the BBB leads to chronic neuropathologic changes in the brain.[7] Blood proteins such as albumin are toxic to brain cells,[8] and BBB disruption allows blood components to enter the brain.

Trans-vascular delivery of genes is also possible without disrupting the BBB by accessing certain endogenous transport systems within the BBB.[9] The capillary endothelium, which forms the BBB, expresses receptor-mediated transcytosis (RMT) systems for certain endogenous peptides such as insulin, transferrin, and others. Either the endogenous peptide or a peptidomimetic monoclonal antibody (mAb) are delivered to brain from blood via the BBB RMT systems. In the case of the peptidomimetic mAb, the antibody binds to an exofacial epitope on the endothelial receptor, which is removed from the binding site for the endogenous ligand, and piggybacks across the BBB on the endogenous RMT system. Since the mAb and the endogenous ligand bind to different sites on the receptor, there is no interference by the mAb with binding of the endogenous ligand,[10,11] unless very high concentrations of the mAb are used.[11,12] High concentrations of the mAb, which would not be used for therapeutic purposes, can have functional effects at the targeted receptor, although the mAb has weak agonist properties compared to the endogenous ligand.[13] The peptidomimetic mAb can be used as molecular Trojan horses to ferry across the BBB any attached drug or gene.[9] In the case of gene delivery, the molecular Trojan horse technology must be merged with special nonviral gene delivery systems utilizing liposomes.

Nonviral gene delivery systems. Nonviral gene transfer technology was developed because of the potential toxicity of viral vectors used in gene therapy. There is a risk of insertional mutagenesis with viral vectors such as retrovirus or adeno-associated virus (AAV). In addition, 90% of the human population has a pre-existing immunity to most viral vectors, which can induce inflammation in the brain.[14] Therefore, a nonviral gene delivery system was considered. Conventional nonviral gene delivery systems utilize cationic polyplexes of the anionic plasmid DNA and a cationic polymer. While these complexes are stable in water, the cationic polyplexes aggregate in saline and embolize in the lung in vivo.[15-17]

The aggregation of the DNA and the nonviral gene delivery system can be eliminated if the DNA is encapsulated in the interior of a nanocontainer such as an 85 nm liposome. This structure is the same size as many viral gene delivery systems. The surface of the liposome must be conjugated with several thousand strands of polyethyleneglycol (PEG), and this PEGylation of the liposome makes the nanocontainer stable in the blood with prolonged blood residence times.[18] PEGylated liposomes carrying small molecule drugs are not immunogenic, and are Food and Drug Administration (FDA)–approved pharmaceuticals. A PEGylated liposome, per se, will not cross the BBB.[19] To enable transport across the BBB via receptor-mediated transport, the tips of 1 to 2% of the PEG strands must be conjugated with a BBB molecular Trojan horse. This formulation is called a pegylated immunoliposome or PIL.

The immunogenic component of the PIL is the molecular Trojan horse, which may be a targeting mAb. However, the immunogenicity of the mAb can be eliminated with genetic engineering and the formation of chimeric or humanized mAb. Genetically engineered mAb are FDA-approved drugs.

Gene delivery to the primate brain. The global expression of an exogenous gene in the entire Rhesus monkey brain following an IV injection of PIL is shown in the figure, D. An expression plasmid encoding for bacterial β-galactosidase was encapsulated in the interior of PIL, which were targeted with a mAb to the human insulin receptor (HIR). The animal was killed 48 hours later and frozen sections of the brain were treated with a chromagen that is hydrolyzed to a blue reaction product if the bacterial β-galactosidase gene is expressed in brain.[20] In the absence of this gene, there is no histochemical reaction, as shown on the left hemisphere of the figure, D, which is taken from a healthy control Rhesus monkey. However, in the primate treated with the PIL gene delivery system, there is global expression of the transgene throughout the entire brain, as shown in the right hemisphere of the figure, D. Confocal microscopy showed the transgene was expressed in neurons.[20] Neuronal expression was possible, because the insulin receptor is expressed both at the BBB and the neuronal cell membrane. Therefore, the HIRMAb molecular Trojan horse delivered the PIL carrying the exogenous gene both across the BBB and across the neuronal plasma membrane. For applications in humans, the HIRMAb has been genetically engineered for use in humans and is transported across the primate brain just as well as the original murine HIRMAb.[21]

Brain specific gene expression. The delivery of an exogenous gene to brain with a molecular Trojan horse that targets the insulin receptor could potentially lead to ectopic gene expression in nonbrain organs, which also express the insulin receptor. However, if the therapeutic gene is under the influence of a brain specific gene promoter, then ectopic gene expression in peripheral organs is eliminated.[22,23] Within the brain, there are certain genes that are only expressed in specific regions of the brain. For example, the gene encoding the glutamate recep-

tor β2 subunit (GluRβ2) is only expressed in the Purkinje cell layer of the brain.[24] Depending on the neurologic disease, it may be preferred to restrict expression of the exogenous gene to a defined region of the brain, and this is possible with specific promoters.

Persistence of gene expression. There are two fundamentally different approaches to gene therapy: permanent integration of the host genome or episomal gene expression. It is possible to obtain permanent, yet random, integration of the host genome without viral vectors, if the gene expression cassette is flanked by terminal inverted repeat (IR) gene elements, which mediate chromosomal integration.[25] However, random integration in the host genome can lead to insertional mutagenesis and cancer, which has complicated the use of retroviral gene therapy vectors.[26] Until the human genome can be targeted with chromosomal integration that does not cause mutagenesis, the alternative approach is to use gene therapy vectors that do not integrate in the host genome, but instead function as nuclear episomal structures or mini-chromosomes. Episomal gene expression systems are degraded by the nuclear DNAse leading to a loss in gene expression, and this requires repeat administration of the gene. The interval of repeat gene therapy is a function of the persistence of the episomal structure. The survival time of mice with intracranial experimental brain cancer was increased 100% with repeat weekly IV antisense gene therapy directed at the human epidermal growth factor receptor. This antisense gene was delivered to the brain cancer using the PIL delivery technology.[27] In experimental parkinsonism rats were treated with an intracerebral injection of the neurotoxin 6-hydroxydopamine in the medial forebrain bundle. Striatal tyrosine hydroxylase (TH) was normalized after an IV injection of the TH gene delivered to brain with the PIL system. The TH gene expression decayed 50% and 90% at 6 and 9 days after a single IV administration.[28] In adult Rhesus monkeys, the level of gene expression is still in the therapeutic range for 2 to 3 weeks after a single IV injection.[23] Thus, the period of repeat administration in humans may be on the order of a month. The challenge of episomal-based gene therapy in the future is to develop plasmid formulations that have improved resistance to nuclear degrading enzymes. Greater persistence of the transgene will reduce the frequency of repeat gene administration. The chronic repeat administration of episomal-based gene medicines may cause either tissue toxicity or inflammation. However, the chronic weekly IV administration of exogenous genes with the PIL formulation has no toxic side effects and causes no inflammation in organs, including the brain.[29] The long-term effects of gene therapy in humans over many years are not known. However, the component of the PIL that is potentially immunogenic is the targeting mAb, which will be genetically engineered for chronic use in humans. Genetically engineered or humanized mAb-based therapeutics are FDA-approved drugs, and are presently given for the treatment of chronic disease.

Brain gene therapy candidates: inherited disease. Many inborn errors of metabolism have devastating effects on the brain, and a partial list is given in the table, along with the GenBank accession number of the affected human gene. These conditions are prime candidates for brain gene therapy, because the mutated gene is generally not functional and normal phenotype could be restored by replacement gene therapy. The mucopolysaccharidoses affect the brain and could be treatable with brain gene therapy.[30] Canavan disease is an autosomal recessive leukodystrophy caused by mutations in the aspartoacylase (ASPA) gene.[31] The loss of ASPA activity leads to neurotoxicity in the brain with features of spongiform degeneration of oligodendrocytes, neurodevelopmental retardation, and a life expectancy of up to 10 years. Phase I clinical trials of Canavan disease have been designed, with the use of AAV as the vector for the ASPA gene; in this trial, a total of 10 billion AAV particles are injected in six different areas of the brain.[32] Based on a 1% transduction efficiency, this treatment regimen is intended to transduce only 180 million brain cells, which is $\leqslant$1% of the total brain cells affected in Canavan disease.

The gene therapy of certain inherited conditions may be more complex where the therapeutic strategy may be the knockout of allele-specific dominant genes. In this case, the combination of RNA interference (RNAi) and gene transfer technology may be required. Recent studies suggest it is possible to knock down a pathogenic allele that differs from the wild type allele by a single nucleotide mismatch using RNAi technology.[33]

Brain gene therapy candidates: acquired disease. The treatment of acquired brain disease with gene therapy is also possible, but potentially more complicated than the treatment of inborn errors that arise from the mutation of a single gene. Acquired brain diseases that could benefit from gene therapy include Parkinson disease (PD) and other neurodegenerative conditions,[34-36] brain cancer,[37-40] neuro-AIDS and other brain infections, multiple sclerosis,[41] brain trauma, acute neurologic insults, and retinal disorders.[42] Experimental forms of PD have responded to gene therapy that augments the expression of TH, the rate-limiting enzyme in dopamine production. Striatal TH is 99% depleted in experimental PD, and striatal TH can be completely normalized with a single IV injection of a TH expression plasmid, encapsulated in targeted PIL.[28] The normalization of striatal TH is possible with the delivery of only 5 to 10 plasmid DNA molecules per brain cell, which illustrates the high level of efficiency of the PIL brain gene targeting technology. However, the therapy of PD must also be aimed at slowing the neurodegeneration of this condition, and this may be possible with gene therapy that augments the production of neuro-

trophins such as glial derived neurotrophic factor within the nigro-striatal tract.

Brain gene therapy of acquired brain disease such as brain cancer or neuro-AIDS may be more straightforward where the goal is to suppress the expression of either oncogenes or viral specific genes. A new form of genetic knockdown in adult animals is RNAi. In this approach a short hairpin RNA (shRNA) molecule is produced from an expression vector, and the shRNA of defined sequence hybridizes with the target mRNA to cause transcript degradation and knockdown of gene expression. RNAi is a powerful new technology, but RNAi is another form of gene therapy; the delivery issues limiting gene therapy also apply and will limit RNAi-based gene therapy. RNAi-expressing plasmids have been delivered to experimental brain cancer with the PIL gene targeting technology, and this results in 90% knockdown of brain cancer specific gene expression.[43]

Regulation of expression of exogenous genes in brain. Once the brain gene delivery problem is solved, a concern with the administration of gene therapeutics to the brain is whether the exogenous gene is overexpressed. However, this may be a problem in only a minority of clinical settings. The expression of certain exogenous genes in brain will be tightly regulated within a normal range by endogenous mechanisms. This is illustrated in the case of tyrosine hydroxylase gene therapy. The enzyme activity of tyrosine hydroxylase arising from the expression of an exogenous gene is regulated within the normal range.[28] In other cases of RNAi gene therapy, the maximal expression of the exogenous gene is desired.[43] In the event that the expression of an exogenous gene is not regulated by brain, and that overexpression of the exogenous gene has adverse effects, then it is possible to reduce the level of gene expression simply by reducing the dose of the exogenous gene.[28] Alternatively, the regulation of expression of the exogenous gene may be controlled by ligand dependent promoters, such as the tetracycline inducible promoter.[44]

References

1. Martin J. Gene therapy and pharmacological treatment of inherited neurological disorders. Trends Biotechnol 1995;13:28–35.
2. Pardridge WM. Drug and gene delivery to the brain: the vascular route. Neuron 2002;36:555–558.
3. Krewson CE, Klarman ML, Saltzman WM. Distribution of nerve growth factor following direct delivery to brain interstitium. Brain Res 1995; 680:196–206.
4. Yan Q, Matheson C, Sun J, et al. Distribution of intracerebral ventricularly administered neurotrophins in rat brain and its correlation with Trk receptor expression. Exp Neurol 1994;127:23–36.
5. Morrison PF, Laske DW, Bobo H, Oldfield EH, Dedrick RL. High-flow microinfusion: tissue penetration and pharmacodynamics. Am J Physiol 1994;266:R292–R305.
6. Bar T. The vascular system of the cerebral cortex. Adv Anat Embryol Cell Biol 1980;59:1–62.
7. Salahuddin TS, Johansson BB, Kalimo H, Olsson Y. Structural changes in the rat brain after carotid infusions of hyperosmolar solutions. An electron microscopic study. Acta Neuropathol 1988;77:5–13.
8. Nadal A, Fuentes E, Pastor J, McNaughton PA. Plasma albumin is a potent trigger of calcium signals and DNA synthesis in astrocytes. Proc Natl Acad Sci USA 1995;92:1426–1430.
9. Pardridge WM. Drug and gene targeting to the brain with molecular Trojan horses. Nat Rev Drug Discov 2002;1:131–139.
10. Skarlatos S, Yoshikawa T, Pardridge WM. Transport of [^{125}I]transferrin through the rat blood-brain barrier in vivo. Brain Res 1995;683: 164–171.
11. Pardridge WM, Kang Y-S, Buciak JL, Yang J. Human insulin receptor monoclonal antibody undergoes high affinity binding to human brain capillaries in vitro and rapid transcytosis through the blood-brain barrier in vivo in the primate. Pharm Res 1995;12:807–816.
12. Ueda F, Raja KB, Simpson RJ, Trowbridge IS, Bradbury MWB. Rate of ^{59}Fe uptake into brain and cerebrospinal fluid and the influence thereon of antibodies against the transferrin receptor. J Neurochem 1993;60:106–113.
13. Wilden PA, Siddle K, Harang E, et al. The role of insulin receptor kinase domain autophosphorylation in receptor-mediated activities. J Biol Chem 1992;267:13719–13727.
14. Driesse MJ, Kros JM, Avezaat CJJ, et al. Distribution of recombinant adenovirus in the cerebrospinal fluid of nonhuman primates. Hum Gene Ther 1999;10:2347–2354.
15. Hofland HEJ, Nagy D, Liu J-J, et al. In vivo gene transfer by intravenous administration of stable cationic lipid/DNA complex. Pharm Res 1997;14:742–749.
16. Hong K, Zheng W, Baker A, Papahadjopoulos D. Stabilization of cationic liposome-plasmid DNA complexes by polyamines and poly(ethylene glycol)-phospholipid conjugates for efficient in vivo gene delivery. FEBS Lett 1997;400:233–237.
17. Song YK, Liu F, Chu S, Liu D. Characterization of cationic liposome-mediated gene transfer in vivo by intravenous administration. Hum Gene Ther 1997;8:1585–1594.
18. Shi N, Pardridge WM. Noninvasive gene targeting to the brain. Proc Natl Acad Sci USA 2000;97:7567–7572.
19. Huwyler J, Wu D, Pardridge WM. Brain drug delivery of small molecules using immunoliposomes. Proc Natl Acad Sci USA 1996;93:14164–14169.
20. Zhang Y, Schlachetzki F, Li JY, Boado RJ, Pardridge WM. Global non-viral gene transfer to the primate brain following intravenous administration. Mol Ther 2003;7:11–18.
21. Coloma MJ, Lee HJ, Kurihara A, et al. Transport across the primate blood-brain barrier of a genetically engineered chimeric monoclonal antibody to the human insulin receptor. Pharm Res 2000;17:266–274.
22. Shi N, Zhang Y, Boado RJ, Zhu C, Pardridge WM. Brain-specific expression of an exogenous gene following intravenous administration. Proc Natl Acad Sci 2001;98:12754–12759.
23. Zhang Y, Schlachetzki F, Li JY, Boado RJ, Pardridge WM. Organ-specific gene expression in the Rhesus monkey eye following intravenous non-viral gene transfer. Mol Vis 2003;9:465–472.
24. Kitayama K, Abe M, Kakizaki T, et al. Purkinje cell-specific and inducible gene recombination system generated from C57BL/6 mouse ES cells. Biochem Biophys Res Commun 2001;281:1134–1140.
25. Izsvak Z, Ivics Z, Plasterk RH. Sleeping beauty, a wide host-range transposon vector for genetic transformation in vertebrates. J Mol Biol 2000;302:93–132.
26. Cavazzana-Calvo M, Hacein-Bey S, de Saint Basile G, et al. Gene therapy of human severe combined immunodeficiency (SCID)-X1 disease. Science 2000;288:669–672.
27. Zhang Y, Zhu C, Pardridge WM. Antisense gene therapy of brain cancer with an artificial virus gene delivery system. Mol Ther 2002;6:67–72.
28. Zhang Y, Calon F, Zhu C, Boado RJ, Pardridge WM. Intravenous nonviral gene therapy causes normalization of striatal tyrosine hydroxylase and reversal of motor impairment in experimental parkinsonism. Hum Gene Ther 2003;14:1–12.
29. Zhang YF, Boado RJ, Pardridge WM. Absence of toxicity of chronic weekly intravenous gene therapy with pegylated immunoliposomes. Pharm Res 2003;20:1779–1785.
30. Yamaguchi A, Katsuyama K, Suzuki K, Kosaka K, Aoki I, Yamanaka S. Plasmid-based gene transfer ameliorates visceral storage in a mouse model of Sanhoff disease. J Mol Med 2003;81:185–193.
31. Leone P, Janson CG, McPhee SJ, During MJ. Global CNS gene transfer for a childhood neurogenetic enzyme deficiency: Canavan disease. Curr Opin Mol Ther 1999;1:487–492.
32. Janson C, McPhee S, Bilniuk L, et al. Gene therapy of Canavan disease: AAV-2 vector for neurosurgical delivery of aspartoacylase gene (ASPA) to the human brain. Hum Gene Ther 2002;13:1391–1412.
33. Xia XG, Zhou H, Ding H, Affar EB, Shi Y, Xu Z. An enhanced U6 promoter for synthesis of short hairpin RNA. Nucl Acids Res 2003;31: e100.
34. Tenenbaum L, Chtarto A, Lehtonen E, et al. Neuroprotective gene therapy for Parkinson's disease. Curr Gene Ther 2002;2:451–483.
35. Siderowf A, Stern M. Update on Parkinson disease. Ann Intern Med 2003;138:651–658.
36. Kordower JH. In vivo gene delivery of glial cell line-derived neurotrophic factor for Parkinson's disease. Ann Neurol 2003;53:S120–S134.
37. Lam PYP, Breakefield XA. Potential of gene therapy for brain tumors. Hum Mol Genet 2001;10:777–787.
38. Lang FF, Bruner JM, Fuller GN, et al. Phase I trial of adenovirus-mediated p53 gene therapy for recurrent gliomas: biological and clinical results. J Clin Oncol 2003;21:2508–2518.

39. Lebedeva IV, Su ZZ, Sarkar D, Fisher PB. Restoring apoptosis as a strategy for cancer gene therapy: focus on p53 and mda-7. Semin Cancer Biol 2003;13:169–178.
40. Mischel PS, Cloughesy TF. Targeted molecular therapy of GBM. Brain Pathol 2003;13:52–61.
41. Baker D, Hankey DJR. Gene therapy in autoimmune, demyelinating disease of the central nervous system. Gene Ther 2003;10:844–853.
42. Chaum E, Hatton M. Gene therapy for genetic and acquired retinal diseases. Surv Ophthalmol 2002;47:449–469.
43. Zhang Y, Boado RJ, Pardridge WM. In-vivo knock-down of gene expression in brain cancer with intravenous RNAi in adult rats. J Gene Med 2003;5:1039–1045.
44. Gossen M, Freundlieb S, Bender G, et al. Transcriptional activation by tetracyclines in mammalian cells. Science 1995;268:1766–1769.

THE JOURNAL OF GENE MEDICINE
J Gene Med 2004; **6**: 906–912.
Published online 30 March 2004 in Wiley InterScience (www.interscience.wiley.com). **DOI:** 10.1002/jgm.575

RESEARCH ARTICLE

Organ-specific expression of the lacZ gene controlled by the opsin promoter after intravenous gene administration in adult mice

Chunni Zhu
Yun Zhang
Yu-feng Zhang
Jian Yi Li
Ruben J. Boado
William M. Pardridge*

Department of Medicine, UCLA, Los Angeles, CA 90024, USA

*Correspondence to:
William M. Pardridge, UCLA, Warren Hall 13-164, 900 Veteran Avenue, Los Angeles, CA 90024, USA.
E-mail:
wpardridge@mednet.ucla.edu

Received: 21 October 2003
Revised: 18 January 2004
Accepted: 19 January 2004

Abstract

Background The tissue-specific expression of an exogenous gene, under the influence of a tissue-specific promoter, has been examined in the past with pro-nuclear injections of the transgene and the development of transgenic mouse models. 'Adult transgenics' is possible with the acute expression of an exogenous gene that is administered to adult animals, providing the transgene can be effectively delivered to distant sites following an intravenous administration.

Methods The organ specificity of exogenous gene expression in adult mice was examined with a bacterial β-galactosidase (LacZ) expression plasmid under the influence of the bovine rhodopsin gene promoter. The 8-kb plasmid DNA was delivered to organs following an intravenous administration with the pegylated immunoliposome (PIL) non-viral gene transfer technology. The PIL carrying the gene was targeted to organs with the rat 8D3 monoclonal antibody (MAb) to the mouse transferrin receptor (TfR).

Results The rhodopsin/β-galactosidase gene was expressed widely in both the eye and the brain of adult mice, but was not expressed in peripheral tissues, including liver, spleen, lung, or heart. Ocular expression included the retinal-pigmented epithelium, the iris, and ciliary body, and brain expression was observed in neuronal structures throughout the cerebrum and cerebellum.

Conclusions The expression of trans-genes in adult animals is possible with the PIL non-viral gene transfer method. The opsin promoter enables tissue-specific gene expression in the eye, as well as the brain of adult mice, whereas gene expression in peripheral tissues, such as liver or spleen, is not observed.

Keywords brain; gene therapy; non-viral gene transfer; rhodopsin; liposomes; transferrin receptor

Introduction

Tissue-specific gene expression in the brain under the influence of a specific promoter is generally examined with transgenic mice following pro-nuclear injection of the gene and development of the embryo into mature animals. The expression of trans-genes in adult animals within 24 h is possible with intravenous administration and non-viral gene targeting technology. A new approach to non-viral gene transfer encapsulates plasmid DNA inside pegylated immunoliposomes (PILs) [1].

The PIL gene transfer technology has been used in adult mice, rats, and adult rhesus monkeys [2–4]. The non-viral plasmid DNA is encapsulated in the interior of an 85-nm liposome, and the surface of the liposome is conjugated with several thousand strands of 2000 Da poly(ethylene glycol) (PEG). This pegylation of the liposome stabilizes the nanocontainer *in vivo*, and allows for prolonged blood residence time [5]. The pegylated liposome is targeted across biological barriers in the brain using targeting ligands that are conjugated to the tips of 1–2% of the PEG strands. The targeting ligand may be an endogenous peptide or a peptidomimetic monoclonal antibody (MAb) that targets a cell surface receptor, and enables transport of the PIL across the membrane barrier. For gene targeting to the brain, the PIL must be delivered across both the brain capillary endothelial wall, which forms the blood-brain barrier (BBB) *in vivo*, and the brain cell plasma membrane. The transferrin receptor (TfR) is expressed at both the BBB [6] and the brain cell membrane [7]. Peptidomimetic MAbs that target the TfR enable the transport of PILs into brain cells in either rats or mice *in vivo* following intravenous administration [2,3]. Peptidomimetic MAbs that target the human insulin receptor (HIR) enable global gene expression within the adult rhesus monkey brain following an intravenous injection [4]. The exogenous gene is expressed in brain 24–48 h after gene administration.

The use of brain-specific promoters, such as the 5′-flanking sequence (FS) of the glial fibrillary acidic protein (GFAP) gene, enables brain-specific gene expression, and eliminates expression of the transgene in non-brain organs following intravenous administration [2]. In searching for other promoters that may allow for brain-specific expression of exogenous genes, the present studies examine the specificity of tissue expression of the lacZ gene that is regulated by the opsin promoter. Transgenic mice expressing the lacZ gene under the influence of the bovine opsin promoter demonstrate expression of the transgene in brain as well as structures of the eye [8]. This finding is consistent with other work showing that opsin genes are expressed in the central nervous system (CNS) [9], and that brain produces proteins that bind to the opsin promoter [10]. The present studies describe the production of PILs carrying an expression plasmid encoding the lacZ gene under the influence of the bovine opsin promoter. The PIL is injected intravenously and is targeted to brain and other organs in adult mice *in vivo* with the rat 8D3 MAb to the mouse TfR as the targeting ligand on the PIL. Gene expression in brain, eye, and peripheral tissues is measured with β-galactosidase histochemistry.

Materials and methods

Materials

Adult female BALB/c albino mice (25–30 g) were purchased from Harlan (Indianapolis, IN, USA). The β-galactosidase staining kit was purchased from Invitrogen (San Diego, CA, USA). The 8D3 hybridoma line, secreting a rat IgG to the mouse transferrin receptor, was obtained from Dr. Britta Engelhardt (Max Planck Institute, Bad Nauheim, Germany), and the 8D3 MAb was purified as described previously [2]. The 1D4 mouse monoclonal antibody against bovine rhodopsin [11] was obtained from Dr. Dean Bok (UCLA School of Medicine, Los Angeles, CA, USA). The vector mouse-on-mouse (M.O.M.) immunodetection kit, the 3-amino-9-ethylcarbazole (AEC) substrate kit for peroxidase and hematoxylin QS counter-stain were purchased from Vector Laboratories (Burlingame, CA, USA). Tissue-Tek embedding compound was purchased from Sakura FineTek (Torrance, CA, USA). All other reagents were purchased from Sigma (St Louis, MO, USA).

LacZ expression plasmid

The LacZ expression plasmid under the influence of the bovine rhodopsin promoter is designated rhodopsin/β-galactosidase, and was provided by Dr. Don Zack (Johns Hopkins University), and has been described previously [8]. This 8-kb plasmid includes nucleotides −2174 to +70 of the bovine rhodopsin gene. The presence of this portion of the bovine rhodopsin promoter within the plasmid was confirmed by DNA sequencing using a M13 reverse sequencing primer followed by custom sequencing primers. Digestion of the rhodopsin/β-galactosidase plasmid with BamHI released the 3.0-kb insert from the 5.0-kb vector backbone. In addition, the lacZ expression plasmid under the influence of the SV40 promoter, pSV-β-galactosidase (Promega), was encapsulated in 8D3 PILs, as described previously [12].

In vivo administration of PILs

The preparation of the 8D3 PIL carrying β-galactosidase expression plasmids has been described previously [2,12]. The liposome is 85–100 nm in diameter and the surface of the liposome is conjugated with several thousand strands of 2000 Da poly(ethylene glycol) (PEG). The tips of about 1–2% of the PEG strands are conjugated with the rat 8D3 MAb to the mouse TfR. Any plasmid DNA not encapsulated in the interior of the liposome is quantitatively removed by exhaustive nuclease treatment [5]. In a typical synthesis, 21% of the initial plasmid DNA (200 μg) was encapsulated within 20 μmol of lipid, and each liposome had on average 48 8D3 MAb molecules conjugated to the PEG strands.

Female BALB/c mice of 25–30 g body weight were anesthetized with ketamine (50 mg/kg) and xylazine (4 mg/kg) intraperitoneally. Experimental animals were injected intravenously through the jugular vein with 8D3 PIL carrying either the rhodopsin/β-galactosidase or the pSV-β-galactosidase plasmid DNA; the injection dose was 5 μg DNA/per mouse. In some animals, the 8D3-targeting MAb was replaced with a control rat IgG that does not

recognize the TfR, as described previously [2,12]. Mice injected with the 8D3 PIL or rat IgG PIL were sacrificed at 48 h after the single intravenous injection of the gene. A total of 12 adult mice were used for this study. Organs were removed and frozen in OCT embedding medium on dry ice and stored at −70 °C.

β-Galactosidase histochemistry

β-Galactosidase histochemistry was performed on frozen sections of organs as described previously [2]. Frozen sections of 18 μm thickness were cut on an HM505 microtome cryostat (Micron Instruments, San Diego, CA, USA), and fixed with 0.5% glutaraldehyde in 0.01 M phosphate-buffered saline (PBS, pH 7.4) for 5 min. After washing in PBS, sections were incubated in X-gal staining solution (4 mM potassium ferricyanide, 4 mM potassium ferrocyanide, 2 mM $MgCl_2$ and 1 mg/ml X-gal, pH 7.4) at 37 °C overnight, where X-gal = 5-bromo-4-chloro-3-indoyl-β-D-galactoside. The pH of the incubation was maintained at 7.4 throughout the incubation. After the staining with X-gal, sections were briefly washed in distilled water. Eye sections were lightly counter-stained with hematoxylin, whereas sections of brain, liver, spleen, heart, lung or kidney were not counter-stained. Frozen sections of mouse kidney were also processed in the histochemistry assay. Kidneys from control, uninjected mice express endogenous β-galactosidase-like enzyme activity that is active at neutral pH [3]. Therefore, including kidney sections in the β-galactosidase histochemistry assay serves as a positive internal control, and indicates the absence of histochemical product in other organs represents a lack of β-galactosidase gene expression in that organ.

Immunohistochemistry

Immunohistochemistry for rhodopsin was performed with the avidin-biotin immunoperoxidase method (Vector Labs, Burlingame, CA, USA). Frozen sections of the eyes were fixed in 2% paraformaldehyde for 20 min at 4 °C, and immunocytochemistry with the 1D4 MAb to rhodopsin was performed as described previously [12].

Results

The β-galactosidase histochemistry of brain, heart, spleen, lung, liver, and kidney is shown in Figure 1 at 48 h after the intravenous injection of 5 μg/mouse of plasmid DNA encapsulated in the PIL targeted with the rat 8D3 MAb to the mouse TfR. The lacZ gene is expressed in brain, but not in heart, spleen, lung, or liver. The β-galactosidase histochemical product in kidney does not represent exogenous gene expression, but rather demonstrates that kidney contains high amounts of endogenous β-galactosidase that is active at neutral pH [2,3]. Kidney

Figure 1. β-Galactosidase histochemistry in multiple organs of adult mice sacrificed 48 h after intravenous administration of 5 μg/mouse of the rhodopsin-lacZ plasmid encapsulated in a PIL targeted with the rat 8D3 MAb to the mouse TfR. The kidney histochemistry is a positive control of the assay, as the kidney of normal mice not injected with the transgene normally expresses high amounts of β-galactosidase that is active at neutral pH

β-galactosidase histochemistry serves as a positive control for the assay. The presence of histochemical product in kidney indicates the negative histochemical signal in heart, spleen, lung, or liver, is not a methologic problem

related to the histochemical assay, but is indicative of a lack of lacZ gene expression in these tissues.

The lacZ gene under the influence of the bovine opsin promoter is widely expressed in the mouse CNS, as shown by serial coronal sections (Figure 2). In the rostral diencephalon, lacZ gene expression is seen in the choroid plexus, the motor cortex, the thalamus/hypothalamus, and gene expression is particularly dense at the base of the brain in the region of the suprachiasmatic nucleus (SCN), which is adjacent to the third ventricle. In the rostral mesencephalon, lacZ gene expression is seen in the visual cortex, the hippocampus, the pontine gray matter, and the periaqueductal gray. In the caudal mesencephalon, lacZ expression is high in gray matter structures of the cortex, and is minimal in white matter structures of the external capsule; lacZ expression is also seen in the periaqueductal gray regions. In the rostral cerebellum, lacZ expression is high in the Purkinje cell layer and in the pons. Light microscopy of selected brain regions shows high lacZ expression in the SCN and lateral hypothalamus around the third ventricle (Figure 3A), the hippocampal dentate gyrus (Figure 3B), the hippocampal statum pyramidale (Figure 3C), the visual cortex (Figure 3D), the Sylvian aqueduct (Figure 3E), and the Purkinje cell layer of the cerebellum (Figure 3F).

The lacZ gene driven by the bovine opsin promoter is expressed in the outer retina, the iris, and the ciliary body of the eye when the PIL is targeted with the TfRMAb (Figure 4A). However, there is no lacZ gene expression in the eye when the PIL is targeted with a control isotype rat IgG (Figure 4B). Light microscopy of β-galactosidase histochemistry in the region of the outer retina is shown in Figure 4C for animals injected with the rhodopsin/β-galactosidase plasmid and in Figure 4E for animals injected with the pSV-β-galactosidase plasmid. Parallel sections were also taken for rhodopsin immunocytochemistry, as shown in Figure 4D. Rhodopsin immunoreactivity is detected in the outer segments (OS) of the retina, but not in the retinal-pigmented epithelium (RPE), the inner segments (IS), or the outer nuclear layer (Figure 4D). The parallel β-galactosidase histochemistry (Figure 4C) and the rhodopsin immunocytochemistry (Figure 4D) show that the lacZ gene is expressed only in the RPE of the mouse retina, and not in the outer nuclear layer or inner and outer segments of the retinal photoreceptor cells, following injection of 8D3 PILs carrying the rhodopsin/β-galactosidase plasmid DNA. Similarly, lacZ gene expression is confined to the RPE following injection of 8D3 PILs carrying the pSV/β-galactosidase plasmid DNA (Figure 4E).

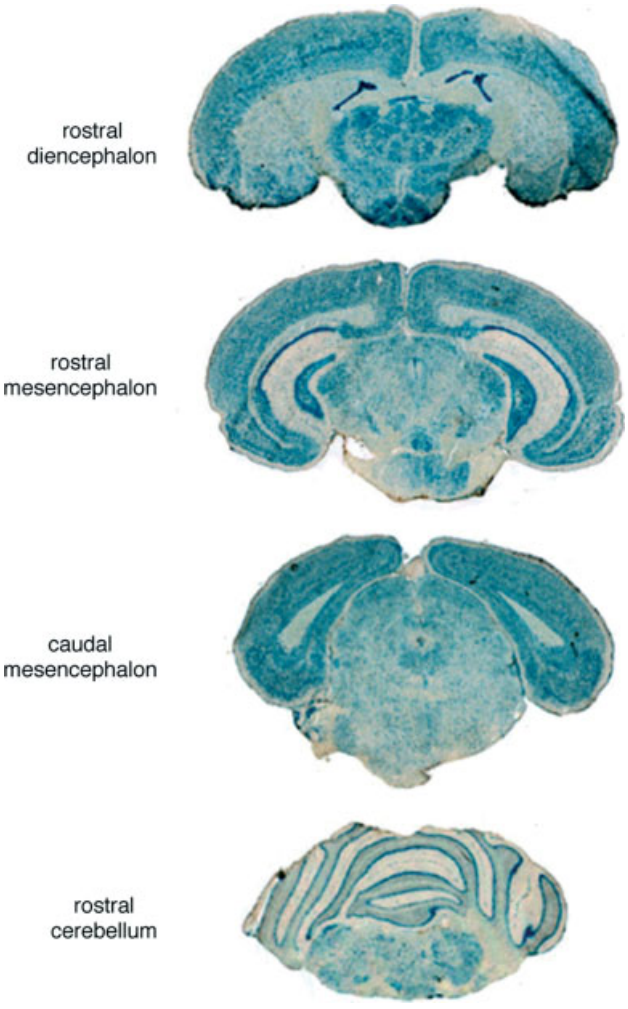

Figure 2. β-Galactosidase histochemistry in mouse brain 48 h after intravenous administration of 5 μg/mouse of the rhodopsin-lacZ plasmid encapsulated in a PIL targeted to brain with the 8D3 MAb to the mouse TfR. Sections through the rostral diencephalon, the rostral mesencephalon, the caudal mesencephalon, and the rostral cerebellum are shown

Discussion

The results of these studies are consistent with the following conclusions. First, the lacZ gene driven by the bovine opsin promoter is selectively expressed in mouse brain and eye following intravenous expression, but not in peripheral tissues such as liver, spleen, heart, or lung (Figure 1). Second, structures of the brain expressing the lacZ gene under the influence of the opsin promoter include neuronal structures in the cerebral cortex (Figure 2), the hippocampus and cerebellum (Figure 3), and the epithelium lining the choroid plexus (Figure 2) or the Sylvian aqueduct (Figure 3E). Third, the lacZ gene under the influence of the opsin promoter is expressed in ocular structures of the mouse including the RPE, the iris, and ciliary body (Figure 4).

Gene expression in organs such as heart or lung is not expected following intravenous administration of TfRMAb-targeted PILs, because these organs have capillaries with continuous endothelial barriers that do not express significant levels of the TfR [3]. The circulating PIL is too large to non-specifically cross the continuous endothelial barrier, and cannot access the parenchymal cells in organs such as heart or lung

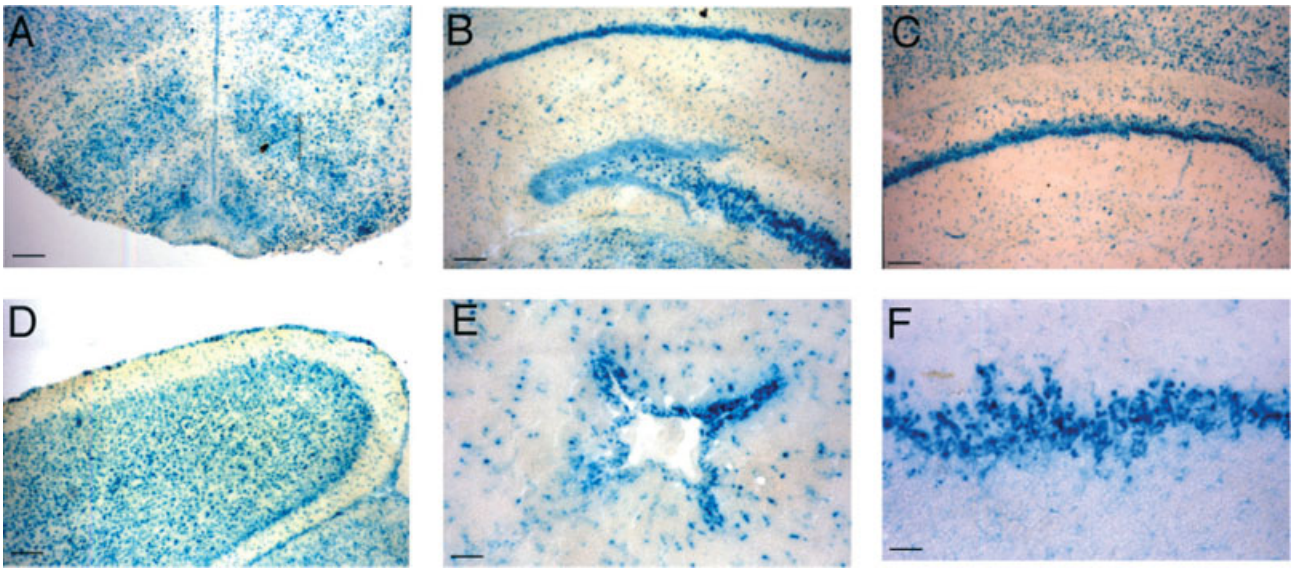

Figure 3. Light microscopy of β-galactosidase histochemistry of mouse brain 48 h after intravenous administration of the rhodopsin-lacZ plasmid shows selective gene expression in the suprachiasmatic nucleus and lateral hypothalamus around the third ventricle (A), the dentate gyrus of the hippocampus (B), the hippocampal stratum pyramidale (C), the visual cortex (D), the epithelium lining the Sylvian aqueduct (E), and cells of the Purkinje cell layer (F). Magnification bar: 125 μm (A–D) and 28 μm (E, F)

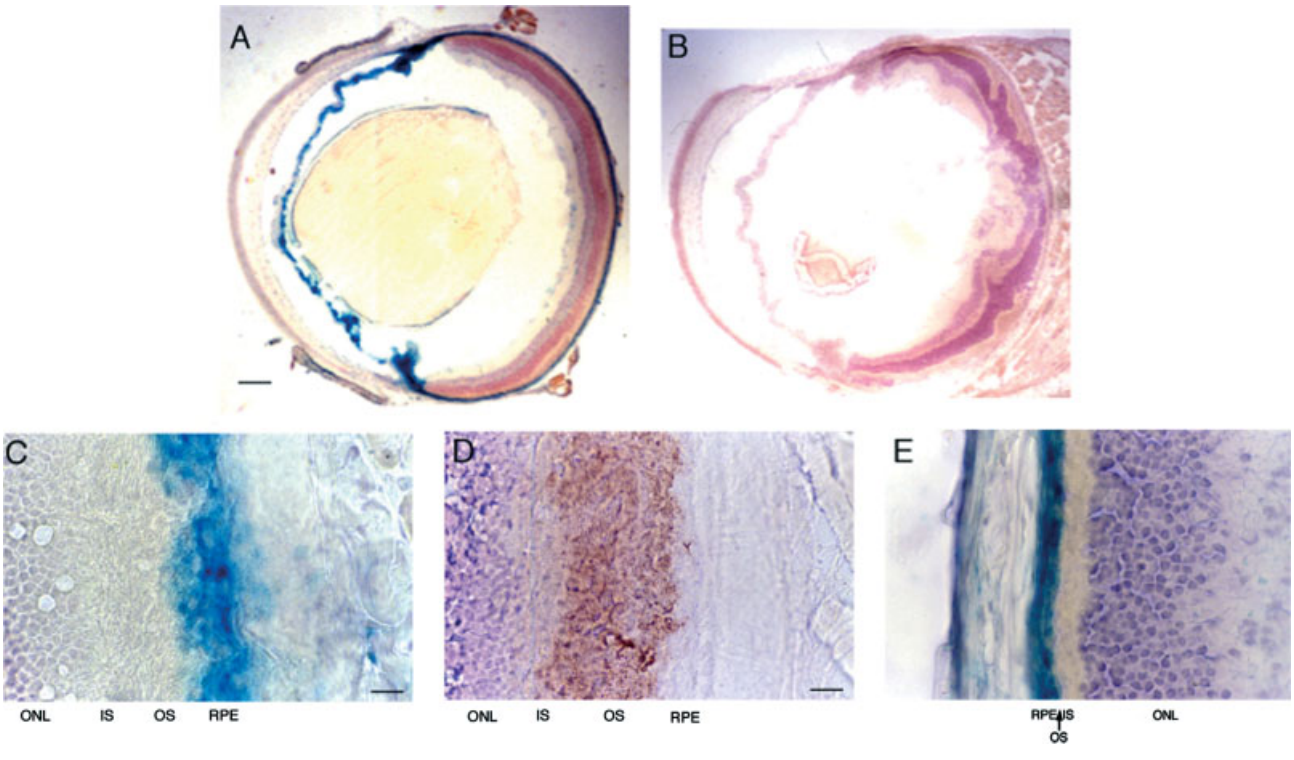

Figure 4. β-Galactosidase histochemistry (A, B, C, E) and rhodopsin immunocytochemistry (D) in the eye of mice at 48 h after intravenous injection of 5 μg/mouse of the lacZ plasmid encapsulated in a PIL targeted with either the rat 8D3 MAb to the mouse TfR (A, C, D), or the rat IgG isotype control antibody (B); the lacZ expression plasmid was under the influence of either the bovine rhopsin promoter (A–D) or the SV40 promoter (E). (A) The principal sites of rhodopsin promoter-lacZ gene expression in the eye are the outer retina, iris, and ciliary body when the PIL is targeted to the eye with the TfRMAb. (B) When the PIL carrying the lacZ gene is targeted to the eye with a rat IgG isotype control antibody, which does not recognize any receptor, there is no lacZ histochemical product in the eye. (C, D) Comparison of the β-galactosidase histochemistry (C) and the rhodopsin immunocytochemistry (D) shows the lacZ gene is not expressed in the photoreceptor cells of the retina, which includes the outer nuclear layer (ONL), the inner segments (IS), and the outer segments (OS). The lacZ gene is expressed in the retinal-pigmented epithelium (RPE). The localization of lacZ gene expression to the RPE is comparable for either the rhodopsin promoter (C) or the SV40 promoter (E). Magnification bar: 210 μm (A) and 10 μm (C, D)

with continuous endothelium lacking endothelial TfR. In contrast, organs such as liver or spleen are perfused by sinusoidal microvasculatures that are highly porous. The PIL freely crosses the microvascular barrier in organs with sinusoidal microcirculations and enters the parenchymal space of organs such as liver or spleen. The parenchymal cells in liver or spleen express TfR, which allows for cellular uptake of the PIL. This uptake is followed by expression of the exogenous gene encapsulated within the PIL, providing the gene is under the influence of a widely expressed promoter such as the SV40 promoter [3,4]. However, the present studies show that if the lacZ gene is under the influence of an opsin promoter, there is no measurable gene expression in liver or spleen. Similar findings were reported when the lacZ gene was under the influence of the human GFAP promoter [2]. These observations suggest that the trans-acting factors that activate the opsin or GFAP promoter are not expressed in peripheral organs such as liver or spleen.

The lacZ gene under the influence of the opsin promoter is expressed in brain following the intravenous injection of the TfRMAb-targeted PIL carrying the expression plasmid (Figures 2 and 3). This observation is consistent with previous work showing that there is a family of opsin genes, and that opsin genes are expressed in the CNS. Encephalopsin is expressed in brain and particularly in the Purkinje cell layer [9]. The encephalopsin gene is homologous with the retinal opsin gene. Brain of certain species produces proteins that bind to the rhodopsin promoter [10], which is in accord with the finding of the present study that the lacZ gene under the influence of the rhodopsin promoter is expressed in mouse brain. The results of this study reproduce the findings reported previously in transgenic mice, wherein the lacZ gene under the influence of the rhodopsin promoter is expressed in transgenic mouse brain [8]. However, the lacZ gene under the influence of the bovine rhodopsin promoter is not expressed in adult rhesus monkey brain [13]. This observation suggests that the brain of higher animals may not express proteins that activate the rhodopsin promoter. The present studies in adult mice show that an exogenous gene under the influence of the bovine rhodopsin promoter, and administered intravenously, is widely expressed throughout the CNS. There is higher gene expression in gray matter as compared with white matter, and the gene is expressed in structures of both the neocortex and the paleocortex (Figures 2 and 3).

In the eye, the expression of the lacZ gene under the influence of the bovine opsin promoter is primarily expressed in the RPE, the iris, and the ciliary body, and to a lesser extent in the iridocorneal angle, the corneal endothelium, the inner retina, the lens capsule, the conjunctiva, as well as scattered cells in the ganglion cell layer of the inner retina (Figure 4A). Comparison of the β-galactosidase histochemistry with rhodopsin immunocytochemistry (Figure 4C-D) indicates the lacZ transgene is not expressed in the photoreceptor cells of the mouse eye following delivery with TfRMAb-targeted PILs. The failure to detect lacZ gene expression in the photoreceptor cells is due to the minimal TfR expression in the outer nuclear layer (ONL) [12]. The minimal expression of the TfR in the ONL of the retina parallels the very low level of iron and ferritin within this part of the retina [14]. Similarly, when the lacZ gene was targeted to adult mouse retina under the influence of the widely expressed SV40 promoter, no gene expression in the photoreceptor cells was observed [12], and this finding is replicated in the present study (Figure 4E). In contrast, high expression of the lacZ gene under the influence of either the SV40 promoter or the rhodopsin promoter is observed in the photoreceptor cells of the adult rhesus monkey 48 h after the intravenous injection of the plasmid encapsulated in PILs targeted with an MAb to the HIR [13]. The exogenous gene was expressed in the cell bodies of the ONL, and in the outer and inner segments of the photoreceptor cells of the primate retina [13]. Although the cell bodies of the photoreceptor cells have minimal expression of the TfR, these structures do express the insulin receptor [13,15]. The differential expression of the TfR and insulin receptor in the ONL may account for the selective expression of exogenous genes in the photoreceptor cells following delivery to the eye with targeting ligands that bind to either the insulin receptor or the TfR. These findings indicate the expression of an exogenous gene in a target organ is a function of both the (a) receptor specificity of the targeting ligand, and (b) tissue specificity of the promoter regulating expression of the trans-gene. If the tissue does not express either the targeted receptor or trans-acting factors that bind to the gene promoter, then there is minimal expression of the trans-gene in tissues following intravenous administration in adult animals.

The lacZ gene under the influence of the bovine rhodopsin promoter is highly expressed in the iris and ciliary body of the adult mouse eye, as well as the corneal endothelium and lens capsule (Figure 4A). These findings parallel observations made in transgenic mice expressing the lacZ gene under the influence of the bovine rhodopsin promoter, where gene expression in the iris and ciliary body was observed [8]. The iris or ciliary body is embryologically related to the photoreceptor cells of the retina. Transfection of iris and ciliary body with the Crx homeobox gene expressed in photoreceptor cells results in synthesis of rhodopsin in the non-photoreceptor structures of the eye [16]. The expression of the lacZ gene under the influence of the rhodopsin promoter in multiple structures of the eye is consistent with prior work showing the TfR is widely expressed in multiple structures of the eye, including the iris, ciliary body, corneal endothelium, the conjunctival epithelium [17], as well as the RPE, the retinal endothelium, and cells of the inner retina [14]. The TfR is also expressed in cells of the choroid [14], although the TfR expression on endothelium of choroidal capillaries is less than the expression of the TfR on the endothelium of retinal capillaries [18]. The choroidal expression of the TfR is consistent with the detection of lacZ gene expression the choroid layer of the eye (Figure 4E).

In summary, these studies indicate that the opsin promoter, like the GFAP promoter [2], enables tissue-specific gene expression in the CNS of the mouse, and eliminates ectopic expression of the trans-gene in peripheral tissues such as liver or spleen that also express the targeted receptor such as the TfR [3]. The non-viral plasmid DNA is expressed episomally and gene expression is transient, although gene expression in the primate eye is still in the therapeutic range for at least 2 weeks after a single intravenous injection of the gene [13]. While the opsin or GFAP promoters may enable CNS-specific gene expression, these promoters have relatively broad profiles of expression within the CNS, and the exogenous gene is expressed in both cerebral and ocular structures. The discovery of gene promoters that are expressed at a more regional level within the CNS will be necessary to achieve regional expression of exogenous genes within specific structures of the brain or eye.

Acknowledgements

This work was supported by a grant from the Neurotoxin Exposure Treatment Research Program of the U.S. Department of Defense.

References

1. Pardridge WM. Gene targeting in vivo with pegylated immunoliposomes. *Methods Enzymol* 2003; **373**: 507–528.
2. Shi N, Zhang Y, Boado RJ, Zhu C, Pardridge WM. Brain-specific expression of an exogenous gene after i.v. administration. *Proc Natl Acad Sci U S A* 2001; **98**: 12 754–12 759.
3. Shi N, Boado RJ, Pardridge WM. Receptor-mediated gene targeting to the tissues in the rat in vivo. *Pharm Res* 2001; **18**: 1091–1095.
4. Zhang Y, Schlachetzki F, Pardridge WM. Global non-viral gene transfer to the primate brain following intravenous administration. *Mol Ther* 2003; **7**: 11–18.
5. Shi N, Pardridge WM. Non-invasive gene targeting to the brain. *Proc Natl Acad Sci U S A* 2000; **97**: 7567–7572.
6. Pardridge WM, Eisenberg J, Yang J. Human blood-brain barrier transferrin receptor. *Metabolism* 1987; **36**: 892–895.
7. Mash DC, Pablo J, Flynn DD, Efange SMN, Weiner WJ. Characterization and distribution of transferrin receptors in the rat brain. *J Neurochem* 1990; **55**: 1972–1979.
8. Zack DJ, Bennett J, Wang Y, *et al*. Unusual topography of bovine rhodopsin promoter-lacZ fusion gene expression in transgenic mouse retinas. *Neuron* 1991; **6**: 187–199.
9. Blackshaw S, Snyder SH. Encephalopsin: a novel mammalian extraretinal opsin discretely localized in the brain. *J Neurosci* 1999; **19**: 3681–3690.
10. Sheshberadaran H, Takahashi JS. Characterization of the chicken rhodopsin promoter: identification of retina-specific and glass-like protein binding domains. *Mol Cell Neurosci* 1994; **5**: 309–318.
11. MacKenzie D, Arendt A, Hargrave P, McDowell JH, Molday RS. Localization of binding sites for carboxyl terminal specific anti-rhodopsin monoclonal antibodies using synthetic peptides. *Biochemistry* 1984; **23**: 6544–6549.
12. Zhu C, Zhang Y, Pardridge WM. Widespread expression of an exogenous gene in the eye after intravenous administration. *Invest Ophthalmol Vis Sci* 2002; **43**: 3075–3080.
13. Zhang Y, Schlachetzki F, Pardridge WM. Organ-specific gene expression in the rhesus monkey eye following intravenous non-viral gene transfer. *Mol Vis* 2003; **9**: 465–472.
14. Yefimova MG, Jeanny J-C, Guillonneau X, *et al*. Iron, ferritin, transferrin, and transferrin receptor in the adult rat retina. *Invest Opthalmol Vis Sci* 2000; **41**: 2343–2351.
15. Naeser P. Insulin receptors in human ocular tissues: immunohistochemical demonstration in normal and diabetic eyes. *Upsala J Med Sci* 1997; **102**: 35–40.
16. Haruta M, Kosaka M, Kanegae Y, *et al*. Induction of photoreceptor-specific phenotypes in adult mammalian iris tissue. *Nat Neurosci* 2001; **4**: 1163–1164.
17. Baudouin C, Brignole F, Fredj-Reygrobelle D, Negre F, Bayle J, Gastaud P. Transferrin receptor expression by retinal pigment epithelial cells in proliferative vitreoretinopathy. *Invest Ophthalmol Vis Sci* 1992; **33**: 2822–2829.
18. Hofman P, Hoyng P, van der Werf F, Vrensen GFJM, Schlingemann RO. Lack of blood-brain barrier properties in microvessels of the prelaminar optic nerve head. *Invest Ophthalmol Vis Sci* 2001; **42**: 895–901.

Tyrosine Hydroxylase Replacement in Experimental Parkinson's Disease with Transvascular Gene Therapy

William M. Pardridge

Department of Medicine, UCLA, Los Angeles, California 90024

Summary: Transvascular gene therapy of Parkinson's disease (PD) is a new approach to the gene therapy of PD and involves the global distribution of a therapeutic gene to brain after an intravenous administration and transport across the blood-brain barrier (BBB). This is enabled with the development of a nonviral gene transfer technology that encapsulates plasmid DNA inside pegylated immunoliposomes or PILs. An 85- to 100-nm liposome carries the DNA inside the nanocontainer, and the liposome surface is conjugated with several thousand strands of 2000-Da polyethyleneglycol (PEG). This PEGylation of the liposome stabilizes the structure in the blood stream. The liposome is targeted across the BBB via attachment to the tips of 1-2% of the PEG strands of a receptor-specific monoclonal antibody (mAb) directed at a BBB receptor, such as the insulin receptor or transferrin receptor (TfR). Owing to the expression of the insulin receptor or the TfR on both the BBB and the neuronal plasma membrane, the PIL is able to reach the neuronal nuclear compartment from the circulation. Brain-specific expression is possible with the combined use of the PIL gene transfer technology and brain-specific gene promoters. In the 6-hydroxydopamine rat model of experimental PD, striatal tyrosine hydroxylase (TH) activity is completely normalized after an intravenous administration of TfRmAb-targeted PILs carrying a TH expression plasmid. A treatment for PD may be possible with dual gene therapy that seeks both to replace striatal TH gene expression with TH gene therapy, and to halt or reverse neurodegeneration of the nigro-striatal tract with neurotrophin gene therapy. **Key Words:** Blood-brain barrier, liposomes, transferrin receptor, monoclonal antibody, targeting.

INTRODUCTION

Parkinson's disease (PD) affects nearly 1% of the U.S. population over 65 years and nearly 1 million individuals in the U.S.[1] The neurodegeneration of the nigral-striatal tract results in a loss of dopaminergic neurons in the substantia-nigra, a loss of tyrosine hydroxylase containing nerve endings in the striatum, and diminished striatal dopamine production causing abnormal motor behavior.[2] Dopamine replacement therapy with dopamine is not possible in PD because this monoamine does not cross the brain capillary endothelial wall, which forms the blood-brain barrier (BBB) *in vivo*. However, the precursor to dopamine, L-dihydroxyphenylalanine (L-DOPA), does cross the BBB owing to transport via the BBB large neutral amino acid transporter, which is expressed by the LAT1 gene.[3] After its transport across the BBB, L-DOPA is decarboxylated to dopamine by aromatic amino acid decarboxylase (AAAD). The rate-limiting step in cerebral production of dopamine is normally the conversion of tyrosine to L-DOPA via tyrosine hydroxylase (TH).

L-DOPA replacement therapy has been the mainstay of Parkinson's treatment for 40 years. However, L-DOPA therapy is not without complications. Owing to ubiquitous expression of both AAAD in brain and LAT1 at the BBB, circulating L-DOPA is converted to dopamine throughout all parts of the brain including the striatum. Dopamine is an inhibitory neurotransmitter, and the ectopic production throughout the brain has side effects. An alternative approach to dopamine replacement therapy in PD is TH gene therapy, wherein an exogenous TH gene is expressed only in the circumscribed regions of the brain forming the dopaminergic nerve tracts.

OVERVIEW OF GENE THERAPY IN PARKINSON'S DISEASE

There are dual goals of gene therapy in PD: 1) replace striatal TH and 2) halt or even reverse the neurodegeneration of nigral-striatal neurons. The latter can be accomplished with local expression of neuroprotective neurotrophins such as glial-derived neurotrophic factor

Address correspondence and reprint requests to William M. Pardridge, M.D., Department of Medicine, UCLA Warren Hall 13-164, 900 Veteran Avenue, Los Angeles, CA 90024. E-mail: wpardridge@mednet.ucla.edu.

(GDNF).[4] The current approach to gene therapy of PD, and gene therapy of brain disorders in general, is the combined use of craniotomy as a delivery system, and viral vectors as a gene expression system. The transcranial injection of viral gene therapy vectors is clearly effective, including primate models, and allows for the local production of therapeutic genes.[4] The single injection into the human or animal brain of either adenovirus or herpes simplex virus results in inflammatory reaction leading to astrogliosis and demyelination,[5,6] and more recent viral gene therapy approaches employ either adeno-associated virus (AAV) or retrovirus. AAV vectors generally need to be given at some repeat intervals, and 90% of the human population has a pre-existing immunity to AAV.[7] Both AAV and retrovirus permanently and randomly integrate into the host genome.[8,9] Neither AAV nor retrovirus crosses the BBB. Therefore, it is necessary to administer the virus via craniotomy and an intracerebral injection. However, the most intense expression of the therapeutic gene is generally limited to the injection site, owing to limited diffusion of the virus within the brain. The treatment volume can be increased with convection-enhanced diffusion (CED). However, a recent study of CED in the primate brain shows an astrogliotic reaction over the entire region of the primate brain that is perfused during the CED procedure.[10] Current limitations of brain gene therapy approaches can be eliminated with the development of a transvascular delivery approach to gene therapy. However, this would require the formulation of plasmid DNA in such a way that the exogenous gene was able to cross the BBB and enter brain via the transvascular route after an intravenous injection. This is now possible with the use of a pegylated immunoliposomes that target genes across the BBB with receptor-specific molecular Trojan horses.[11]

PEGYLATED IMMUNOLIPOSOMES—A NEW APPROACH TO TRANSVASCULAR GENE THERAPY OF THE BRAIN

Exogenous genes incorporated in plasmid DNA can be widely distributed throughout the entire brain after an intravenous injection with the use of a new form of transvascular gene transfer technology that uses pegylated immunoliposomes, or PILs. The plasmid DNA is encapsulated in the interior of a 100-nm liposome.[12] The surface of the liposome is decorated with several thousand strands of 2000-Da polyethyleneglycol (PEG), and this pegylation process alters the surface of the liposome such that the liposome is not rapidly cleared by the reticulo-endothelial system after an intravenous administration. The pegylated liposome is relatively inert and does not cross the BBB.[13] However, transvascular transport of the PIL can be induced by conjugating receptor specific monoclonal antibodies (mAbs) to the tips of 1-2% of the PEG tails so that each 100-nm liposome is conjugated with approximately 50 mAb molecules.[12,13] A drawing of a PIL is shown in Figure 1A. An actual PIL is visualized with electron microscopy as shown in Figure 1B. In this study, a conjugate of 10 nm gold and a secondary antibody was attached to the surface of the PIL to demonstrate the relationship of the targeting mAb to the surface of the PIL.[14] The size of a 10-nm gold particle is approximately the size of the targeting mAb, as depicted in Figure 1B. The plasmid DNA is encapsulated in the interior of the liposome, which renders the DNA insensitive to the ubiquitous exo- and endonucleases in the circulation.[12]

The PIL is to be contrasted with conventional cationic liposomes that are a mixture of anionic DNA and a cationic polymer. Cationic liposome/DNA complexes are unstable in blood, aggregate in a saline environment, and are more than 99% cleared by the pulmonary circulation after a single intravenous injection.[15,16] Cationic liposomes do not distribute to the brain after an intravenous administration.[17]

PILs act as an artificial virus in that the PILs are approximately the same size as a virus, the DNA is contained inside the nanocontainer, and the surface of the nanocontainer has proteins that trigger uptake across membrane barriers. The targeting component of the PIL is a receptor-specific mAb that is conjugated to the tips of 1-2% of the PEG strands on the liposome surface.[12] The transferrin receptor (TfR) or the insulin receptor are expressed at both the BBB and on neuronal cell membranes. Therefore, a PIL, targeted with a mAb to either the TfR or the insulin receptor, is able to undergo sequential receptor-mediated transcytosis across the BBB, followed by receptor-mediated endocytosis into neurons.[18,19] The PIL rapidly enters the nuclear compartment after endocytosis into the cell, as demonstrated by confocal microscopy.[20] In this study, the plasmid DNA was fluoresceinated with nick translation before encapsulation into PIL. The PIL was targeted to human U87 glioma cells using the murine 83-14 mAb to the human insulin receptor (HIR). The HIRmAb-targeted PIL was added to U87 cells and incubated for 3 or 24 h, followed by fixation and confocal microscopy. As shown in Figure 1C, the DNA is largely confined to the cytoplasmic compartment at 3 h, although DNA is detected within intranuclear vesicular structures at 3 h. By 24 h, virtually all of the intracellular DNA is found in the nuclear compartment (FIG. 1C).

Global expression of transgene in rhesus monkey brain

The intravenous administration of PILs carrying an expression plasmid encoding bacterial β-galactosidase under the influence of the simian virus 40 (SV40) promoter to the adult rhesus monkey leads to global expres-

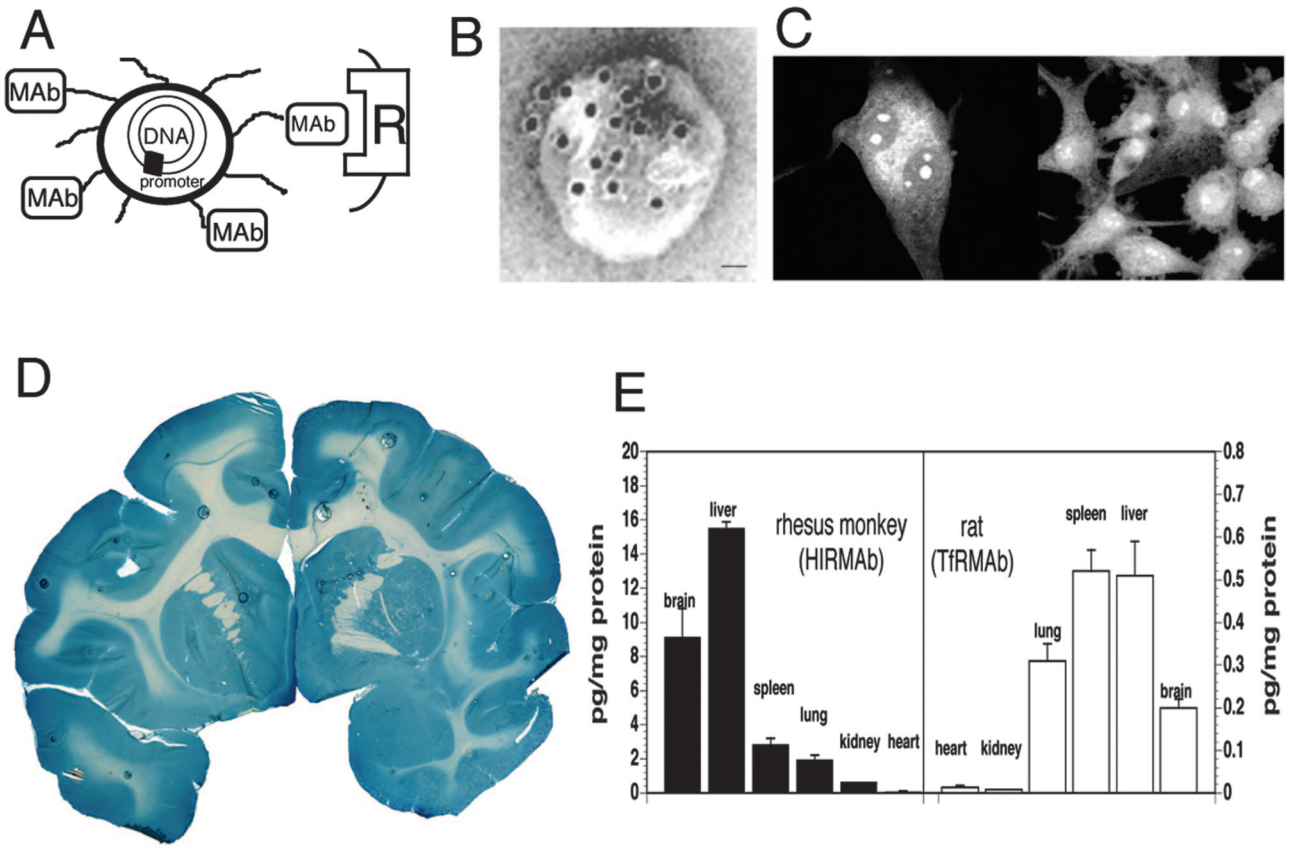

FIG. 1. A: Diagram of a super-coiled expression plasmid DNA encapsulated in an 85 nm pegylated PIL targeted to a cell membrane receptor (R) with a receptor-specific, endocytosing mAb. Tissue-specific expression of the plasmid can be controlled by the promoter inserted 5′ of the gene. Panels A and B are reproduced with permission from Zhang et al. Intravenous nonviral gene therapy causes normalization of striatal tyrosine hydroxylase and reversal of motor impairment in experimental parkinsonism. *Hum Gene Ther* 14:1–12. Copyright © 2003, Mary Ann Leibert, Inc. All rights reserved.[14] B: Transmission electron microscopy of a PIL. The mAb molecule tethered to the tips of the 2000-Da PEG is bound by a conjugate of 10 nm gold and a secondary antibody. The position of the gold particles shows the relationship of the PEG extended mAb and the liposome. Magnification bar = 20 nm.[14] C: Confocal microscopy of U87 human glioma cells after either a 3-h (left panel) or a 24-h (right panel) incubation of fluorescein conjugated clone 882 DNA (fluoro-DNA) encapsulated within HIRmAb-PILs. The inverted grayscale image is shown. There is primarily cytoplasmic accumulation of the fluoro-DNA at 3 h, whereas the fluoro-DNA is largely confined to the nuclear compartment at 24 h. Fluoro-DNA entrapped within intranuclear vesicles is visible at both 3 and 24 h. Panel C is reproduced with permission from Zhang et al. Receptor-mediated delivery of an antisense gene to human brain cancer cells. *J Gene Med* 4:183–194. Copyright © 2002, John Wiley & Sons, Ltd. All rights reserved.[20] D: β-Galactosidase histochemistry of brain removed 48 h after the intravenous injection of a β-galactosidase expression plasmid encapsulated in HIRmAb-PILs in the adult rhesus monkey. Panels D and E are reproduced with permission from Zhang et al. Global non-viral gene transfer to the primate brain following intravenous administration. *Mol Ther* 7:11–18. Copyright © 2003, Academic Press. All rights reserved.[19] E: Luciferase gene expression in the brain and other organs of the adult rhesus monkey (left panel) and adult rat (right panel) measured at 48 h after a single intravenous injection of the PIL carrying the plasmid DNA. Data are mean ± SEM. The plasmid DNA encoding the luciferase gene used in either species is clone 790, which is driven by the SV40 promoter.[19] The PIL carrying the DNA was targeted to primate organs with an HIRmAb and to rat organs with a TfRmAb.[19]

sion of the trans-gene throughout the primate brain as demonstrated in Figure 1D. The PIL was targeted with a mAb to the HIR, and this mAb cross reacts with the Old World primate insulin receptor.[21] There is widespread expression of the transgene throughout the primate brain with a greater enrichment in gray matter relative to white matter (FIG. 1D). Similar findings of global expression of a trans-gene throughout the entire brain after an intravenous injection of PILs has been demonstrated in mice using the rat 8D3mAb to the murine TfR,[18] and in rats using the murine OX26mAb to the rat TfR.[22] The targeting mAbs are species specific, and the 8D3mAb is not effective in rats, and the 83-14 HIRmAb is effective in humans and Old World primates such as rhesus monkeys, but is not effective in New World primates such as squirrel monkeys, and is not effective in rodents. The insulin receptor normally serves to deliver its endogenous ligand, insulin, to the nuclear compartment, and therefore, the insulin receptor is an ideal conduit for gene delivery.[23] Because of this nuclear targeting property of the insulin receptor, levels of gene expression in human cells or Old World primates can be 10- to 50-fold higher than comparable levels of gene expression in rodents,[19,23] as demonstrated for the luciferase reporter gene (FIG. 1E). The luciferase expression plasmid was encapsulated in TfRmAb-targeted PILs and injected into

TABLE 1. *TH Activity in Cultured Rat RG2 Glioma Cells or Human U87 Glioma Cells after Delivery of either SV40 Promoter (clone 877) or GFAP Promoter (Clone 951) TH Expression Plasmid Encapsulated in mAb-Targeted PIL*

	TH Activity (pmol-L-DOPA/h · mg_p)		
Days	Clone 877 in rat RG2 cells	Clone 877 in human U87 cells	Clone 951 in human U87 cells
2	65 ± 7	214 ± 14	231 ± 10
4	375 ± 26	1458 ± 99	1576 ± 33
6	39 ± 9	177 ± 10	311 ± 22

Mean ± SE (n = 3 dishes per time point). PILs carrying either clone 877 or clone 951 are targeted to rat RG2 glioma cells with the TfRmAb and to human U87 glioma cells with the HIRmAb.[14,25]

adult rats, and was separately encapsulated in HIRmAb-targeted PILs and injected into adult rhesus monkeys.[19] The animals were sacrificed 48 h after the intravenous injection for measurements of luciferase enzyme activity in brain and other organs. These studies show that luciferase expression is 50-fold higher in the primate as compared with rat. In addition to brain, the luciferase transgene is expressed in peripheral tissues such as liver or spleen, that also express the TfR or insulin receptor. However, this ectopic expression of the exogenous gene in nonbrain organs can be eliminated with the use tissue-specific gene promoters, as demonstrated for β-galactosidase gene expression in mice[18] or rhesus monkeys,[24] and discussed below in the case of TH gene therapy studies in rats.

TH GENE THERAPY OF EXPERIMENTAL PARKINSON'S DISEASE WITH PEGYLATED IMMUNOLIPOSOMES

Experimental PD was produced in adult rats with the intracerebral injection of a neurotoxin, 6-hydroxydopamine.[14,25] The toxin was injected in the medial forebrain bundle of one side of the rat brain under stereotaxic guidance. Three weeks later, animals were tested with apomorphine, which causes aberrant rotation behavior in those animals with a successful biochemical lesion of the nigral-striatal tract. Before treatment of these animals with TH gene therapy, it is first necessary to synthesize TH expression plasmids. Because one goal of this work was to localize TH gene expression in the brain, two different expression plasmids were produced.[14,25] The first plasmid, designated clone 877, encodes for the rat TH cDNA under the influence of the widely read SV40 promoter.[14] The second expression plasmid, designated clone 951,[25] is identical, except that the SV40 promoter is replaced with 2 kb of the 5′-flanking sequence (FS) of the human GFAP gene. The GFAP gene is expressed only in brain, and not in peripheral tissues. This was demonstrated in initial studies with a β-galactosidase reporter gene. When the β-galactosidase expression plasmid under the influence of the SV40 promoter was encapsulated in TfRmAb-targeted PILs and injected into rodents, the gene was expressed not only in brain, but TfR-rich peripheral organs such as liver or spleen.[22] However, when the β-galactosidase expression plasmid was under the influence of the GFAP promoter, the transgene was expressed only in brain, and ectopic gene expression in peripheral tissues was eliminated.[18]

The biologic activity of clone 877 or clone 951 was initially evaluated in cell culture with either cultured RG2 rat glioma cells or cultured U87 human glioma cells. The TH gene is not expressed in cells unless there is local production of tetrahydrobiopterin, a critical TH cofactor. GTP-cylcohydrolase (GTPCH) is the rate-limiting enzyme in the pathway leading to the production of tetrahydrobiopterin, and cultured rat glioma cells[26] and cancer cell lines[27] produce the GTPCH enzyme, although glial cells in brain do not normally express the GTPCH gene.[28] Both clone 877 and clone 951 produce TH enzyme activity in either cultured rat glioma cells or cultured human U87 glioma cells (Table 1). There is a 5- to 8-fold higher level of TH gene expression in human cells, which are targeted with the HIRmAb, as opposed to TH gene expression in rat glioma cells, which are targeted with the TfRmAb. As noted above in the discussion of Figure 1E, PILs targeted with the insulin receptor normally yield a much higher level of gene expression than that obtained with PILs targeted with the TfRmAb.[19,23]

The TfRmAb-targeted PILs carrying either clone 877 or clone 951 were injected intravenously into adult rats and TH enzyme activity was measured with a radioenzymatic assay at 3 days after a single intravenous injection in rats that had apomorphine-proven 6-hydroxydopamine lesions. The striatal TH was 98% depleted, as indicated by the very low TH level in the saline treated animals in the striatum ipsilateral to the 6-hydroxydopamine injection (Table 2). The control is the contralateral striatum, which shows a more than 50-fold higher level of TH enzyme activity in the same rat brain (Table 2). Both clone 877, the SV40 promoter driven plasmid, and clone 951, the GFAP promoter driven plasmid, were equally effective in restoring striatal TH enzyme activity in the ipsilateral striatum of the lesioned animals.[14,25]

TABLE 2. *TH in Brain and Peripheral Organs in the Rat 3 Days after Intravenous Injection of Gene Therapy*

Organs	Saline (pmol/h/mg_p)	TfRmAb-PIL/877 (pmol/h/mg_p)	TfRmAb-PIL/951 (pmol/h/mg_p)
Ipsilateral striatum	128 ± 27	5177 ± 446*	5536 ± 395*
Contralateral striatum	6445 ± 523	5832 ± 391	5713 ± 577
Ipsilateral cortex	176 ± 30	132 ± 16	184 ± 38
Contralateral cortex	150 ± 36	150 ± 24	135 ± 25
Heart	29 ± 3	45 ± 8	31 ± 3
Liver	13 ± 2	130 ± 28*	18 ± 6
Lung	42 ± 13	74 ± 22	30 ± 6
Kidney	24 ± 2	35 ± 5	31 ± 8

*$p < 0.01$ difference from saline group (ANOVA with Bonferroni correction; n = 4 rats per group). Rats were lesioned with intracerebral injections of 6-hydroxydopamine; 3 weeks after toxin injection the rats were tested for apomorphine-induced rotation behavior; those rats testing positively to apormorphine were selected for gene therapy, which was administered intravenously 4 weeks after toxin administration; all animals were euthanized 3 days after gene administration. Clones 877 and 951 are eukaryotic expression plasmids encoding the rat TH cDNA under the influence of either the widely expressed SV40 promoter, or the brain-specific GFAP promoter, respectively.[25]

Clone 877 also produced a 10-fold increase in hepatic TH because the SV40 promoter is expressed in this peripheral tissue. However, clone 951 caused no change in hepatic TH enzyme activity, and there was no ectopic expression of the TH gene in any of the peripheral tissues examined (Table 2). Administration of the TH gene did not result in any change in cortical TH enzyme activity. This is because the GTPCH gene is not expressed in cortex,[29] and local production of the tetrahydrobiopterin cofactor is an obligatory requirement for local TH gene expression. The biochemical assays of TH enzyme activity were corroborated with immunocytochemistry and measurements of immunoreactive TH (FIG. 2). This study shows the results from six different rats, all of which had apomorphine proven 6-hydroxydopamine lesions on the right side of the brain. The three animals in panels A, B, and C of Figure 2 were treated with the TH gene encapsulated in PILs targeted with the TfRmAb. The three animals shown in D, E, and F of Figure 2 were treated with the TH gene encapsulated in PILs targeted with the mouse IgG2A isotype control, which had no receptor specificity. This immunocytochemical study shows complete normalization of striatal immunoreactive TH on the lesioned side with PIL gene therapy,

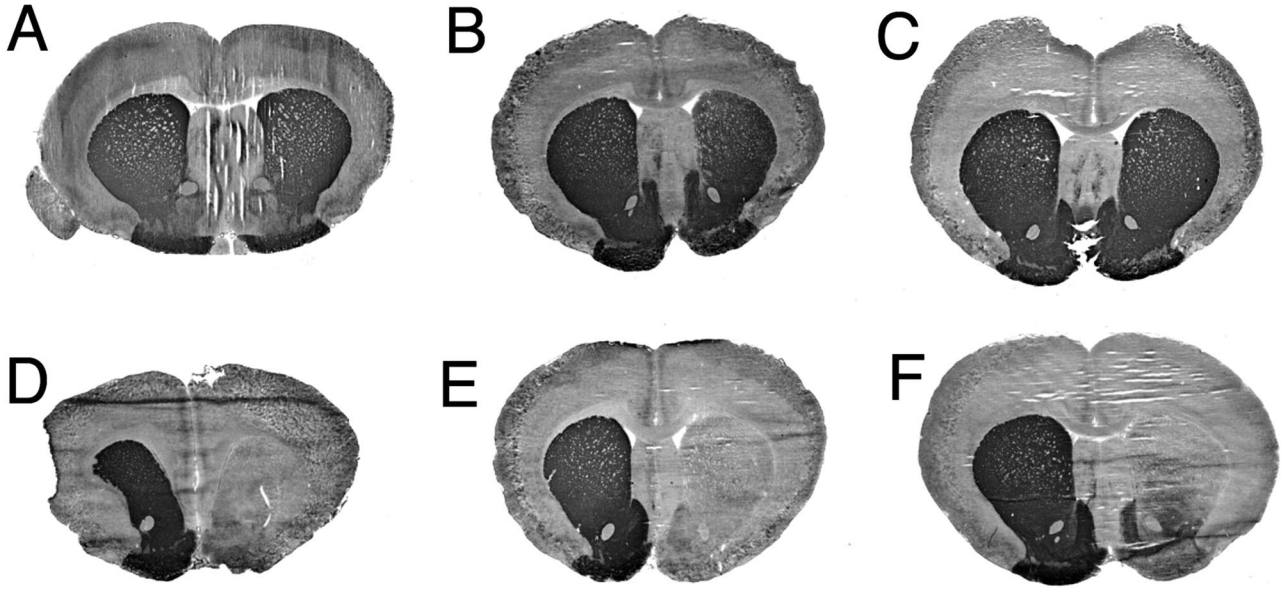

FIG. 2. Tyrosine hydroxylase immunocytochemistry of rat brain removed 72 h after a single intravenous injection of 10 μg per rat of clone 951 plasmid DNA encapsulated in PIL targeted with either the TfRmAb (panels A–C) or with the mouse IgG2a isotype control (panels D–F). Coronal sections are shown for three different rats from each of the two treatment groups. Clone 951 is the TH expression plasmid under the influence of the human GFAP promoter. The 6-hydroxydopamine was injected in the medial forebrain bundle of the right hemisphere, which corresponds to right side of the figure. Sections are not counterstained. Reproduced with permission from Zhang et al. Normalization of striatal tyrosine hydroxylase and reversal of motor impairment in experimental parkonsinism with intravenous nonviral gene therapy and a brain-specific promotor. *Hum Gene Ther* 15:339–350. [25]

providing a receptor active targeting mAb is used. If an identical formulation is employed, except the TfRmAb targeting agent is replaced with a nontargeting agent, then no TH gene expression is observed. These results were corroborated by confocal microscopy using antibodies to TH, GFAP, the NeuN neuronal nuclear antigen, or the 200-kDa neurofilament protein (FIG. 3). The fibers in the striate body ipsilateral to the lesion were immunoreactive for TH after intravenous administration of the TH gene encapsulated in TfRmAb targeted PILs (FIG. 3C), but there was no expression of immunoreactive TH in these fibers when the PIL was targeted with the mouse IgG isotype control (FIG. 3B). The expression of the immunoreactive TH in the striatum was confined to nerve endings as there was no colocalization of immunoreactive TH and astrocytic GFAP in the striate body of the gene therapy-treated animals (FIG. 3, G–I). Confocal microscopy of the substantia nigra showed production of immunoreactive TH in nigral neuron cell bodies after a TH gene therapy (FIG. 3, K and L). The normalization of striatal TH immunoreactive TH and striatal TH enzyme activity was correlated with the normalization of pharmacologic behavior in response to apomorphine.[14,25] There was an 80% reduction in apomorphine induced rotation behavior in animals treated with intravenous TH gene therapy using PILs targeted with the TfRmAb (FIG. 4). In contrast, in those lesioned animals that were treated with the TH gene encapsulated in PILs targeted with the nonspecific mouse IgG isotype control, there was no affect on apomorphine induced rotation behavior (FIG. 4).

Time-response and dose-response studies

The persistence of TH gene expression in the striate body ipsilateral to the 6-hydroxydopamine lesion was determined with measurements of striatal TH enzyme activity at 3, 6, and 9 days after a single intravenous injection of clone 877 plasmid DNA encapsulated in the TfRmAb-targeted PILs.[14] These data show striatal TH enzyme activity peaks at 3 days and decreases 50% by 6 days and approximately 90% by 9 days after a single intravenous injection (FIG. 5A). A dose-response study was performed by measurement of TH enzyme activity in the striatum at 3 days after the intravenous injection of clone 877 plasmid DNA encapsulated in TfRmAb-targeted PILs at a dose of 1, 5, or 10 μg plasmid DNA per rat.[14] There was no increase in striatal TH after the 1 μg DNA/rat dose; there was an intermediate TH response after the intravenous injection of the 5 μg DNA/rat dose, and there was complete normalization of striatal TH enzyme activity after the 10 μg DNA/rat dose (FIG. 5B). A per rat dose of 10 μg of the 6.0 kb clone 877 plasmid DNA delivers 1.2×10^9 plasmid molecules per gram of brain, as 0.07% of the injected PIL dose is delivered per gram of rat brain.[14] Assuming 10^8 cells per gram brain, the 10 μg/rat dose delivers ~12 plasmid DNA molecules per brain cell. Conversely, only approximately one plasmid molecule per brain cell is delivered with 1 μg/rat dose. These observations suggest that there is a very high efficiency of cell transfection with the PIL gene transfer technology, and that the cellular delivery of only 5-10 plasmid DNA molecules per cell is required for a full pharmacologic response from the gene therapy. After delivery of the TH gene across the BBB in the region of the substantia nigra in brain, the gene is incorporated into the neuronal nuclear compartments of the substantia nigra where the gene is transcribed and the TH protein is translated from the TH mRNA produced from the exogenous plasmid. The TH enzyme may then be transported to the striatum via one of two mechanisms. First, there is intense neuronal sprouting from the substantia nigra to the striatum that follows the intracerebral injection of 6-hydroxydopamine, such that the density of dopaminergic terminals in the striatum is returned nearly to normal, albeit these nerve fibers do not produce TH in the absence of gene therapy.[30,31] Second, intracerebral fluorogold injection studies have shown that approximately 30% of nigral striatal neurons are intact after intracerebral injection of 6-hydroxydopamine.[32] Both GTPCH and the tetrahydrobiopterin cofactor levels in the striatum of the 6-hydroxydopamine-lesioned rat are still one third the concentrations in nonlesioned animal,[33] owing to striatal inputs from monoaminergic regions outside the substantia nigra.

The PIL gene transfer technology enables adult transgenics in 24-48 h and gives a picture similar to that obtained with conventional transgenics technology that requires pronuclear injections of genes into embryos. Transgenic mice expressing the human TH gene produce no TH mRNA in the cortex of these animals,[34] because there is no GTPCH gene expression or cofactor production in the cortex. Similarly, there is no change in TH gene expression in the cortex of adult rats administered the TH gene via the PIL gene transfer technology (Table 2). The level of TH gene expression is tightly regulated within the brain so that supraphysiological levels of TH are not generated in the brain. Despite a 50-fold increase in TH mRNA in the substantia nigra of human TH transgenic mice, there is only a minor increase in TH protein in the striatum of these animals.[34] This finding is consistent with the observations made with the PIL gene transfer technology, where the level of TH enzyme activity is restored to normal but not supranormal levels by intravenous TH gene therapy (Table 2).

Brain gene expression driven by the GFAP promoter

The confocal studies show that the TH gene is expressed in neurons when the transgene is under the influence of GFAP promoter (FIG. 3). Moreover, there is

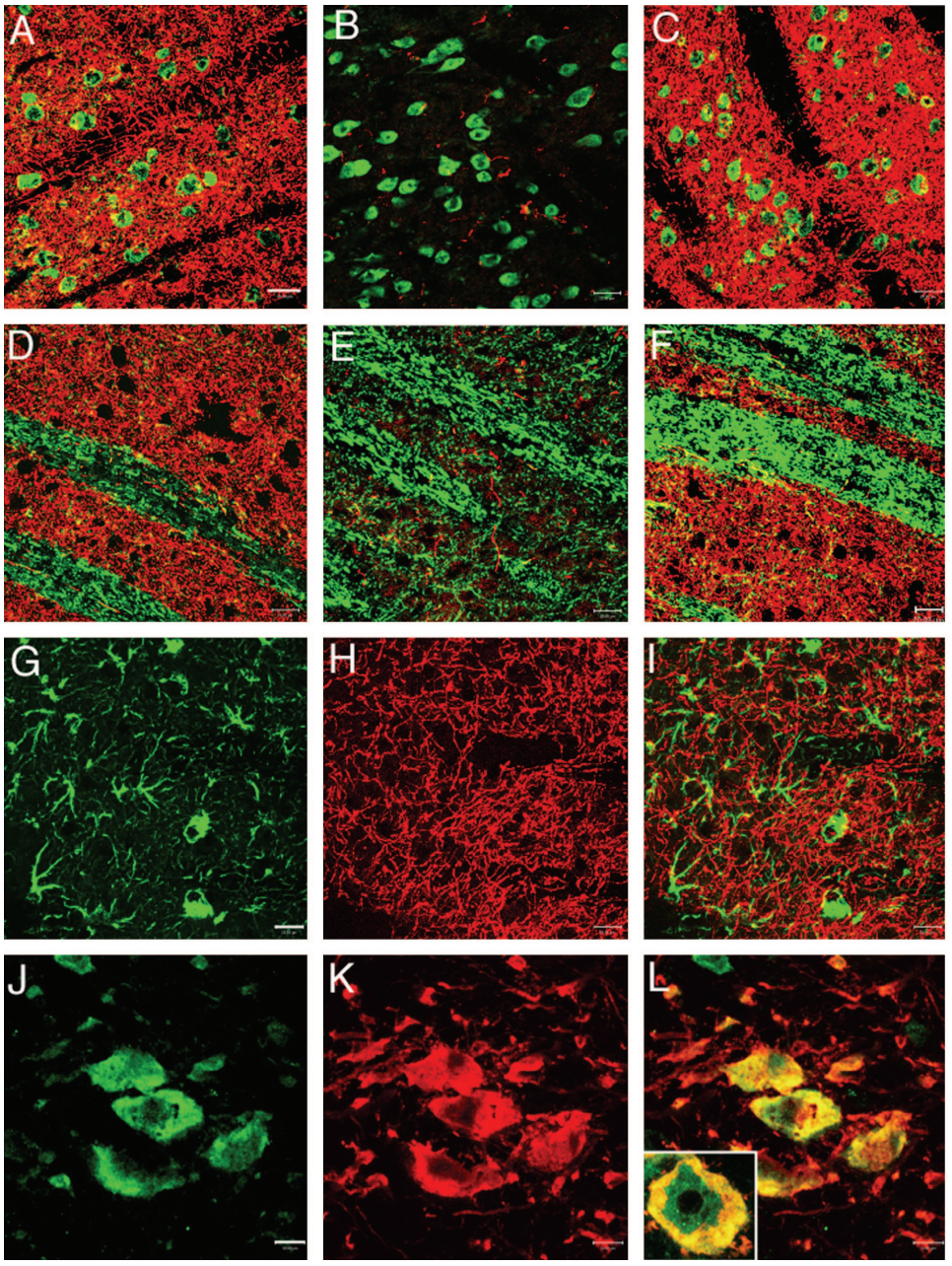

FIG. 3. Confocal microscopy of striatum and substantia nigra in 6-hydroxydopamine-lesioned rats sacrificed at 3 days after intravenous injection of clone 951 plasmid DNA encapsulated in PILs targeted either with mouse IgG2a (panels B and E) or with the TfRmAb (panels A, C, D, F, and G–L). Panels A and D are from the striatum contralateral to the lesion, and panels B, C, E, F, and G–I are from the striatum ipsilateral to toxin injection. Panels J to L are from the substantia nigra ipsilateral to the lesion. Panels A–C show striatum colabeled with a mouse monoclonal antibody to NeuN (green) and a rabbit polyclonal antibody to TH (red). Panels D–F show striatum colabeled with a mouse monoclonal antibody to the 200-kDa neurofilament protein (green) and a rabbit polyclonal antibody to TH (red). The magnification bar in panel A is 20 μm. All images are three-dimensional projection views of multiple planar images. The yellow color is an artifact from the three-dimensional projection because there was no overlap observed in the single planar views. Panels G and J show immune staining (green channel) with monoclonal antibodies to GFAP and NeuN, respectively. Panels H and K show immune staining (red channel) with a rabbit polyclonal antibody to TH. The overlap image of TH and GFAP in striatum is shown in panel I; the overlap image of TH and NeuN in substantia nigra is shown in panel L. The inset of panel L is a 100× oil immersion view of colabeling of TH (red), NeuN (green), and the overlap (yellow) in a neuron in the substantia nigra. The magnification bars in panels G and J are 20 and 10 μm, respectively. All images are three-dimensional projection views of multiple planar images. Reproduced with permission from Zhang et al. Normalization of striatal tyrosine hydroxylase and reversal of motor impairment in experimental parkinsonism with intravenous nonviral gene therapy and a brain-specific promotor. *Hum Gene Ther* 15:339–350. Copyright © 2004, Mary Ann Liebert, Inc. All rights reserved.[25]

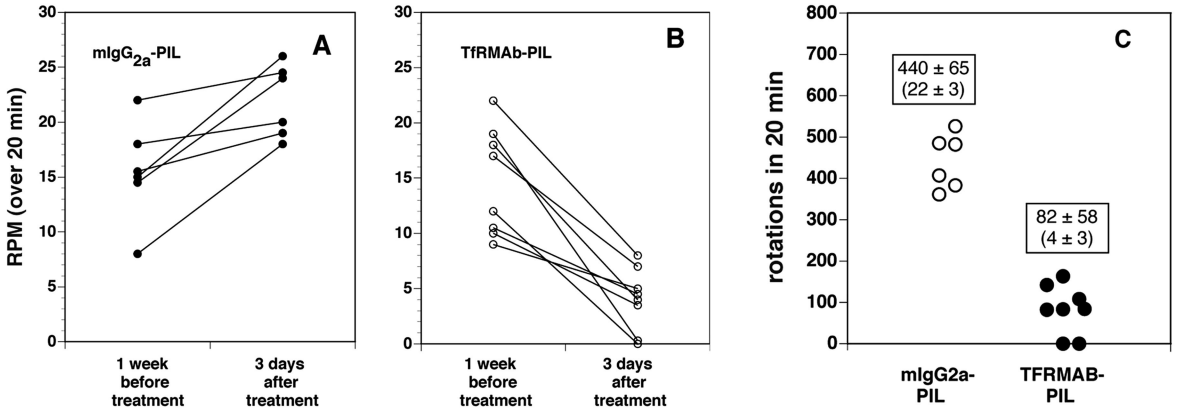

FIG. 4. A: Apomorphine-induced rotations per minute (RPM) over a 20-min period measured in individual rats at 1 week before treatment and at 3 days after a single intravenous injection of 10 μg per rat of clone 951 plasmid DNA encapsulated in a PIL targeted with the mouse IgG2a isotype control antibody. B: Apomorphine-induced RPM over a 20 min period measured in individual rats at 1 week before treatment and at 3 days after a single intravenous injection of 10 μg per rat of clone 951 plasmid DNA encapsulated in a PIL targeted with the TfRmAb. C: Comparison of the total rotations in the two groups at 3 days after treatment. The average RPM is 22 ± 3 and 4 ± 3 (mean ± SD) in animals treated with the mIgG2a-PIL and the TfRmAb-PIL, respectively. The difference in rotation between the two groups is significant at the $p < 0.005$ level. Reproduced with permission from Zhang et al. Normalization of striatal tyrosine hydroxylase and reversal of motor impairment in experimental parkonsinism with intravenous nonviral gene therapy and a brain-specific promotor. *Hum Gene Ther* 15:339–350. Copyright © 2004, Mary Ann Liebert, Inc. All rights reserved.[25]

no detectable expression of the TH gene in astrocytes based on confocal microscopy and colabeling with antibodies to TH and GFAP (FIG. 3I). This finding is consistent with the observation that astrocytes under normal conditions do not express the GTPCH gene.[28] The intracerebral injection of TH expression plasmids under the influence of the GFAP promoter can lead to astrocyte gene expression in brain when the expression plasmid is mixed with cationic liposomes.[35] However, cationic liposomes cause a brain injury reaction,[36] and the GTPCH gene is expressed in reactive astrocytes.[37] The finding of neuronal expression of the TH gene under the influence of the GFAP 5′-FS is consistent with earlier observations that the GFAP 5′-FS confers brain specificity of gene expression, but not astrocyte-specific gene expression. Astrocyte specific expression of the GFAP gene requires coordinated interactions between regulatory elements in both the 5′-FS and more distal parts of the gene, including the 3′-FS.[38,39] Recent work in transgenic mouse models show that the 5′-FS of the GFAP gene enables widespread neuronal expression of transgene throughout the brain,[40] and these findings are consistent with the

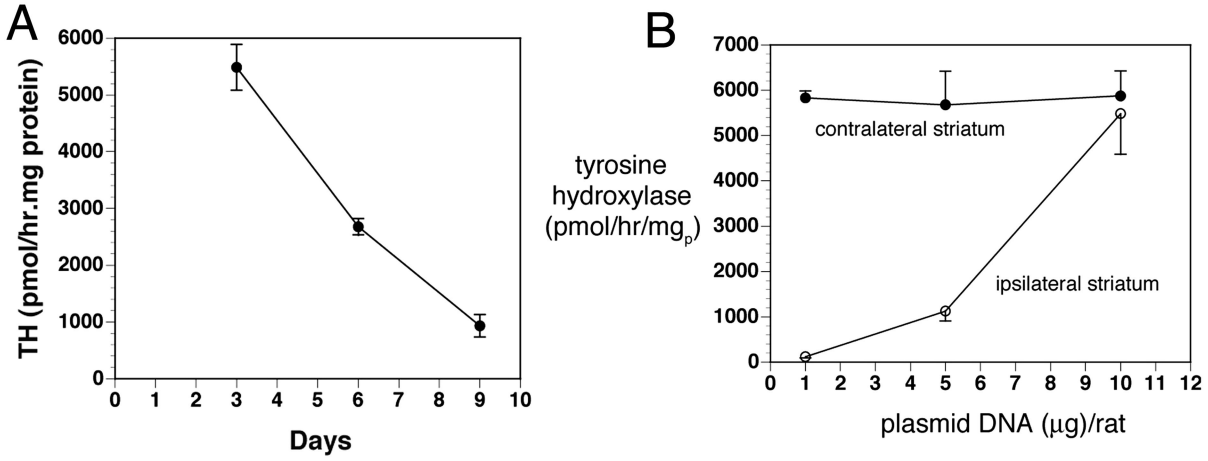

FIG. 5. A: The striatal TH activity ipsilateral to the 6-hydroxydopamine lesion is plotted *versus* time after a single intravenous injection of 10 μg/rat of clone 877 plasmid DNA encapsulated in the TfRmAb-PIL at day 0. Data are mean ± SD (n = 3 rats per point). Clone 877 is the TH expression plasmid under the influence of the SV40 promoter. B: The striatal TH activity either ipsilateral or contralateral to the 6-hydroxydopamine lesion is plotted *versus* the dose of clone 877 plasmid DNA encapsulated in the TfRmAb-PIL. Data are mean ± SD (n = 3 rats per point). Striatal TH was measured at 3 days after the single intravenous administration of the DNA. Reproduced with permission from Zhang et al. Intravenous nonviral gene therapy causes normalization of striatal tyrosine hydroxylase and reversal of motor impairment in experimental parkinsonism. *Hum Gene Ther* 14:1–12. Copyright © 2003, Mary Ann Liebert, Inc. All rights reserved.[14]

observations of other studies that neurons produce transacting factors that interact with the 5′-FS of the GFAP gene.[41]

FUTURE DIRECTIONS

Gene expression in brain after administration of PILs is reversible and extrachromosomal. The plasmid DNA functions as an extrachromosomal episome, and persistence of expression of the transgene decays with time as the plasmid DNA is degraded. Southern blot studies show no chromosomal integration of the plasmid DNA.[22] The reversible nature of episomal-based gene therapy is considered desirable and advantageous over viral delivery systems that cause permanent integration into the host genome. With episomal-based gene therapy, the risk of chromosomal integration is nil, and the gene is given chronically at repeat occasions as with any other therapeutic. The interval of repeat administration is determined by the persistence of the transgene expression, which is a function of the structural elements engineered within the plasmid DNA. If the plasmid DNA incorporates chromosomal derived elements, then the expression plasmid can attract transacting factors within brain cells, which stabilize the plasmid against degradation by DNase I, which may produce more prolonged periods of gene expression. Gene therapy needs to move from the sole reliance on cDNA-based forms of therapeutic genes, to chromosomal-derived genes that include both the coding region and important 5′ flanking sequence elements, and either intronic or 3′ flanking sequence elements that contribute to stability of gene expression within the cell.

PILs can be administered to humans chronically as the only immunogenic component of the formulation is the antibody and the immunogenicity of the antibody can be eliminated with genetic engineering and the use of chimeric or humanized antibodies. A genetically engineered chimeric HIRmAb has been produced and has identical affinity for the HIR as does the original murine 83-14 HIRmAb.[42] PILs have been administered chronically by weekly intravenous administration to rats without any toxicologic effects and no inflammation within the brain.[43] Multiple genes can be delivered to brain with the PIL gene transfer technology, and an ideal form of gene therapy of PD would be aimed at the dual goals of TH replacement gene therapy and neuroprotection gene therapy.

Acknowledgments: This work was supported by a grant from the U.S. Department of Defense Neurotoxin Exposure and Treatment Research Program.

REFERENCES

1. Shastry BS. Parkinson disease: etiology, pathogenesis and future of gene therapy. *Neurosci Res* 41:5–12, 2001.
2. Booij J, Bergmans P, Winogrodzka A, Speelman JD, Wolters EC. Imaging of dopamine transporters with [123I]FP-CIT SPECT does not suggest a significant effect of age on the symptomatic threshold of disease in Parkinson's disease. *Synapse* 39:101–108, 2001.
3. Boado RJ, Li JY, Nagaya M, Zhang C, Pardridge WM. Selective expression of the large neutral amino acid transporter at the blood-brain barrier. *Proc Natl Acad Sci USA* 96:12079–12084, 1999.
4. Kordower JH, Emborg ME, Bloch J, Ma SY, Chu Y, Leventhal L, et al. Neurodegeneration prevented by lentiviral vector delivery of GDNF in primate models of Parkinson's disease. *Science* 290:767–773, 2000.
5. Dewey RA, Morrissey G, Cowsill CM, Stone D, Bolognani F, Dodd NJ, et al. Chronic brain inflammation and persistent herpes simplex virus 1 thymidine kinase expression in survivors of syngeneic glioma treated by adenovirus-mediated gene therapy: implications for clinical trials. *Nat Med* 5:1256–1263, 1999.
6. McMenamin MM, Byrnes AP, Charlton HM, Coffin RS, Latchman DS, Wood MJ. A γ34.5 mutant of herpes simplex 1 causes severe inflammation in the brain. *Neuroscience* 83:1225–1237, 1998.
7. Chirmule N, Propert K, Magosin S, Qian Y, Qian R, Wilson J. Immune responses to adenovirus and adeno-associated virus in humans. *Gene Ther* 6:1574–1583, 1999.
8. Miller DG, Rutledge EA, Russell DW. Chromosomal effects of adeno-associated virus vector integration. *Nat Genet* 30:147–148, 2002.
9. Laufs S, Gentner B, Nagy KZ, Jauch A, Benner A, Naundorf S, et al. Retroviral vector integration occurs in preferred genomic targets of human bone marrow-repopulating cells. *Blood* 101:2191–2198, 2003.
10. Ai Y, Markesbery W, Zhang Z, Grondin R, Elseberry D, Gerhardt GA, et al. Intraputamenal infusion of GDNF in aged rhesus monkeys: distribution and dopaminergic effects. *J Comp Neurol* 461: 250–261, 2003.
11. Pardridge WM. Drug and gene targeting to the brain with molecular Trojan horses. *Nat Rev Drug Discov* 1:131–139, 2002.
12. Shi N, Pardridge WM. Non-invasive gene targeting to the brain. *Proc Natl Acad Sci USA* 97:7567–7572, 2000.
13. Huwyler J, Wu D, Pardridge WM. Brain drug delivery of small molecules using immunoliposomes. *Proc Natl Acad Sci USA* 93: 14164–14169, 1996.
14. Zhang Y, Calon F, Zhu C, Boado RJ, Pardridge WM. Intravenous nonviral gene therapy causes normalization of striatal tyrosine hydroxylase and reversal of motor impairment in experimental parkinsonism. *Hum Gene Ther* 14:1–12, 2003.
15. Plank C, Tang MX, Wolfe AR, Szoka FC Jr. Branched cationic peptides for gene delivery: role of type and number of cationic residues in formation and in vitro activity of DNA polyplexes. *Hum Gene Ther* 10:319–332, 1999.
16. Hong K, Zheng W, Baker A, Papahadjopoulos D. Stabilization of cationic liposome-plasmid DNA complexes by polyamines and poly(ethylene glycol)-phospholipid conjugates for efficient in vivo gene delivery. *FEBS Lett* 400:233–237, 1997.
17. Osaka G, Carey K, Cuthbertson A, Godowski P, Patapoff T, Ryan A, et al. Pharmacokinetics, tissue distribution, and expression efficiency of plasmid [33P]DNA following intravenous administration of DNA/cationic lipid complexes in mice: use of a novel radionuclide approach. *J Pharm Sci* 85:612–618, 1996.
18. Shi N, Zhang Y, Zhu C, Boado RJ, Pardridge WM. Brain-specific expression of an exogenous gene after i.v. administration. *Proc Natl Acad Sci USA* 98:12754–12759, 2001.
19. Zhang Y, Schlachetzki F, Pardridge WM. Global non-viral gene transfer to the primate brain following intravenous administration. *Mol Ther* 7:11–18, 2003.
20. Zhang Y, Jeong Lee H, Boado RJ, Pardridge WM. Receptor-mediated delivery of an antisense gene to human brain cancer cells. *J Gene Med* 4:183–194, 2002.
21. Pardridge WM, Kang YS, Buciak JL, Yang J. Human insulin receptor monoclonal antibody undergoes high affinity binding to human brain capillaries in vitro and rapid transcytosis through the blood-brain barrier in vivo in the primate. *Pharm Res* 12:807–816, 1995.
22. Shi N, Boado RJ, Pardridge WM. Receptor-mediated gene targeting to tissues in vivo following intravenous administration of pegylated immunoliposomes. *Pharm Res* 18:1091–1095, 2001.
23. Zhang Y, Boado RJ, Pardridge WM. Marked enhancement in gene

expression by targeting the human insulin receptor. *J Gene Med* 5:157–163, 2003.
24. Zhang Y, Schlachetzki F, Li JY, Boado RJ, Pardridge WM. Organ-specific gene expression in the rhesus monkey eye following intravenous non-viral gene transfer. *Mol Vis* 9:465–472, 2003.
25. Zhang Y, Schlachetzki F, Zhang YF, Boado RJ, Pardridge WM. Normalization of striatal tyrosine hydroxylase and reversal of motor impairment in experimental parkinsonism with intravenous nonviral gene therapy and a brain-specific promoter. *Hum Gene Ther* 15:339–350, 2004.
26. Vann LR, Payne SG, Edsall LC, Twitty S, Spiegel S, Milstien S. Involvement of sphingosine kinase in TNF-α-stimulated tetrahydrobiopterin biosynthesis in C6 glioma cells. *J Biol Chem* 277: 12649–12656, 2002.
27. Nussler AK, Liu ZZ, Hatakeyama K, Geller DA, Billiar TR, Morris SM Jr. A cohort of supporting metabolic enzymes is coinduced with nitric oxide synthase in human tumor cell lines. *Cancer Lett* 103:79–84, 1996.
28. Nagatsu I, Ichinose H, Sakai M, Titani K, Suzuki M, Nagatsu T. Immunocytochemical localization of GTP cyclohydrolase I in the brain, adrenal gland, and liver of mice. *J Neural Transm Gen Sect* 102:175–188, 1995.
29. Shimoji M, Hirayama K, Hyland K, Kapatos G. GTP cyclohydrolase I gene expression in the brains of male and female hph-1 mice. *J Neurochem* 72:757–764, 1999.
30. Parish CL, Finkelstein DI, Tripanichkul W, Satoskar AR, Drago J, Horne MK. The role of interleukin-1, interleukin-6, and glia in inducing growth of neuronal terminal arbors in mice. *J Neurosci* 22:8034–8041, 2002.
31. Stanic D, Finkelstein DI, Bourke DW, Drago J, Horne MK. Time-course of striatal re-innervation following lesions of dopaminergic SNpc neurons of the rat. *Eur J Neurosci* 18:1175–1188, 2003.
32. Kozlowski DA, Connor B, Tillerson JL, Schallert T, Bohn MC. Delivery of a GDNF gene into the substantia nigra after a progressive 6-OHDA lesion maintains functional nigrostriatal connections. *Exp Neurol* 166:1–15, 2000.
33. Levine RA, Miller LP, Lovenberg W. Tetrahydrobiopterin in striatum: localization in dopamine nerve terminals and role in catecholamine synthesis. *Science* 214:919–921, 1981.
34. Kaneda N, Sasaoka T, Kobayashi K, Kiuchi K, Nagatsu I, Kurosawa Y, et al. Tissue-specific and high-level expression of the human tyrosine hydroxylase gene in transgenic mice. *Neuron* 6:583–594, 1991.
35. Segovia J, Vergara P, Brenner M. Astrocyte-specific expression of tyrosine hydroxylase after intracerebral gene transfer induces behavioral recovery in experimental parkinsonism. *Gene Ther* 5:1650–1655, 1998.
36. Bell H, Kimber WL, Li M, Whittle IR. Liposomal transfection efficiency and toxicity on glioma cell lines: in vitro and in vivo studies. *Neuroreport* 9:793–798, 1998.
37. Foster JA, Christopherson PL, Levine RA. GTP cyclohydrolase I induction in striatal astrocytes following intrastriatal kainic acid lesion. *J Chem Neuroanat* 24:173–179, 2002.
38. Kaneko R, Sueoka N. Tissue-specific versus cell type-specific expression of the glial fibrillary acidic protein. *Proc Natl Acad Sci USA* 90:4698–4702, 1993.
39. Galou M, Pournin S, Ensergueix D, Ridet JL, Tchelingerian JL, Lossouarn L, et al. Normal and pathological expression of GFAP promoter elements in transgenic mice. *Glia* 12:281–293, 1994.
40. Zhuo L, Theis M, Alvarez-Maya I, Brenner M, Willecke K, Messing A. hGFAP-cre transgenic mice for manipulation of glial and neuronal function in vivo. *Genesis* 31:85–94, 2001.
41. Gomes FC, Garcia-Abreu J, Galou M, Paulin D, Moura Neto V. Neurons induce GFAP gene promoter of cultured astrocytes from transgenic mice. *Glia* 26:97–108, 1999.
42. Coloma MJ, Lee HJ, Kurihara A, Landaw EM, Boado RJ, Morrison SL, et al. Transport across the primate blood-brain barrier of a genetically engineered chimeric monoclonal antibody to the human insulin receptor. *Pharm Res* 17:266–274, 2000.
43. Zhang YF, Boado RJ, Pardridge WM. Absence of toxicity of chronic weekly intravenous gene therapy with pegylated immunoliposomes. *Pharm Res* 20:1779–1785, 2003.

ASENT Conflict of Interest Statement

The American Society for Experimental NeuroTherapeutics (ASENT) comprises individuals from academia, industry, government, and the advocacy community. The mission of ASENT is to advance treatments for individuals at risk for or affected by disorders of the nervous system. Because ASENT receives financial contributions from industry and organizations in support of its programs, including publications and the annual scientific meeting, such financial relationships need to be fully disclosed. In order to ensure the integrity of its publications, including the journal *NeuroRx*®, an editorial board was established to review the content of ASENT publications. In addition, ASENT has a Publications Oversight Committee to provide further review of real or potential conflicts of interest. All authors of ASENT publications are required to disclose any personal financial relationships with industry or organizations that may influence the content of their authored publication. Such disclosures are reported at the time of publication.

Pharmaceutical Research, Vol. 23, No. 7, July 2006 (© 2006)
DOI: 10.1007/s11095-006-0274-x

Research Paper

Decline in Exogenous Gene Expression in Primate Brain Following Intravenous Administration Is Due to Plasmid Degradation

Chun Chu,[1] Yun Zhang,[1] Ruben J. Boado,[1] and William M. Pardridge[1,2]

Received October 20, 2005; accepted February 21, 2006

Purpose. Nonviral gene transfer to the brain of adult Rhesus monkeys is possible with a single intravenous administration of plasmid DNA that is encapsulated in the interior of pegylated immunoliposomes, which are targeted across membrane barriers *in vivo* with a monoclonal antibody to the human insulin receptor.
Methods. The present studies measure the rate of decay of luciferase gene expression in the Rhesus monkey with luciferase enzyme assays, Southern blotting, and real-time polymerase chain reaction.
Results. Luciferase enzyme activity in frontal cortex, cerebellum, and liver decays with a $t_{1/2}$ of 2.1 ± 0.1, 2.6 ± 0.2, and 1.7 ± 0.01 days, respectively. Luciferase plasmid in brain and liver was detectable by Southern blotting at 2 days, but not at 7 or 14 days. The concentration of luciferase plasmid DNA in brain and liver was measured by real-time polymerase chain reaction, and decayed with $t_{1/2}$ of 1.3 ± 0.3 and 2.7 ± 0.5 days, respectively.
Conclusions. The maximal concentration of luciferase plasmid DNA in Rhesus monkey brain was 3–4 molecules/cell following an i.v. administration of 12 μg/kg pegylated immunoliposome encapsulated plasmid DNA. These results demonstrate that the rate of loss of exogenous gene expression in the primate *in vivo* correlates with the rate of DNA degradation of the exogenous plasmid DNA.

KEY WORDS: insulin receptor; luciferase; nonviral gene transfer; real-time PCR.

INTRODUCTION

Nonviral plasmid gene therapeutics may be delivered to distant target sites *in vivo* following an intravenous administration with the use of the pegylated immunoliposome (PIL) gene targeting technology (1). A single plasmid DNA molecule is encapsulated in the interior of a 100-nm liposome. The surface of the liposome is conjugated with several thousand strands of 2,000-Da polyethyleneglycol (PEG). The tips of 1–2% of the PEG strands are conjugated with a receptor-specific targeting monoclonal antibody (MAb). In prior studies, plasmid DNA encoding luciferase or β-galactosidase was delivered to the brain of adult Rhesus monkeys with an intravenous injection of PILs targeted with an MAb to the human insulin receptor (HIR) (2). The expression of luciferase and β-galactosidase in Rhesus monkey brain was determined 2 days after a single intravenous injection. In parallel studies, luciferase gene expression was measured in the retina of Rhesus monkeys, and luciferase enzyme activity in the retina decayed with a $t_{1/2}$ of 2.0 ± 0.1 days (3). The decay in gene expression may be due either to promoter inactivation, or to plasmid degradation.

The purpose of the present studies was to measure luciferase gene expression in Rhesus monkey brain at periods lasting up to 14 days following a single intravenous injection of HIRMAb-targeted PILs. In parallel with measurements of luciferase enzyme activity in primate brain, the level of the exogenous plasmid DNA in primate brain was measured with real-time polymerase chain reaction (PCR) assays, and by Southern blotting. The correlation of the luciferase enzyme assay and the real-time PCR assay allows for a determination as to whether the loss with time of luciferase gene expression is attributable to promoter inactivation or to plasmid DNA degradation.

MATERIALS AND METHODS

Intravenous Gene Administration in Rhesus Monkeys

Three healthy 5- to 10-year-old, 5- to 6-kg female Rhesus monkeys were purchased from Covance (Alice, TX, USA). A fourth rhesus monkey was sacrificed for removal of control tissues from an uninjected primate. The animals were anesthetized with 10 mg/kg ketamine intramuscular, and 5 mL sterile HIRMAb-PIL containing 70 μg of plasmid DNA was injected into each monkey via the saphenous vein with a 18-gauge catheter. The primates were euthanized at 2, 7, or 14 days after the single PIL injection of the luciferase expression plasmid (3). The brain, liver, spleen, lung, heart, kidney, and triceps skeletal muscle were removed. PIL formulation was prepared as previously described (2). The total dose of HIRMAb that was conjugated to the PIL and administered to each monkey was 1.8 mg or 300 μg/kg of

[1] Department of Medicine, UCLA, UCLA Warren Hall 13-164, 900 Veteran Avenue, Los Angeles, CA 90024, USA.
[2] To whom correspondence should be addressed. (e-mail: wpardridge@mednet.ucla.edu)

antibody. The injection dose of PIL encapsulated plasmid DNA was 12 μg/kg. Murine HIRMAb was purified from hybridoma generated ascites by protein G affinity chromatography. The luciferase expression plasmid is clone 790, as previously described (2,4), and is driven by the SV40 promoter. The research adhered to the provisions of "Principles of Laboratory Animal Care" (NIH Publication #85-23, revised in 1985).

Luciferase Enzyme Activity Measurements

Primate organs were homogenized in 4 vol Promega lysis buffer as previously described (2). The data are reported as pg luciferase activity per mg cell protein. Based on the standard curve, 1 pg luciferase was equivalent to 14,312 ± 2,679 relative light units (RLU), which is the mean ± SE of five assays.

Isolation of Genomic DNA

Genomic DNA was isolated from monkey brain and liver with Genomic-tip 500/G columns from Qiagen (Valencia, CA, USA) according to the manufacturer's instructions. About 350 mg monkey liver tissue or 400 mg monkey brain tissue was homogenized in 0.8 M guanidine, 0.03 M Tris/8.0, 30 mM EDTA, 5% Tween 20, 0.5% Triton X-100, and 0.2 mg/mL RNase A, followed by incubation with 1 mg/mL proteinase K at 50°C for 2 h. Genomic DNA in the homogenate was retrieved by filtration through a Qiagen Genomic tip 500/G column followed with isopropanol precipitation. The A_{260}/A_{280} ratio averaged 2.0, and the yield of genomic DNA was 500 μg. The yield of genomic DNA isolation was 70% based on parallel samples labeled with ^{32}P-DNA internal standard.

Real-Time PCR

Real-time PCR primers that hybridize within the open reading frame of the firefly luciferase gene were identified with the Beacon 2.1 software (Bio-Rad, Hercules, CA, USA), which selects primers with an annealing temperature of 58 ± 2°C and PCR products with 75–150 bp. The sequence for the forward primer is 5′-TCGAAAGAAGTCGGGGAAGC, and the sequence for the reverse primer is 5′-CCTCGGGTG TAATCAGAATAGC.

Table I. Luciferase Enzyme Activity in Rhesus Monkey Organs

	pg luciferase/mg protein		
Organ	2 days	7 days	14 days
Frontal white	3.2 ± 0.3	0.4 ± 0.03	0.020 ± 0.002
Cerebellum gray	7.0 ± 1.6	1.9 ± 0.2	0.080 ± 0.009
Cerebellum white	4.0 ± 0.4	0.4 ± 0.03	0.025 ± 0.0006
Heart	0.014 ± 0.003	0.003 ± 0.0007	<0.01
Liver	15.5 ± 0.4	2.9 ± 0.2	0.14 ± 0.023
Spleen	2.8 ± 0.4	0.6 ± 0.03	0.015 ± 0.0007
Lung	1.9 ± 0.3	0.3 ± 0.03	0.017 ± 0.002
Kidney	0.6 ± 0.1	0.05 ± 0.003	<0.01
Skeletal muscle	0.13 ± 0.02	0.011 ± 0.001	<0.01

Data are mean ± SE (n = 3 replicates from a single monkey at each time point).

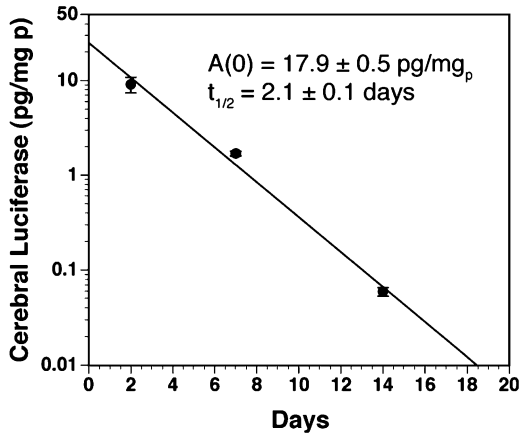

Fig. 1. Luciferase enzyme activity in Rhesus monkey frontal cortex gray matter is plotted vs. time after a single i.v. injection of HIRMAb-targeted PILs carrying clone 790 luciferase expression plasmid DNA. The y-intercept, $A(0)$, and the slope were determined by linear regression analysis. The $t_{1/2}$ of decay was determined from ln 2/slope.

Real-time PCR was performed by using Bio-Rad MBR Green Supermix and an iCycler IQ™ Real-time Detection System from Bio-Rad. For each reaction in 25 μL, 200 ng genomic DNA and 2.5 μL of 2.5 μM primer mixture were added. PCR was initiated by a 3-min incubation at 95°C, followed by 40 cycles consisting of 10 s annealing at 57.9°C, 10 s extension at 72°C, and 10 s denaturing at 95°C. Melting curves of each PCR product were determined by measuring the ratio of single-strand DNA vs. double-strand DNA at every 0.5°C temperature increase from 55 to 94°C. For quantification of luciferase DNA, the clone 790 luciferase expression plasmid was diluted into 5 ng/μL, 50 pg/μL, 500 fg/μL, 5 fg/μL, and 0.05 fg/μL aliquots containing 100 ng/μL genomic DNA isolated from normal monkey brain tissue. Real-time PCR was performed as described above, using 2 μL DNA standard solution as the template. A series of threshold cycle (C_t) values were obtained. A standard curve of luciferase DNA was generated by plotting C_t values against the logarithm of plasmid mass (fg). Plasmid mass was converted into number of plasmid molecules based on the molecular weight of the luciferase expression plasmid, 10.6 kb, and 665 Da per base pair. The standard curve was linear over 8 log orders of luciferase DNA (10^{-4} to 10^4 pg DNA).

Southern Blotting

Genomic DNA (10 μg) from brain or liver were digested with 15 U *Hin*dIII for 1 h at 37°C, resolved by gel electrophoresis in 0.8% agarose, blotted to a GeneScreen Plus membrane, and hybridized with the ^{32}P-labeled, *Hin*dIII linearized luciferase expression plasmid designated clone 734 (4). Autoradiograms were developed following exposure of Kodak Biomax film for 3 days at −70°C.

RESULTS

The luciferase enzyme activity in brain and peripheral tissues of adult Rhesus monkeys at 2, 7, and 14 days after a single intravenous injection of the HIRMAb targeted PIL is

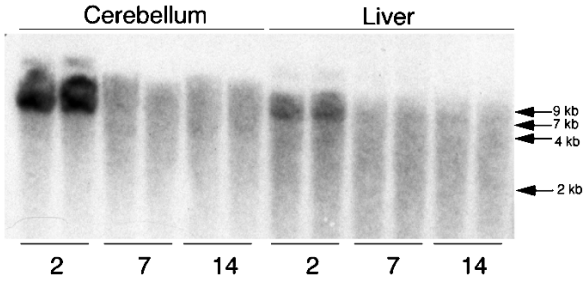

Fig. 2. Southern blot analysis of genomic DNA isolated from Rhesus monkey cerebellum and liver at 2, 7, and 14 days after a single i.v. injection of HIRMAb-targeted PILs carrying clone 790 luciferase expression plasmid DNA. The size of molecular weight standards is shown on the right side of the figure. The top of the gel is shown, indicating the sample DNA has migrated into the gel.

shown in Table I. For brain, the data in Table I include luciferase enzyme activity for frontal cortex white matter, cerebellar gray matter, and cerebellar white matter. The luciferase enzyme activity levels in frontal cortex gray matter at the 3 different days after intravenous administration are given in Fig. 1. The luciferase enzyme activity decays monoexponentially with a $t_{1/2}$ of 2.1 ± 0.1 days (Fig. 1). The luciferase data for cerebellar gray matter and for primate liver were also analyzed by a monoexponential function that yielded a $t_{1/2}$ of 2.6 ± 0.2 days for cerebellar gray matter and 1.7 ± 0.01 days for primate liver ($r = 0.99$).

Extracts of genomic DNA isolated from the primate brain 2, 7, and 14 days after administration were analyzed by Southern blot analysis. Plasmid DNA in cerebellum and liver was detectable at 2 days after i.v. administration, and barely detectable at 7 and 14 days after administration (Fig. 2). Levels of luciferase DNA in primate brain were quantitated by real-time PCR. A luciferase standard curve was established, and this standard curve was linear over 8 log orders of luciferase plasmid DNA concentration (Materials and Methods). Luciferase plasmid DNA concentrations in brain and liver were estimated from the real-time PCR C_t value (Table II) and the luciferase C_t standard curve. The concentrations of plasmid DNA in brain and liver at 2, 7, and 14 days after i.v. administration are given in Table II. The luciferase plasmid standard curve allowed for the conversion of C_t values into fg of luciferase plasmid DNA per 200 ng genomic DNA, or ng of luciferase plasmid DNA per 100 g tissue wet weight (Table II). Based on the size of the luciferase plasmid DNA, 10.6 kb, ng of plasmid DNA were converted into molecules of plasmid DNA per 200 ng genomic DNA (Table II). The luciferase plasmid concentrations in brain and liver (Table II) were analyzed by a monoexponential decay curve, and the intercept and slopes are given in Table III. These data show that the half-life of decay of luciferase plasmid DNA in primate brain and liver is 1.3 ± 0.3 and 2.7 ± 0.5 days, respectively.

Table III. Linear Regression Analysis of Luciferase Plasmid DNA Content in Rhesus Monkey Brain following IV Administration of PILs

Organ	Parameter	Value
Brain	$A(0)$	798 ± 123 fg luciferase DNA/200 ng DNA
	k	0.55 ± 0.11 days^{-1}
	$t_{1/2}$	1.3 ± 0.3 days
Liver	$A(0)$	248 ± 18 fg luciferase DNA/200 ng DNA
	k	0.26 ± 0.04 days^{-1}
	$t_{1/2}$	2.7 ± 0.5 days

Parameters were computed from the data in Table II by linear regression analysis. $A(0)$ and k are the y-intercept and slope, respectively. The $t_{1/2}$ was computed from ln 2/k. The correlation coefficients of the linear regression analysis were 0.98 and 0.99 for brain and liver, respectively. Tissue analyzed is frontal brain matter.

DISCUSSION

The results of these studies are consistent with the following conclusions. First, luciferase gene expression in primate brain and liver decays with a $t_{1/2}$ of about 2 days following a single i.v. injection of the luciferase expression plasmid encapsulated inside PILs targeted to brain and liver with an HIRMAb. Second, the cause of the transient duration of luciferase gene expression is plasmid degradation, because the $t_{1/2}$ of decay of luciferase plasmid DNA concentration in brain and liver, 1–2 days (Table III), approximates the $t_{1/2}$ of decay of luciferase enzyme activity (Fig. 1).

Episomal plasmid DNA gene expression is generally transitory in cultured cells *in vitro* or in organs *in vivo*, where the vector DNA is not permanently integrated into the host genome. One cause for loss of exogenous gene expression is gene silencing without loss of vector DNA (6), owing to promoter inactivation (7). Another potential cause of loss of gene expression is vector DNA degradation. Plasmid DNA is unstable in the cytosol owing to cellular DNase (8), and is degraded with a $t_{1/2}$ of 50–90 min following DNA microin-

Table II. Quantitation of Luciferase cDNA in Rhesus Monkey Brain and Liver by Real-Time PCR

Organ	Days	C_t	luc DNA (fg/200 ng DNA)	luc DNA (ng/100 g tissue)	luc DNA (molecules/200 ng DNA)
Brain	2	22.5 ± 0.1	417 ± 45	284 ± 31	34,528 ± 3,784
	7	27.7 ± 0.1	7.6 ± 0.7	5.2 ± 0.5	631 ± 60
	14	31.3 ± 0.2	0.48 ± 0.07	0.33 ± 0.05	40 ± 6
Liver	2	23.6 ± 0.08	177 ± 11	120 ± 8	14,656 ± 944
	7	25.9 ± 0.08	30.6 ± 1.8	21 ± 1	2,534 ± 147
	14	27.7 ± 0.07	7.8 ± 0.4	5.3 ± 0.3	642 ± 32

Real-time PCR C_t values were converted into fg luciferase (luc) plasmid DNA per 200 ng genomic DNA with the luciferase standard curve (Methods). The mass of luciferase plasmid DNA was converted into molecules of plasmid DNA with the molecular size, 10.6 kb, of the luciferase expression plasmid. Data are mean ± SD (n = 3–4). Tissue analyzed is frontal brain matter.

jection into the cell (9). Unlike chromosomal DNA, which has a highly ordered chromatin structure that makes the DNA inaccessible to DNase (10), plasmid DNA lacks a higher-order chromatin structure, and is particularly vulnerable to cellular endonucleases, at "hot spots," or DNase-hypersensitive sites (11). The present studies show that the basis for the transitory expression of the luciferase expression plasmid in primate brain and liver *in vivo* following intravenous administration and delivery with PILs is plasmid degradation. Southern blot (Fig. 2) shows the loss of measurable luciferase plasmid DNA, and rate of plasmid DNA degradation is quantitated with real-time PCR (Table II). The luciferase transcriptional unit incorporated in the plasmid DNA is composed of the SV40 promoter, the luciferase cDNA, followed by SV40 3′-untranslated region (UTR). The luciferase expression plasmid used in these studies lacks any chromosomal derived gene sequences that can interact with the nuclear matrix, such as a matrix attachment region (MAR). Such sequences allow plasmid DNA to attach to the nuclear matrix (12), which may inhibit the access of cellular nuclease to the exogenous DNA.

Real-time PCR allows for quantitation of the concentration of luciferase plasmid DNA in brain and liver. The level of luciferase gene expression in cerebellum and cortex is comparable (Table I), which parallels previous studies on the level of β-galactosidase gene expression in Rhesus monkey (2). The peak luciferase enzyme activity in liver is about 2-fold greater than in brain (Table I). However, the peak luciferase plasmid DNA concentration in brain is about 3-fold greater than in liver (Table III), and this reflects organ differences in genomic DNA. The luciferase plasmid DNA concentration in brain and liver is expressed relative to the amount of genomic DNA (Tables II and III). The concentration of genomic DNA in liver is about 3-fold greater than the concentration of genomic DNA in brain (13). The earliest time point of analysis of gene expression in these studies was 2 days. Prior work on β-galactosidase gene expression shows the exogenous gene does not reach maximal expression until 2 days after injection, and is submaximal at 1 day after administration (14). The time course of luciferase gene expression is believed to parallel the time course of β-galactosidase gene expression, because the bacterial β-galactosidase enzyme and the luciferase enzyme are both rapidly degraded *in vivo*. The half-time of the luciferase enzyme in cells is about 3 h (15). Although the half-time of the bacterial β-galactosidase protein in cultured cells is about 20 h (16), this protein is degraded much faster *in vivo* in animals. Bacterial β-galactosidase is completely degraded within 4 h after administration in mice (17,18). Therefore, both the luciferase and bacterial β-galactosidase proteins have short half-times *in vivo*, which means the duration of expression of enzyme activity parallels the persistence of the transgene.

Estimates are made on the number of luciferase plasmid DNA molecules in brain per 200 ng of genomic DNA, based on the molecular size of the plasmid DNA. These data are given in Table II for both brain and liver at 2, 7, and 14 days after intravenous administration of the exogenous gene. Results of a linear regression analysis of the luciferase plasmid levels are shown in Table III, which gives $A(0)$, the maximal mass of luciferase plasmid DNA in brain or liver after an i.v. injection. The level of luciferase DNA in brain and liver decays with a half-time of 1.3 ± 0.3 and 2.7 ± 0.5 days, respectively (Table III). Therefore, the half-time of decay of luciferase enzyme activity (Fig. 1) closely parallels the half-time of plasmid DNA in monkey brain or liver *in vivo* (Table III). This observation suggests that the luciferase enzyme is rapidly degraded *in vivo*, such that the limiting factor controlling the level of luciferase enzyme activity is the concentration of luciferase plasmid DNA. This observation corroborates other work showing the half-time of luciferase enzyme activity *in vivo* is only 2–3 h (15).

The $A(0)$ for primate brain is 798 ± 123 fg luciferase plasmid DNA per 200 ng of genomic DNA (Table III). Based on the molecular size of the luciferase expression plasmid, 10.6 kb (19), the $A(0)$ corresponds to 65,342 ± 1,563 molecules per 200 ng genomic DNA. Assuming there are 10 pg of genomic DNA per cell (13,20), these calculations indicate the maximum number of luciferase plasmid DNA molecules per primate brain cell is 3.3. These calculations are consistent with other studies in rats showing that pharmacologic effects in brain, e.g., experimental Parkinson's disease, are achieved with the delivery of 5–10 plasmid DNA molecules per brain cell (21). Therefore, therapeutic levels of plasmid DNA in brain cells of the adult Rhesus monkey are achieved with an intravenous dose of PIL-encapuslated plasmid DNA of 70 μg (Materials and Methods). The level of luciferase plasmid DNA at 2 days after injection is 0.28 μg per 100 g brain (Table II). Because the Rhesus monkey brain weighs 100 g (5), the brain uptake of the plasmid DNA is 0.4% of the 70 μg injected dose at 2 days after i.v. administration. Therefore, the uptake of PIL encapsulated plasmid DNA approximates the measured peak uptake of the nonliposome conjugated HIRMAb at 3 h after an i.v. injection, which is 2% of the injected dose per Rhesus monkey brain (5).

In summary, 3–4 plasmid DNA molecules are delivered per brain cell following the i.v. injection of PIL encapsulated plasmid DNA, at a dose of 70 μg DNA per 6 kg animal or 12 μg/kg in the adult Rhesus monkey. The exogenous gene expression decays with time in parallel with the degradation of the exogenous plasmid DNA. It is possible that the persistence of plasmid DNA in the brain of higher animals may be sustained for longer periods with reformulations of the plasmid DNA that render the vector less sensitive to cellular nuclease activity.

ACKNOWLEDGMENTS

This work was supported by a grant from the Neurotoxin Exposure Treatment Research Program of the U.S. Department of Defense, and by NIH grant NS-53540.

REFERENCES

1. W. M. Pardridge. Gene targeting *in vivo* with pegylated immunoliposomes. *Methods Enzymol. (Liposomes, Part C)* **373**:507–528 (2003).
2. Y. Zhang, F. Schlachetzki, and W. M. Pardridge. Global non-viral gene transfer to the primate brain following intravenous administration. *Mol. Ther.* **7**:11–18 (2003).
3. Y. Zhang, F. Schlachetzki, J. Y. Li, R. J. Boado, and W. M. Pardridge. Organ-specific gene expression in the Rhesus mon-

key eye following intravenous non-viral gene transfer. *Mol. Vis.* **9**:465–472 (2003).
4. R. J. Boado and W. M. Pardridge. Ten nucleotide *cis* element in the 3′-untranslated region of the GLUT1 glucose transporter mRNA increases gene expression via mRNA stabilization. *Mol. Brain Res.* **59**:109–113 (1998).
5. W. M. Pardridge, Y.-S. Kang, J. L. Buciak, and J. Yang. Human insulin receptor monoclonal antibody undergoes high affinity binding to human brain capillaries *in vitro* and rapid transcytosis through the blood–brain barrier *in vivo* in the primate. *Pharm. Res.* **12**:807–816 (1995).
6. Z. Y. Chen, C. Y. He, L. Meuse, and M. A. Kay. Silencing of episomal transgene expression by plasmid bacterial DNA elements *in vivo*. *Gene Ther.* **11**:856–864 (2004).
7. N. S. Yew, M. Przybylska, R. J. Ziegler, D. Liu, and S. H. Cheng. High and sustained transgene expression *in vivo* from plasmid vectors containing a hybrid ubiquitin promoter. *Mol. Ther.* **4**:75–82 (2001).
8. D. P. Howell, R. J. Krieser, A. Eastman, and M. A. Barry. Deoxyribonuclease II is a lysosomal barrier to transfection. *Mol. Ther.* **8**:957–963 (2003).
9. D. Lechardeur, K. J. Sohn, M. Haardt, P. B. Joshi, M. Monck, R. W. Graham, B. Beatty, J. Squire, H. O'Brodovich, and G. L Lukacs. Metabolic instability of plasmid DNA in the cytosol: a potential barrier to gene transfer. *Gene Ther.* **6**:482–497 (1999).
10. H. J. Lipps, A. C. W. Jenke, K. Nehlsen, M. F. Scinteie, I. M. Stehle, and J. Bode. Chromosome-based vectors for gene therapy. *Gene* **304**:23–33 (2003).
11. S. C. Ribeiro, G. A. Monteiro, and D. M. F. Prazeres. The role of polyadenylation signal secornary structures on the resistance of plasmid vectors to nucleases. *J. Gene Med.* **6**:565–573 (2004).
12. B. H. C. Jenke, C. P. Fetzer, I. M. Stehle, F. Jonsson, F. O. Fackelmayer, H. Conradt, J. Bode, and H. J. Lipps. An episomally replicating vector binds to the nuclear matrix protein SAF-A *in vivo*. *EMBO J.* **3**:349–354 (2002).
13. F. H. Biase, M. M Franco, L. R. Goulart, and R. C. Antunes. Protocol for extraction of genomic DNA from swine solid tissues. *Genet. Mol. Biol.* **25**:313–315 (2002).
14. N. Shi, Y. Zhang, C. Zhu, R. J. Boado, and W. M. Pardridge. Brain-specific expression of an exogenous gene after i.v. administration. *Proc. Natl. Acad. Sci. USA* **98**:12754–12759 (2001).
15. H. Carlsen, J. O. Moskaug, S. H. Fromm, and R. Blomhoff. *In vivo* imaging of NF-κB activity. *J. Immunol.* **168**:1441–1446 (2002).
16. A. Bachmair, D. Finley, and A. Varshavsky. *In vivo* half-life of a protein is a function of its amino-terminal residue. *Science* **234**:179–186 (1986).
17. A. Scherpereel, R. Wiewrodt, M. Christofidou-Solomidou, R. Gervais, J. C. Murciano, S. M. Albelda, and V. R. Muzykantov. Cell-selective intracellular delivery of a foreign enzyme to endothelium *in vivo* using vascular immunotargeting. *FASEB J.* **15**:416–426 (2001).
18. Y. Zhang and W. M. Pardridge. Delivery of β-galactosidase to mouse brain via the blood–brain barrier transferrin receptor. *J. Pharmacol. Exp. Ther.* **313**:1075–1081 (2005).
19. Y. Zhang, R. J. Boado, and W. M. Pardridge. Marked enhancement in gene expression by targeting the human insulin receptor. *J. Gene Med.* **5**:157–163 (2003).
20. P. Chomczynski, K. Mackey, R. Drews, and W. Wilfinger. DNAzol: a reagent for the rapid isolation of genomic DNA. *BioTechniques* **22**:550–553 (1997).
21. Y. Zhang, F. Calon, C. Zhu, R. J. Boado, and W. M. Pardridge. Intravenous nonviral gene therapy causes normalization of striatal tyrosine hydroxylase and reversal of motor impairment in experimental Parkinsonism. *Hum. Gene Ther.* **14**:1–12 (2003).